VARIABILITY IN LEVANTINE TREE-RING RECORDS AND ITS APPLICATIONS IN DENDROCHRONOLOGICAL DATING, PROVENANCING, AND PALEOENVIRONMENTAL RECONSTRUCTION IN THE SOUTHERN LEVANT

A Dissertation

Presented to the Faculty of the Graduate School

of Cornell University

In Partial Fulfillment of the Requirements for the Degree of

Doctor of Philosophy

by

Brita Elizabeth Lorentzen

August 2015

VARIABILITY IN LEVANTINE TREE-RING RECORDS AND ITS APPLICATIONS IN DENDROCHRONOLOGICAL DATING, PROVENANCING, AND PALEOENVIRONMENTAL RECONSTRUCTION IN THE SOUTHERN LEVANT

Brita Elizabeth Lorentzen, Ph.D.

Cornell University 2015

The East Mediterranean littoral (the Levant) is a bioclimatically diverse region with a rich cultural heritage. Such bioclimatic diversity creates important regional variations in vegetation growth and (potentially) human-landscape interactions, and critically impacts how one interprets and uses the region's paleoenvironmental data. This study examines how to use dendrochronology to investigate paleoenvironmental change and date and source historical/archaeological timbers in such a varied landscape, focusing on the southern Levant (southern Lebanon, Israel/Palestine, Jordan, and the northern Sinai Peninsula).

Chapter 1 introduces the Levant's physical geography and climate. I review basic dendrochronological principles and applications in dating, provenancing, and climate reconstruction, and previous dendrochronological research in the Levant. In Chapter 2, I investigate variability in tree-ring growth patterns and climate responses of multiple tree species sampled along ecological gradients in the southern Levant. In Chapter 3, I compare tree-ring growth patterns and climate responses of *Pinus halpensis* Mill. and *Pinus brutia* Ten. sampled along bioclimatic gradients in both the

southern and northern Levant. Finally, in Chapters 4 and 5, I use dendrochronological techniques to date and source timbers from al-Aqsa Mosque in Jerusalem, and two late 19th century buildings in Jaffa, Israel.

I demonstrate that the northern and southern Levant have distinct tree-ring patterns (with a transition zone located in Lebanon), and that there is clear variability in tree-ring growth along altitudinal gradients in the northern Levant. Consequently tree-ring data from the northern Levant should not be used for reconstructing climate in the southern Levant, especially at high frequency timescales, because of the critical bioclimatic differences and differing climate proxy data that can be derived from tree-rings along the Levantine latitudinal gradient. Tree-ring chronologies from multiple altitudinal zones in the northern Levant and a separate chronology for the southern Levant should be used for dating historical/archaeological timbers from these regions. One can use these distinct dendrochronological 'zones' to identify whether timber was procured from the northern or southern Levant. Dendrochronological data can then be combined with available archaeological/historical, textual, or other paleoenvironmental data to gain new insights on human use of forest resources from the Levant and beyond.

BIOGRAPHICAL SKETCH

Brita Lorentzen received her B.A. in archaeology with a concentration in Jewish Studies from Cornell University in 2006. As part of her studies at Cornell, she took Peter Kuniholm's dendrochronology course and began working in the Cornell Tree-Ring Lab as an undergraduate research assistant in 2004. She worked on archaeological projects in Greece and Israel, which further developed her interest in paleoenvironmental studies in the Mediterranean. While working at the Tel Dor Archaeological Excavations in Israel, she also worked with researchers from the Weizmann Institute of Science, which sparked her interest in conducting dendrochronological research in Israel and the southern Levant.

After receiving her undergraduate degree, she worked as a research technician in the Cornell Tree-Ring Laboratory under Sturt Manning and participated in dendrochronological field projects in Northeast North America, Crete, and Cyprus. She also worked in the Cornell Quaternary Paleoecology Laboratory with Michelle Goman, who encouraged her to pursue graduate studies in Quaternary paleoecology.

During her PhD studies at Cornell, Brita has worked on dendrochronological research projects in the Northeast US, Eastern Europe, the Balkans, and Turkey, in addition to her main research in the southern Levant. She also works as a dendrochronologist and wood identification specialist on multiple archaeological projects in the Near East, including the Jaffa Cultural Heritage Project, the Akko Bay and Dor-Tantura Underwater Excations in Israel, the Cyprus Archaeomagnetic Project, and the Edom Lowlands Regional Archaeological Project in Jordan.

This work is dedicated to the memory of Leon H. Lorentzen, a wonderful archaeologist whom I was fortunate to count as a mentor and family.

ACKNOWLEDGMENTS

Several research grants were vital in financing this work, including: the Council of American Overseas Research Centers-American Center of Oriental Research Pre-Doctoral Fellowship; the Mario Einaudi Center for International Studies travel grant; multiple Hirsch travel grants from the Cornell Archaeology Program; multiple Kroll Travel Awards from the Cornell Near Eastern Studies Department; the Donavan Family Scholarship and additional research funds from the Geological Sciences Department; a Cornell Graduate School Research Travel Grant; and several generous financial contributions from the Cornell Tree-Ring Lab and the Malcolm H. Wiener Foundation. I have also been supported at Cornell by numerous TA appointments in the Department of Earth and Atmospheric Sciences, a Foreign Language and Area Studies scholarship, and funds from the Classics Department.

This project is the result of extensive collaboration with many individuals in several different countries. It's been a fantastic journey, and I'm sure that I could fill many more pages than I have here to express my gratitude. First, I would like to thank the members of my committee, Sturt Manning, Michelle Goman, Tim Fahey, and Peter Kuniholm, for their instruction and guidance during my graduate studies. It would take forever to list out the many ways that they have assisted me, so I'll just be succinct and give them a heartfelt THANK YOU for everything that they've done. You all have made me a better scientist. Their editorial comments that have helped improve this text are especially appreciated.

I would also like to thank my unofficial fifth and sixth committee members,

Carol Griggs and Tomasz Ważny, who have graciously donated many hours of their free time to help me with this work. Tomasz, thanks for encouraging me and helping me develop my research skills in wood anatomy and dendroprovenancing. Thank you also for bringing me along with you to the field in Europe. I never thought that I'd get to experience crossing Transylvania in a Volkswagen while listening to Black Sabbath, being chased by Bulgarian water buffalo, or moonlight chain-sawing subfossil oaks in Bosnia! Carol, thanks for all your help in answering my many questions about climate and statistics, and most of all, thanks for being a fantastic office-mate. Thanks also for bringing me with you to the field to dig in Late Pleistocene mud and drill holes in people's attics (and demolish the occasional wall)!

Elisabetta Boaretto at the Kimmel Center for Archaeological Science at the Weizmann Institute of Science was instrumental in helping me make the contacts necessary for accessing archaeological and forest materials in Israel. She has also on multiple occasions helped me find and store equipment and provided me with food, transport, and lodging. It's fair to say that this project wouldn't have happened without her help. Kimmel Center researchers Lior and Johanna Regev showed great hospitality and helped with forest sampling (which included a lesson in removing stuck increment borers). Lior, I look forward to working on many new exciting tree-ring projects in Israel!

Both the Israel Nature and Parks Authority and Jewish National Fund (JNF) generously gave me access to Israel's nature reserves and planted forests. I'd particularly like to thank Didi Kaplan, Talya Oron, Natan Elbaz, and Naama Tessler from the Nature and Parks Authority and David Brand and Amikam Riklin from the

JNF for their help in sampling and providing ecological information about the forests. Nature and Parks staff members Dotan Rotem, Yossi Karni, Eyal Miller, and Eli Sliječević, and JNF staff members Yoram Goldring, Amir Zehavi, Ezra Stein, Ido Rasis, and Haim Teperberg also provided valuable field assistance, information, and occasional transport through some of Israel's more rugged forest trails.

For my research in Jordan, I would especially like to thank Barbara Porter, Christopher Tuttle, and the rest of the staff at the American Center of Oriental Research for their hospitality and assistance. I would also like to thank Engineers Eid Al-Zouabi and Al-Shourman from the Forestry Department of the Jordanian Ministry of Agriculture for letting me sample in the Dibeen Reserve, and Dr. Abu Hazim (Director General of the Jordan Meteorological Department) for the climate data from the Shobauk and Ras Muneef stations. Hazim Nusaibeh and Abu-Khaled-M'hd Talih Youseli Bari Hamdan showed me great hospitality and gave helpful assistance with sampling at Dibeen. Jennie Bradbury, Ameen Al-Duqs (Jordanian Ministry of Agriculture), and Linah Ababneh also provided valuable field assistance. I also thank Sara Rich, who generously took time away from her own PhD project to sample the pines from Ehden, and Dr. Nabil Nemer at the Tannourine and Ehden Forest Reserves, who was instrumental in making collection in Lebanon possible.

Brendan Buckley at the Lamont Doherty Tree-Ring Lab at Columbia University donated his spare time to teach me how to use Arstan and made the chronology standardization process comprehensible and much less painful. Ramzi Touchan at the Laboratory of Tree-Ring Research at University of Arizona offered valuable background information about his Levantine tree-ring data and kindly gave

me access to his tree-ring measurements from Mt. Carmel. Nesibe Köse generously took time out of her very busy teaching and research schedule at Istanbul University to teach me how to use the DendroClim program and to help me with statistical and climate response analyses.

For the work at al-Aqsa, I would specifically like to thank Ze'ev Ehrlich for access to the al-Aqsa timber collection; Kurt Nicolussi, Katarina Čufar, and Mauro Bernabei for use of their larch reference chronologies and their additional helpful comments about working with that species; Bernd Kromer for providing radiocarbon dates; David Powers for translating the Kufic inscription; and Beatrice St. Laurent for her helpful insights about the history of the *Haram* and al-Aqsa.

For the work at Jaffa, Aaron Burke and Martin Peilstöcker, the co-directors of the Jaffa Cultural Heritage Project, have been wonderful collaborators and helped in accessing both historical and archaeological material, and provided important contextual information. Yoav Arbel (Israel Antiquities Authority) was instrumental in helping me gain access to the Ottoman buildings (and gave me free lodging in Tel Aviv). I think that we've just scratched the surface of Jaffa's dendrochronological potential, and I look forward to continuing this research collaboration.

The Cornell Tree-Ring Lab has been a huge part of both my undergraduate and graduate career. Charlotte Pearson has been a constant source of advice and encouragement, and worked tirelessly for many years to make sure that the lab ran smoothly. Thanks so much for everything you did, Charlie! Peter Brewer saved me from numerous computer and ArcGIS-related difficulties. Mary Jaye Bruce helped me greatly with organizing paperwork and field season budgeting, especially during

the early years. The lab's past and present research aides, Kate Seufer, Jen Watkins, LeAnn Canady, and Kayla Altand, all helped me immensely as well. I would also like to thank the students from the introductory dendrochronology course and "old-timers" working in the lab for their help with sample prep and measurements. It's been a pleasure to work with all of you down in the depths of Goldwin Smith.

I have also been very fortunate to be part of a wonderful, supportive research community in Cornell's geology department. I would especially like to thank Larry Brown and Lou Derry for their support and guidance. The staff at Snee, particularly Savannah Sawyer, Judy Starr, Amy Colvin, and Steve Gallow, are some of Cornell's best and have helped navigate me through many administrative and technological difficulties. My fellow graduate students, especially Mary Kosloski, Veronica Prush, Kyle Trostle, Gregg McElwee, Sander Hunter, Ursula Smith, and Greg Kirkpatrick, made Snee a fun place to work while I was here and gave a lot of moral support along the way. I also want to thank Will Guerra, my fellow paleoecologist, for assisting me in the field in Israel and sharing in my enthusiasm for old dead plants.

Special thanks go to Jessica Herlich, who quickly became a trusted friend and confidante when we took Peter Kuniholm's dendrochronology course together and then worked in the lab as undergraduates and post-graduates. Jess also had the unenviable task of being my first field assistant in Israel when I was still learning the intricacies of the Israeli road system, which provided us with many colorful tales from the field. Since then, she has remained a constant source of emotional support throughout graduate school. Thanks for voluntarily becoming my sister, Jess!

Finally, I would like to thank my parents, Lance and Elizabeth Lorentzen, and

my brother and sister-in-law, Josh and Katie Bottorff. Their never-ending support and encouragement helped get me out the door to Cornell and through the many long years of hard work that this project has entailed. I wouldn't be here without you guys!

TABLE OF CONTENTS

LIST OF FIGURES

Chapter 5

LIST OF TABLES

Chapter 5

CHAPTER 1:

THE SOUTHERN LEVANT AS A POTENTIAL REGION FOR DENDROCHRONOLOGICAL RESEARCH

INTRODUCTION

The East Mediterranean littoral between Anatolia and Egypt, or the "Levant," is an area of dramatic contrast and confluence, linking multiple geographic, climatic, and biological zones. The region–wedged between the Mediterranean Sea and the Syrio-Arabian and Sinai Deserts–is a narrow physical land bridge joining Europe, Asia, and Africa, and four biogeographic zones (Mediterranean, Irano-Turanian, Saharo-Sindian, and Sudano-Deccanian) (Zohary 1973). The area also has unique topography (due in part to its location along the Dead Sea transform fault system), in which there are drastic changes in elevation over relatively short distances (Freiwan and Kadıoğlu 2008; Zohary 1973). This has created a diverse mosaic of climatic and ecological zones with exceptionally rich biodiversity (Blondel and Aronson 1999).

In addition to its unique biological and climatic features, the Levant has been a cultural crossroads with an extensive archaeological record of long-term human (and earlier hominid) habitation (Broodbank 2013; Horden and Purcell 2000; Rosen 2007). Charred and worked wood remains in the northern Jordan River Valley indicate hominid exploitation of the Levant's local woody plant and forest resources by at least 780,000 years ago (Werker 2006). In turn, human exploitation of timber resources had broader regional impacts on Mediterranean forests, as long-distance timber trading

networks evolved. For instance, remains of cedar of Lebanon (*Cedrus libani*) timbers, which were likely imported from Lebanon, have been found in Early Bronze Age Ashkelon (Gophna and Liphschitz 1996) and the Egyptian Predynastic site of Maadi (Kuniholm et al. 2007), indicating that long-distance timber trade to the southern Levant existed by as early as the 4th millennium BC. The Levant is therefore a bioclimatically unique region, in which researchers may study the feedback between humans and their climate/environment on both local and regional scales over several millennia.

This study concentrates on the development of tree-ring chronologies and using dendrochronology (tree-ring dating) to investigate paleoenvironmental change and to date and provenance historical/archaeological timbers in the southern Levant. I particularly compare and contrast the year-to-year growth patterns of tree-ring chronologies built from forest sites in the southern and northern Levant, as well as the climatic variables regulating tree-ring growth at these sites. Understanding such variability in the Levantine tree-ring record is critical for understanding what climatic variables may be reconstructed when using tree-rings from different sites as a climate proxy and the spatial extent over which such reconstructions may be applied. Additionally, understanding tree-ring variability throughout the Levant helps in defining appropriate strategies for building and using tree-ring chronologies to date and provenance wood from the southern Levant's many rich historical and archaeological sites.

The southern Levant was chosen as a study area, because it is on the periphery of the Mediterranean forest zone (Blondel and Aronson 1999) and is particularly

sensitive to changes in climate (Lindner et al. 2010; Lionello et al. 2006, 2008). The southern Levant also lacks forests with large volumes of high-quality timber resources. Consequently, during antiquity and more recent historical periods, it was necessary to supplement timber from native forests with imported wood from different forests in the Mediterranean and beyond, which can be dated and sourced using dendrochronological techniques. There are, therefore, multiple opportunities to use the tree-ring record to reveal new information about the rich environmental and cultural histories of this region, where dendrochronological research has thus far remained underdeveloped.

GEOGRAPHY OF THE STUDY REGION

Terminology

For the purposes of this study, the 'northern Levant' will be defined as the geographic area including modern Cyprus, the Mediterranean coast of southern Turkey, coastal Syria, northern Lebanon (i.e., the area including the Lebanon/Anti-Lebanon Mountains and the coastal strip above 34ºN latitude), and Mt. Hermon in the Golan Heights (Figure 1.1). The 'southern Levant' will be defined as the geographic area including present-day southern Lebanon (i.e., the coastal strip below 34ºN latitude), Israel/Palestine, the Eastern Highlands of Jordan, and the northern Sinai Peninsula.

This is somewhat broader than the traditional geographic boundaries of the Levant, but is meant to include areas in the south that have relict populations of Mediterranean vegetation (Cordova 2007; Danin 1999; El-Bana et al. 2010), and areas in both the north and south of the region that are in the Mediterranean climate zone

and (secondarily) with which the Levant *sensu stricto* had frequent cultural and economic contact (Horden and Purcell 2000). The dividing line between the 'northern' and 'southern' Levant is based on phytogeographic and topographic features, since the Lebanon/Anti-Lebanon chain marks the southern latitudinal limits of several Mediterranean forest species found in Blondel and Aronson's (1999) 'oro-, montane-, and supra- Mediterranean life zones' (e.g., *Cedrus libani*, *Quercus cerris*, *Juniperus excelsa*, and *Abies cilicica*) (Abi-Saleh and Safi 1998; Quézel and Médail 2003). The northern-southern Levantine boundary along the coastal plain roughly follows the latitude at which the ranges of *Pinus brutia* Ten. and *Pinus halepensis* Mill.–two common Mediterranean pine species (part of the 'thermo- and meso-Mediterranean' life zones)–overlap (Blondel and Aronson 1999; Quézel and Médail 2003; Talhouk et al. 2001). However, this boundary is tentative, because anthropogenic impacts (both deforestation and afforestation) have considerably altered the landscape and distributions of these species in particular (Blondel and Aronson 1999; Talhouk et al. 2001).

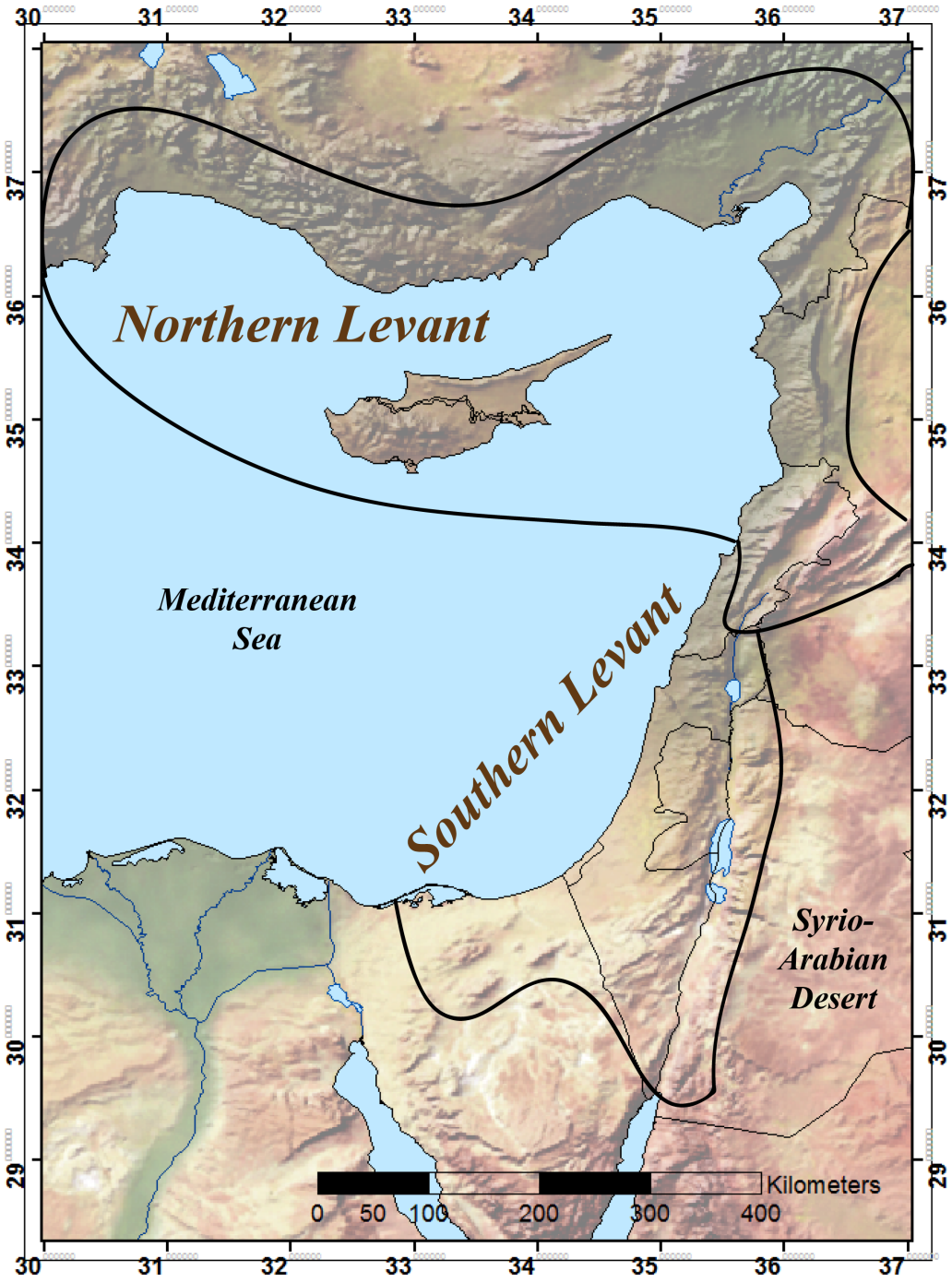

Figure 1.1. Geographic extent of the northern and southern Levant as defined in this study.

Physical setting

The southern Levant can be broadly divided into the following four longitudinal belts: the coastal plain, the Western Highlands, the Rift Valley, and the Eastern Highlands (adapted from: Cordova 2007; Zohary 1962) (Figure 1.2).

The low-lying coastal plain runs parallel to the Mediterranean and widens toward the south. Headlands and promontories often interrupt the coastline in the north, including Mt. Carmel and the Rosh HaNiqra cliffs in northern Israel and Ras al-Madfun and Ras el-Biyada in southern Lebanon (Flexer et al. 2005; Zohary 1973). Anthropogenic impacts in this area are particularly high, as the coastal plain has been subject to heavy cultivation and urban development (Talhouk et al. 2001; Zohary 1962).

The Western Highlands are an extension of a coastal mountain chain (including the Lebanon/Anti-Lebanon Mountains) that stretches from southeastern Turkey to the Sinai Peninsula. The highlands are comparatively lower in elevation than the coastal mountain chains further north; Mt. Meron in Israel is the highest peak at 1,208 meters a.s.l. The highlands are characterized by gentle western slopes and abrupt eastern slopes. Occasional valleys associated with secondary faults running perpendicular to the Rift Valley dissect the highlands and create flat latitudinal plains, including the Jezreel Valley in northern Israel (Flexer et al. 2005; Zohary 1973). The highlands curve to the southwest in the Sinai Peninsula and include three anticlines–Jebel Halal, Jebel Yelleq, and Jebel Maghara–oriented parallel to the northern Sinai's Mediterranean coast (Kusky and El-Baz 2000).

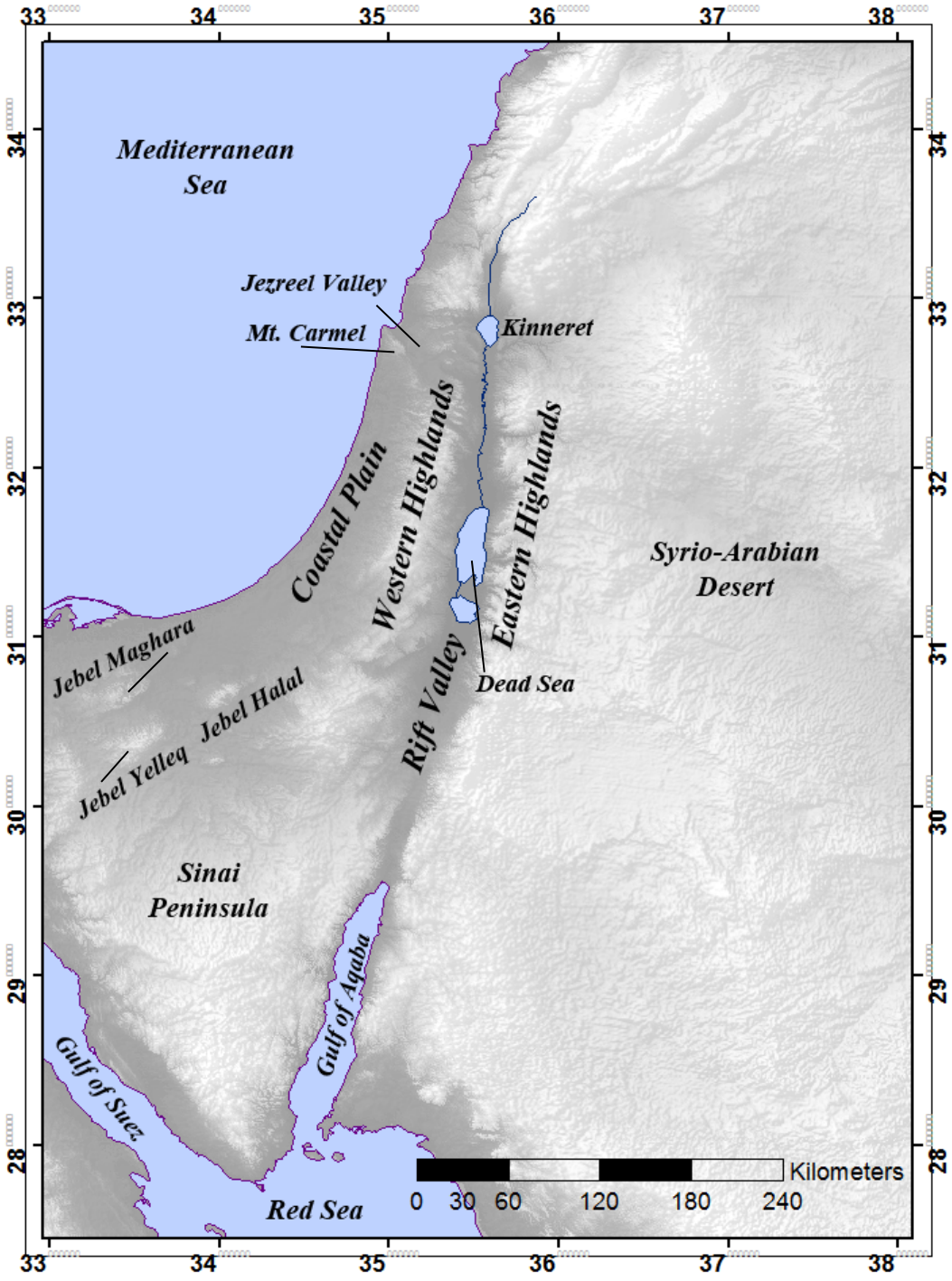

Figure 1.2. Physiographic units and features of the southern Levant.

The Rift Valley (which continues south into the Gulf of Aqaba and the Red Sea and to the northeast into Lebanon) is a series of steep-sided basins that includes the Kinneret (Sea of Galilee), Jordan River Valley, Wadi Araba, and the Aqaba Valley. It also includes the lowest terrestrial point on Earth in the Dead Sea basin (396 m below sea level) (Zohary 1973).

The Eastern Highlands consist of a series of raised plateaus, mountains, and other complex highland morphologies which run parallel to the Rift Valley, and which are dissected by a series of valleys and canyons through which the region's main perennial streams and wadis drain (Cordova 2007). The western slopes facing the Rift Valley form steep escarpments, while their eastern side slopes more gently into the Syrio-Arabian Desert. The highlands reach about 1,150 m a.s.l. in the north and about 1,500 m a.s.l. in the south, with a maximum height of 1,734 m a.s.l. at Jebel Ram in the south (Cordova 2007; Freiwan and Kadıoğlu 2008).

Climate

The southern Levant receives most of its annual precipitation during October through April. Precipitation primarily results from cold fronts associated with extratropical cyclones originating over the eastern Mediterranean (i.e., 'Cyprus lows') (Goldreich 2003). These cyclones generally move to the east and northeast, and (less frequently) to the southeast (Freiwan and Kadıoğlu 2008). Since the southern Levant is on the southern edge of the typical storm track for Cyprus lows, this means that even small variations in cyclone trajectories during the winter can have a large effect on the region's total annual rainfall. In contrast, summer months in the southern Levant are hot and completely dry with minimal cloud cover. This is because of

influence from a northward shift in the subtropical high and the Persian trough (a shallow, low-pressure trough that extends from the Asian monsoon depression

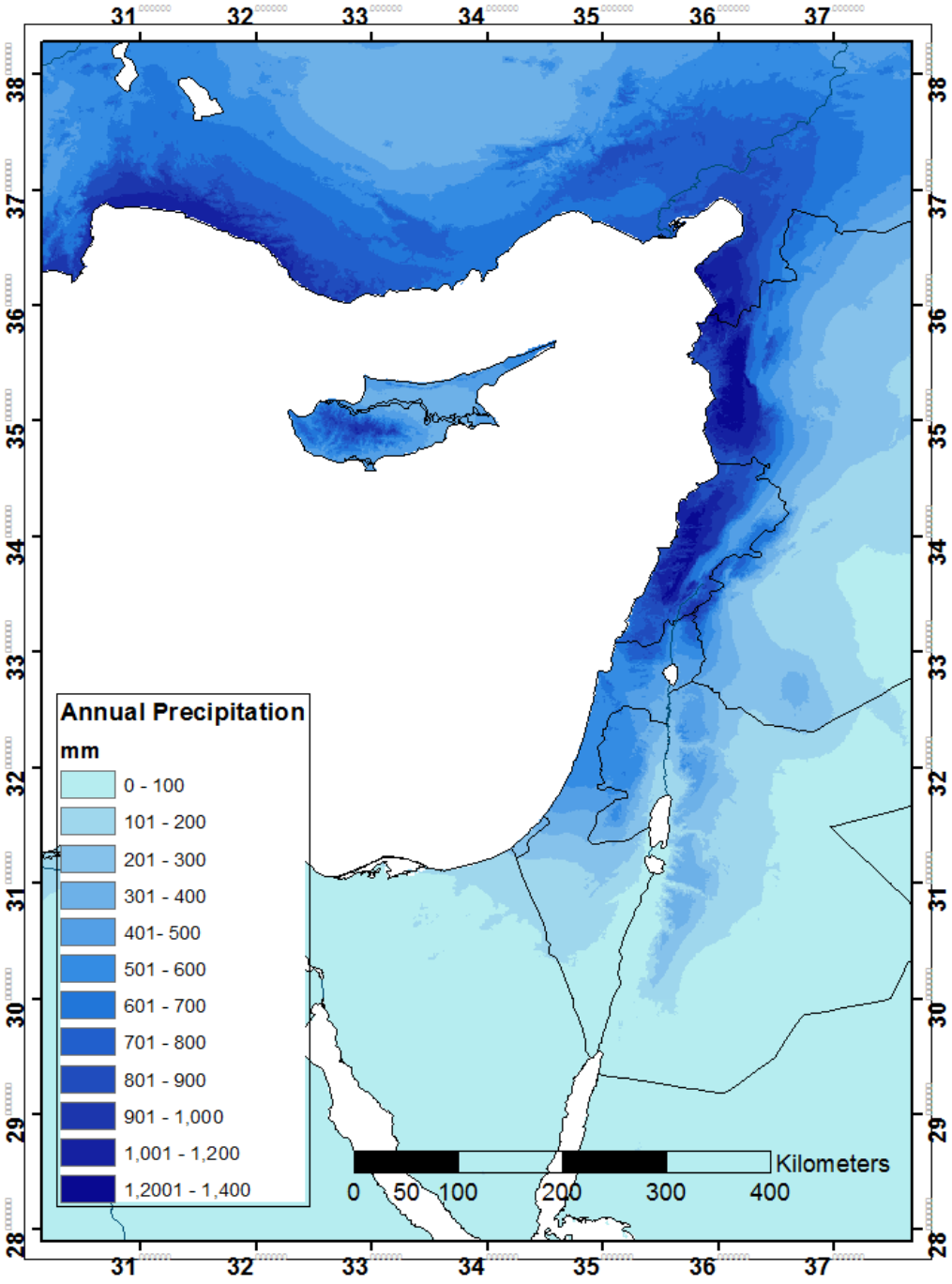

Figure 1.3. Average annual rainfall in the eastern Mediterranean (1950-2000) (adapted from the dataset of Hijmans et al. 2005).

centered over Pakistan), which leads to predominantly northwesterly winds in the eastern Mediterranean during summer (Price et al. 1999; Ziv et al. 2004).

Overall, average annual precipitation in the southern Levant decreases from north to south and west to east (Black et al. 2011; Freiwan and Kadıoğlu 2008; Goldreich 2003) (Figure 1.3). Precipitation declines from west to east with increasing distance from the Mediterranean Sea. The north-south contrast in precipitation results from differences in the trajectories of the winter frontal depressions (Black et al. 2011). When the primarily westerly winds from these systems bring moist air from the Mediterranean to the north, this causes precipitation; however, in the south, the same westerly systems bring dry desert air from the Sinai, causing little rain (Black et al. 2011; Freiwan and Kadıoğlu 2008).

Topography also influences the distribution of precipitation in the southern Levant. Because of orographic effects, higher elevation areas like Mt. Carmel, and the Western and Eastern Highlands receive greater precipitation. Conversely, the Rift Valley, which is in the rain shadow of the Western Highlands, is drier (Freiwan and Kadıoğlu; Goldreich 2003). Mean temperatures in the low-lying Rift Valley and coastal plain are also generally higher (Cordova 2007; Goldreich 2003).

REGIONAL PALEOENVIRONMENTAL AND PALEOCLIMATE RESEARCH

Researchers have conducted paleoclimatological and paleoecological studies in the Levant using a variety of proxies, including pollen (e.g., Baruch and Bottema 1999; Hajar et al. 2008, 2010; Kadosh et al. 2004; Rambeau 2010; Schwab et al. 2004; Yasuda et al. 2000); coral (Al-Rousan et al. 2007; Felis et al. 2000); speleothem (e.g.,

Almogi-Labin et al. 2009; Bar-Matthews et al. 1997; Verheyden et al. 2008); and sedimentary/geomorphological (e.g., Kadosh et al. 2004; Migowski et al. 2006) records. Other studies have used charred wood and pollen remains from archaeological sites (e.g., Baruch and Goring-Morris 1997; Hunt et al. 2007; Liphschitz 2007; Mithen et al. 2007), although such analysis requires careful sample selection strategies and consideration of sample context (Asouti and Austin 2005).

Multiple, comprehensive reviews (e.g., Cordova 2007; Finné et al. 2011; Rambeau 2010; Rambeau and Black 2011; Robinson et al. 2006; Rosen 2007) summarizing paleoenvironmental research in the southern Levant (and, more broadly, the eastern Mediterranean) have been written recently and are available elsewhere. These studies note that successful reconstruction of the southern Levant's paleoenvironmental history and human use of forest resources requires: i) improving the dating precision of various environmental and climate proxies; ii) improving the spatial coverage of paleoenvironmental studies, particularly in the region's more arid areas; and iii) determining the spatial extent over which paleoenvironmental proxy data may be used. Several recent studies (e.g., Finné et al. 2011; McCormick et al. 2013; Manning 2013, Riehl 2012) emphasize that understanding societal response to climate and human impact on the Mediterranean environment requires using proxy data that provides paleoenvironmental information on a local scale at high temporal (i.e., decadal and sub-decadal) resolution, particularly because of the great climatological and environmental variability in the region.

DENDROCHRONOLOGY AND ITS RESEARCH APPLICATIONS

Dendrochronological Principles

Dendrochronology, or tree-ring dating, is a valuable tool for ecological, climatological, and archaeological research, because it provides paleoenvironmental proxy data and dates for when a tree was cut at an annual (and, in some cases, seasonal) resolution. Several comprehensive reviews are available describing basic dendrochronological principles and applications (e.g., Baillie 1982; Cook and Kairiukstis 1990; Fritts 1976; Hughes et al. 2011; Schweingruber 1989, 1996), so only a brief description is given here.

Dendrochronological research is possible, because trees growing in the same forest area grow an overall similar annual sequence of wide and narrow rings in response to common climatic and ecological conditions. A tree's ring-widths can be measured to build a time series of consecutive annual tree-ring widths that are each assigned to the year in which they were formed. The tree's outermost ring (below the bark and vascular cambium) dates to the year in which the tree was cut down or sampled. Tree-ring measurement sequences from the same site can therefore be synchronized ('crossdated') and averaged together to build a site chronology that is representative of the overall year-to-year growth conditions at a site. Site chronologies from the same geographic area and experiencing common climatic and ecological conditions (and therefore having similar ring-width patterns) can be synchronized and averaged together to build regional chronologies.

Dendrochronological dating and provenancing

The ring-widths of wood from historical, archaeological, and paleoenvironmental sites can be measured and their year-to-year ring-widths crossdated with sequences sampled from timbers of the same species to build a site chronology of relatively dated samples. Site chronologies can then be crossdated against absolutely dated reference chronologies that include modern samples. If the historical, archaeological, or paleoenvironmental wood includes either the tree's bark or vascular cambium, the precise year (and sometime season) in which the tree was cut can be determined. If these anatomical features are not present, then the date of the sample's last extant ring is a precise *terminus post quem* for the tree's cutting date. These older, dendrochronologically dated timbers can then be incorporated into reference chronologies, thereby extending the region's tree-ring record further back in time beyond the earliest chronological extent of modern forest samples.

With a large network of available tree-ring datasets, regional chronologies from known geographic areas can be compared and divided into zones with tree-ring patterns unique to a specific region (e.g., Haneca et al. 2005). These regional reference chronologies can then be used to identify the forest area from which historical and archaeological timbers were cut. With this technique, called 'dendroprovenancing' (Bonde et al. 1997), tree-ring chronologies built from historical or archaeological timbers (whose origin is unknown) are compared with reference chronologies from known sites in different regional zones. The timber's likely area of origin can be identified when there is significant correlation with a group of site chronologies clustered in the same geographic area/dendrochronological zone. The

origin is estimated to be closest to the area where correlation with the site chronology is highest. The historical and archaeological tree-ring chronologies can then be incorporated into regional chronologies to extend them further back in time, although one must carefully assess whether a site chronology has a clear match with the tree-rings from one geographic area before doing so (Bridge 2012; Eckstein and Wrobel 2007; Haneca et al. 2005).

This method is advantageous, in that unlike other provenancing methods, such as wood DNA (e.g., Dumlin-Lapègue et al. 1999) and isotope analyses (e.g., English et al. 2001; Kagawa and Leavitt 2010; Rich et al. 2012), tree-ring dendroprovenancing is relatively inexpensive and does not destroy the wood. Dendroprovenancing methods have been used successfully in northern Europe to reconstruct timber trade and changes in forest usage between the Baltic States and the Low Countries, United Kingdom (Eckstein et al. 1986; Haneca et al. 2005; Ważny 2002), and Scandinavia (Daly 2007), as well as in Germany (Eißing and Dittmar 2011). These methods are now being applied in the eastern Mediterranean (Ważny 2011a). Further development of complementary provenancing research using $^{87}Sr/^{86}Sr$ ratios in wood (e.g., Rich et al. 2012) may provide an independent technique for corroborating the forest sources of Mediterranean wood that have been identified using tree-ring based dendroprovenancing methods.

Dendroclimatology

Since trees respond to certain climate parameters (e.g., precipitation or temperature) during their growing season, which is reflected in their annual ring width, the overall year-to-year ring-width variability in the tree-ring chronologies can

be used as a high resolution proxy to reconstruct past climate conditions predating modern meteorological records (Fritts 1976; Hughes et al. 2011). Multi-millennial tree-ring chronologies that are sensitive to climate have already been used in other regions, such as central Europe (Büntgen et al. 2013, 2011), central Asia (D'Arrigo et al. 2001), southeast Asia (Cook et al. 2010), and the southwest United States (Dean 1996) to reconstruct long-term paleoclimatic and paleoenvironmental conditions. Researchers have then compared these high-resolution paleoclimate records with local and regional archaeological/historical records to analyze interactions between humans and their environment and climate.

Year-to-year and intra-year variations in tree-ring stable isotope ratios, particularly in stable carbon ($\delta^{13}C$), oxygen ($\delta^{18}O$), and hydrogen (δD) isotopic ratios of tree-ring cellulose, can also be used as proxies to reconstruct climatic variables (for a review of stable isotope dendroclimatology, see: McCarroll and Loader 2004). Stable isotope proxy data may also allow reconstruction of climatic variables that do not have a strong relationship with radial tree growth (i.e., tree-ring width). Investigation of the climatic signals recorded in tree-ring stable isotope chronologies, as well as climate reconstructions from the data, have begun relatively recently in the East Mediterranean by Mutlu et al. (2011) and Heinrich et al. (2013).

Dendrochronological Sampling Criteria

While the specific criteria for samples most suited for dendrochronological analysis varies depending on the specific research project (e.g., dendroclimatological vs. archaeological studies), in order to be used for traditional, tree-ring width-based dendrochronological analysis, wood samples must have the following: i) clearly

visible ring boundaries; ii) single, annually produced tree-rings; and iii) a year-to-year ring pattern that will crossdate with those of other trees, in order to build chronologies.

For limited, within-site studies, trees need to crossdate only with other trees within the same stand, but for regional climate and environmental studies, and especially for archaeological dating, tree-ring sequences should have a common year-to-year growth pattern with, and be able to crossdate with, tree-ring chronologies from other sites in a given region. Correlation strength and the distance over which tree-ring chronologies can crossdate varies, due to several variables controlling tree-ring growth, including species physiology, ecological amplitude, and phenotypic plasticity. Abiotic factors like regional geography, climate regimes and large-scale circulation patterns, and physical and chemical properties of an area's bedrock and soils may also play an important role (Schweingruber 1996).

Trees that are responsive ('sensitive') to year-to-year changes in climate and environmental conditions, creating variable year-to-year ring-widths, are best suited for dendrochronological dating and climate studies. Sites and samples experiencing minimal anthropogenic disturbance and impacts (e.g., areas where pruning, watering, terracing, and grazing are absent to minimal) should also be selected, since these activities create localized variation ('noise') in the sample ring-width pattern, which can make successful crossdating more difficult, and sometimes impossible. Long-lived tree species and chronologies (≥ 50–100 rings) are required for climate and environmental reconstructions, and successful dating, since they provide a longer growth pattern record that can extend reconstructions further back in time, and that

can be compared visually and statistically against reference chronologies for a more secure crossmatch and dendrochronological date.

Dendrochronological Research in the Southern Levant

A vast database of modern and historical/archaeological tree-ring chronologies has been created for the northern Levant and the Aegean for dating historical/archaeological wood (e.g., Kuniholm 2000a; Kuniholm and Striker 1987; Kuniholm et al. 2007; Pearson et al. 2012; Ważny 2011a) and paleoclimate reconstruction (e.g., Akkemik and Aras 2005; Chalabi et al. 1981; D'Arrigo and Cullen 2001; Griggs et al. 2007, 2013; Heinrich et al. 2013; Hughes et al. 2001; Köse et al. 2011; Mutlu et al. 2011; Touchan et al. 2005, 2007, 2014a, b). However, dendrochronological research in the southern Levant is still largely on *terra nova*.

There are, to date, only two published dendroclimatological studies (both from the same research project) from the southern Levant (Touchan and Hughes 1999; Touchan et al. 1999) that have used more recent and statistically robust methods of chronology building, standardization, and modeling tree-ring climate response (e.g., Cook 2006, 1985; Cook and Peters 1997; Osborne et al. 1997). Unfortunately, with the exception of Touchan and Hughes (1999) and Touchan et al.'s (1999) studies, the tree-ring measurement data from previous studies has also not been published or archived, and thus these datasets (and in some cases, also the physical samples) have been lost and cannot be re-examined more closely.

Earlier studies comparing tree-ring and climate in the southern Levant (e.g., Felix 1968; Kaplan 1984; Lev-Yadun et al. 1981; Liphschitz 2007: 145–152 and references contained therein; Liphschitz and Waisel 1967) usually focused on tree-ring

growth at a single site (or closely adjacent sites). Studies that did compare tree-ring chronologies from multiple sites and their climate responses did so using only visual comparison (e.g., Gindel 1944; Tamari 1976; Waisel and Liphschitz 1968). Liphschitz and Mendel (1987) compared tree-ring growth in different species at the same site by comparing their correlations with seasonal rainfall and calculated the Pearson correlation coefficient between the two chronologies. Still, inter-site correlation values were not calculated. Time periods of relative narrow or wide ring growth were compared using chronologies built from several different species sampled from multiple sites at a wider scale in the eastern Mediterranean by visually comparing the tree-ring curves (e.g., Tamari 1976; Waisel and Liphschitz 1968). However, in some cases, these observed growth trends may be the result of local stand dynamics or the standardization curves used for these chronologies.

The southern Levant's regional tree-ring teleconnections or heteroconnections (that is: correlation between tree-ring chronologies from different species) have therefore not been investigated with a robust, well-replicated multi-site tree-ring network. Regional teleconnections at wider scales, particularly between the northern and southern Levant, also have not been systematically investigated.

Previous dendrochronological and paleoethnobotanical research of the southern Levant's numerous historical and archaeological sites demonstrates the vast potential for applying dendrochronological and dendroprovenancing techniques. In particular, Liphschitz's (2007, and the references contained therein) work in identifying wood species at numerous archaeological and historical sites in Israel has highlighted use of both native and imported wood species that might be dated and provenanced using

dendrochronology. Unfortunately, only in rare instances (e.g., Biger and Liphschitz 1993; Liphschitz and Biger 1988; Liphschitz et al. 1996) were historical tree-ring chronologies built and successfully crossdated to obtain an absolute date for the timber, and all of these studies analyzed either imported European or American tree species. In contrast, while tree-ring chronologies of Mediterranean species have been built from historical and archaeological timbers from sites in the southern Levant, they have all been 'floating chonologies' that have not been crossdated with reference chronologies to obtain an absolute date (Liphschitz 2007: 154–164, and references contained therein). These chronologies have remained either only relatively dated, or absolutely dated by obtaining single radiocarbon dates from the samples (e.g., Liphschitz 2007: 154–164), which is considerably less precise than dendrochronological dating.

Both Liphschitz (2007) and Lev-Yadun (2008) note that in the southern Levant (and in drier areas bordering the northern Levant), there are fewer native tree species that are long-lived and produce clear annual growth rings. They also note that the region generally lacks high-quality building timber. Consequently, timber was used more sparingly in building construction, or (in special cases) imported, and wood was often re-used during antiquity. This has meant that there are fewer timber remains that are suitable for dendrochronological analysis in the southern Levant than in the northern Levant and the Aegean. Therefore, they argue that there are fewer opportunities to date historical and archaeological material using dendrochronology, and it is more difficult to build long reference chronologies of species native to the southern Levant that might also be used in dendroclimatological reconstructions.

Liphschitz (2007) goes on to argue that it is difficult to build master reference chronologies for Israel and the southern Levant, because many tree species have asymmetric growth or produce false growth rings, and therefore cannot be crossdated. She also argues that historical timber sections often cannot be sampled for dendrochronological dating, since they are supporting building roofs. Imported timbers, she also argues, have an unknown origin that limits successful crossdating, and reference chronologies from the eastern Mediterranean (e.g., Turkey, Lebanon, and Cyprus) for dating imported timbers are unreliable.

It is beyond the scope of this work to discuss the issues that Liphchitz (2007: 161–164) raises regarding the reliability of East Mediterranean reference chronologies, and they have been addressed elsewhere (Griggs and Manning 2009; Kuniholm et al. 2011; Manning et al. 2001, 2003, 2009, 2010, 2011). Careful sample selection, adequate sample size, preparation of samples, and careful sample crossdating that uses a combination of visual assessment and statistical methods (including those used in the program COFECHA, which specifically assesses the quality of crossmatching and likelihood of locally absent rings within a chronology) (Holmes 1983) help address many of the difficulties in building modern reference chronologies that Liphschitz (2007) describes. Additionally, when it is required, historical samples, including roof timbers and decorated woodwork, can be sampled using minimally destructive methods, such as drilling cores, *in situ* measurement, and extremely high-resolution scanning and digital photography (for a few successful examples, see: Bernabei and Bontadi 2012; Bill et al. 2012; Haneca et al. 2009; Kuniholm 2000a,b; Ważny 2011b). Careful consideration of available historical and

archaeological data and sample context can help identify possible signs of timber re-use when interpreting dendrochronological dates.

Imported timbers with unclear origins present an excellent opportunity for dendroprovenancing analysis. Historical and archaeological data can also be used in tandem with botanical data to deduce the imported timbers' possible origins and select tree-ring reference chronologies that will most likely date samples successfully. Access to a wide network of tree-ring reference chronologies–including those from modern and historical material–from multiple sites throughout the Mediterranean and Europe (and not only one country) is critical for successfully carrying out dating and provenancing analyses. The development of online databases, such as the Digital Collaboratory for Cultural Dendrochronology (DCCD) (Jansma et al. 2012a) and International Tree-Ring Data Bank (http://www.ncdc.noaa.gov/paleo/treering.html), as well as the standardization of sample data and metadata (Jansma et al. 2012b) have improved access to a vast network of tree-ring reference chronologies and provide a means of archiving previous research results in a standardized format. Consequently, these recent advances have opened up new possibilities and improved the ability to build, analyze, and use a large database of modern and ancient tree-ring networks, including those from the southern Levant.

PROJECT OBJECTIVES

The aim of this work is to examine tree-ring variability in the Levant at multiple spatial scales, in order to provide an organized framework for developing further dendrochronological research in the southern Levant. My overall objectives are to:

- Determine if there is a coherent signal in tree-ring chronologies for the Mediterranean forest zone of the southern Levant, which will allow crossdating between sites and between tree-ring chronologies from archaeological/historical sites and reference chronologies.
- Delineate the boundaries between regional dendrochronological zones in the southern Levant and between the northern and southern Levant, in order to determine the spatial scale over which historical/archaeological samples may be provenanced.
- Compare tree-ring responses to climate in chronologies from a network of forest sites sampled along the Mediterranean forest ecological gradients in the southern Levant, in order to identify sites that are especially sensitive to climate and the distance over which trees have a common climate response.
- Apply dendrochronological dating and provenancing techniques to historical material sampled from sites in the southern Levant, in order to build up the database of dendrochronologically dated and provenanced materials in the region and demonstrate this method's potential in reconstructing broader regional timber trade and environmental histories.

I use the results from the following four chapters to argue that the development of tree-ring chronologies for the southern Levant for both paleoenvironmental and archaeological research requires that the tree-ring data be analyzed and considered over multiple spatial scales. Other paleoclimate proxies and other tree-ring datasets from the eastern Mediterranean can provide paleoenvironmental data over broader temporal and regional scales. However, obtaining tree-ring data that is representative

of the southern Levant's local bioclimatic conditions is critical, particularly for considering the effects that climatic fluctuations have had on human populations in an area that is located at the margins of where rain-fed agriculture is possible (Rosen 2007) and at the limits of the Mediterranean forest ecosystem. Fine-scale, as well as regional, comparisons of tree-ring growth across the region's ecological gradients also identify variations in significant limiting factors that affect other vegetation, including crops and forest timbers that have provided important ecosystem services to the region's human inhabitants.

Dendrochronological dating and provenancing applications should also analyze wood samples from the southern Levant's historical and archaeological sites within a multi-scale research framework. I propose a two-pronged strategy, in which separate reference chronologies specifically for the southern Levant are built from native species that are suitable for dendrochronology. Nonnative, imported timbers may be crossdated and provenanced using pre-existing chronologies from the northern Levant (and in some cases, Europe) and additional chronologies built from sites located along both spatial and altitudinal gradients.

Building a dense tree-ring network for the Levant along the region's bioclimatological gradients is a large, long-term research undertaking. However, it is also a necessary task, so that the tree-ring record adequately represents the diverse mosaic of phytogeographical and bioclimatic zones present in the Levant's forest ecosystems.

REFERENCES

Abi-Saleh, B., Safi, S., 1998. Carte de la vegatation du Liban. *Ecologia Mediterranea* XIV (1/2): 123–141.

Akkemik, Ü., Aras, A., 2005. Reconstruction (1689–1994) of April–August precipitation in southwestern part of central Turkey. *International Journal of Climatology* 28: 173–183.

Al-Eisawi, D., 1985. Vegetation in Jordan. In: Hadidi, A. (Ed.), *Studies in the History and Archaeology of Jordan 2*. Department of Antiquities of Jordan, Amman, pp. 81–93.

Almogi-Labin, A., Bar-Mathhews, M., Shriki, D., Kolosovsky, E., Paterne, M., Schilman, B., Ayalon, A., Aizenshtat, Z., Matthews, A., 2009. Climatic variability during the last ~90 ka of the southern and northern Levantine Basin as evident from marine records and speleothems. *Quaternary Science Reviews* 28: 2882–2896.

Al-Rousan, S., Felis, T., Manasrah, R., Al-Horani, F., 2007. Seasonal variations in the stable oxygen isotopic composition in *Porites* corals from the northern Gulf of Aqaba, Red Sea. *Geochemical Journal* 41: 333–340.

Asouti, E., Austin, P., 2005. Reconstructing woodland vegetation and its exploitation by past societies based on the analysis and interpretation of archaeological wood charcoal macro-remains. *Environmental Archaeology* 10: 1–18.

Baillie, M.G.L., 1989. *Tree-Ring Dating and Archaeology*. University of Chicago Press, Chicago.

Bar-Matthews, M., Ayalon, A., Kaufman, A., 1997. Late Quaternary paleoclimate in the eastern Mediterranean region from stable isotope analysis of speleothems at Soreq cave, Israel. *Quaternary Research* 47: 155–168.

Baruch, U., Bottema, S., 1999. A new pollen diagram from Lake Hula. In: Kawanabe, H., Coulter, G.W., Roosevelt, A.C. (Eds.), *Ancient Lakes: Their Cultural and Biological Diversity*. Kenobi Productions, Ghent, pp. 75–86.

Baruch, U., Goring-Morris, N., 1997. The arboreal vegetation of the Central Negev Highlands, Israel, at the end of the Pleistocene: evidence from archaeological charred wood remains. *Vegetation History and Archaeobotany* 6: 249–259.

Bernabei, M., Bontadi, J., 2012. Dendrochronological analysis of the timber structure of the Church of the Nativity in Bethlehem. *Journal of Cultural Heritage* 13 (4) supplement: e54–e60.

Biger, G., Liphschitz, N., 1993. Tree ring research of the 19th century American constructions in Israel. *Dendrochronologia* 11:139–150.

Bill, J., Daly, A., Johnsen, Ø., Dalen, K.S., 2012. DendroCT– Dendrochronology without damage. *Dendrochronologia* 30: 223–230.

Black, E., Hoskins, B., Slingo, J., Brayshaw, D., 2011. The present-day climate of the Middle East. In: Mithen, S., Black, E. (Eds.), *Water, Life and Civilisation: Climate, Environment and Society in the Jordan Valley*. Cambridge University Press, Cambridge, pp. 13–24.

Blondel, J., Aronson, J., 1999. *Biology and Wildlife of the Mediterranean Region*. Oxford University Press, New York.

Bonde, N., Tyers, I., Ważny, T., 1997. Where does timber come from? Dendrochronological evidence of timber trade in northern Europe. In: Sinclair, A., Slater, E., Gowlett, J. (Eds.), *Archaeological Science 1995*. Oxbow, Oxford, pp. 201–204.

Bridge, M., 2012. Locating the origins of wood resources: a review of dendroprovenancing. *Journal of Archaeological Science* 39: 2828–2834.

Broodbank, C., 2013. *The Making of the Middle Sea: A History of the Mediterranean from the Beginning to the Emergence of the Classical World*. Thames and Hudson, London.

Büntgen, U., Kyncl, T., Ginzler, C., Jacks, D.S., Esper, J., Tegel, W., Heussner, K.U., 2013. Filling the Eastern European gap in millennium-long temperature reconstructions. *Proceedings of the National Academy of Sciences* 110 (5): 1773–1778.

Büntgen, U., Tegel, W., Nicolussi, K., McCormick, M., Frank, D., Trouet, V., Kaplan, J.O., Herzig, F., Heussner, K.U., Wanner, H., Luterbacher, J., Esper, J., 2011. 2500 years of European climate variability and human susceptibility. *Science* 331: 578–582.

Chalabi, M.N., Serre-Bachet, F., 1981. Analyse dendroclimatologique de deux stations syriennes de *Quercus cerris* ssp. *pseudocerris*. *Ecologia Mediterranea* 7 (1): 3–21.

Cook, E.R., Anchukaitis, K.J., Buckley, B.M., D'Arrigo, R.D., Jacoby, G.C., Wright, W.E., 2010. Asian monsoon failure and megadrought during the last millennium. *Science* 328: 486–489.

Cook, E.R., and Kairiukstis, L.A. (Eds.), 1990. *Methods of Dendrochronology*. Kluwer Academic Publishers, Dordrecht.

Cordova, C.E., 2007. *Millennial Landscape Change in Jordan: Geoarchaeology and Cultural Ecology*. University of Arizona Press, Tucson.

D'Arrigo, R., Cullen, H.M., 2001. A 350-year (AD 1628–1980) reconstruction of Turkish precipitation. *Dendrochronologia* 19: 169–177.

D'Arrigo, R., Jacoby, G., Frank, D., Pederson, N., Cook, E., Buckley, B., Baatarbileg, N., Mijiddorj, R., Dugarjav, C., 2001. 1738 years of Mongolian temperature variability inferred from a tree-ring width chronology of Siberian pine. *Geophysical Research Letters* 28 (3): 543–546.

Daly, A., 2007. *Timber, Trade, and Tree-Rings.* Unpublished Ph.D. dissertation, University of Southern Denmark, Odense.

Dean, J.S., 1996. Dendrochronology and the study of human behavior. In: Dean, J.S., Meko, D.M., Swetnam, T.W. (Eds.), *Tree Rings, Environment and Humanity: Proceedings of the International Conference, Tucson, AZ, 17–21 May 1994*. Radiocarbon, Tucson, pp. 461–469.

Dumlin-Lapègue, S., Pemonge, M.H., Gielly, L., Taberlet, P., Petit, R.J., 1999. Amplification of oak DNA from ancient and modern wood. *Molecular Ecology* 8: 2137–2140.

Eckstein, D., Ważny, T., Bauch, J., Klein, P., 1986. New evidence for the dendrochronological dating of Netherlandish paintings. *Nature* 320 (3): 465–466.

Eckstein, D., Wrobel, S., 2007. Dendrochronological proof of origin of historic timber–retrospect and perspectives. In: Haneca, K., Verheyden, A., Beeckman, H., Gärtner, H., Helle, G., Schleswer, G. (Eds.), *Proceedings of the Symposium on Tree Rings in Archaeology, Climatology, and Ecology, April 20–22, 2006.* Vol. 5. Tervuren, pp. 8–20.

Eißing, T., Dittmar, C., 2011. Timber transport and dendro-provenancing in Thuringia and Bavaria. In: Fraiture, P. (Ed.), *Tree Rings, Art, and Archaeology*. Proceedings of the Conference, Royal Institute for Cultural Heritage, Brussels, 10–12th February 2010. Scientia artis collection, Brussels, pp. 137–149.

English, N., Betancourt, J., Dean, J., Quade, J., 2001. Strontium isotopes reveal distant sources of architectural timber in Chaco Canyon, New Mexico. *Proceedings of the National Academy of Sciences* 98: 11891–11896.

Felis, T., Pätzold, J., Loya, Y., Fine, M., Nawar, A.H., Wefer, G., 2000. A coral oxygen isotope record from the northern Red Sea documenting NAO, ENSO, and North Pacific teleconnections on Middle East climate variability since the year 1750. *Paleoceanography* 15 (6): 679–694.

Felix, Y., 1968. Trees and wood in the Golan. *Teva ve'Aretz* 10: 168–178. (Hebrew)

Finné, M., Holmgren, K., Sundqvist, H.S., Weiberg, E., Lindblom, M., 2011. Climate in the eastern Mediterranean and adjacent regions, during the past 6000 years–a review. *Journal of Archaeological Science* 38: 3153–3173.

Flexer, A., Hirsch, F., Hall, J.K., 2005. Israel: Introduction. In: Hall, J.K., Krasheninnikov, V.A., Hirsch, F., Benjamini, C., Flexer, A. (Eds.), *Geological Framework of the Levant, Volume 2: The Levantine Basin and Israel*. vol. 2. Historical Productions-Hall, Jerusalem, pp. 215–268.

Freiwan, M., Kadıoğlu, M., 2008. Spatial and temporal analysis of climatological data in Jordan. *International Journal of Climatology* 28: 521–535.

Fritts, H.C., 1976. *Tree Rings and Climate*. Laboratory of Tree-Ring Research, University of Arizona: Tucson.

Gindel, J., 1944. Aleppo pine as a medium for tree-ring analysis. *Tree-Ring Bulletin* 11 (1): 6–8.

Goldreich, Y., 2003. *The Climate of Israel: Observation, Research, and Application.* Kluwer Academic Publishers, New York.

Gophna, R., Liphschitz, N., 1996. Ashkelon trough settlements in the Early Bronze Age I: new evidence of maritime trade. *Tel Aviv* 23: 143-153.

Griggs, C.B., Pearson, C.L., Manning, S.W., Lorentzen, B., 2013. A 250-year annual precipitation reconstruction and drought assessment for Cyprus from *Pinus brutia* (Ten.) tree-rings. *International Journal of Climatology* 34: 2702–2714.

Griggs, C.B., DeGaetano, A.T., Kuniholm, P.I., Newton, M.W., 2007. A regional reconstruction of May-June precipitation in the north Aegean from oak tree-rings, AD 1089–1989. *International Journal of Climatology* **27**: 1075–1089.

Griggs, C.B., Manning, S.W., 2009. A reappraisal of the dendrochronology and dating of Tille Höyük (1993). *Radiocarbon* 51: 711–720.

Hajar, L., Haïdar-Boustani, M., Khater, C., Cheddadi, R., 2010. Environmental changes in Lebanon during the Holocene: Man vs. climate impacts. *Journal of Arid Environments* 74: 746–755.

Hajar, L., Khater, C., Cheddadi, R., 2008. Vegetation changes during the Late Pleistocene and Holocene in Lebanon: a pollen record from the Bekaa Valley. *The Holocene* 18 (7): 1089–1099.

Haneca, K., Čufar, K., Beeckman, H., 2009 Oaks, tree-rings and wooden cultural heritage: a review of the main characteristics and applications of oak dendrochronology in Europe. *Journal of Archaeological Science* 36: 1–11.

Haneca, K., Ważny, T., Van Acker, J., Beeckman, H., 2005. Provenancing Baltic timber from art historical objects: success and limitations. *Journal of Archaeological Science* 32: 261–271.

Heinrich, I., Touchan, R., Dorado Liñán, I., Vos, H., Helle, G., 2013. Winter-to-spring temperature dynamics in Turkey derived from tree rings since AD 1125. *Climate Dynamics* 41: 1685–1701.

Hijmans, R.J., Cameron, S.E., Parra, J.L., Jones, P.G., Jarvis, A., 2005. Very high resolution interpolated climate surfaces for global land areas. *International Journal of Climatology* 25: 1965–1978.

Holmes, R.L., 1983. Computer-assisted quality control in tree-ring dating and measurement. *Tree-Ring Bulletin* 43: 69–78.

Hordon, P., Purcell, N., 2000. *The Corrupting Sea: A Study of Mediterranean History*. Blackwell Publishers, Oxford.

Hughes, M.K., Kuniholm, P.I., Eischeid, J.K., Garfin, G., 2001. Aegean tree-ring signature years explained. *Tree-Ring Research* 57 (1): 67–73.

Hughes, M.K., Swetnam, T.W., Diaz, H.F. (Eds.), 2011. *Dendroclimatology: Progress and Prospects*. Developments in Paleoenvironmental Research, vol. 11. Springer, Dordrecht.

Hunt, C.O., Gilbertson, D.D., El-Rishi, H.A., 2007. An 8000-year history of landscape, climate, and copper exploitation in the Middle East: the Wadi Faynan and the Wadi Dana National Reserve in southern Jordan. *Journal of Archaeological Science* 34: 1306–1338.

Jansma, E., Van Lanen, R.J., Brewer, P.W., Kramer, R., 2012a. The DCCD: a digital data infrastructure for tree-ring research. *Dendrochronologia* 30: 249–251.

Jansma, E., Van Lanen, R., Sturgeon, K., Mohlke, S., Brewer, P.W., 2012b. TRiDaBASE: A stand-alone database for storage, analysis and exchange of dendrochronological metadata. *Dendrochronologia* 30: 209–211.

Kadosh, D., Sivan, D., Kutiel, H., Weinstein-Evron, M., 2004. A Late Quaternary paleoenvironmental sequence from Dor, Carmel Coastal Plain, Israel. *Palynology* 28: 143–157.

Kagawa, A., Leavitt, S.W., 2010. Stable carbon isotopes of tree rings as a tool to pinpoint the geographic origin of timber. *Journal of Wood Science* 56: 175–183.

Köse, N., Akkemik, Ü., Dalfes, H.N., Özeren, M.S., 2011. Tree-ring reconstructions of May–June precipitation for western Anatolia. *Quaternary Research* 75 (3): 438–450.

Kuniholm, P.I., 2000a. Dendrochronologically dated Ottoman monuments. In: Baram, U., Carroll, L. (Eds.), *A Historical Archaeology of the Ottoman Empire: Breaking New Ground*. Plenum Press, New York, pp. 93–136.

Kuniholm, P.I., 2000b. Dendrochronology (tree-ring dating) of panel paintings. In: Taft, S.W., Mayer, J.W. (Eds.), *The Science of Paintings*. Springer Verlag, New York, pp. 206–215.

Kuniholm, P.I., Griggs, C.B., Newton, M.W., 2007. Evidence for early timber trade in the Mediterranean. In: Belke, K., Kislinger, E., Küler, A., Stassinopoulou, M.A. (Eds.), *Byzantina Mediterranea: Festschrift für Johannes Koder zum 65. Geburtstag*. Böhlau Verlag, Vienna, pp. 365–385.

Kuniholm, P.I., Newton, M.W., Liebhart, R.F., 2011. Dendrochronology at Gordion. In: Rose, C.B., Darbyshire, G. (Eds.), *The New Chronology at Iron Age Gordion*. Gordion special studies 6. University of Pennsylvania Museum of Archaeology and Anthropology, Philadelphia, pp. 79–122.

Kuniholm, P.I., Striker, C.L., 1987. Dendrochronological investigations in the Aegean and neighboring regions, 1983–1986. *Journal of Field Archaeology* 14: 385–398.

Kusky, T., El-Baz, F., 2000. Neotectonics and fluvial geomorphology of the northern Sinai Peninsula. *Journal of African Earth Sciences* 31 (2): 213–215.

Lev-Yadun, S., 2008. Wood remains from archaeological excavations: A review with a Near Eastern perspective. *Israel Journal of Earth Sciences* 56: 139–162.

Lindner, M., Maroschek, M., Netherer, S., Kremer, A., Barbati, A., Garcia-Gonzalo, J., Seidl, R., Delzon, S., Corona, P., Kolström, M., Lexer, M.J., Marchetti, M., 2010. Climate change impacts, adaptive capacity, and vulnerability of European ecosystems. *Forest Ecology and Management* 259: 698–709.

Lionello, P., Malanotte-Rizzoli, P., Boscolo, T., Alpert, P., Artale, V., Li, L., Luterbacher, J., May, W., Trigo, R., Tsimplis, M., Ulbrich, U., Xoplaki, E., 2006. The Mediterranean climate: an overview of the main characteristics and issues. In: Lionello, P., Malanotte-Rizzoli, P., Boscolo, R. (Eds.), *Mediterranean Climate Variability*. Elsevier, Amsterdam, pp. 1–27.

Lionello, P., Platon, S., Rodó, X., 2008. Preface: Trends and climate change in the Mediterranean region. *Global and Planetary Change* 63: 87–89.

Liphschitz, N., 2007. *Timber in Ancient Israel: Dendroarchaeology and Dendrochronology*. Monograph Series of the Institute of Archaeology of Tel Aviv University, 26. Emery and Claire Yass Publications in Archaeology, Tel Aviv.

Liphschitz, N., 1986. Overview of the dendrochronology and dendroarchaeology in Israel. *Dendrochronologia* 4: 37–58.

Liphschitz, N., Biger, G., 1988. Identification of timber and dating of historical buildings in Eretz Israel (Palestine), by dendrochronological methods. *Dendrochronologia* 6: 99–110.

Liphschitz, N., Mendel, Z., 1987. Comparative radial growth of *Pinus halepensis* Mill. and *Pinus brutia* in Israel. *Forêt Méditerranéenne* 9 (2): 115–117.

Liphschitz, N., Waisel, Y., 1967. Dendrochronological studies in Israel. *Quercus boissieri* of Mt. Meron. *La-Yaaran* 17: 78-90, 111–115. (Hebrew with English summary)

Manning, S.W., 2013. The Roman world and climate: context, relevance of climate change, and some issues. In: Harris, W.V. (Ed.), *The Ancient Mediterranean Environment between Sciences and History*. Brill, Leiden, pp. 103–170.

Manning, S.W., Kromer, B., 2011. Radiocarbon dating Iron Age Gordion and the Early Phrygian destruction in particular. In: Rose, C.B., Darbyshire, G. (Eds.), *The New Chronology at Iron Age Gordion*. Gordion special studies 6. University of Pennsylvania Museum of Archaeology and Anthropology, Philadelphia, pp. 79–122.

Manning, S.W., Kromer, B., Bronk Ramsey, C., Pearson, C.L., Talamo, S., Trano, N., Watkins, J., 2010. ^{14}C record and wiggle-match placement for the Anatolian (Gordion area) juniper tree-ring chronology ~1729 to 751 cal BC, and typical Aegean/Anatolian (growing season related) region ^{14}C offset assessment. *Radiocarbon* 52: 1571–1597.

Manning, S.W., Kromer, B., Kuniholm, P.I., Newton, M.W., 2003. Confirmation of near-absolute dating of east Mediterranean Bronze-Iron dendrochronology. *Antiquity* 77: 295.

Manning, S.W., Kromer, B., Kuniholm, P.I., Newton, M.W., 2001. Anatolian tree rings and a new chronology for the East Mediterranean Bronze-Iron Ages. *Science* 294: 2532–2535.

Manning, S.W., Pulak, C., Kromer, B., Talamo, S., Bronk Ramsey, C., Dee, M., 2009. Absolute age of the Uluburun shipwreck: a key Late Bronze Age time-capsule for the east Mediterranean. In: Manning, S.W., Bruce, M.J. (Eds.), *Tree-Rings, Kings and Old World Archaeology and Environment: Papers Presented in Honor of Peter Ian Kuniholm*. Oxbow Books, Oxford, pp. 163–187.

McCarroll, D., Loader, N.J., 2004. Stable isotopes in tree rings. *Quaternary Science Reviews* 23: 771–801.

McCormick, M., Büntgen, U., Cane, M.A., Cook, E.R., Harper, K., Huybers, P., Litt, T., Manning, S.W., Mayewski, P.A., More, A.F.M., Nicolussi, K., Tegel, W., 2012. Climate change during and after the Roman Empire: reconstructing the past from scientific and historical evidence. *Journal of Interdisciplinary History* 43 (2): 169–220.

Meadows, J., 2005. The Younger Dryas episode and the radiocarbon chronologies of the Lake Huleh and Ghab Valley pollen diagrams, Israel and Syria. *The Holocene* 15 (4): 631–636.

Meiggs, R., 1982. *Trees and Timber in the Ancient Mediterranean World*. Clarendon Press, Oxford.

Migowski, C., Stein, M., Prasad, S., Negendank, J.F.W., Agnon, A., 2006. Holocene climate variability and cultural evolution in the Near East from the Dead Sea sedimentary record. *Quaternary Research* 66: 421–431.

Mithen, S., Austen, P., Kennedy, A., Emberson, H., Lancaster, N., Finlayson, B., 2007. Neolithic woodland composition and exploitation in the Southern Levant: a comparison between archaeobotanical remains from WF16 and present-day woodland at Hammam Adethni. *Environmental Archaeology* 12: 49–70.

Mutlu, H., Köse, N., Akkemik, Ü., Aral, D., Kaya, A., Manning, S.W., Pearson, C.L., Dalfes, N., 2011. Environmental and climatic signals from stable isotopes in Anatolian tree rings, Turkey. *Regional Environmental Change* 12 (3): 559–570.

Pearson, C., Griggs, C.B., Kuniholm, P.I., Brewer, P.W., Ważny, T., Canady, L., 2012. Dendroarchaeology of the mid-first millennium AD in Constantinople. *Journal of Archaeological Science* 39: 3402–3414.

Quézel, P., Médail, F., 2003. *Écologie et Biogéographie des Forêts du Bassin Méditerranéen*. Elsevier, Paris.

Rambeau, C., 2010. Paleoenvironmental reconstruction in the southern Levant: synthesis, challenges, recent developments and perspectives. *Philosophical Transactions of the Royal Society A* 368: 5225–5248.

Rambeau, C., Black, S., 2011. Palaeoenvironments of the southern Levant 5,000 BP to present: linking the geological and archaeological records. In: Mithen, S., Black, E. (Eds.), *Water, Life and Civilisation: Climate, Environment and Society in the Jordan Valley*. Cambridge University Press, Cambridge, pp. 94–104.

Riehl, S., 2012. Variability in ancient Near Eastern environmental and agricultural development. *Journal of Arid Environments* 86: 113–121.

Robinson, S.A., Black, S., Sellwood, B.W., Valdes, P.J., 2006. A review of palaeoclimates and palaeoenvironments in the Levant and Eastern Mediterranean from 25,000 to 5000 years BP: setting the environmental background for the evolution of human civilisation. *Quaternary Science Reviews* 25: 1517–1541.

Rosen, A.M., 2007. *Civilizing Climate: Social Responses to Climate Change in the Ancient Near East*. AltaMira Press, Lanham.

Schwab, M., Neumann, F., Litt, T., Negendank, J.F.W., Stein, M., 2004. Holocene palaeoecology of the Golan Heights (Near East): investigation of lacustrine sediments from Birkat Ram crater lake. *Quaternary Science Reviews* 23 (16–17): 1723–1731.

Schweingruber, F.H., 1996. *Tree Rings and Environment Dendroecology*. Verlag Paul Haupt, Bern.

Talhouk, S.N., Zurayk, R., Khuri, S., 2001. Conservation of the coniferous forests of Lebanon: past, present and future prospects. *Oryx* 35 (3): 206–215.

Tamari, A., 1976. *Climatic Fluctuations in the Eastern Basin of the Mediterranean Based on Dendrochronological Analysis*. Unpublished Ph.D. thesis, Tel Aviv University. (Hebrew)

Touchan, R., Akkemik, Ü., Hughes, M.K., Erkan, N., 2007. May–June precipitation reconstruction of southwestern Anatolia, Turkey during the last 900 years from tree rings. *Quaternary Research* 68: 196–202.

Touchan, R., Anchukaitis, K.J., Shishov, V.V., Sivrikaya, F., Attieh, J., Ketmen, M., Stephan, J., Mitsopoulos, I., Christou, A., Meko, D.M., 2014a. Spatial patterns of eastern Mediterranean climate influence on tree growth. *The Holocene* 24 (4): 381–392.

Touchan, R., Christou, A.K., Meko, D.M., 2014b. Six centuries of May–July precipitation in Cyprus from tree rings. *Climate Dynamics* 43: 3281–3292.

Touchan, R., Hughes, M.K., 1999. Dendrochronology in Jordan. *Journal of Arid Environments* 42: 291–303.

Touchan, R., Meko, D., Hughes, M.K., 1999. A 396-year reconstruction of precipitation in southern Jordan. *Journal of the American Water Resources Association* 35 (1): 49–59.

Touchan, R., Xoplaki, E., Funkhouser, G., Luterbacher, J., Hughes, M.K., Erkan, N., Akkemik, Ü., Stephan, J., 2005. Reconstructions of spring/summer precipitation for the eastern Mediterranean from tree-ring widths and its connection to large-scale atmospheric circulation. *Climate Dynamics* 25: 75–98.

Verheyden, S., Nader, F.H., Cheng, H.J., Edwards, L.R., Swennen, R., 2008. Paleoclimate reconstruction in the Levant region from the geochemistry of a Holocene stalagmite from the Jeita cave, Lebanon. *Quaternary Research* 70: 368–381.

Waisel, Y., Liphschitz, N., 1968. Dendrochronological studies in Israel II: *Juniperus phoenicea* of north and central Sinai. *La-Yaaran* 8: 2-22, 63–67. (Hebrew with English summary)

Ważny, T., 2011a. Dendro-provenancing between the Baltic Sea and East Mediterranean. In: Fraiture, P. (Ed.), *Tree Rings, Art, and Archaeology*. Proceedings of the Conference, Royal Institute for Cultural Heritage, Brussels, 10–12th February 2010. Scientia artis collection, Brussels, pp. 99–105.

Ważny, T., 2011b. Secrets of a Rembrandt school still life: a Baltic oak panel and its many layers. In: Weislogel, A. (Ed.), *The New and Unknown World: Art, Exploration, and Trade in the Dutch Golden Age*. Herbert F. Johnson Museum of Art, Cornell University, Ithaca, pp. 22–29.

Ważny, T., 2002. Baltic timber in Western Europe–an exciting dendrochronological question. *Dendrochronologia* 20 (3): 313–320.

Werker, E., 2006. 780,000-year-old wood from Gesher Benot Ya'aqov, Israel. *Israel Journal of Plant Sciences* 54: 291–300.

Yasuda, Y., Kitagawa, H., Nakagawa, T., 2000. The earliest record of major anthropogenic deforestation in the Ghab Valley, northwest Syria: a palynological study. *Quaternary International* 73/74: 127–136.

Ziv, B., Saaroni, H., Alpert, P., 2004. The factors governing the summer regime of the eastern Mediterranean. *International Journal of Climatology* 24: 1859–1871.

Zohary, M., 1973. *Geobotanical Foundations of the Middle East*. Vol. 2. Gustav Fischer Verlag, Stuttgart.

Zohary, M., 1962. *Plant Life of Palestine: Israel and Jordan*. Ronald Press, New York.

CHAPTER 2:

TREE-RING GROWTH AND RESPONSE TO CLIMATE ACROSS ECOLOGICAL GRADIENTS IN THE SOUTHERN LEVANT

SUMMARY

Variability in annual tree-ring growth response to climate is investigated at 11 forest sites that are located along north-south and west-east ecological gradients in the southern Levant. Inter-species comparisons of tree-ring chronologies of native tree species (*Pinus halepensis* Mill., *Quercus macrolepis* Kotschy, and *Juniperus phoenicea* L.) and of non-native tree species (*Pinus pinea* L. and *Pinus brutia* Ten.) are made. The results indicate that in the Mediterranean forest zone of the southern Levant, there are two dendrochronological zones in which the tree-ring signals of different sites are coherent and have significant correlation. The boundary between these zones is located near Jerusalem along the 400 mm/year isohyet. Tree-ring chronologies from the northern dendrochronological zone generally have significant positive growth responses to December–February precipitation and significant negative growth responses to monthly mean temperature during December–January and April. The tree-ring signal and climate responses are similar across species and sites, although there is slight variability, primarily along a latitudinal gradient, corresponding to the annual precipitation gradient. The southern zone, which is in a more arid bioclimatic zone with a greater annual temperature range, has a significant

response only to precipitation, particularly during the months at the beginning (October) and end (April) of the rainy season.

INTRODUCTION

As discussed in chapter 1, the southern Levant is a phytogeographical and climatic transition zone, in which the landscape changes from Mediterranean forest to semi-arid steppes and desert over relatively short distances, with equally dramatic changes in topography. Such climatic and environmental changes are especially apparent across north-south and west-east transects in the region, over which the overall average annual rainfall decreases. The southern Levant's bioclimatic heterogeneity can potentially cause high variability in year-to-year tree-ring growth throughout the region, which may inhibit or complicate successful dendrochronological crossdating and development of reference chronologies for tree-ring research in the region at a macro-scale.

The primary objectives of this study are to examine variability in tree-ring growth and tree-ring response to climate at forest sites in the southern Levant sampled along west-east and north-south gradients, and identify the climatic factors that most influence tree-ring growth. With this information, tree-ring growth patterns and climate responses can therefore be placed into meaningful groups, in order to determine the coherence of tree-ring signals in the southern Levant for dendrochronological crossdating and to delineate geographic zones with common tree-ring patterns for future dendroprovenancing studies. Determining groups of forest sites with similar responses to climate also identifies forests that are most sensitive to

climate and thus most affected by projected long-term changes in climate in the Mediterranean.

Previous Research

Although previous dendrochronological studies have been undertaken in the southern Levant and some have examined tree-ring climate response, many are restricted to a single site (e.g., Kaplan 1984; Lev-Yadun et al. 1981; Liphschitz and Waisel 1967; Touchan et al. 1999; Waisel and Liphschitz 1968). Studies including inter-site comparisons have generally explored correlation among only two or three sites (e.g., Gindel 1944; Touchan and Hughes 1999), sometimes at considerable distances from one another, and have compared only different species that occupy different bioclimatological zones (e.g., Tamari 1976). With the exception of Touchan and Hughes (1999) and Touchan et al. (1999), these analyses of site variability and climate response generally occurred prior to, or did not use, more recent dendroclimatological standardization methods (e.g., Cook 2006, 1985; Cook and Peters 1997; Osborne et al. 1997) and statistically robust multivariate analysis techniques for determining tree-ring response to climate, particularly response function analysis (Fritts 1976; Guiot 1991).

This study is therefore the first analysis undertaken in the southern Levant using these techniques to determine and categorize climate response and spatial variability of a robust network of tree-ring chronologies sampled across ecological gradients in the southern Levant's Mediterranean forest zone. This dataset includes 11 new tree-ring chronologies sampled from native and planted forests in Israel and northern Jordan. Two additional chronologies that Touchan et al. (1999) and Touchan and

Hughes (1999) built from Bani Kenana in northern Jordan and the Shobauk Plateau in southern Jordan are also examined as part of the overall dataset.

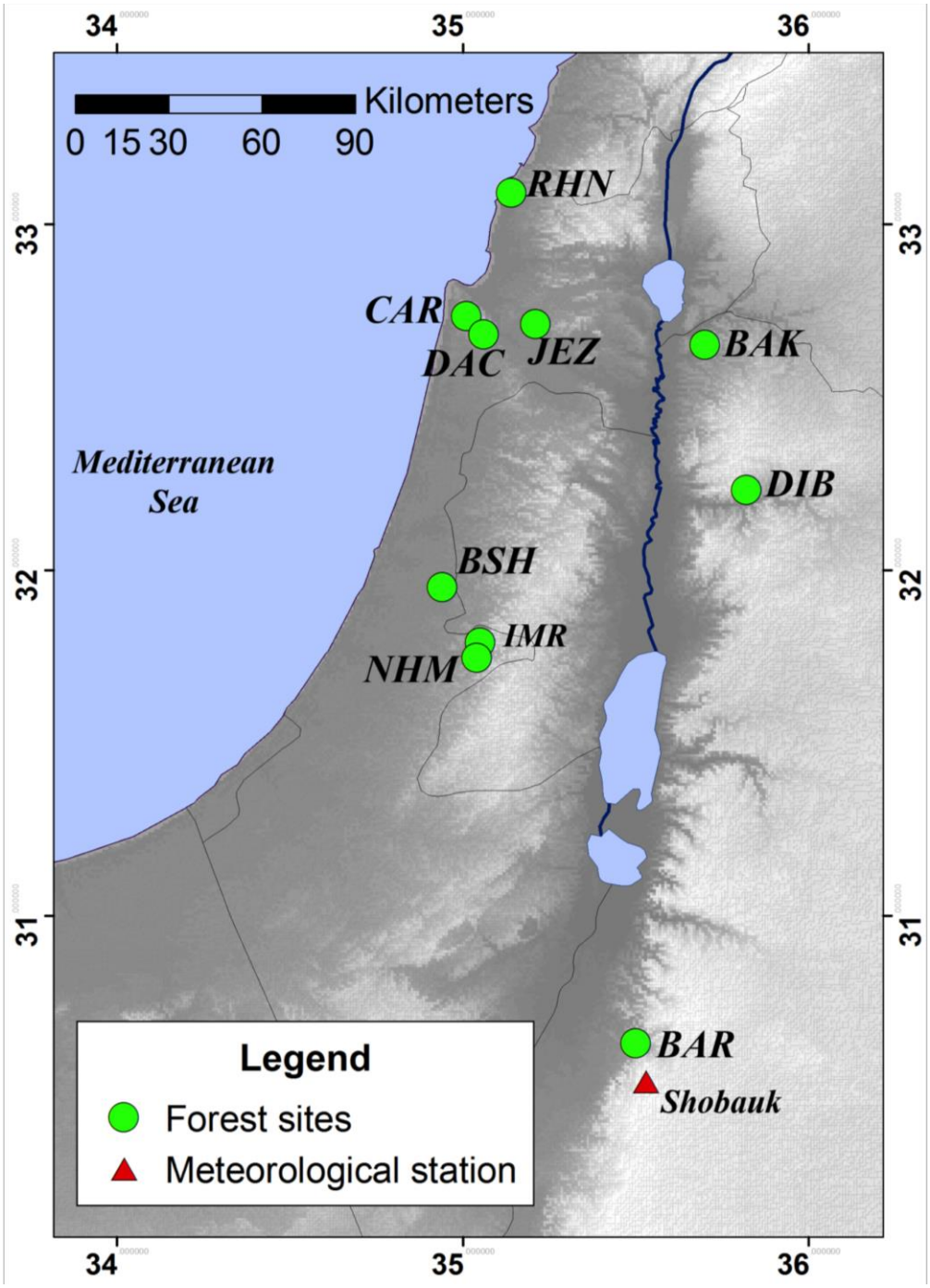

Figure 2.1. Locations of the tree-ring sites (*squares*) and meteorological station (*triangle*) which provided precipitation data for climate analysis.

Study Area

The geographic extent of the entire sampled area ranges from 33º–30.65ºN latitude and 34.93º–35.82ºE longitude (Figure 2.1), and the elevations of the sampled sites range from 106 to 1400 meters a.s.l., with the majority of the sampled sites located at elevations below 800 meters a.s.l. The location and elevation range of each sampled site is given in Table 2.1.

The climate type of all of the sampled sites may be broadly categorized as Mediterranean, which is characterized by warm, rainless summers, and cold, rainy winters (Cordova 2007; Freiwan and Kadıoğlu 2008; Goldreich 2003). October–September precipitation (the Levantine hydrological year) is also consistent in year-to-year anomalies (i.e., relative 'wet' years and 'dry' years) at different locations within the study area (Table 2.2). However, there are critical variations in climate (particularly in total annual precipitation and the annual temperature range) within the southern Levant that affect plant species distribution and influence tree-ring growth. The bioclimatic variability among forest sites in the study area is explored and characterized using the classification systems described in the following section.

Table 2.1. Description of the site locations and tree-ring chronologies. Site codes consist of a three-letter code for the site name and a four-letter code for the species sampled, which include: *Pinus halepensis* (PIHA), *Pinus brutia* (PIBR), *Pinus pinea* (PIPN), *Quercus macrolepis* (QUMA), and *Juniperus phoenicea* (JUPH).

Country	Site name	Site code	Species	Latitude °N	Longitude °E	Elevation range (m)	Years spanned	Total years	No. of trees	No. of cores/ radii
Israel	Shephelah, Ben Shemen	BSH-PIBR	*Pinus brutia*	31.95	34.94	106–147	1932–2009	78	24	37
	Shephelah, Ben Shemen	BSH-PIHA	*Pinus halepensis*	31.95	34.94	106–147	1928–2009	82	12	20
	Mt. Carmel	CAR-PIHA	*Pinus halepensis*	32.69–32.77	34.98–35.04	175–529	1910–2011	102	29	44
	Mt. Carmel, Daliyat al-Carmel	DAC-PIPN	*Pinus pinea*	32.68	35.01	408–421	1933–2009	77	22	43
	Judean Hills, Masreq	IMR-PIHA	*Pinus halepensis*	31.79	35.05	505–632	1846–2009	164	23	44
	Jezreel, Tel Shimron	JEZ-PIHA	*Pinus halepensis*	32.71	35.21	154–173	1935–2008	74	21	34
	Judean Hills, Nes Harim	NHM-PIHA	*Pinus halepensis*	31.75	35.04	436–711	1935–2009	75	14	22
	Judean Hills, Nes Harim	NHM-PIPN	*Pinus pinea*	31.75	35.04	566–711	1932–2009	78	21	37
	Rosh HaNiqra	RHN-PIHA	*Pinus halepensis*	33.09	35.14	273–332	1889–2010	122	14	27
Jordan	Bani Kenana	BAK-QUAE	*Quercus macrolepis*	32.65	35.70	300–410	1906–1995	90	12	12
	Shobauk Plateau	BAR-JUPH	*Juniperus phoenicea*	30.63	35.50	1100–1400	1469–1995	527	17	17
	Dibeen	DIB-PIHA	*Pinus halepensis*	32.23	35.82	600–1134	1884–2011	128	31	48

Table 2.2. Pearson correlation coefficients between normalized October–September precipitation (1961–1990) at different locations in the study area. The climate data includes 0.5º gridded datasets available from the Climate Research Unit (CRU) at the University of East Anglia (Hulme 1992; Mitchell and Jones 2005), and local precipitation data from the Shobauk meteorological station in southern Jordan. Each CRU gridded dataset is listed according to the geographic coordinates of the grid's center.

	31.75º, 35.25º			
32.75ºN, 35.25ºE	0.632***	**32.75º, 35.25º**		
33.25ºN, 35.25ºE	0.553***	0.923***	**33.25º, 35.25º**	
32.25ºN, 35.75ºE	0.760***	0.763***	0.702***	**32.75º, 35.75º**
32.75ºN, 35.75ºE	0.655***	0.845***	0.856***	0.880***
Shobauk	0.411**	0.408**	0.427**	0.453**

***** Significant at the 0.01% level.**
**** Significant at the 1% level.**
*** Significant at the 5% level.**

Bioclimatic classification of the study area

Various classification systems have been used to divide the southern Levant–including the study area examined here–into meaningful bioclimatic zones (e.g., Al-Eisawi 1985; Danin 1999; Dufour-Dror and Ertaş 2004; Goldreich 2003; Peel et al. 2007; Zohary 1973). In this study, I characterize different bioclimatic zones in the study area by using two of the most common bioclimatic classification systems–the Köppen (Köppen 1931; Peel et al. 2007) and Emberger (1955, 1971) systems. I also calculate the length of the dry season (*LDS*), dry season water deficit (*DSWD*), and monthly potential evapotranspiration (*PET*) for different locations in the study area. For these calculations, I used precipitation and temperature data obtained from the high-resolution climate dataset CRU TS 3.1, which is gridded at 0.5º intervals and available from the Climate Research Unit at the University of East Anglia (Hulme

1992; Mitchell and Jones 2005), as well as local meteorological station data obtained from the Jordanian Meteorological Service.

The Köppen classification system determines bioclimatic zones using an empirical set of thresholds for defining aridity and seasonal rainfall that were determined by examining changes in climate relative to natural vegetation distribution (Köppen 1931; Peel et al. 2007). The system combines average annual and monthly temperatures and precipitation to divide climates into five main groups (assigned an uppercase letter 'A–E'). Groups are then sub-divided, based on their precipitation pattern (e.g., the dry winter sub-group 'w' or dry summer subgroup 's') and the degree of summer heat; subgroups are identified by a lowercase letter. This system has been criticized for its use in the Mediterranean (which is in the 'Group C' category), because it creates overly broad bioclimatic zones, in which there is dramatic variation (Dufour-Dror and Ertaş 2004), although the system is still widely used in biogeographic studies.

The bioclimatic zone *sensu* Emberger offers a more fine-scale, quantitative classification of bioclimatic zones in the Mediterranean climatic zone than the Köppen system and is the most frequently used classification method for the Mediterranean region (Al-Eisawi 1985; Blondel and Aronson 1999; Dufour-Dror and Ertaş 2004). The Emberger system defines bioclimatic zones by using the following two quantitative criteria: i) the climate's global humidity, which is calculated according to Emberger's pluviothermic quotient (Q_2); and ii) the severity of the winter (the 'thermal variant'), which is a function of temperature (Emberger 1955, 1971). The pluviothermic quotient is calculated with the following formula:

$$Q_2 = \frac{2000P}{(M + m + 546.24)(M \quad m)}$$

where P is the mean annual precipitation in mm, M is the mean of the maxima of the hottest month in ºC, and m is the mean of the minima of the coldest month in ºC. Severity of winter is defined according to the value of m. Up to six categories of humidity and thermal variants can be distinguished using this method (Blondel and Aronson 1999; Dufour-Dror and Ertaş 2004; Emberger 1971).

It has been argued that Emberger's method does not account for differences in annual rainfall distribution in the Mediterranean (Blondel and Aronson 1999; Daget 1977; Nahal 1981) or the severity of dry season water deficit, which previous research has found is one of the most useful systems for characterizing Mediterranean bioclimates (Blondel and Aronson 1999; Dufour-Dror and Ertaş 2004; Gaussen 1954). Therefore the length and severity of the dry season throughout the study range is also calculated and examined here.

LDS is calculated as the average number of 'dry' months in a year by using Gaussen's method (Gaussen 1954). A month is considered 'dry' if the amount of rainfall (P in mm) in a given month is less than, or equal to, twice the value of the average temperature (T in ºC) of that month (i.e., $P < 2T$).

The severity of water deficit for a plant is related to the amount of moisture stored in the soil. The balance between precipitation, which recharges soil moisture, and evapotranspiration, which removes water from the soil, plays a critical role in determining the amount of moisture available to plants in Mediterranean forest ecosystems (Dufour-Dror and Ertaş 2004; Schiller and Cohen 1995; Strahler and

Strahler 2006; Yaseef et al. 2009). The overall water deficit of a given month (*WD*) is a quantitative value that is expressed in mm and calculated as follows:

$$WD = p - PET$$

where p is the average monthly rainfall amount (mm) and *PET* is the monthly potential evapotranspiration (mm) (Dufour-Dror and Ertaş 2004).

Potential evapotranspiration is defined as the amount of water that would be evaporated from an area if an unlimited supply of water were available (i.e., the atmosphere's 'drying power') (Bruins 2012; Hulme et al. 1992; Strahler and Strahler 2006). There are multiple equations that have been developed to calculate *PET*. One of the most widely used formulas for calculating *PET* in biophysical studies is that proposed by Penman (1948). The Penman formula is considered one of the most accurate formulas for estimating *PET*, because it uses parameters that directly relate to the atmosphere's drying power, including net solar radiation, wind speed, and relative humidity (Bruins 2012; Hulme et al. 1992; Penman 1948). However, long-term datasets of all of the parameters that the Penman method requires are not available for all locations in the study area, so it is not appropriate to use the Penman method to calculate *PET* in the southern Levant at high spatial resolution.

Instead, I calculate monthly *PET* for different locations in the study area using a simpler formula developed by Thornthwaite (1948), which requires only a location's mean monthly temperature and average number of daylight hours per month (the daylight coefficient). The equations used to calculate monthly *PET* are as follows:

$$PET^{T} = 16C\,(10T/I)^{a}$$

$$I = \Sigma\,(T/5)^{1.51}$$

$$a = (67.5 \bullet 10^{-8}\, I^{3}) - (77.1 \times 10^{-6}\, I^{2}) + (0.0179\, I) + (0.492)$$

where *PET* is the potential evapotranspiration in mm; *C* is the daylight coefficient; *T* is the average monthly temperature in ºC; and *a* is an empirically derived exponent, which is a function of the heat index (*I*). Daylight coefficient values vary according to a location's latitude. The daylight coefficient values for the center of each climate grid point or meteorological station in the study area were obtained from data available online from the US Naval Observatory (USNO 2013).

The severity of the dry season at each location was quantified by calculating water deficit (monthly *P-PET*) of each dry season month, and then calculating the total cumulative water deficit. Dry season months were identified using Gaussen's method, described above (Dufour-Dror and Ertaş 2004). However, it should be noted that Thornthwaite's (1948) formula was originally developed for calculating *PET* in the United States, which means that it often underestimates *PET* for locations in hot, semi-arid and arid environments (particularly areas in which annual precipitation is less than 500 mm) (Hulme et al. 1992). Monthly *PET* and *DSWD* may therefore be somewhat underestimated.

The bioclimatic characteristics and classifications for each climate grid point or meteorological station in the study area are summarized below in Table 2.3 (for water balance diagrams of each climate grid and meteorological station, see: Appendix 2.1).

Table 2.3. Characteristics and bioclimatic classifications of the 0.5º CRU grids and station data used in this study. Since the CRU grids cover a broader area than individual meteorological stations and may not capture small-scale climatic variations, the Emberger classification of each CRU grid was compared to individual climate station data from the Israeli and Jordanian Meteorological Services and Dufour-Dror and Ertaş's (2004) results. The bioclimatic designations generally correspond well, although small-scale variations exist in the CRU grid centered at 31.75ºN, 35.25ºE. The Ben Shemen site has a hot sub-humid/ semi-arid climate, while Nes Harim and Masreq have warm semi-arid bioclimates. The *LDS* values are consistent throughout this gridded zone.

Climate dataset	Köppen zone	Emberger zone	Oct–Sep *P* (mm)	*M* (ºC)	*m* (ºC)	Q_2	*LDS* (months)	*DSWD* (mm)
CRU (31.75ºN, 35.25ºE)	Csa	warm semi-arid	468.4	31.3	6.0	63.36	7	-734
Ben Shemen		*hot sub-humid/ semi-arid*						
Masreq/ Nes Harim		*warm semi-arid*						
CRU (32.75ºN, 35.25ºE)		hot sub-humid	585.9	30.9	7.2	84.47	7	-713
CRU (33.25ºN, 35.25ºE)		hot sub-humid	738.8	30.4	7.4	110.04	6	-670
CRU (32.25ºN, 35.75ºE)	Csa/Csb	warm semi-arid	427.2	31.3	6.2	58.44	7	-683
CRU (32.75ºN, 35.75ºE)	Csa/Csb	warm semi-arid	469.2	31.9	5.7	61.34	7	-738
Shobauk station	Csb	cold semi-arid	302.6	27.2	-1.3	37.17	8	-555

Examination of the bioclimatic data and previous studies of the region's climate and vegetation (e.g., Al-Eisawi 1985; Danin 1999; Freiwan and Kadıoğlu 2008; Zohary 1973) indicate that the study area is divided into two main forest zones, the sub-humid/semi-arid Mediterranean zone and the cold semi-arid Mediterranean

zone. The main characteristics and vegetation of each of these forest ecosystems are described below.

Sub-humid/semi-arid Mediterranean (SHAM) forest zone

The trees analyzed in this study are primarily located in the northern part of the southern Levant's sub-humid/semi-arid Mediterranean (hereafter SHAM) forest zone. This zone generally has a warm temperate Mediterranean climate (type 'Csa') using the Köppen climate classification system (Goldreich 2003; Köppen 1931; Peel et al. 2007). One high altitude site sampled from the SHAM forest zone for this study (Dibeen in northern Jordan) has a cool temperate Mediterranean climate (Köppen climate classification 'Csb'), which experiences slightly milder summers and colder winters than type 'Csa' (Cordova 2007; Köppen 1931). The sites are all located in the hot to warm thermal variants of the Emberger bioclimatic zones (Dufour-Dror and Ertaş 2004; Emberger 1955, 1971) (Table 2.3).

Precipitation in the SHAM forest zone occurs only during the autumn, winter, and spring months (October–April), with the majority of rainfall occurring during December–February. Mean annual precipitation ranges from 427 to 739 mm (Hijmans et al. 2005; Hulme 1992; Mitchell and Jones 2005). Higher elevation areas like Dibeen (as well as Mt. Kenaan and Mt. Meron in Israel) also receive snowfall, which may remain on the ground for several days, during colder, wetter years (Cordova 2007; Goldreich 2003). The length of the dry season (*LDS*) throughout this area is generally 7 months, except at the coastal site of Rosh HaNiqra in the north, where the *LDS* is a slightly shorter 6 months (Table 2.3; Appendix 2.1). During the dry season, there is severe water deficit and high *PET* throughout the area.

Mean annual temperature ranges from 18.5º to 19ºC. August is the hottest month of the year, with an average maximum temperature of 30.4º to 31.3ºC, while January is the coldest month of the year, with an average minimum ranging from 5.7º to 7.4ºC in the study area (Table 2.3; Appendix 2.1).

The soils in the SHAM forest zone are calcareous brown and pale rendzinas, occasionally mixed with clayey *terra rossa*, which are less calcareous and have lower water retaining capacity (Cordova 2007; Shapiro 2006; Singer 2007). The bedrock in these areas is composed of calcareous chalks, marls, dolomites, cherts, and limestone (Cordova 2007; Flexer et al. 2005; Schiller 1982).

Two common woodland types of the SHAM forest zone are analyzed in this study. The first is dominated by a relatively open canopy of *Pinus halepensis* and has a subordinate canopy composed of *Quercus calliprinos* Webb., *Pistacia lentiscus* L., *Pistacia palaestina* Boiss., and *Arbutus andrachne* L. The second type is a park forest, consisting of deciduous Valonia oak (*Quercus macrolepis* Kotschy.; alternatively known as *Quercus aegilops* or *Quercus ithaburensis*) that grows in pure or in mixed stands with *Pistacia atlantica* Desf., *Ceratonia siliqua* L., and *Styrax officinalis* L. (Zohary 1973).

In the native pine forests sampled for this study, there is generally an inverse relationship between tree age and density (i.e., trees in older age classes are less abundant than those in younger age classes). However, the age distributions of *P. halepensis* may vary at smaller scales within different parts of the forests because of localized disturbance and variable seed dispersal.

The planted forests that were sampled for this study are generally dominated by *Pinus halepensis*, with smaller populations of nonnative *Pinus brutia* Ten., *Pinus pinea* L., and (at Ben Shemen) *Pinus canariensis* C.Sm. The age distributions of the *Pinus halepensis* populations at two of these sites (Ben Shemen and Nes Harim) are uneven, because planting has occurred over multiple years and because of natural regeneration. *Pinus brutia* populations in these forests are generally younger (with most in the 10- to 40-year age range) than *P. halepensis*. The *Pinus pinea* populations at Ben Shemen and Nes Harim are relatively even-aged, with most in the 70–80-year age range (i.e., the same age as the oldest *P. halepensis* age class). Two other planted sites–Daliyat al-Carmel and Tel Shimron–have pure, even-aged stands of planted *Pinus pinea* and *Pinus halepensis*, respectively. Much of the underlying vegetation at the planted sites is similar to the native forests, although the percent ground cover and overall species diversity is generally lower. Stand density is also generally higher in the planted forests than in the native forests, although the forests have been periodically thinned (Bonneh 2000; Orni 1978).

Fire plays an important role in shaping the stand structure and composition of the forest ecosystems in the sub-humid/semi-arid Mediterranean zone, although most recent forest fires in the southern Levant have been caused by human activity (Kaplan and Gutman 1999; Tessler et al. 2008). There are both written records (e.g., Tessler et al. 2008; Triepke et al. 2012) and field evidence (e.g., basal scarring and burnt vegetation) of forest fires in all of the native forests and some of the planted forests (e.g., Nes Harim and Tel Shimron) studied here.

Cold semi-arid Mediterranean (CSAM) forest zone

The Shobauk Plateau in southern Jordan has a cool temperate Mediterranean climate (type 'Csb') according to the Köppen climate classification (Cordova 2007; Köppen 1931; Peel et al. 2007). According to Al-Eisawi's (1985) bioclimatic classification, which uses the Emberger pluviothermic quotient, it is part of the cold semiarid Mediterranean (hereafter CSAM) forest zone (Table 2.3). Like the rest of the study area further north, the Shobauk Plateau has cold, rainy winters and hot, dry summers, with the majority of annual rainfall concentrated during December–February.

The Shobauk area has a more xeric environment than that of the SHAM forest zone further north and a greater annual temperature range (Freiwan and Kadıoğlu 2008). Mean annual precipitation at the Shobauk meteorological station is 303 mm (Table 2.3), although there is considerable year-to-year variation in precipitation. The average annual temperature of the Shobauk meteorological station is around 13ºC. August is the hottest month of the year, with an average maximum temperature of 27.2ºC, while January is the coldest month of the year, with an average minimum temperature of -1.25ºC (Table 2.3; Appendix 2.1). The areas where Touchan et al. (1999) sampled, which are above 1100 meters, regularly receive snowfall during the winter months. Up to a meter of snow cover, lasting up to one month, has been reported in this area (Black et al. 2011).

The colder winter temperatures and cooler summer temperatures at high-altitude locations on the Shobauk Plateau contribute to lower winter and summer *PET* values in the CSAM zone than in the SHAM forest zone further north (Table 2.3).

However, while less water is lost through evapotranspiration in this area than in forest sites further north, the CSAM zone receives less precipitation, meaning that there is a lower input to the CSAM zone's water budget than in the SHAM zone. The CSAM zone's dry season is slightly longer (8 months), and the balance between water surplus and water deficit is more precarious throughout the year than further north (see: Appendix 2.1). However, as altitude decreases from the Shobauk Plateau into the Rift Valley, precipitation decreases, while mean winter and summer temperatures and *PET* increase (Cordova 2007; Wade et al. 2011)

The main soil type in the CSAM zone is a shallow, calcareous loam with low organic content, which is highly eroded on steeper slopes (Cordova 2007; Touchan et al. 1999). Soils in the area's rock crevices and wadis have higher clay content and moisture-holding capacity than soils in the surrounding area. The underlying bedrock in this area is composed of smooth-faced limestone and sandstones, which direct large amounts of runoff into the crevices and wadis in these formations. This provides enough moisture to create microhabitats supporting relict populations of Mediterranean trees, shrubs, and herbaceous plants (Danin 1999; Zohary 1973). Relict populations of Mediterranean flora also grow at higher elevations, often near springs, where there is moisture-retaining alluvium covering soft sandstones (Danin 1999).

Red juniper (*Juniperus phoenicea* L.) dominates the wadi beds and crevices, although higher elevation areas, especially those near springs, also support *Pistacia atlantica* Desf. and *Quercus calliprinos* Webb. Groundcover in these areas is relatively sparse, and includes common steppe shrubs like *Artemisia herba-alba* Asso,

Gymnocarpos decandrum Forsk. var. lasiocalyx Svent., *Retama raetam* (Forssk.) Webb, *Onopodum ambiguum* Fresen., as well as grasses and herbs like *Anchusa strigosa* Banks & Sol., *Origanum syriacum* L., and *Hordeum glaucum* Steud. (Danin 1999; Mithen et al. 2007; Touchan et al. 1999).

Tree Species

Aleppo pine (*Pinus halepensis* Mill.) is the primary species from the SHAM forest zone analyzed in this study. Aleppo pine (alternatively known as Jerusalem pine) is the most widely distributed pine in the Mediterranean basin. Its range extends in the western Mediterranean from montane areas in Morocco to Tunisia, along with a small population in northern Libya, northward through the Mediterranean coastal ranges in Spain across to the southern Balkans. Although there are isolated populations of Aleppo pine in eastern Turkey, the majority of *P*. *halepensis* in the eastern Mediterranean is found in the southern Levant, in southern Lebanon, Israel/Palestine, and Jordan (Nahal 1963; Quézel 2000). *P*. *halepensis* stands in the southern Levant therefore mark the southeastern limit of the species' distribution in the Mediterranean and are also the southernmost limit of the genus *Pinus* in the Mediterranean ecological zone (Zohary 1973).

Although phenological, anatomical, and physiological differences exist among its different (and numerous) genetic provenances (Melzack et al. 1981; Schiller 2000; Weinstein 1989) and the species exhibits great plasticity, *P*. *halepensis* is generally a thermophilous species with low frost resistance that grows in areas (normally at lower altitudes) with a mean minimum temperature above 0ºC and an annual average temperature above 13º–17ºC. While the species can grow where annual rainfall

ranges from 200 mm to more than 1500 mm, it is most abundant in semi-arid to sub-humid zones whose annual rainfall is 350–700 mm (Quézel 2000). *P*. *halepensis* is well adapted to the Mediterranean climate and drought (Schiller 2000). It is also capable of adapting to a wide variety of soil and bedrock types, although it prefers calcareous soils and marl, and does not tolerate poorly drained soils (Quézel 2000; Schiller 1982).

Since it is fast-growing, *P*. *halepensis* has been a popular species in Mediterranean afforestation efforts. In Israel, planted forest stands were composed largely (and often exclusively) of *P*. *halepensis* from the mid-1920s until the 1970s, when, due to die-back from pine bast scale, nonnative *Pinus brutia* and native broadleaf species became more popular (Bonneh 2000; Liphschitz and Biger 2000). The species has also established itself beyond native and planted forest areas through colonization of abandoned land during the 20th century (Cordova 2007; Lavi et al. 2005). As a result, *Pinus halepensis* is the most common naturally growing and planted conifer in Israel, covering about 32,000 hectares, which represents approximately 9% of the area of the Mediterranean forest zone (Lavi et al. 2005). In Jordan, *P*. *halepensis* has also been an important species in afforestation, although the natural range of the species is restricted to the Ajloun Mountains in northwestern Jordan (Al-Eisawi 1985). The largest population of native *P*. *halepensis* in Jordan is in the Dibeen Nature Reserve, where Aleppo pine accounts for approximately 52.9% of the forest's total basal area (Triepke et al. 2012).

Aleppo pine forests play an important role (particularly when they are part of a multi-species planting strategy using native genetic provenances; see: Maestre and

Cortina 2004) in protecting soils (Castillo 1997), stabilizing hillslopes, and providing recreational areas (Schiller 2001). The wood of both *P*. *halepensis* and *P*. *brutia* has also been commonly used as low-quality firewood and building material throughout the Levant (Liphschitz 2007; Meiggs 1982).

Cambial activity and wood formation play a critical role in plant performance and survival (Liphschitz and Lev-Yadun 1986). Because of Aleppo pine's ecological and biogeographic importance in the southern Levant, further information about how *P*. *halepensis* tree-rings in native and planted stands respond to climate across the tree's distribution in the southern Levant is useful for forest management and planning (Serre-Bachet and Tessier 1990). This information may be particularly critical, since forests in the southern Levant are especially vulnerable to, and may be greatly impacted by, global climate change and projected increases in temperature and drought in the region (Lindner 2010).

P. *halepensis* has been used in multiple recent dendroclimatic studies around the Mediterranean (e.g., De Luis 2009; Touchan and Hughes 1999; Touchan et al. 2008) and is therefore a species suitable for dendrochronological analysis. Its physiology and seasonal cambial growth rhythms have been widely studied in Israel (Lev-Yadun 2000; Liphchitz and Lev-Yadun 1986; Liphschitz et al. 1984) and elsewhere in the Mediterranean (Attolini et al. 1990; Cherubini et al. 2003; De Luis et al. 2007, 2009; Esteban et al. 2010; Serre 1976). *P*. *halepensis* also has the widest geographic distribution in the southern Levant of all the native species identified as suitable for dendrochronology, thereby allowing comparison of tree-ring growth for the same species across the greatest geographic area.

It is therefore because of its ubiquity, biogeographic and ecological significance, and the relative wealth of physiological data that *P*. *halepensis* has been chosen as the primary species for this study. The tree-ring growth and climate responses of umbrella pine (*Pinus pinea* L.) and Calabrian pine (*Pinus brutia* Ten.) are also analyzed and compared with the *P*. *halepensis* data, in order to determine if there is a coherent, macroscale signal in tree-ring growth across species in the Mediterranean forest zone of the southern Levant. *P*. *brutia* and *P*. *pinea* are two nonnative species that are commonly found in the southern Levant's planted forests and have been previously used in dendrochronological studies (e.g., Akkemik 2000; De Luis et al. 2009; Griggs et al. 2014; Kienast et al. 1987; Sarris et al. 2007, 2011; Touchan et al. 2005).

Touchan and Hughes' (1999) Valonia oak (*Quercus macrolepis* Kotschy.) tree-ring chronology from Jordan is also analyzed and compared to the *P*. *halepensis* data. Because *P*. *halepensis* does not naturally grow in the CSAM forest zone of southern Jordan, chronologies from the SHAM forest zone are compared with Touchan et al.'s red juniper (*Juniperus phoenicea* L.) chronology that was sampled from this region.

METHODS

Sample Collection

Pinus halepensis samples were collected from four native forest stands in nature reserves in Israel and Jordan, and the five planted forests in Israel in 2008–2012. Both *Pinus pinea* and *Pinus halepensis* were sampled at Nes Harim, and *Pinus brutia* and *Pinus halepensis* were sampled at Ben Shemen. Nonnative *Pinus pinea* was

sampled from a planted stand near the village of Daliyat al-Carmel in the southeastern foothills of Mt. Carmel (Table 2.1).

Two to four forest cores were sampled from each tree with a 5 mm diameter Swedish increment borer at approximately breast height (ca. 1.3 m). At Masreq, Mt. Carmel, Ben Shemen, and Dibeen, full cross-sections of pine were also cut from available extant stumps. In dendroclimatic studies, it is recommended to sample 'pristine' forests free of anthropogenic disturbance, so as to reduce the potential of non-climatic 'noise' altering or hiding the tree-ring climate signal (Fritts 1976). Due to the southern Levant's long history of human settlement and alteration of the landscape, it is not possible to find sites entirely free from human impact. Areas where anthropogenic disturbance was minimal (e.g., away from roads, terraces, and grazing areas) and trees that had not obviously been heavily pruned or injured were therefore targeted for sampling. Mature, dominant trees were targeted for sampling, in order to obtain tree-ring records that extended as far back in time as possible, and to reduce the potential effects of stand dynamics and competition on the tree-ring data. Attempts were made to sample the entire radii from the trees (i.e., from the bark to the pith), so that the longest tree-ring sequences possible could be obtained from the trees. However, in some cases this was not possible, particularly for trees with rotten centers or trees with asymmetric ring growth.

Laboratory Measurement and Chronology Building

The cores were mounted on strips of channeled wood, and they and the cut sections were sanded and polished, so that the tree-rings and cell anatomy were clearly visible for dendrochronological analysis. Each sample's tree-ring widths were then

measured to the nearest 0.01 mm on a measurement table under a dissecting microscope, using the Tellervo TRiDaS (Brewer et al. 2010) and TSAP (Rinn 1996) dendrochronological analysis packages. Notable anatomical features were also marked and described for each ring using the same programs. Samples that had a high percentage of rings with unclear boundaries between their earlywood and latewood (preventing accurate ring measurement) were not measured.

Tree-ring sequences sampled from the same tree species at the same site were crossdated with one another by visually matching their similar growth patterns and recorded anatomical features; this synchronized the sample sequences and allowed each of their ring-width measurements to be assigned to a specific calendar year. The synchronized ring-width measurement sequences were averaged together to build a master chronology for each species collected from each site.

In some cases, it was evident that samples had either 'false rings' or locally absent rings. False rings occur when cambial activity briefly ceases during the growing season, or when the cambium is briefly re-activated during its quiescence period. Consequently the tree may either produce earlywood-like cells within latewood or latewood-like cells within the earlywood (Schweingruber 1996), creating the impression of an additional small ring (Figure 2.2). Multiple biotic or abiotic agents may cause the production of false rings. In general, false rings in the samples could be identified by wood anatomical examination, since the transition from earlywood to latewood in a false ring is more gradual and the earlywood-latewood boundary is more diffuse than in an actual tree-ring boundary (Cherubini et al. 2003).

Tree-ring sequences containing false rings were also compared with other tree-ring sequences from the same site to verify if an actual ring was present.

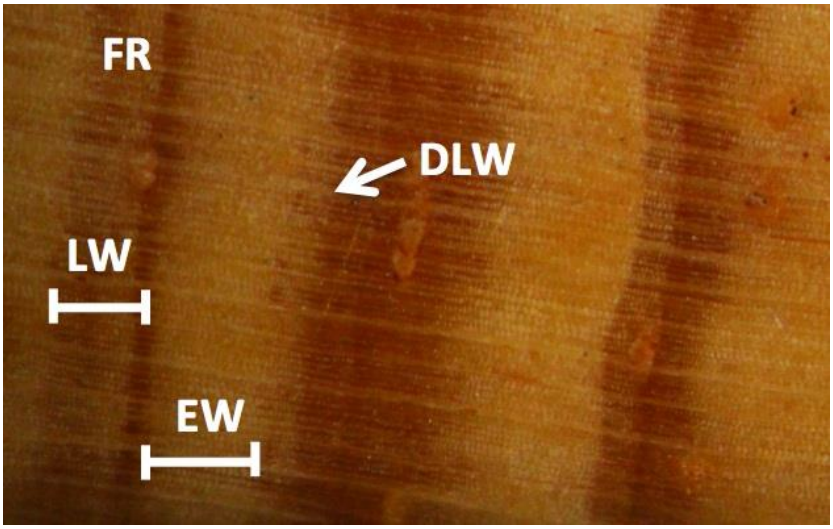

Figure 2.2. ***Pinus halepensis*** **core from Rosh HaNiqra (6x magnification) with false rings and diffuse latewood. The earlywood (*EW*) and latewood (*LW*) boundaries of one ring (year 1979) are shown. A false ring (*FR*) is present in the ring's latewood. During the previous year, the tree's cambium was not completely dormant at the end of the growing season, creating a diffuse latewood boundary (*DLW*).**

During years when conditions do not favor ring growth, a tree may not produce xylem around the entire circumference of the tree, with the result that this particular year's ring-growth may be 'locally absent' from a core or section. Missing rings were identified and their exact placements were determined by examining the sample wood and comparing sequences with missing rings against the tree-ring sequences of other radii sampled from the same tree and trees from the same site (especially younger, more robust trees). Samples that had a high proportion of missing rings were either excluded from further analysis or were truncated, so that the segments with disproportionately high numbers of missing rings were excluded from analysis.

The accuracy of the measurements and crossmatches, as well as the quality of interseries correlation in each chronology, was checked using COFECHA version 6.06 (Holmes 1983). COFECHA assesses crossdating quality in a chronology by using segmented time series correlation techniques (Grissino-Mayer 2001; Holmes 1983). The correlation of each tree-ring sequence in a chronology was tested versus the master site chronology (which is adjusted to remove the series being tested) in succeeding 40 or 50-year segments (depending on the length of the master chronology). Successive segments were lagged 25 years.

COFECHA also checks the correlation of each series segment to determine if higher correlation occurs when a series is crossmatched at alternative positions shifted up to ten years earlier or ten years later from the given dating placement (Grissino-Mayer 2001), which helps detect missing or extra rings in a tree-ring sequence. The program additionally flags "outlier" ring measurements that lie in the outer portions of the distributions of all tree-ring widths in all series in a given year. The dating placements and measurements of tree-ring series that COFECHA flagged with possible missing/extra rings or with outlier tree-ring measurements were re-examined. Any measurement series that had low correlation with the site master chronology or several flagged outlier values was excluded from further analysis.

After crossdating, the chronologies were standardized using the program ARSTAN 41d version 10.5 (Cook 1985; Cook and Krusic 2006). First, an adaptive power transformation (based on the local series mean and standard deviation) was applied to the data. This is a two-step procedure that stabilizes the variance and reduces potential end-fitting bias by calculating residuals rather than ratios from the

expected growth curve (Cook and Peters 1997). Since the tree-ring series in each chronology were sampled from multiple tree age classes, the variance of the chronologies was further stabilized using the weighted Rbar method outlined in Osborn et al. (1997), in order to reduce the effects on the changing sample size.

All tree-ring series were then smoothed individually, in order to remove growth trends related to age and stand dynamics, and to maximize the common tree-ring signal. In this process, tree-ring measurements are fitted to different selected curves, including negative exponential, regression, cubic smoothing splines of varying stiffness, and Friedman super-smoother curves (Friedman 1984) (see: Appendix 2.2 for a list of curves used at each site). Since the objective of this study was to determine the role of both temperature and precipitation as limiting factors to tree-ring growth, curves–particularly the Friedman super-smoother–were selected that would preserve low-frequency variance (some of which is related to long-term trends in temperature) while being locally adaptive enough to remove obvious disturbances from stand dynamics.

In their previous studies, Touchan et al. (1999) and Touchan and Hughes (1999) had selected curves that had removed most of the low-frequency variance from their *J. phoenicea* and *Q. macrolepis* chronologies, since the authors were primarily interested in using the tree-ring chronologies for precipitation reconstruction. Therefore, for the current study, their chronologies were re-standardized in ARSTAN using curves that preserved greater low-frequency variance, in order to investigate tree-ring responses to temperature at these sites as well.

Each tree-ring series was then 'pre-whitened' in ARSTAN, using a low order autoregressive (AR) model (see: Appendix 2.2 for the order of AR model used for each chronology) to remove year-to-year autocorrelation not related to climate variations. The 'pre-whitened' time series were then combined together into a single site chronology using a 'biweight robust estimate of the mean,' which is a technique designed to reduce the influence of isolated outlier values (Cook 1985).

The mean sensitivity (MS) was calculated from each residual chronology. Mean sensitivity is the mean percent change from each measured annual ring-width value to the next. First-order autocorrelation (AC1) was also calculated from each standardized chronology, prior to the removal of significant autocorrelation from the time series in the pre-whitening process. First order autocorrelation measures the correlation between a given ring-width value in a time-series and its predecessor, and therefore the effect that environmental conditions, stress, and growth during the previous year have on tree-ring growth during the following year (Fritts 1976). Both statistical parameters (MS and AC1) indicate the sensitivity of a tree species to environmental factors in a given area.

Climate Response Functions

The relationship between tree-ring growth and climate was analyzed by determining the response function coefficients for each chronology using the DENDROCLIM2002 program (Biondi and Waikul 2004). Fritts (1976) developed response function analysis as a more mathematically objective alternative to simple or multiple regression analysis (Serre-Bachet and Tessier 1990). In response function analysis, the predictor variable set (usually monthly precipitation and mean

temperature) is transformed to a set of principal components to correct for naturally occurring correlation between monthly precipitation and temperature and month-to-month correlation among climate indices. Linear regression of the tree-ring indices is then performed on the climate principal components to calculate the regression coefficients, and then the necessary matrix algebra is performed to express the regression coefficients in terms of the original monthly climate variables (Fritts 1976). The DENDROCLIM program then applies a bootstrap process (Guiot 1991) to assess the statistical significance of the regression coefficients.

Since previous studies (Boydak 2004; De Luis 2007; Lev-Yadun 2000; Liphschitz and Lev-Yadun 1986) indicate that *P. halepensis*, *P. brutia*, and *P. pinea* are all intolerant of cold temperatures, and high temperatures increase evapotranspiration and drought stress, I also investigated tree-ring response to different temperature indices. Therefore three sets of response function coefficients using monthly mean, maximum, and minimum temperatures each with monthly precipitation rates were calculated. The hydrological year in the southern Levant usually begins in early to mid-October and ends in late September to mid-October. In order to analyze the entire possible duration of the study region's hydrological year, response function coefficients were calculated using monthly climate data from October of the previous year to October of the current year. Thus each calculated response function includes 13 coefficients associated with either monthly mean, maximum, or minimum temperature and 13 coefficients associated with the variables of monthly total precipitation.

Monthly precipitation and temperature data were obtained from the CRU TS 3.1 dataset gridded at 0.5º intervals (Hulme et al. 1992; Mitchell and Jones 2005), and local meteorological station data obtained from the Israeli and Jordanian Meteorological Services. During preliminary analysis, it was found that the gridded data was generally more robust, longer, free from missing data, and had higher correlation with the tree-ring chronologies than local meteorological station data. Therefore I preferred to use the closest grid point climate data to each site. However, for the Shobauk site in southern Jordan, I used precipitation data from the Shobauk meteorological station, because the CRU gridded dataset, which likely includes station data from desert areas, does not accurately reflect the Shobauk Plateau's climatological regime and growing season length. The Shobauk precipitation dataset was truncated up to 1946, after which the climate data is homogeneous with relatively uniform variance.

The monthly climate data were used as predictors and the standardized site chronologies as predictands over a common period of 1943–2008 for the pine chronologies; thus climate data from October–December of the previous year (1942) were also used. This common period was chosen, because all of the sampled pine chronologies have a subsample signal strength (SSS, calculated in ARSTAN) above 0.85 after 1943. Subsample signal strength is the correlation coefficient between the average of a time series *N* and the average of an arbitrary subset of this series, *n* (Wigley et al. 1984). This value allows one to assess how well a subset of a time series will represent the overall average and is especially useful in identifying when in the early years of a chronology (where sample replication is generally lower) there is

adequate replication for reliable statistical analysis. The response functions for Touchan and Hughes (1999) and Touchan et al.'s *J*. *phoenicea* and *Q*. *macrolepis* chronologies were calculated over a shorter time interval (1947–1995, and 1943–1995, respectively) to accommodate the shorter length of the available tree-ring and precipitation data for these sites.

The stability of the climate signal in each of the tree-ring chronologies was also computed in DENDROCLIM by computing the response functions using a moving interval with different base lengths of 52 (the minimum available interval), 60, and (when data was available) 70 years. Therefore, the program calculates climate response functions for multiple 52, 60, or 70-year increments that are progressively slid backward by one year over a set period of time (Biondi and Waikul 2004). Moving interval response functions for each chronology were computed between the years 1930 and 2008 for the pine chronologies, or between 1930 and 1995 for the Bani Kenana chronology of Touchan and Hughes (1999). The overlap between Touchan et al.'s (1999) *Juniperus phoenicea* chronology and available meteorological data is too short to calculate moving interval response functions in the DENDROCLIM program. Since the SSS of five of the chronologies (Ben Shemen-*P*. *brutia*, Daliyat al-Carmel, Tel Shimron, Nes Harim-*P*. *brutia* and *P*. *halepensis*) is below 0.85 until after 1930 (Table 2.4), moving interval response functions were calculated from the year in which SSS >0.85 until 2008 for each of these sites.

Inter-Site and Inter-Species Growth Variability

Variability in tree-ring growth among different species and among different sites was evaluated using multiple different statistical analyses, including Pearson

correlation and multivariate techniques, specifically principal component analysis (PCA) and hierarchical cluster analysis (HCA). All analyses were conducted over a common period of AD 1943–2008. This time period was selected, so that each chronology would have adequate sample depth, particularly in the earliest years of the chronologies, while still maximizing the number of years analyzed.

Inter-site and inter-species correlation was measured by determining the Pearson correlation coefficient (r) between chronologies. Correlation was calculated over the entire overlapping time period available for each pair of chronologies as well as over the shorter AD 1943–2008 common period, in order to examine the effects of increasing the number of overlapping years. Although their overlapping periods (n=53) with the other chronologies are shorter than the 66-year common period, correlation values were also calculated for the Valonia oak and red juniper chronologies of Touchan and Hughes (1999) and Touchan et al. (1999) for the period of AD 1943–1995.

Hierarchical cluster analysis (HCA) and principal component analysis (PCA) were performed to sort chronologies into meaningful groups and subgroups. Both analyses were performed over the 1943–2008 common period and again over a shorter common period of 1943–1995, so that the present study's chronologies could be compared with the *Q. macrolepis* and *J. phoenicea* chronologies of Touchan and Hughes (1999) and Touchan et al. (1999).

HCA was used as an initial means of exploratory data analysis, in order to identify which chronologies had greatest similarity to one another. After testing multiple linkage methods (which yielded very similar results) (Rencher 2002: 456–

479), Ward's method linkage of cluster analysis was selected for analyzing the chronologies, in order to prevent reversals and minimize variance and influence of outliers.

PCA was performed for the correlation matrix of the 10 residual pine chronologies, in order to evaluate shared variance among the chronologies. The most representative principal components from the PCA, which explain most of the variance in tree-ring growth, were selected according to Kaiser's rule, where eigenvalues >1 are retained (Kaiser 1992). VARIXMAX rotation was then performed on the retained components. This operation rotates the retained number of principal components and makes the distribution of explained variance among the retained components more uniform, thereby aiding in the interpretation of individual chronology loadings on each eigenvector.

RESULTS

Tree-Ring Chronologies

The length, number of samples, and the general statistics of each chronology are given in Tables 2.2 and 2.4. The residual chronologies are plotted in Figure 2.3.

Touchan and Hughes' (1999) *P. halepensis* chronology from Dibeen has excellent correlation (r=0.79; n=75; p<0.001) with this study's chronology. Likewise, the Mt. Carmel chronology from *P. halepensis* sampled for this study has excellent correlation (r=0.77; n=82; p<0.001) with Touchan and Hughes' (1999) *P. halepensis* chronology from Mt. Carmel, and since their chronology was sampled from a different location in the Mt. Carmel Reserve, their sequences are included in the Mt. Carmel chronology analyzed here. This study's new tree-ring chronologies from Dibeen and

Mt. Carmel both lengthen the chronologies that Touchan and Hughes (1999) developed for these sites and update them to include the last 16 years of tree-ring growth with greater sample replication.

Table 2.4. Descriptive statistics for the samples and chronologies (site codes listed in Table 2.1). First order autocorrelation (AC1) is calculated from the standardized chronology. All other statistics are calculated from the residual chronologies, in which significant autocorrelation in each tree-ring time series has been removed.

Site code	Standard deviation	Skewness	Kurtosis	Mean sample segment length	Mean inter-series correlation	1st year SSS >0.85	MS	AC1
BAK-QUMA[a]	0.199	0.02	0.09	71	0.260	1924	0.222	0.191
BAR-JUPH[a]	0.240	0.02	0.04	326	0.438	1549	0.288	0.394
BSH-PIBR	0.194	-0.18	-0.33	59	0.480	1933	0.258	0.251
BSH-PIHA	0.238	0.00	-0.18	75	0.478	1930	0.278	0.249
CAR-PIHA	0.016	0.01	-0.10	68	0.407	1911	0.209	0.198
DAC-PIPN	0.161	-0.01	-0.28	66	0.516	1936	0.221	0.270
DIB-PIHA	0.211	-0.14	-0.11	74	0.541	1915	0.272	0.297
IMR-PIHA	0.202	-0.05	0.02	82	0.539	1851	0.242	0.294
JEZ-PIHA	0.027	0.15	-0.13	64	0.542	1938	0.330	0.129
NHM-PIHA	0.180	0.00	-0.35	62	0.449	1943	0.231	0.247
NHM-PIPN	0.231	0.01	-0.30	63	0.614	1941	0.276	0.279
RHN-PIHA	0.204	0.01	0.08	80	0.469	1914	0.235	0.275

[a] **Tree-ring measurements from Touchan et al. (1999) and Touchan and Hughes (1999).**

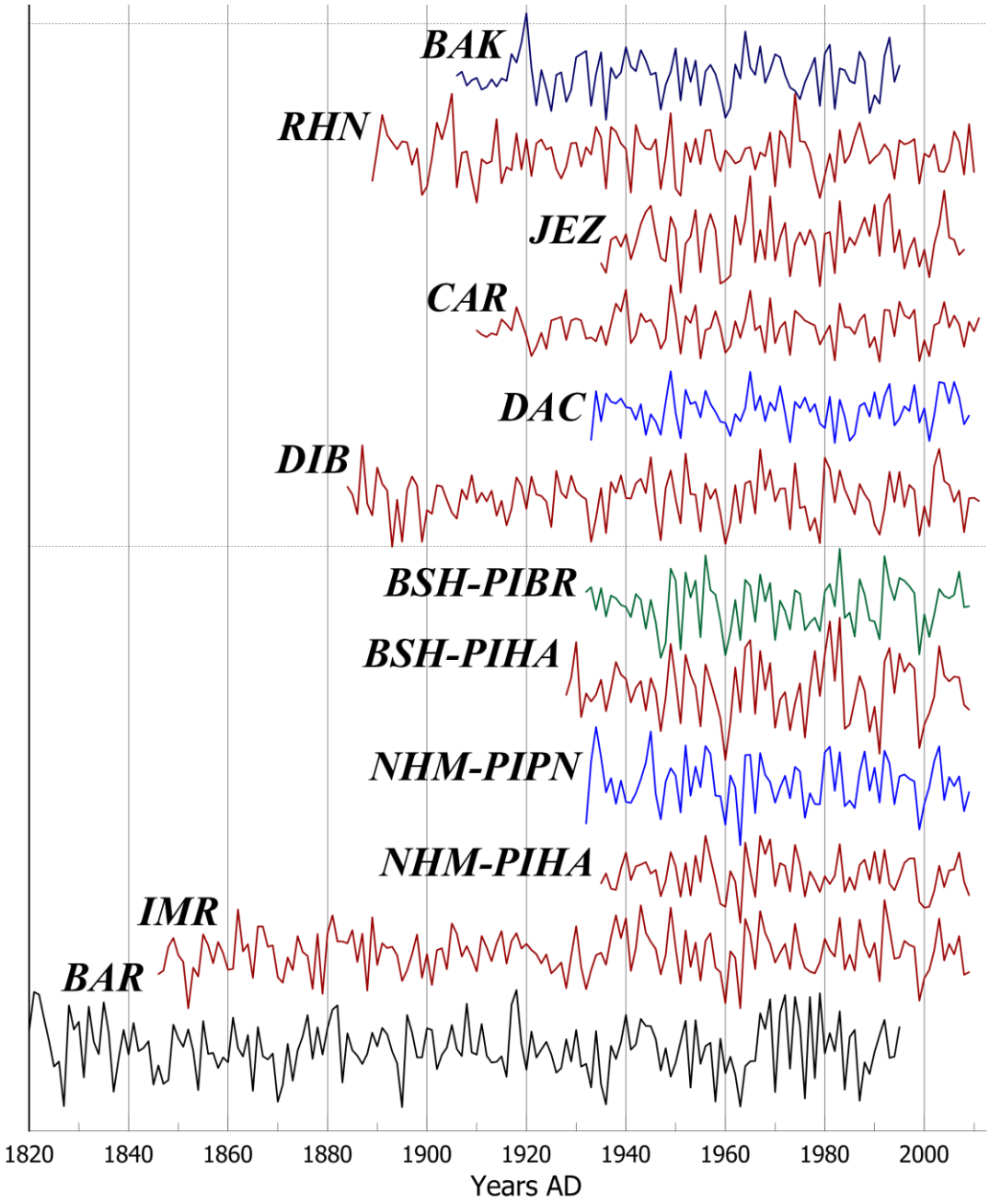

Figure 2.3. Residual site chronologies from the southern Levant with their relative measurements (site codes listed in Table 2.1). *Pinus halepensis* chronologies are shown in red, *P. brutia* chronologies in green, *P. pinea* chronologies in blue, *Q. macrolepis* in purple, and *Juniperus phoenicea* in black. Touchan et al.'s (1999) *J. phoenicea* extends back to 1469, but has been truncated to 1820 here, in order to display the chronology (relative to the other, much shorter chronologies) more clearly.

Touchan et al.'s (1999) 326-year *Juniperus phoenicea* chronology from the Shobauk plateau (BAR) is by far the longest tree-ring chronology in the southern Levant. The 164-year *Pinus halepensis* chronology from Masreq (IMR) built for the present study is the oldest pine chronology from a native forest recorded in the southern Levant so far. The *Pinus halepensis* chronologies from Dibeen (DIB) (128 years), Rosh HaNiqra (RHN) (122 years), and Mt. Carmel (CAR) (109 years) also are over a century in length. However, the mean ages of *P. halepensis* and *Q. macrolepis* sampled in the Israeli and Jordanian nature reserves (BAK, CAR, DIB, IMR, and RHN), and also the majority of the total number of trees sampled from each of these sites (i.e., both sampled trees included in the site chronologies and those that were not), are much younger and germinated after World War I during the mid-1920s through early 1950s. Therefore most of the trees in the nature reserves are approximately the same age, or even younger, than the oldest trees in Israel's planted forests.

Mean sensitivity is moderate for most of the chronologies, ranging from 0.209–0.288, and has little variation among different sites and different species. The exception is the *P. halepensis* chronology from Tel Shimron, which had higher mean sensitivity (MS=0.330). After de-trending (but prior to pre-whitening for the climate and series intercorrelation analyses), Touchan et al.'s (1999) *Juniperus phoenicea* chronology still has a first-order autocorrelation (AC1) value that is substantially higher than the AC1 values of the other chronologies analyzed here. This indicates that juniper tree-ring growth at Shobauk in a given year is more strongly influenced by growth during the previous year than at the other sites. This may occur, because the Shobauk Plateau is a more xeric environment, which may cause a lag in the recovery

of tree-ring growth after especially harsh drought years. Generally, there is little variation in the AC1 values among the pine and oak chronologies at different sites or between species.

Locally absent rings are most common in *P. halepensis* sequences from Masreq and in the *J. phoenicea* sequences from Shobauk, which are two of the most arid sites in the study area. Missing rings most frequently occur during known drought years (e.g., 1928, 1932, 1936, 1963, 1999, 2001), in which other tree-ring sequences from the Shobauk and Masreq sites (as well as those from other sites) have abnormally low ring-growth. Conversely, false rings and diffuse latewood are most common in younger, more robust *P. halepensis* and *P. brutia* samples. (Many of these samples were not included in the site chronologies analyzed below, because their sequences are highly complacent.) False rings are most common in trees sampled from Rosh HaNiqra and Ben Shemen. This may indicate that trees in this area have access to local water reserves during the dry season, or (in the case of Rosh HaNiqra) that the site more frequently receives early autumn rainfall before the main winter rainy season. False rings and diffuse latewood are extremely rare in *P. pinea* samples, likely because the species has a more fixed period of seasonal cambial activity than *P. halepensis*, whose cambial activity exhibits great plasticity, depending on soil moisture availability (De Luis et al. 2007; Liphschitz et al. 1984; see: discussion below).

Correlation Among Site Chronologies

Pearson correlation values among different sites and species over the 1943–2008 common period (along with the 1943–1995 common period for comparisons

against the Bani Kenana and Shobauk sites) are given in Table 2.5. The results show that there is generally significant correlation ($p<0.05$ and often $p<0.01$) among all site chronologies and across species. Strength in correlation is largely a function of distance (Figure 2.4), that is: correlation is generally higher between chronologies from sites that are closer to one another.

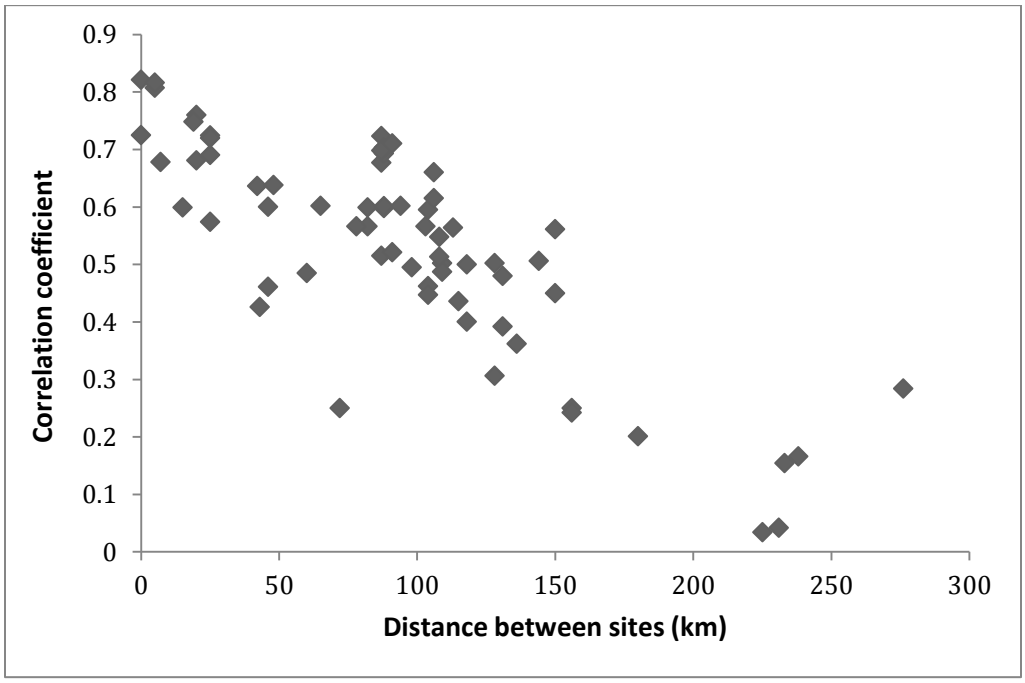

Figure 2.4. Pearson correlation values between tree-ring chronologies from different sites in the southern Levant (*y*-axis) as a function of the distance between the sites (*x*-axis).

Touchan et al.'s (1999) *Juniperus phoenicea* chronology from the Shobauk plateau (BAR) has overall poor correlation with most of the chronologies in the study area, except with IMR and both pine chronologies (*Pinus halepensis* and *Pinus pinea*) from Nes Harim (NHM), which are the southernmost pine chronologies in the study area and closer to Shobauk.

Table 2.5. Pearson correlation (*r*-value) and distance (km) among site tree-ring chronologies for the 1943–2008 common period. Correlation against the BAK and BAR chronologies is over a shorter 1943–1995 common period. Pearson correlation values marked with a '' indicate correlation significant at p< 0.05, while values marked with '*' are significant at p<0.01. Sites whose correlation is significant at p<0.05 or below are shaded in green.**

	BSH_PIHA										
BSH_PIBR	r= 0.821** 0 km	BSH-PIBR									
CAR-PIHA	*r*= 0.677** 87 km	*r*= 0.723** 87 km	CAR								
DAC-PIPN	*r*= 0.566** 82 km	*r*= 0.599** 82 km	*r*= 0.678** 7 km	DAC							
IMR-PIHA	*r*= 0.681** 20 km	*r*= 0.760** 20 km	*r*= 0.595** 104 km	*r*= 0.495** 98 km	IMR						
JEZ-PIHA	*r*= 0.598** 88 km	*r*= 0.601** 88 km	*r*= 0.748** 19 km	*r*= 0.599** 15 km	*r*= 0.566** 103 km	JEZ					
NHM-PIHA	*r*= 0.574** 25 km	*r*= 0.724** 25 km	*r*= 0.502** 109 km	*r*= 0.462** 104 km	*r*= 0.807** 5 km	*r*= 0.513** 108 km	NHM-PIHA				
NHM-PIPN	*r*= 0.690** 25 km	*r*= 0.720** 25 km	*r*= 0.487** 109 km	*r*= 0.447** 104 km	*r*= 0.816** 5 km	*r*= 0.548** 108 km	*r*= 0.725** 0 km	NHM-PIPN			
RHN-PIHA	*r*= 0.306* 128 km	*r*=0.502** 128 km	*r*= 0.558** 42 km	*r*= 0.461** 46 km	*r*= 0.506** 144 km	*r*= 0.426** 43 km	*r*= 0.561** 150 km	*r*= 0.450** 150 km	RHN		
DIB-PIHA	*r*= 0.693** 88 km	*r*= 0.703** 88 km	*r*= 0.636** 94 km	*r*= 0.515** 87 km	*r*= 0.698** 87 km	*r*= 0.566** 78 km	*r*= 0.521** 91 km	*r*= 0.710** 91 km	*r*= 0.436** 115 km	DIB	
BAK-QUMC	*r*= 0.660** *n*= 53 106 km	*r*= 0.615** *n*= 53 106 km	*r*= 0.602** *n*= 53 65 km	*r*= 0.485** *n*= 53 60 km	*r*= 0.564** *n*= 53 113 km	*r*= 0.600** *n*= 53 46 km	*r*= 0.400** *n*= 53 118 km	*r*= 0.500** *n*= 53 118 km	*r*= 0.250 *n*= 53 72 km	*r*= 0.638** *n*= 53 48 km	BAK
BAR-JUPH	*r*= 0.250 *n*= 53 156 km	*r*= 0.242 *n*= 53 156 km	*r*= 0.166 *n*= 53 238 km	*r*= 0.042 *n*= 53 231 km	*r*= 0.362** *n*= 53 136 km	*r*= 0.154 *n*= 53 233 km	*r*= 0.480** *n*= 53 131 km	*r*= 0.392** *n*= 53 131 km	*r*= 0.284* *n*= 53 276 km	*r*= 0.201 *n*= 53 180 km	*r*= 0.034 *n*= 53 225 km

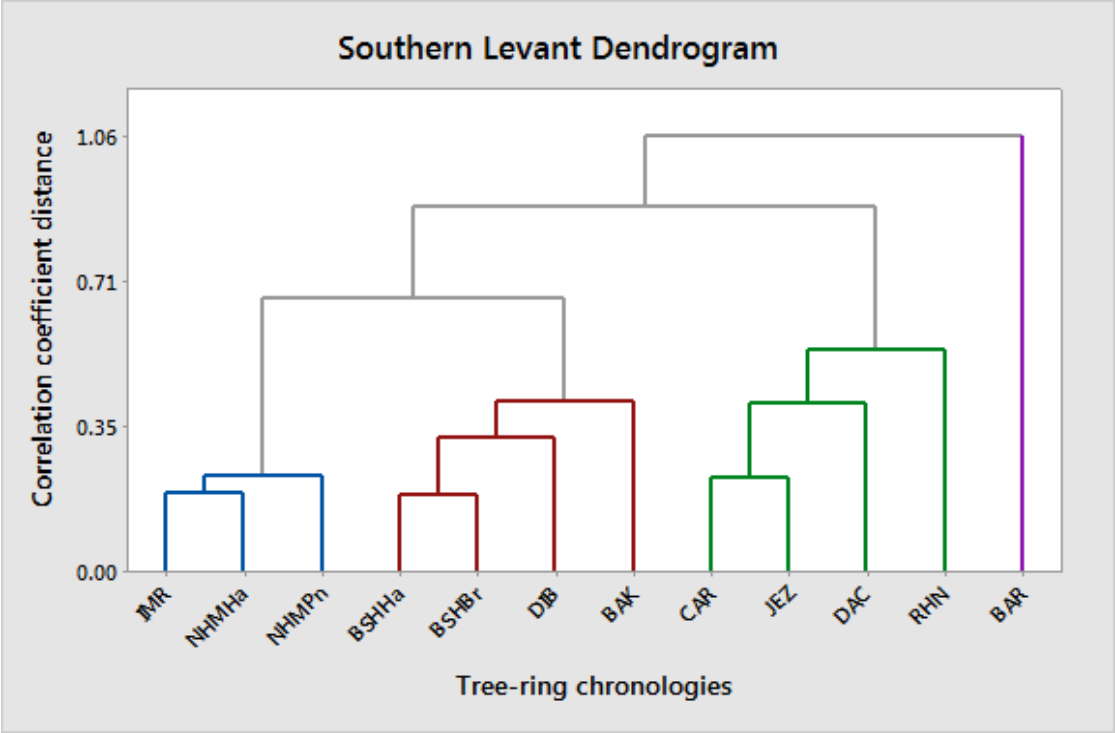

Figure 2.5. Dendrogram resulting from the cluster analysis (Ward's linkage method) of the tree-ring chronologies in the study area over the 1943–1995 common period. The names of the site chronologies are labeled using the site codes given in Table 2.1. In cases where there are chronologies of different pine species at the same site, the site code is followed by a species abbreviation (Ha= *Pinus halepensis*; Br= *Pinus brutia*; and Pn= *Pinus pinea*).

Hierarchical cluster analysis of the pine chronologies over the 1943–2008 common period (*not shown*) and of the pine, juniper, and oak chronologies over the 1943–1995 common period (Figure 2.5) reveal similar groupings for the chronologies. When all of the chronologies are included, two main groups and three additional subgroups are created. The Shobauk juniper chronology is placed in its own distinct group with the greatest correlation coefficient distance from all of the other chronologies. The remainder of the chronologies are placed into the following four subgroups: i) IMR and both NHM pine chronologies (*P*. *halepensis* and *P*. *pinea*); ii)

DIB, BAK, and both BSH pine chronologies (*P*. *halepensis* and *P*. *brutia*); and iii) CAR, JEZ, DAC; and RHN.

These subgroups are largely divided by latitude; one notable exception is the Bani Kenana (BAK) oak chronology. BAK is placed in the second sub-group (BSH and DIB), despite the fact that the site's location is closer to the sites in third sub-group (JEZ, CAR, DAC, and RHN). It is possible that this is because the BAK site is further inland and experiences greater drought stress than sites in the third subgroup, which are all within 25 km of the Mediterranean. In contrast, BSH and DIB are located further inland than sites in the third sub-group and slightly further south, so these sites have a more arid environment.

Principal component analysis of the pine chronologies over the 1943–2008 common period generates one principal component, which explains 64.4% of the variance in the original data set. The loadings for each individual chronology in PC1, 2, 3, and 4 are given in Table 2.6. All of the individual chronologies have a positive loading in PC1. RHN has the lowest loading in PC1, suggesting that a higher proportion of other (likely more site-specific) factors are responsible for explaining variance within the chronology. In general, though, the amount of variance explained by one principal component (i.e., eigenvalue >1) for all the pine chronologies suggests an overall coherence in the datasets and in factors creating inter-site and inter-species variability.

Table 2.6. Summary statistics of the PCA over the 1943–2001 common period for the *Pinus* spp. chronologies, and the individual loadings for each site. The principal component with the highest loading for each chronology is noted in bold. The names of the site chronologies are listed using the site codes given in Table 2.1.

Summary statistics	**PC1**	**PC2**	**PC3**	**PC4**
Eigenvalue	6.443	0.929	0.786	0.437
Proportion variance (%)	0.644	0.093	0.079	0.044
Cumulative variance (%)	0.644	0.737	0.816	0.859
Site code				
BSH-PIBR	**0.355**	-0.072	0.113	-0.071
BSH-PIHA	0.329	-0.032	**0.443**	-0.038
CAR-PIHA	0.324	**0.447**	0.019	0.113
DAC-PIPN	0.283	**0.479**	-0.009	-0.339
DIB-PIHA	0.321	-0.070	0.227	**0.698**
IMR-PIHA	0.343	-0.339	-0.053	-0.086
JEZ-PIHA	0.302	**0.362**	0.099	-0.176
NHM-PIHA	0.315	-0.358	-0.302	**-0.470**
NHM-PIPN	0.327	**-0.411**	0.060	0.059
RHN-PIHA	0.249	0.130	**-0.795**	0.341

When Touchan and Hughes (1999) and Touchan et al.'s (1999) chronologies from Shobauk and Bani Kenana are included in the PCA over a shorter common period of 1943–1995, this generates two principal components that together explain 70.1% of the variance in the original data set. The summary statistics and loadings for each individual chronology in PC1 and 2 after VARIMAX rotation are given in Table 2.7 and are plotted in Figure 2.6.

Table 2.7. Summary statistics of the PCA over the 1943–1995 common period, and the rotated principal components and individual loadings for each site retained in PCA. The rotated principal component with the highest loading for each chronology is noted in bold. The names of the site chronologies and species sampled are listed using the site codes given in Table 2.1.

Summary statistics	**PC1**	**PC2**
Eigenvalue	7.078	1.337
Proportion variance (%)	0.590	0.111
Cumulative variance (%)	0.590	0.701
Site code		
BAK-QUMC	**0.426**	-0.08
BAR-JUPH	-0.347	**0.594**
BSH-PIBR	**0.277**	0.198
BSH-PIHA	**0.318**	0.107
CAR-PIHA	**0.392**	0.012
DAC-PIPN	**0.371**	-0.020
DIB-PIHA	**0.281**	0.144
IMR-PIHA	0.122	**0.354**
JEZ-PIHA	**0.346**	0.067
NHM-PIHA	-0.018	**0.475**
NHM-PIPN	0.094	**0.371**
RHN-PIHA	0.077	**0.277**

In general, the individual loadings in PC1 and PC2 are divided along a latitudinal gradient. Chronologies sampled from the southern part of the study region have the highest loading in PC1, and chronologies from sites sampled toward the northern part of the study region have the highest loading in PC2. Touchan et al.'s (1999) *Juniperus phoenicea* chronology (BAR) has the highest loading of all of the chronologies in PC1. RHN is the only site from the northern part of the study area with the highest loading in PC2, although PC2 explains only 27.7% of year-to-year ring-width variance at this site.

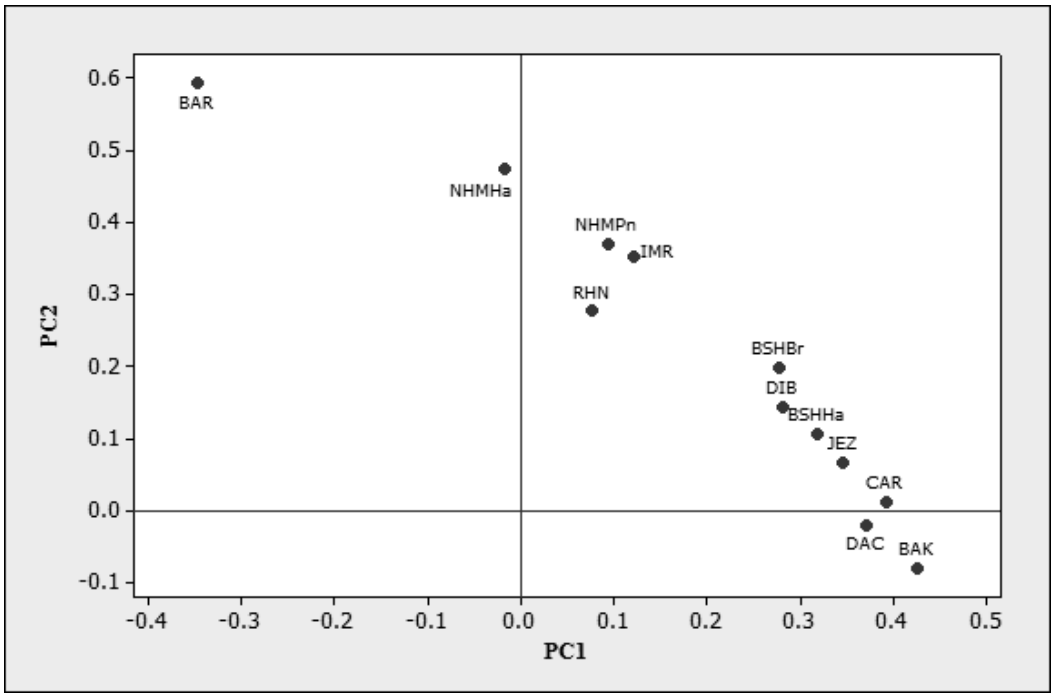

Figure 2.6. Biplot showing the relationship among the different tree-ring chronologies (labeled by site codes given in Table 2.1) for the common period 1943–1995 in terms of their individual loadings in PC1 (*x*-axis) and PC2 (*y*-axis). The names of the site chronologies are labeled using the site codes given in Table 2.1. In cases where there are chronologies of different pine species at the same site, the site code is followed by a species abbreviation (Ha= *Pinus halepensis*; Br= *Pinus brutia*; and Pn= *Pinus pinea*).

Climate response function analysis

Monthly temperature and precipitation values that have significant correlation ($p<0.05$) with each of the tree-ring chronologies over the 1943–2008 common period, and their relative stability over the moving intervals, are given in Table 2.8 (for individual response function plots for each chronology, see: Appendix 2.3).

Overall, both monthly precipitation and mean temperature are important factors influencing tree-ring growth in the SHAM forest zone. Tree-ring growth at all of the sampled sites is positively correlated with monthly precipitation values,

Table 2.8. Summary of significant response function coefficients of the 12 tree-ring chronologies to monthly precipitation and mean temperature anomalies over the 1943–2008 common period (1947–1995 for site BAR-JUPH and 1943–1995 for site BAK-QUMA). A '+' signifies significant positive correlation, while a '-' signifies significant negative correlation. Months shaded in gray had significant response function coefficients throughout the moving interval analysis; the length of the BAR chronology and corresponding climate dataset was too short for moving interval analysis in DENDROCLIM. The names of the site chronologies and species sampled are listed using the abbreviations given in Table 2.1.

Precipitation

Site	Oct	Nov	Dec	Jan	Feb	Mar	Apr	May	Jun	Jul	Aug	Sep	Oct
BAK-QUMA	+		+										
BAR-JUPH	+						+						
BSH-PIBR			+	+									
BSH-PIHA													
CAR-PIHA		+	+	+									
DAC-PIPN			+										
DIB-PIHA		+	+	+	+								
IMR-PIHA	+	+	+	+	+	+							
JEZ-PIHA		+	+	+									
NHM-PIHA				+									
NHM-PIPN			+	+									
RHN-PIHA													

Mean Temperature

Site	Oct	Nov	Dec	Jan	Feb	Mar	Apr	May	Jun	Jul	Aug	Sep	Oct
BAK-QUMA			-				-	-					
BAR-JUPH													
BSH-PIBR			-				-						
BSH-PIHA			-				-						
CAR-PIHA							-						
DAC-PIPN							-						
DIB-PIHA							-						
IMR-PIHA			-	-	-	-	-						
JEZ-PIHA				-									
NHM-PIHA				-			-						
NHM-PIPN				-									
RHN-PIHA							-	-					

meaning that higher (lower) monthly precipitation values correspond to wider (narrower) tree-ring widths. Significant correlations between precipitation and tree-ring growth are concentrated during the rainy season from October through April. The majority of the 12 chronologies have positive responses to either December (7) or January (7) precipitation, or both months (5), when the majority of annual rainfall occurs in the southern Levant. The moving interval response function analysis shows that this relationship is generally stable over time (Table 2.8).

Monthly mean temperature values also have significant negative correlation with tree-ring growth during at least one month for all of the chronologies, indicating that higher (lower) temperatures correspond to narrower (wider) tree-rings. In contrast, monthly maximum and minimum temperatures (*not shown*) yield less significant or no significant responses, and months in which there were significant responses for maximum monthly temperature are generally the same as those in which there are significant mean temperature responses. Nine of the twelve chronologies have significant negative responses to mean temperature in April (i.e., at the end of the rainy season). Chronologies from sites in the southern part of the SHAM forest zone (Nes Harim, Masreq, and Ben Shemen), as well as two of the low-altitude sites further inland in the north (Bani Kenana and Tel Shimron), also have significant negative responses to mean temperatures during December and January at the peak of the rainy season. However, tree-ring response to monthly mean temperature is generally less stable over time.

Climate response does not differ among the different pine species (*P. halepensis*, *P. brutia*, and *P. pinea*). Different species of pine at the same site overall respond to

the same monthly precipitation and temperature values, although chronologies from native forest sites are overall more climatically sensitive than the planted stands. The *P*. *halepensis* chronology from Masreq (IMR) near Jerusalem is the most climatically sensitive of the southern Levant chronologies; correlation between tree-ring growth and both monthly precipitation and mean temperature values is significant or nearly significant throughout most of the rainy season (October–April). The Dibeen (DIB) chronology is also climatically sensitive, but tree-ring growth at this site largely responds to precipitation, rather than temperature. The *P*. *halepensis* chronology from Tel Shimron (JEZ), which is a low-altitude inland site, is the most climatically sensitive of the planted forest sites and is most responsive to November–January precipitation and January mean temperature. In contrast, Rosh HaNiqra (RHN), unlike chronologies from the other native forest sites, is not climatically sensitive and has significant negative responses only to April and May mean temperature.

The climate response of Touchan and Hughes' (1999) *Quercus macrolepis* chronology Bani Kenana (BAK) differs slightly from the pine chronologies. Although the pines and oaks have similar positive and negative responses to precipitation and temperature, respectively, precipitation during the earlier part of the rainy season in October (and to a lesser degree, December) most significantly affects oak tree-ring growth. The oak tree-rings also have a significant negative response to temperature slightly later in spring during May than the pines.

Monthly precipitation is the main limiting factor for Touchan et al.'s (1999) *Juniperus phoenicea* chronology from the Shobauk Plateau (BAR). Tree-ring growth has significant positive correlation with precipitation values in October and especially

April, which mark the beginning and end of the rainy season in southern Jordan. The response function analysis did not yield any significant responses to monthly mean, minimum, or maximum temperature values, which corresponds with Touchan et al.'s results (1999).

DISCUSSION

Tree-Ring Chronologies and the Southern Levant's Environmental History

During the mid to late 19th century and early 20th century, several conflicts and industrial and technological developments led to multiples waves of large-scale deforestation throughout the northern and southern Levant. During the 1830s, the Egyptian general Ibrahim Pasha cut large portions of woodlands in Palestine (Karschon 1982; Rustum 1936) to use as fuel and timber for building the Egyptian naval fleet. From ca. 1876–1921, the Ottomans settled communities of Circassian immigrants in previously sparsely populated areas in modern-day northern Jordan and Israel (Khammash 1986; Shami 1992). These communities used native oaks and pine to construct buildings, wagons, and farm implements (Kaplan 1984; Khammash 1986). Meanwhile, the introduction and expansion of railroads during the late 19th century and early 20th century led to deforestation throughout the Levant, as trees were cut down for fuel and railroad ties. Deforestation escalated during World War I, as Ottoman forces used timber as building material to expand their military railway network and to fuel military train engines and irrigation pumps (Atkinson and Beaumont 1971; Cordova 2007; Karschon 1982, 1984; Liphschitz and Biger 2000). Trees that were not cut down were also damaged, as many of their lower branches were cut to supply additional firewood for railway engines (Karschon 1984).

Following World War I, afforestation efforts increased dramatically in the mandate of Palestine, primarily under the auspices of the Keren Kayemeth LeIsrael/Jewish National Fund (KKL/JNF), whose work had begun prior to the war in the early 20th century. Planting activity under the KKL/JNF escalated further in the 1950s, after the founding of the modern state of Israel in 1948 (Bonneh 2000; Liphschitz and Biger 2000; Orni 1978; Tal 2013). Although subsequent conflicts, agricultural development, grazing, and forest fires have led to destruction of, and injury to, forests in Israel, the establishment of protected nature reserves under the auspices of the Nature and Parks Authority and continued planting efforts have increased the country's overall forest cover (Bonneh 2000; Liphschitz and Biger 2000; Tal 2013; Weinstein-Evron and Lev-Yadun 2000). Tal (2013) estimates that forest cover in Israel/Palestine has increased from less than 37,00 hectares in 1920 to more than 153,800 hectares in 2011.

Post-World War I forest planting efforts also took place under the governments of the Emirate of Transjordan and (after 1946) the Hashemite Kingdom of Jordan (Cordova 2007). The Royal Society for the Conservation of Nature (RSCN) was established in 1966 to safeguard the country's natural resources and environment. Protected nature reserves were established under the RSCN beginning in 1968 and continuing especially during the 1980s–1990s (RSCN 2008). The Dibeen Nature Reserve was established most recently in 2004, expanding the protected forest area from a smaller protected recreation area established in 1975 (RSCN 2008). In the last five years, the RSCN, in collaboration with US Forest Service, has begun intensive inventories of forest structure and biomass in reserves in northern Jordan at Dibeen

and Ajloun (DeMeo et al. 2010; Triepke et al. 2012). The RSCN and Jordanian army also continue afforestation and forest planting campaigns (FAO 2010, 2013; RSCN 2008).

Estimates of forest cover change in modern Jordan from World War I to the present are difficult to quantify, since different surveys in the country have classified areas as "forest" using different criteria (Atkinson and Beaumont 1971; Cordova 2007; Khresat et al. 2008). As of 2011, forest cover in Jordan is estimated at 97,500 hectares (FAO 2013). Atkinson and Beaumont (1971) estimate that forest cover in Jordan was approximately 251,300 hectares in the late 1960s, which is more than 2.5 times greater than the FAO's (2013) modern forest cover estimates. Khresat et al.'s (2008) analysis of forest cover change in northwestern Jordan through satellite imagery and review of records from the Jordanian Ministries of Agriculture and Environment also suggests loss of forest cover. They estimate that forest cover in their 5,830-hectare study area decreased from approximately 2,449 to 2,273 hectares from 1953 to 2002, largely as the result of forest being converted into agricultural land (Khresat et al. 2008). However, it should be noted that the forest cover in the entire country of Jordan has remained more or less unchanged at 97,500 hectares since 1990 (FAO 2010, 2013).

Consequently, although fragments of native, old-growth forest are present in the southern Levant, the majority of forest cover, particularly of *Pinus halepensis*, likely germinated following widespread deforestation events in the late 19th–early 20th centuries. The pine and oak samples analyzed here corroborate the regional ecological history outlined above. Most of the samples germinated following World War I, and many of the trees sampled from Israeli forests germinated in the 1950s during the

large escalation in afforestation, abandonment of farmlands, and establishment of larger nature reserves. Thus, many trees sampled from the nature reserves (Dibeen, Masreq, Mt. Carmel, and Rosh HaNiqra) are no older than many of the trees in the planted forest areas. Many of the pines in the nature reserves may therefore be either the offspring of the older, fragmentary native stands, or of older planted *Pinus halepensis*, which includes several nonnative genetic provenances of the species, mainly from north Africa, Italy, and Greece (Lavi et al. 2005). Touchan and Hughes (1999) and Kaplan (1984) also found that very few *Quercus macrolepis* trees in northwestern Jordan and the Golan Heights pre-date World War I. Additionally, Kaplan (1984) notes that the majority of the oaks in the Yehudia Reserve in the Golan (near Bani Kenana in Jordan) had re-sprouted during the 1930s–1950s from the stumps of previously cut trees.

It is suggestive that the oldest pines sampled from the Masreq Reserve germinated after 1840, when the Ottoman Empire regained control of Palestine, and Muhammad Ali's Egyptian forces were no longer culling ship timbers from the Levantine forests. Older pine samples from Masreq, Dibeen, and Mt. Carmel, as well as Touchan and Hughes' (1999) oaks from Bani Kenana, also show clear signs of injury and disturbance, including resin pockets, traumatic resin ducts, and fire scars during the 1890s and World War I, which would suggest that their branches were likely cut for fuel, and the surrounding forest area was affected by increasing demands for fuel with the development of the railroads.

Sub-humid/semi-arid Mediterranean (SHAM) forest zone

Soil water availability is a key environmental factor influencing cambial activity and wood formation in the Mediterranean forests (De Luis 2007, 2011; Rathgeber et al. 2004; Schiller and Cohen 1995, 1998). In the southern Levant there are dramatic seasonal fluctuations in water availability. Trees must endure a dry period, in which there is severe water deficit, for half or more of the entire year, while precipitation (which replenishes soil water content) is largely concentrated in December and January. Although water can move out of an ecosystem as surface or sub-surface runoff, studies analyzing water balance in forests in sub-humid and semi-arid forest zone (SHAM) in the southern Levant indicate that the majority of water loss in many of these areas is from evapotranspiration (Schiller and Cohen 1995, 1998; Schiller et al. 2010; Ungar et al. 2013). Consequently year-to-year changes in climatic factors that have an important impact on the input and removal of water available to the tree (i.e., the site's water balance) also have a critical influence on annual tree-ring growth at that site.

This is apparent in the response function analysis. For most of the chronologies in the SHAM zone, precipitation has the most significant impact on tree-ring growth. This is consistent with the results of Touchan et al. (1999), Touchan and Hughes (1999), and Tamari (1976), who found a strong correlation between annual precipitation and tree-ring growth in the *Quercus macrolepis*, *Pinus halepensis*, and *Juniperus phoenicea* trees that they sampled from a smaller subset of the tree-ring network presented here. Furthermore, the response function analysis presented here

shows that overall, precipitation in December–January (and, to a lesser degree, November), i.e., the months with the highest rainfall, has an especially critical influence on year-to-year ring growth. This relationship is also generally consistent over time.

The beginning and end of the rainy season and precipitation distribution during autumn and spring months have greater year-to-year variability, while the majority of annual precipitation is consistently during December–January. Consequently, if there is little precipitation during December–January, rainfall during either autumn or spring months will generally not be adequate to make up for the deficit in the soil water content of that given year, leading to narrower ring growth.

Mean temperature, particularly during December–January and April–May, also has an important influence on tree-ring growth in the study area. During winter months, cambial activity in *Pinus halpensis* (as well as the other species analyzed in this study) will cease if temperatures are too cold, and photosynthesis is inhibited (De Luis 2007; Fahn 1953; Lev-Yadun 2000a; Liphschitz et al. 1984). However, mild winters allow trees to maintain efficient winter photosynthesis, and their cambiums remain active (Lev-Yadun 2000a; Schiller and Cohen 1995, 1998; Schiller et al. 2007). High winter temperatures can increase the atmosphere's evaporative demand (i.e., raise *PET*), which both causes loss in soil water content and increases the tree's transpiration rate. In turn, the tree's water use efficiency (that is: the ratio of the amount of biomass that the plant produces to the rate of transpiration) is lowered (Lambers et al. 2008).

The fact that many of the chronologies in the study area have a negative response to winter temperatures suggests that narrow ring growth does not primarily result from cold temperatures limiting photosynthesis. Instead, these negative responses likely indicate the negative effects of water stress and lowered water use efficiency on tree-ring growth. It is also notable that the sites in the SHAM forest zone that do not have significant negative responses to winter temperature are either adjacent to the Mediterranean coast (DAC, CAR, and RHN), or a mid-to-high-altitude site (DIB). The higher humidity of sites along the Mediterranean coast contributes to lower winter *PET*, so that tree water use efficiency is likely not lowered as dramatically during dry winters compared to sites further inland. The trees sampled at Dibeen grow at higher altitudes than those of most of the other sites analyzed here, and winter temperatures and winter *PET* at Dibeen are generally lower than at those at other sites in the SHAM forest zone. The lack of significant radial growth responses to winter temperatures by the Dibeen pines indicates that the site's comparatively lower winter temperatures (which contribute to lower winter *PET*) likely do not lower water use efficiency as dramatically as at other inland sites with warmer winters.

The months of April–May mark the end of the rainy season in the southern Levant, when water input to the soil from precipitation reduces and eventually ceases. Mean temperatures steadily rise during the transition to the summer dry season (Goldreich 2003). The atmosphere's evaporative demand and the tree's transpiration rate rise, and soil water content is depleted. Soil water content eventually drops so low that the tree's roots can no longer supply the tree with water. This induces

stomatal closure and reduction in the transpiration rate, such that photosynthesis eventually ceases (Schiller and Cohen 1995, 1998).

Schiller and Cohen (1995, 1998) observed a sharp drop in the transpiration rates of *Pinus halepensis* in Israel shortly after the last rainfall (>30 days), at which point most of the available water in the main root zone had been extracted. They concluded that the photosynthetically productive period of pine forests in the southern Levant is limited to the rainy season and a short period after the last rainfall, whose length is dependent on soil water content and soil water holding capacity (Schiller and Cohen 1995, 1998).

The common negative response to April temperature (in all but one of the chronologies in the SHAM forest zone) likely relates to the effect of temperature in raising or lowering *PET*. Abnormally warm temperatures during the April–May transition season contribute to higher *PET* and shorten the period of time after the last rainfall in which there is sufficient water available for the tree to remain photosynthetically productive (effectively shortening the tree's growing season). Such high temperatures in late spring (particularly April–June) in the southern Levant may sometimes occur due to greater incidence during these months of hot, dry easterly winds (referred to as *kadim* in Hebrew, or *shurkiyeh* in Arabic) and dust-storms in the southern Levant, followed by a (sometimes severe) dry heat wave (a *sharav* or *khamsin*) that may last for several weeks (Goldreich 2003).

Investigations in Israel on the seasonal dynamics of cambial growth in *Pinus halepensis* (Gindel 1944, 1947; Lev-Yadun 2000; Liphschitz and Lev-Yadun 1986; Liphschitz et al. 1984; Oppenheimer 1945) corroborate the key role of water

availability in affecting annual tree-ring growth. These studies indicate that the cambial activity of *Pinus halepensis* and (also likely) *Pinus brutia* largely responds to local climatic conditions and (particularly) water availability, rather than keeping a set dormancy period. In the southern Levant, *P. halepensis* tree-ring growth begins with the wet season in October–November. The cambium becomes quiescent in mid-winter (December–February) if temperatures are too cold. Cambial activity continues until the beginning of the dry season, when the cambium enters a second rest period, and the ring border is formed. However, if sufficient water is available, the cambium of *Pinus halepensis* will remain active throughout the entire year (Liphschitz and Lev-Yadun 1986; Liphschitz et al. 1984). Studies elsewhere in the Mediterranean (e.g., Attolini et al. 1990; De Luis et al. 2007; Esteban et al. 2010) found similar plasticity in the seasonal cambial activity of *Pinus halepensis*.

Pinus pinea growing in Israel has a set dormancy period during the colder rainy season (October–March) that is more characteristic of trees growing in temperate climates (Liphschitz et al. 1984). Although the cambium of *Pinus pinea* resumes activity later in the rainy season than *Pinus halepensis*, the similar climate response function results for the *Pinus halepensis*, *Pinus brutia*, and *Pinus pinea* chronologies in the present study indicate that site water balance–and in turn, the climate variables that critically influence water balance–exerts an important influence the radial growth of all three pine species (at least for the mature, dominant crown classes sampled for this study). De Luis et al. (2009) also note that the radial growth of mature, dominant crown classes of *P. pinea* and *P. halepensis* in Spain have similar climate responses and sensitivity. Piraino et al. (2012) and Sarris et al. (2011) report similar

dendroclimatic responses related to water balance (i.e., positive responses to rainy season precipitation and negative responses to mean temperature) from *Pinus pinea* and *Pinus brutia* growing in xeric sites in Italy and Greece, respectively.

Seasonal cambial activity, water use, and photosynthesis in *Quercus macrolepis* is more restricted than that of the sampled pine species, since *Quercus macrolepis* is winter deciduous. Oak leaf senescence in northern Israel and Jordan generally occurs around November-December. Initial bud break occurs in February, and leaves and twigs grow to their full size by the end of March–beginning of April (Kaplan 1984; Kaplan and Gutman 1999; Schiller et al. 2007). Transpiration rates increase steadily from leaf flush, reach peak values during April–mid-August, and then decline drastically to low values until autumn leaf abscission (Schiller et al. 2007, 2010). Cambial activity in *Quercus macrolepis* generally initiates in mid-February, and earlywood growth occurs until mid-May (Fahn 1953). Latewood growth continues until about mid-August, when the cambium becomes dormant (Fahn 1953). According to Schiller et al. (2007), *Quercus macrolepis* is able to remain physiologically productive by growing primarily in porous chalky rock and deep soil pockets that retain water from the rainy season and facilitate efficient water movement to the tree roots.

Since there is little to no rainfall after April in the southern Levant, it is not surprising that tree-ring growth at Bani Kenana has a significant positive response to precipitation during one of the rainiest months of the hydrological year (December). Tree-ring growth at Bani Kenana also has a significant (although temporally unstable) response to October precipitation. This may occur, because in years of abnormally

high October rainfall, the trees may be able to produce and store extra reserves of carbon prior to leaf abscission. Since *Quercus macrolepis* maintains high transpiration rates later into the summer dry season than *Pinus halepensis*, late spring temperatures (which, as described above, modulate evapotranspiration and, in turn, water use efficiency) may have a greater impact on oak radial growth. This may explain the significant negative temperature responses of *Q. macrolepis* in both April and May.

Overall, climatic sensitivity–measured in terms of their calculated mean sensitivity, first-order autocorrelation, and number of months with significant climate response function–is relatively uniform among the different pine species and oak growing in similar geographic locations in the SHAM forest zone. Instead, variation in tree-ring climatic sensitivity is largely based on site bioclimatic conditions. For instance, the Dibeen and especially the Masreq chronologies are both located in more arid bioclimatic zones away from the coast with lower annual precipitation and are therefore much more climatically sensitive. Conversely, the Rosh HaNiqra chronology, which is in a more humid bioclimatic zone with a slightly shorter dry season (*LDS*=6), is not particularly climatically sensitive.

However, anthropogenic impact also plays a role in tree-ring climatic sensitivity at some of the sites in the SHAM forest zone, since the planted stands are generally less climatically sensitive (i.e., they have fewer significant responses to monthly temperature and precipitation). For instance, the *Pinus halepensis* chronologies from Ben Shemen and Nes Harim may include trees that belong to genotypes from North Africa that are more drought resistant (Schiller 1982, 2000).

Cold semi-arid Mediterranean (CSAM) forest zone

Touchan et al.'s (1999) *Juniperus phoenicea* chronology differs from the tree-ring chronologies collected from the SHAM zone. The juniper chronology's AC1 value is much higher than the other site chronologies, indicating that climatic conditions from the previous year(s) have a greater impact on juniper radial growth in a given year than on those of pine and oak in the SHAM forest zone. The juniper chronology's MS value is also higher than those of the pine and oak chronologies from the SHAM forest zone, meaning that juniper ring growth has higher year-to-year variability.

The juniper chronology's high sensitivity likely occurs, because the CSAM zone is a more xeric environment, where there is high year-to-year variability in precipitation and more severe drought episodes than in the SHAM forest zone. Drought episodes can lead to defoliation (needle shedding) and stomatal closure, which reduces photosynthetic carbon uptake, and deplete a plant's stored carbon reserves (Galiano et al. 2011; McDowell et al. 2008). Both canopy defoliation and reduction of carbon reserves limit the tree's capacity to create new photosynthetic tissue (and in turn, produce new xylem tissue), which may result in reduced radial growth in years following severe drought episodes.

Precipitation is clearly the main climatic factor limiting juniper radial growth, corroborating the results of Touchan et al. (1999). However, unlike the pine and oak chronologies from the SHAM zone, juniper tree-ring growth has significant responses to April and October precipitation, rather than December–January precipitation. Since the Shobauk site receives lower annual precipitation (with greater year-to-year

variability), tree-ring growth may be more limited by when the rainy season begins (October) and ends (April) and therefore the total length of time during which water is available in the soil. Previous physiological studies (Baquedano and Castillo 2007) comparing *J. phoenicea* and *P. halepensis* have shown that *J. phoenicea* is the more drought tolerant of the two species and capable of water uptake in drier environments at lower water pressure potential values. Therefore it is also possible that the Shobauk junipers can continue water uptake later in the spring than pine and oak species, so precipitation during these later months is critical to juniper ring growth.

Junipers growing at high altitudes in the CSAM zone also experience colder winters and lower winter *PET* than pines and oaks in the SHAM zone. The shallow soils and rocky slopes in which the junipers grow contribute to significant loss of water through surface runoff, particularly in years when annual precipitation is largely the result of short, intense storm systems (Touchan et al. 1999; Wade et al. 2011). These important hydrological differences in the CSAM and SHAM zones likely explain the juniper chronology's lack of significant responses (particularly negative responses) to mean winter temperature. The CSAM zone's cold winter temperatures (particularly in December and January) also likely inhibit photosynthesis and induce a winter quiescent phase of cambial activity in the junipers, which may explain the lack of significant responses in radial growth to precipitation during these cold winter months. However, future research investigating seasonal cambial activity and water use of *Juniperus phoenicea* in Jordan and the Sinai (where relict populations of this species also grow) (El-Bana et al. 2010) is needed to help explain the physiological responses of these trees to climate more fully.

Spatial and Inter-Species Correlation

The patterns resulting from the Pearson correlation, PCA, and HCA are generally independent of species and instead are grouped largely with respect to bioclimatic gradients over the study area. The strong, macro-scale common growth signal among different site chronologies that occurs even among different species indicates that climate is the common factor contributing to year-to-year ring-width variation, which Touchan and Hughes (1999) also suggested, based on their analysis of a sub-set of the tree-ring datasets analyzed here. The similar climate response functions of different pine and oak species in the SHAM forest zone support this assertion.

The two major groups emerging from correlation analyses correspond to the two major bioclimatic zones in the study area. The first dendrochronological group consists of tree-ring chronologies in the SHAM forest zone in the northern and central parts of the study area (referred to here as 'SoLevant A'), while the Shobauk chronology in the CSAM zone in southern Jordan comprises the second group (referred to here as 'SoLevant B') (Figure 2.7). Correlation between 'SoLevant B' and most of the chronologies in 'SoLevant A' is not significant, except for the southernmost sites in 'SoLevant A' (i.e., Masreq and the Nes Harim pine chronologies). These sites are closest to the Shobauk site and are located in a more arid bioclimatic zone than the other sites in 'SoLevant A.'

The critical role of water availability (particularly precipitation) on tree-ring growth exhibited in the response function analysis is also clearly demonstrated in the spatial grouping of the area's tree-ring records. The boundaries of the southern

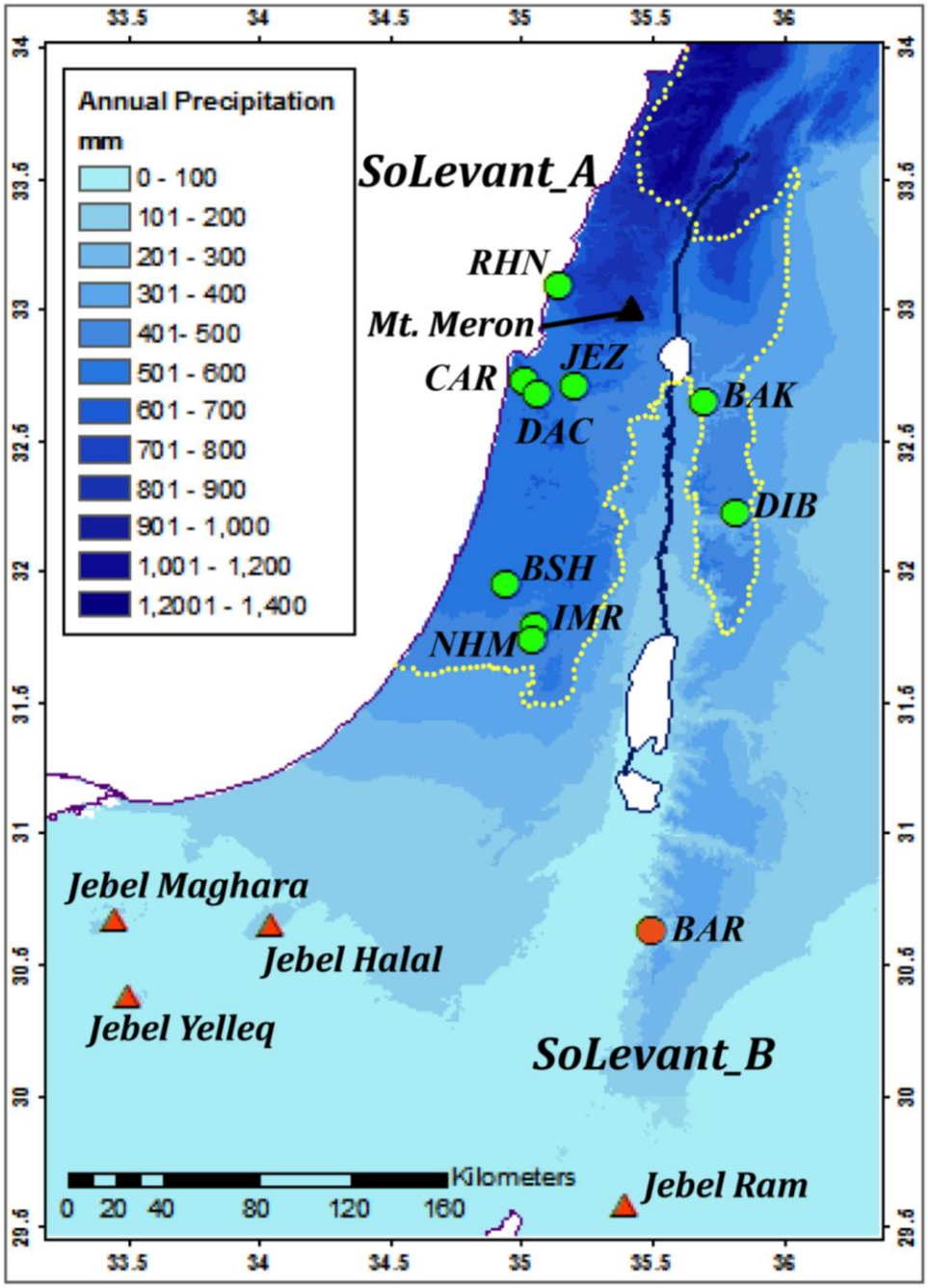

Figure 2.7. Dendrochronological zones, 'SoLevant_A' and 'So_Levant B' identified in this study in relationship to the distribution of annual precipitation in the southern Levant (adapted from the dataset of Hijmans et al. 2005). The boundaries of 'SoLevant_A' are indicated by the dotted yellow line. 'SoLevant_B' likely includes relict Mediterranean forest stands in the Sinai and southern Jordan (*orange triangles*). Mt. Meron in northern Israel (*black triangle*) may also have a unique tree-ring signal because of the area's cooler, more humid microclimate. Sites are labeled using the abbreviations given in Table 2.1.

Levant's dendrochronological zones follows closely the boundaries of the precipitation regions for Jordan given by Freiwan and Kadıoğlu (2008), who separated the 'northern region' (i.e., the area in 'SoLevant A') and Shobauk (i.e., the area in 'SoLevant B') into two precipitation zones, but considered them to be one major region with "a remarkable rainfall gradient."

Within the dendrochronological group 'SoLevant A,' there is an overall high coherence in the tree-ring signal, with small variations due to site location along (primarily) the north-south latitudinal gradient, over which aridity increases toward the south. There is smaller variation in the tree-ring signal along the west-east longitudinal gradient. These results match the analysis of annual rainfall variability by Black et al. (2011) and Enzel et al. (2003), who found a high degree of spatial coherence in rainfall in the northern and central region of the southern Levant and greater north-south rainfall variability. The distance over which correlation among tree-ring chronologies remains significant (ca. 100–150 km) also closely mirrors the distance over which Black et al. (2011) and Enzel et al. (2003) found annual rainfall to be spatially coherent in the southern Levant.

However, site properties (e.g., slope gradient and exposure, soil water holding capacity, and bedrock lithology) also have an important influence on water availability and, consequently, tree growth that is apparent particularly at local (i.e., within site) and meso-scales. Schiller (1982) found that the moisture-retaining characteristics of soil and bedrock have a critical effect on the mean height and diameter at breast height (DBH) of *Pinus halepensis* trees growing in multiple sites in Israel. Sites located on chalk and marl bedrock offer more favorable growth environment than locations on

dolomite or limestone. This is because chalk and marl have higher porosity and lower permeability than dolomite and limestone. Consequently, water may be retained in deep fissures and soil pockets in chalk and marl bedrock, offering a continuous water supply to deep-rooting trees like *Pinus halepensis* and *Pinus brutia*, long after soil water content has been depleted during the dry season (Schiller 1982). "Nari" (calcrete hardpans typically overlying chalk formations) in the bedrock can slow tree growth, since these hard crusts hinder development of deep root systems and lower bedrock permeability, promoting water loss through runoff (Schiller 1982; Schiller et al. 2007).

It is notable that the pines sampled at Rosh HaNiqra (RHN)–whose tree-ring sequences are less climatically sensitive and whose tree-rings had more false rings and rings with diffuse latewood than other sites–grow over chalk and chert bedrock. It was also observed that there was a thick layer of plant litter, particularly on the forest's lower slopes. Thus, both the bedrock and organic layer at Rosh HaNiqra likely facilitate the capture and storage of larger supplies of water that *Pinus halepensis* root systems may access (even during the dry season or during drought years), compared to other sites in the study area.

Slope gradient can also have an important influence on radial growth in the study area. For instance, pines sampled on Mt. Carmel from Givat Aizim have generally wide, complacent rings, in which there is frequently diffuse latewood, despite the fact that the soil at the site is *terra rosa* with a limestone bedrock and should therefore have low water holding capacity. In contrast, another stand of trees growing on Mt. Carmel near Bet Oren have narrower rings than those from Givat Aizim and generally lack diffuse latewood, even though they grow in a theoretically

more favorable rendzina soil and on a chalk and marl bedrock. This may occur because there are several breaks in the slope at Givat Aizim, where it was observed that water collects after winter rainstorms. The site is also downslope from a housing development (Ramat Begin) and may therefore receive runoff from this area.

Both local bedrock lithology and slope gradient certainly play a critical role in the distribution and growth of *Juniperus phoenicea* at Shobauk in the CSAM forest zone. The region's relatively smooth, non-porous limestone and sandstone direct rainfall as runoff into low-lying fissures containing soil pockets with higher water holding capacity than surrounding areas, which capture runoff and produce water-rich micro-environments that support junipers and other Mediterranean hydrophilous species (Danin 1999; Wade et al. 2011). Bedrock lithology and tectonic history also control the distribution and movement of the area's perennial springs. Streams in the Shobauk area largely occur along zones of contact between limestones and sandstone and fault-contacts between sandstones and Precambrian volcanic rocks. Such areas provide another important source of moisture for junipers and other hydrophilous plant species (Cordova 2007; Mithen et al. 2007; Wade et al. 2011).

Use in Dendrochronological Research Applications

The *Juniperus phoenicea* populations of southern Jordan and the Sinai are an especially valuable, long-lived species for reconstructing precipitation for the area within 'SoLevant B' and the southernmost area of 'SoLevant A,' which includes the area around Jerusalem. Since local historical buildings and archaeological sites around southern Jordan (e.g., Al-Bashaireh et al. 2011; Engel 1993; Khammash 1986; Lorentzen, *unpublished data*; Mithen et al. 2007; Warnock 2001) and southern Israel

(Baruch and Goring-Morris 1997; Lev-Yadun et al. 1995; Liphschitz 2007) contain ample remains of juniper, there is great potential for crossdating these timbers against modern forest chronologies, thereby extending both the juniper chronologies and precipitation reconstructions even further back in time. However, this species is highly sensitive and commonly forms locally absent and false rings–particularly in lower elevation sites or locations affected by the Red Sea trough (Goldreich 2003), where annual precipitation is more bimodal. Thus, careful sample selection, crossdating techniques (e.g., skeleton plotting, which is commonly used in the American Southwest; for description, see: Stokes and Smiley 1996), and independent dating verification with radiocarbon wiggle-matching (e.g., Wils et al. 2011) may be required to build such chronologies and climate reconstructions successfully.

Tree-ring chronologies from the 'SoLevant A' zone are still relatively short and require historical and archaeological samples to extend the tree-ring record back in time, in order to be useful for dendroclimatic reconstructions. The common tree-ring signal exhibited in the tree-ring chronologies in the 'SoLevant A' zone indicates that wood samples from trees growing in this zone may be dendrochronologically dated using 'SoLevant A' regional reference chronologies. However, because of the absence of extremely long-lived tree species in this zone, accomplishing this is a more challenging task than for 'SoLevant B'. *Pinus brutia*/*halepensis* wood has been found in historical and archaeological sites around the southern Levant (e.g., Liphschitz 2007; Lorentzen, *unpublished data*; Mor and Kahanov 2006; Warnock 2001), but based on historical records, it is likely that much of this material was actually imported from southern Turkey, which is part of a different dendrochronological zone (see:

Chapter 3). Additionally, since *Pinus halepensis* grows wide juvenile rings, finding timbers of these species (especially those that have been heavily worked and had their smaller, outer rings removed) with an adequate ring count (≥100 rings) for secure dendrochronological crossdating is difficult.

It may be more profitable to focus on building additional forest chronologies of *Quercus macrolepis* in the northern Galilee, Golan, and northern Jordan, since this species generally forms narrower rings and may be easier to use for long chronology building than *Pinus halepensis*. The oak chronologies can then be extended further back in time using historical timbers, like those found in the Circassian buildings in northern Jordan (e.g., Khammash 1986), Ottoman-era shipwrecks (Cvikel and Kahanov 2012; Rustum 1936), and earlier archaeological materials.

However, while *Pinus halepensis* is not the most widely used (nor always the most useful) species for dendroclimatic reconstructions, it is a widespread Mediterranean species that plays an important role in the region's forest ecosystems, and is valuable for regional afforestation, recreation, and as an economic resource. It is therefore useful to have greater information about how this species responds to climate and to identify areas that are particularly sensitive to climate. From this study, it is clear that the Masreq pines, and (to a lesser degree) also the Dibeen, Tel Shimron, and Mt. Carmel pines are particularly sensitive to climate, and that the pines from Masreq, Ben Shemen, and Nes Harim also have a significant negative radial growth response to high temperatures. Thus, trees in these specific areas may be more vulnerable to, and adversely affected by, projected rising temperatures and increased drought stress in the Mediterranean (Allen et al. 2010; Lindner et al. 2010).

Possible negative effects from drought stress are already observed at the Masreq Reserve. Many of the oldest trees studied here had crown die-back and produced so-called 'senescence signals' (Fish et al. 2010), in which tree-ring growth drastically declines, and where ultimately annual rings are produced and water uptake occurs on only a small part of the tree stem. This indicated that several of these older trees are at the end of their life cycle (and indeed, at least three of the trees have died already). Many of these samples started to decline after an especially hot, dry period from 1999–2001. Ungar et al. (2013) also observed drought-induced mortality in relatively young (<50 years) planted *Pinus halepensis* growing in the Yatir Forest, which is located south of the SHAM forest zone in Israel on the northern edge of the Negev Desert. Similar drought-induced mortality was also observed among juniper stands in the Sinai (El-Bana et al. 2010) and southern Jordan (Danin 1999) from the 'SoLevant B' zone. Increased drought severity and frequency may also make these pine forests more vulnerable to large forest fires, like that which destroyed parts of Masreq in 2001 and killed many of the oldest trees (including some trees that were sampled for this study) on Mt. Carmel in 2010.

CONCLUSIONS

The results from this study indicate that tree-ring patterns in the Mediterranean forest zone of the southern Levant may be divided into two main zones that correspond well with the regional precipitation. Tree-rings in the northern zone of the study region ('SoLevant A'), which includes Mediterranean forests on both sides of the Rift Valley, have a tree-ring signal that is generally coherent across species, planted and native forests, and geographic location, with small-scale variations along a

latitudinal gradient. The second dendrochronological zone ('SoLevant B') is located approximately below the 400 mm isohyet and south of the natural limit of *Pinus halepensis* in the southern Levant. Tree-ring chronologies from this zone, represented by the Shobauk juniper chronology in this study, do not have significant correlation with the tree-ring chronologies in the northernmost areas of the southern Levant, but have moderate correlation with trees growing at the southern border of the 'SoLevant A' zone.

Further research on relict juniper populations growing in the northern Sinai, as well as those growing at lower elevations and latitudes in the Eastern Highlands of Jordan (including at Jebel Ram), should be conducted to delineate the extent of the 'SoLevant B' zone. If suitable species for dendrochronological analysis with adequate sample replication can be found, tree-ring response to climate in the Rift Valley, as well as high elevation areas like Mt. Meron and the Golan, and the southern Lebanese coastal plain, should be analyzed to determine how they compare to the regional tree-ring responses described here.

The adverse effects of drought stress in the southern Levant may drastically alter the current forest landscape. Therefore development of suitable mitigation strategies–particularly for the climate sensitive forests in the southern 'SoLevant A' and 'SoLevant B' zones identified here–should be adopted to aid in the survival of these valuable forest ecosystems. Further development of multi-century and multi-millennia tree-ring chronologies in these zones will also provide proxy data for precise, long-term precipitation reconstructions that will improve our understanding of drought cycles and their effects on the southern Levant's forest ecosystems over the long-term.

APPENDIX 2.1

Climate diagrams showing mean monthly temperatures (*black line*), average monthly precipitation total (*dark gray bars*), and average monthly potential evapotranspiration (*light gray bars, shown as negative values*) calculated from each of the gridded CRU datasets and the Shobauk meteorological station in the study area and used in the response function analysis.

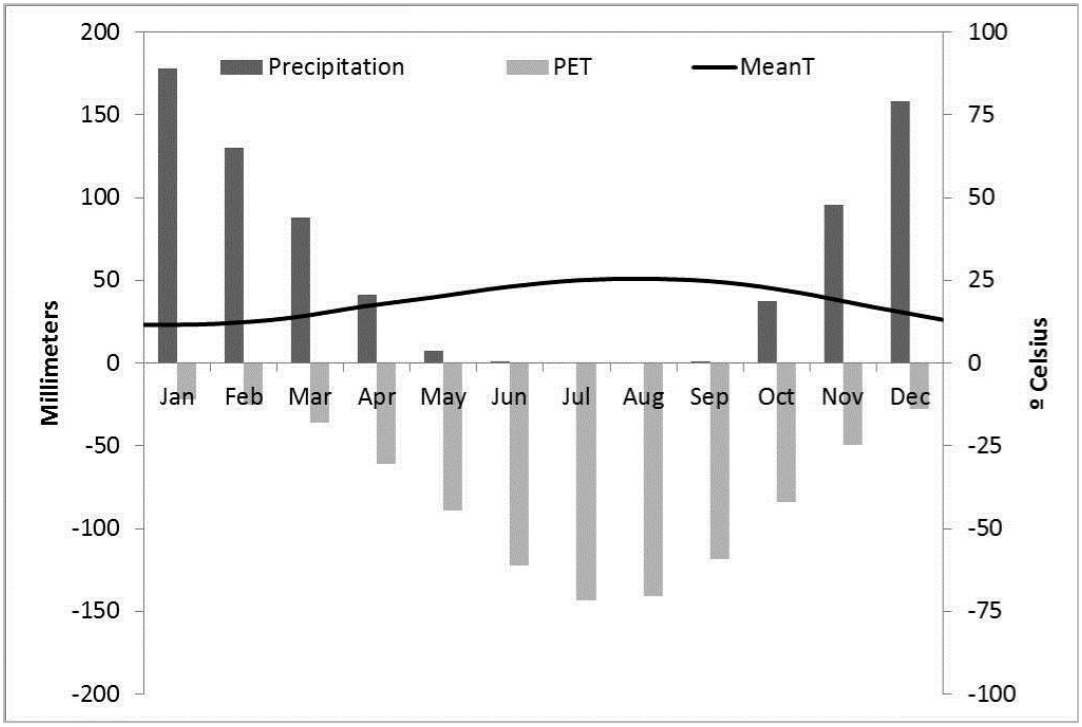

a. CRU (33.25ºN, 35.25ºE)

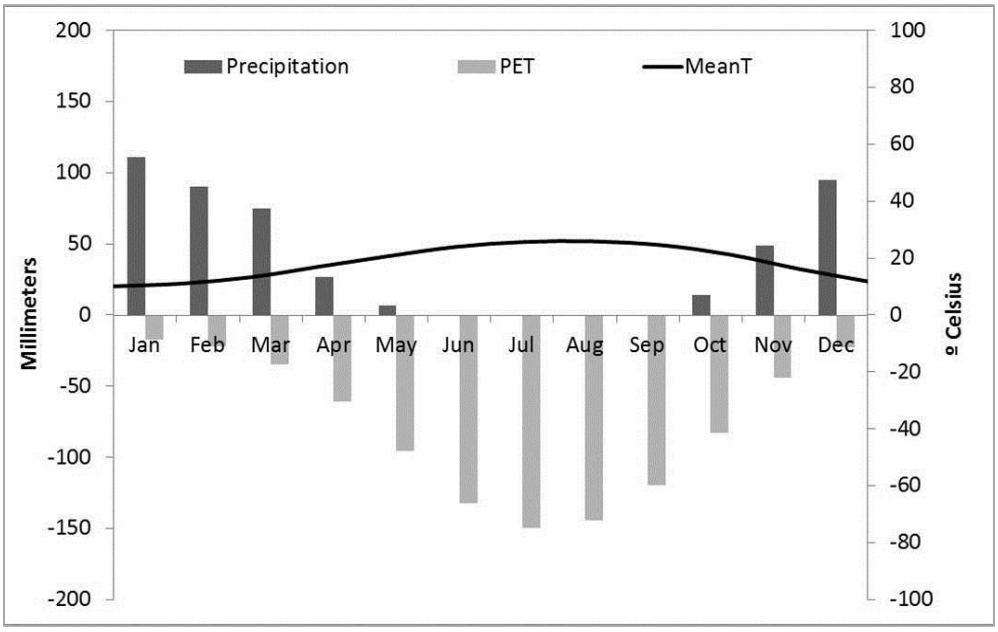

b. CRU (32.75ºN, 35.75ºE)

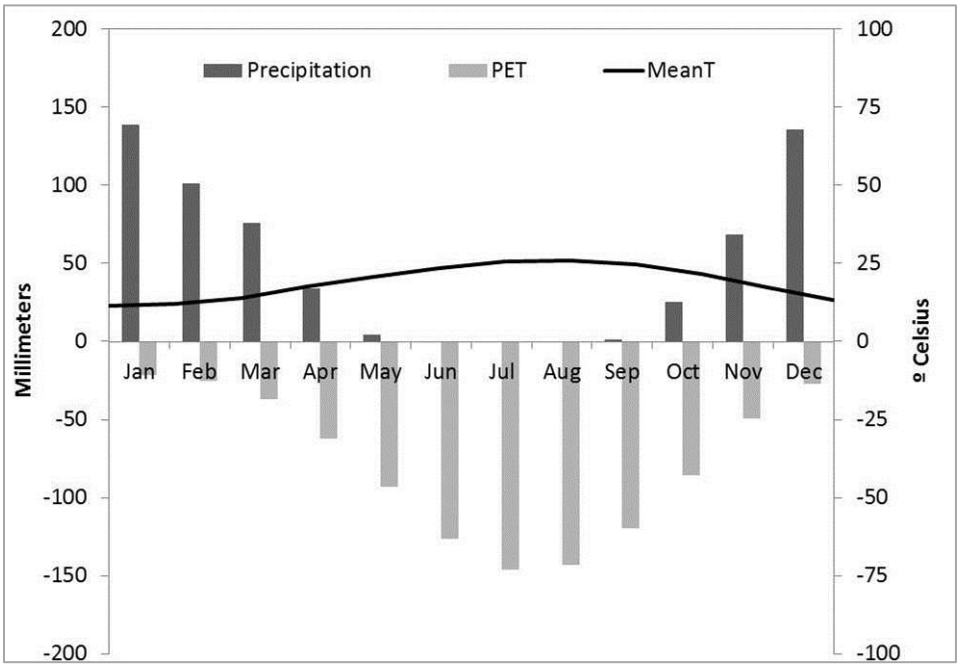

c. CRU (32.75ºN, 35.25ºE)

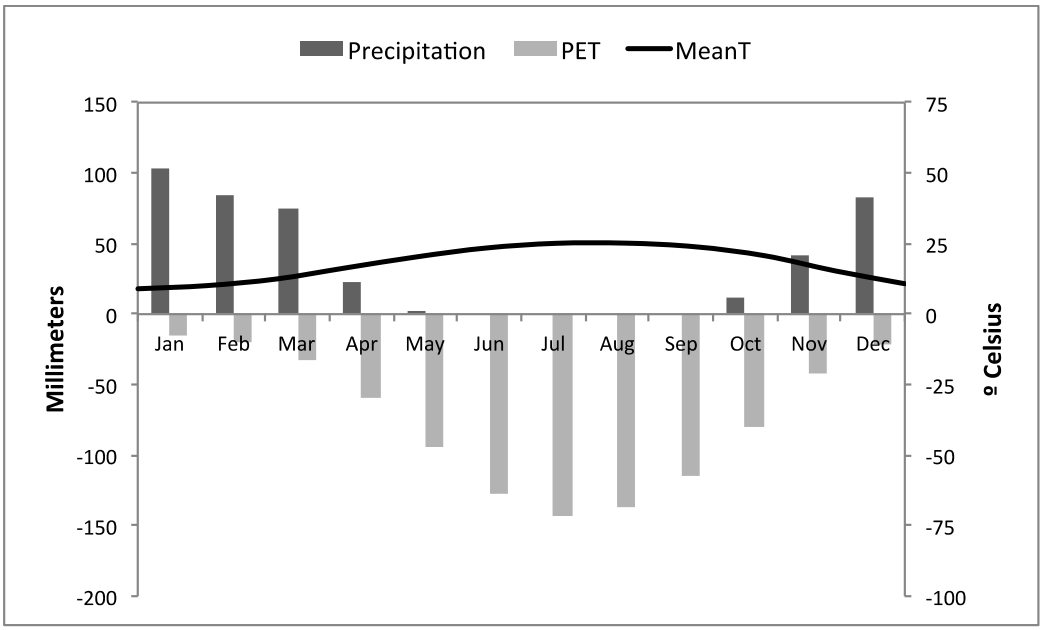

d. CRU (32.25ºN, 35.75ºE)

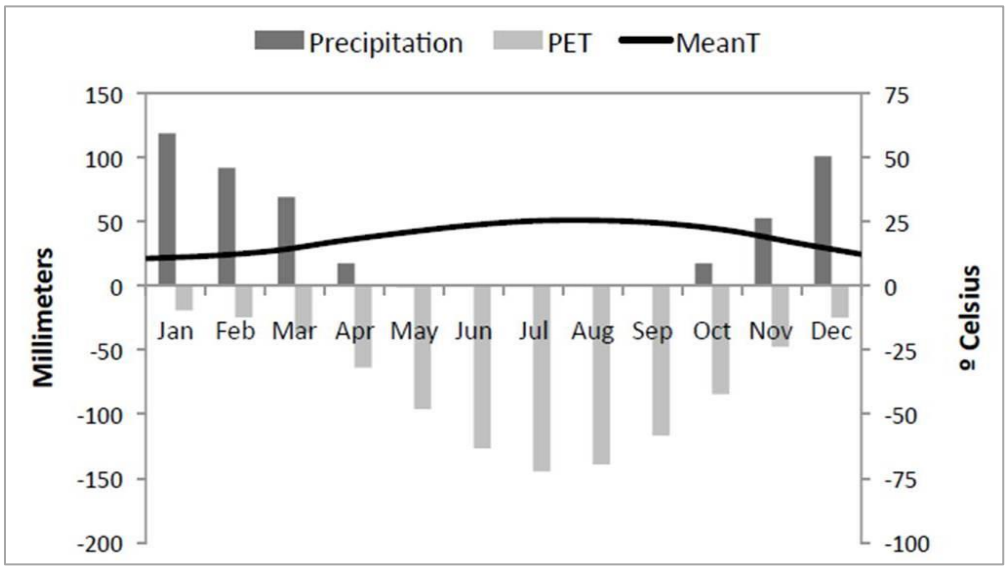

e. CRU (31.75ºN, 35.25ºE)

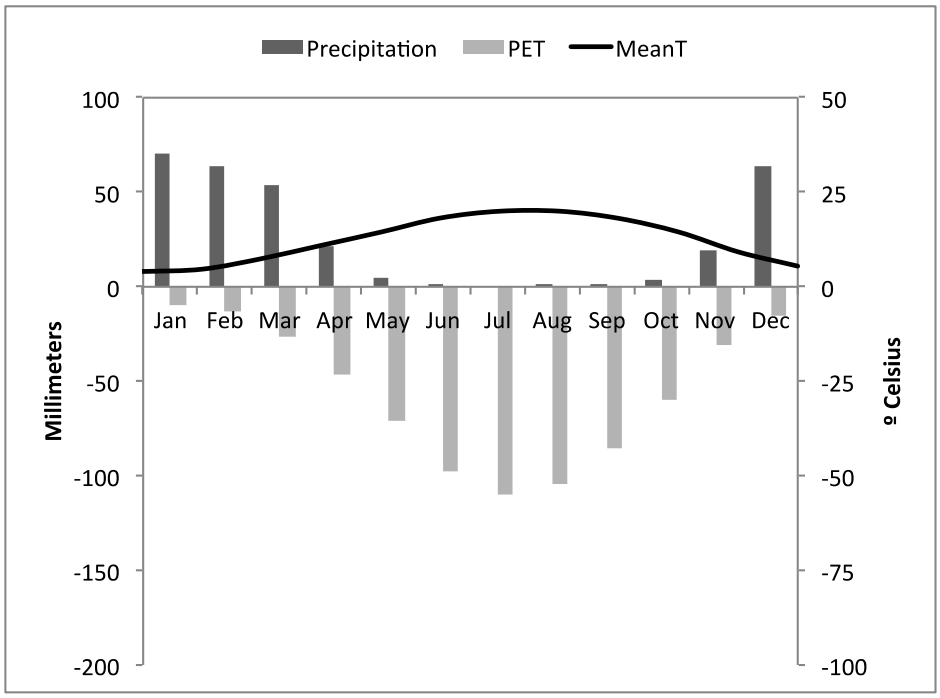

f. Shobauk meteorological station (30.52ºN, 35.53ºE); elevation= 1365 m

APPENDIX 2.2

De-trending curves and order of autoregression model (AR) used for each tree-ring chronology in Chapters 2 and 3.

Site code	Detrending methods	AR model (order)
ARMI-PIBR	negative exponential, Friedman super smoother, linear regression, cubic smoothing spline (30 and 50-year)	1
ATR-PIBR	negative exponential, Friedman super smoother, cubic smoothing spline (20 and 30-year)	2
BAB-PIBR	negative exponential, Friedman super smoother, cubic smoothing spline (20, 30, 40, and 50-year)	1
BAK-QUMC	Friedman super smoother, cubic smoothing spline (30-year)	0
BAR-JUPH	Friedman super smoother, negative exponential, linear regression	3
BSH-PIBR	Friedman super smoother, cubic smoothing spline (20 and 30-year)	4
BSH-PIHA	Friedman super smoother, negative exponential, linear regression, cubic smoothing spline (20-year)	0
CAR-PIHA	Friedman super smoother, negative exponential, linear regression, cubic smoothing spline (40-year)	2
CMH-PIBR	negative exponential, linear regression	2
DAC-PIPN	Friedman super smoother, negative exponential, cubic smoothing spline (20 and 30-year)	3
DIB-PIHA	negative exponential, Friedman super smoother, linear regression	2
DST-PIBR	negative exponential, linear regression	0
EPF-PIBR	Friedman super smoother, cubic smoothing spline (50-year)	2
GOLD-PIBR	negative exponential, Friedman super smoother, linear regression, cubic smoothing spline (50 and 100-year)	1
IMR-PIHA	Friedman super smoother, negative exponential	2
JEZ-PIHA	Friedman super smoother, negative exponential, linear regression	2
NHM-PIHA	Friedman super smoother, negative exponential, linear regression, cubic smoothing spline (20 and 30-year)	2
NHM-PIPN	Friedman super smoother, negative exponential, linear regression	1
RVA-PIBR	negative exponential, linear regression	1
STV-PIBR	negative exponential, linear regression	2
RHN-PIHA	Friedman super smoother, linear regression, cubic smoothing spline (20 and 30-year)	1

APPENDIX 2.3

Response function plots showing response function coefficients (*y*-axis) for tree-ring growth at each site in the study area against mean temperature (*blue*) and precipitation (*red*) values for each month (*x*-axis). An '*' = significant response function coefficient ($p<0.05$) for a given month.

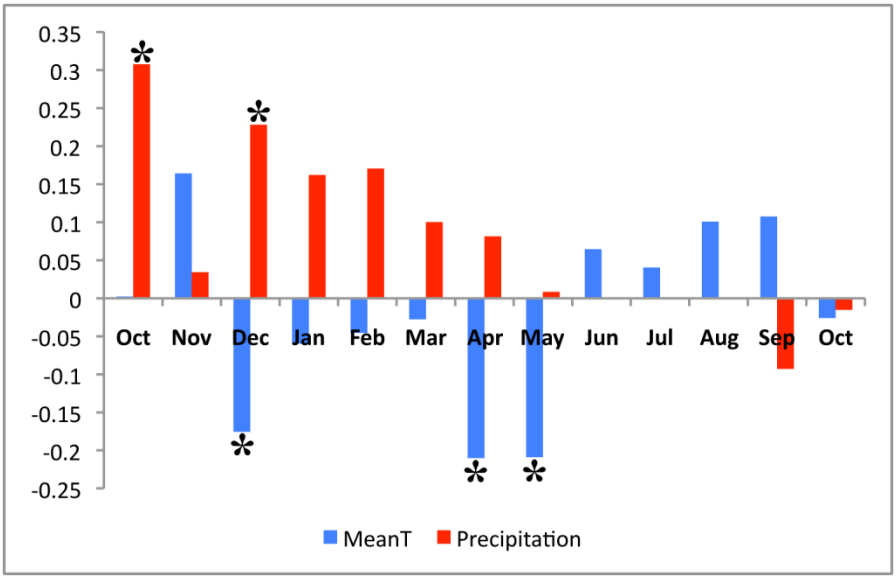

a. Jordan, Bani Kenana, *Quercus macrolepis* (BAK_QUMC)

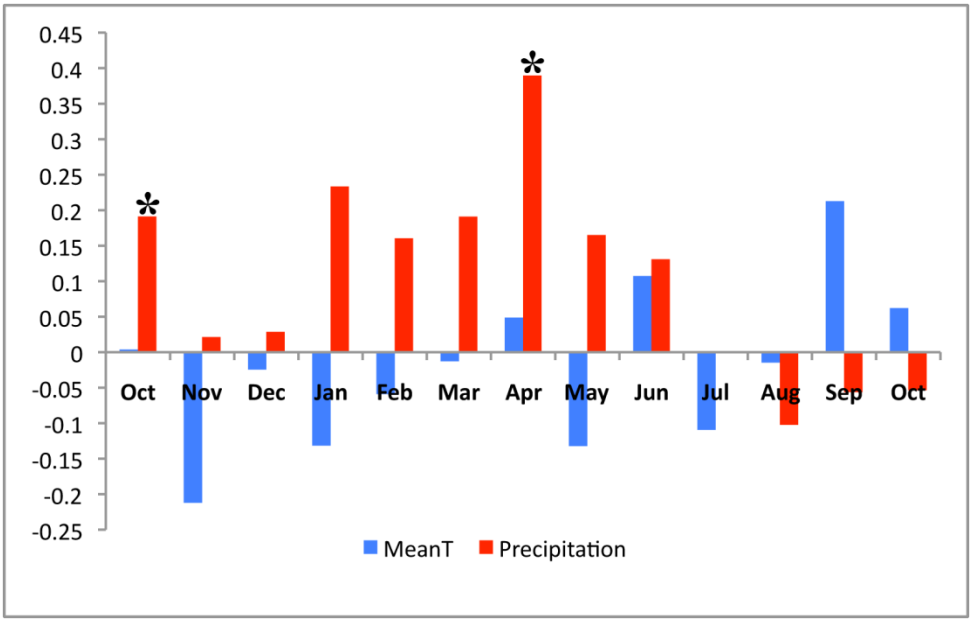

b. Jordan, Shobauk Plateau, *Juniperus phoenicea* (BAR_JUPH)

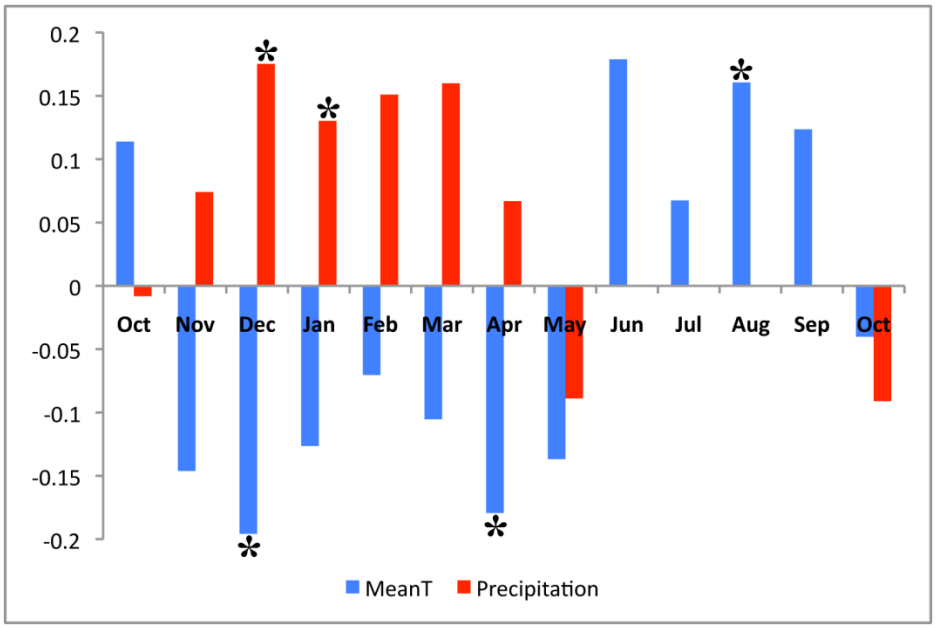

c. Israel, Shephelah, Ben Shemen, *Pinus brutia* (BSH_PIBR)

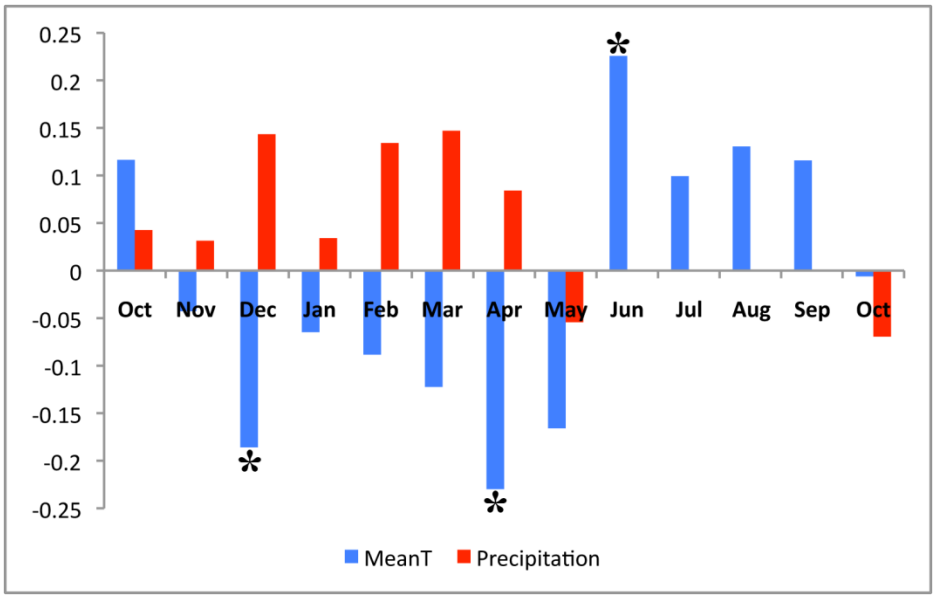

d. Israel, Shephelah, Ben Shemen, *Pinus halepensis* (BSH_PIHA)

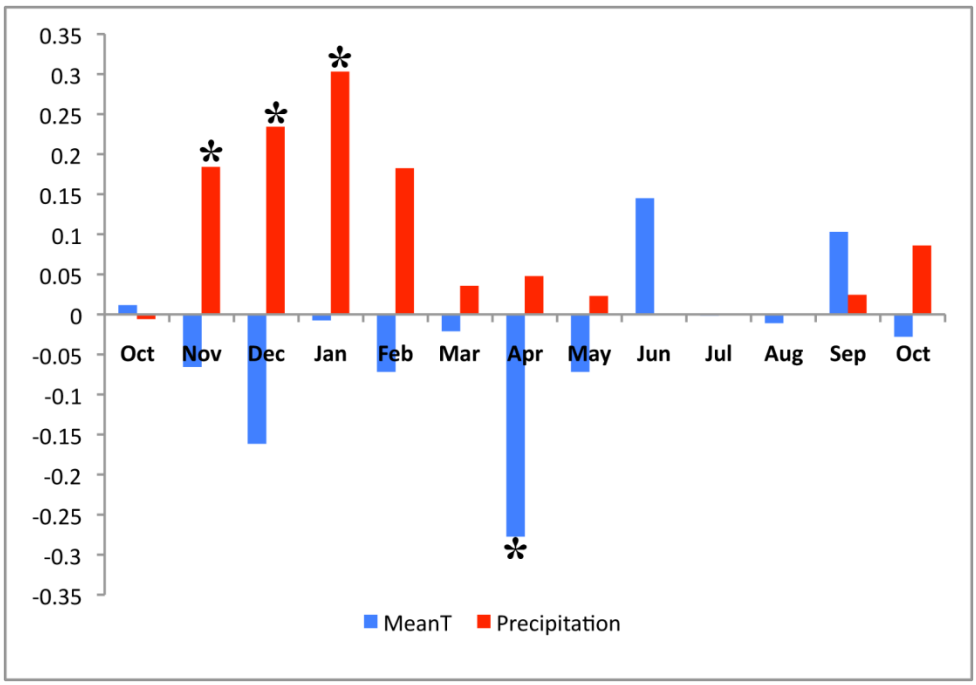

e. Israel, Mt. Carmel, *Pinus halepensis* (CAR_PIHA)

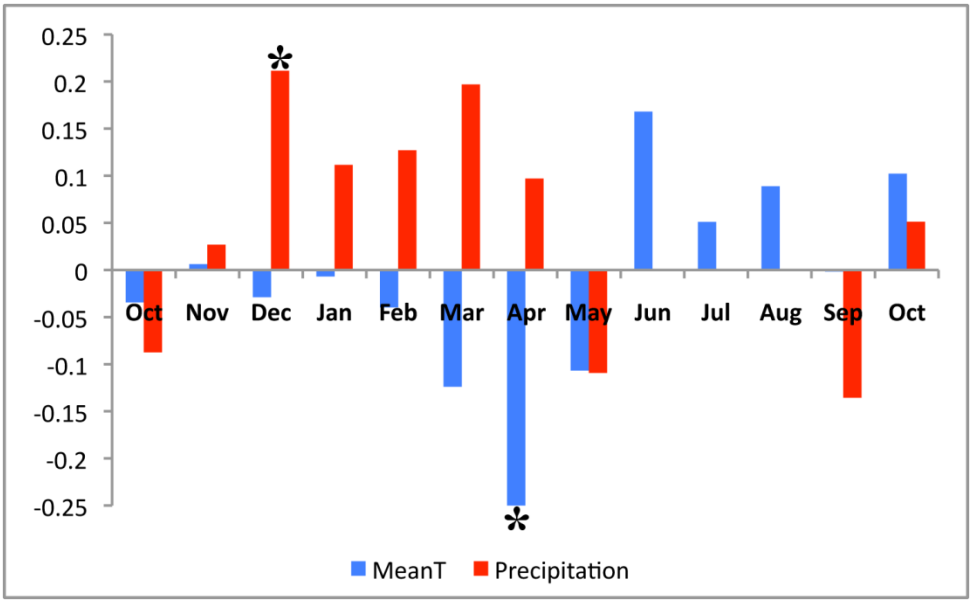

f. Israel, Daliyat al-Carmel, *Pinus pinea* (DAC_PIPN)

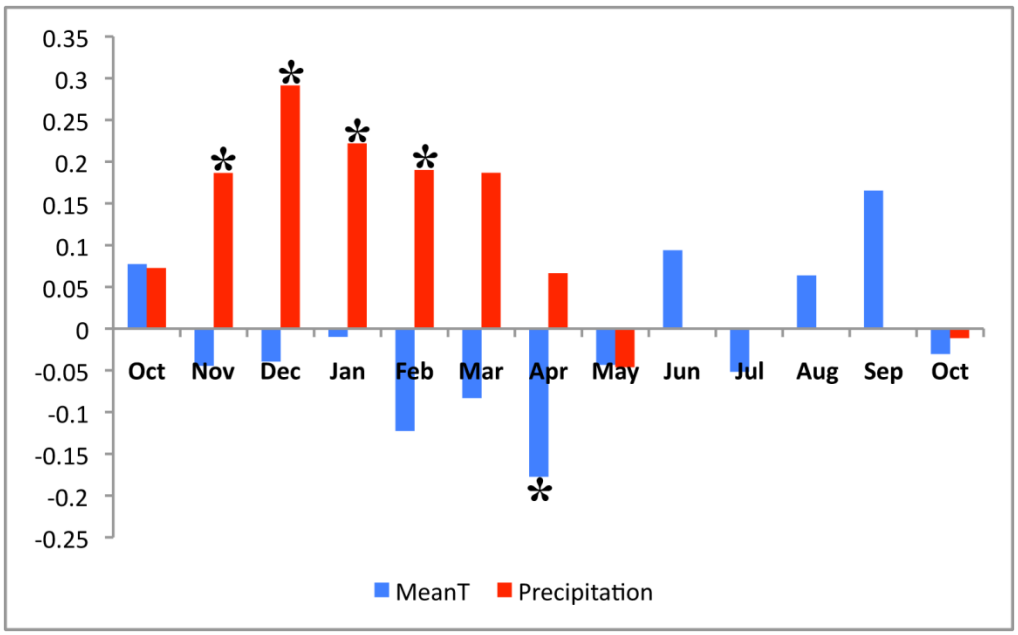

g. Jordan, Dibeen, *Pinus halepensis* (DIB_PIHA)

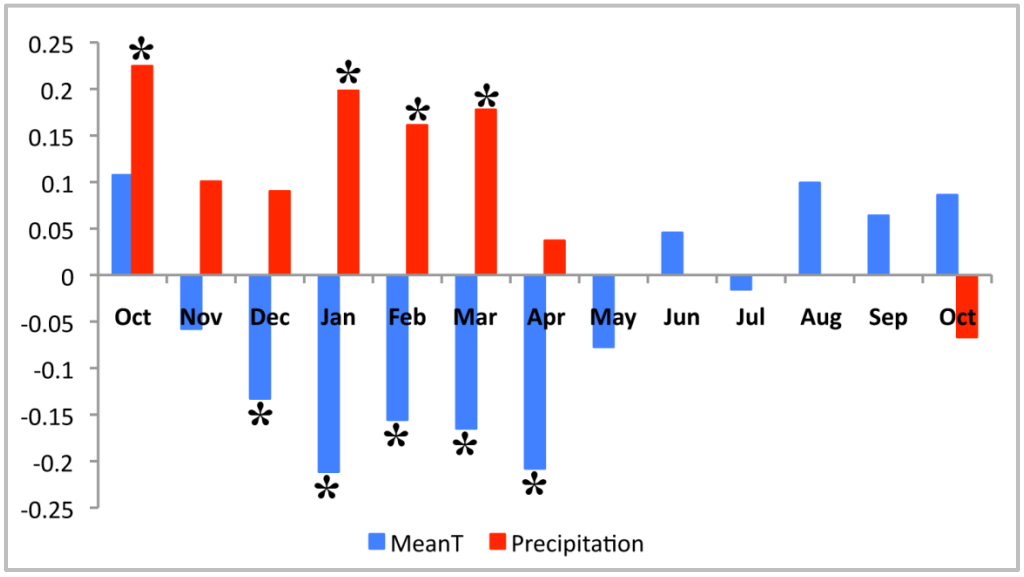

h. Israel, Judean Hills, Masreq, *Pinus halepensis* (IMR_PIHA)

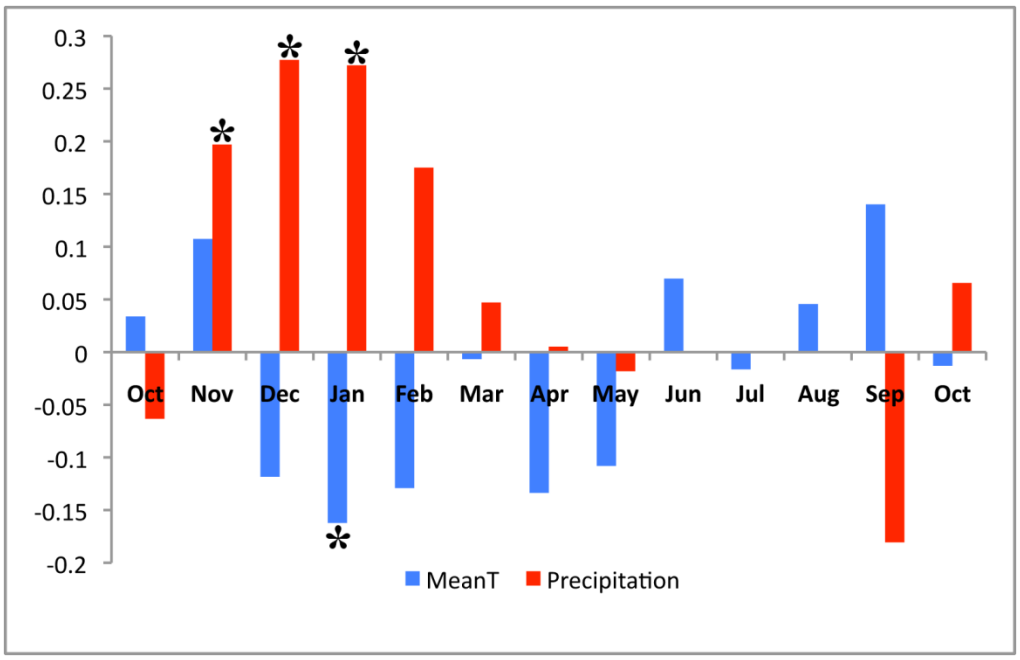

i. Israel, Jezreel Valley, Tel Shimron, *Pinus halepensis* (JEZ_PIHA)

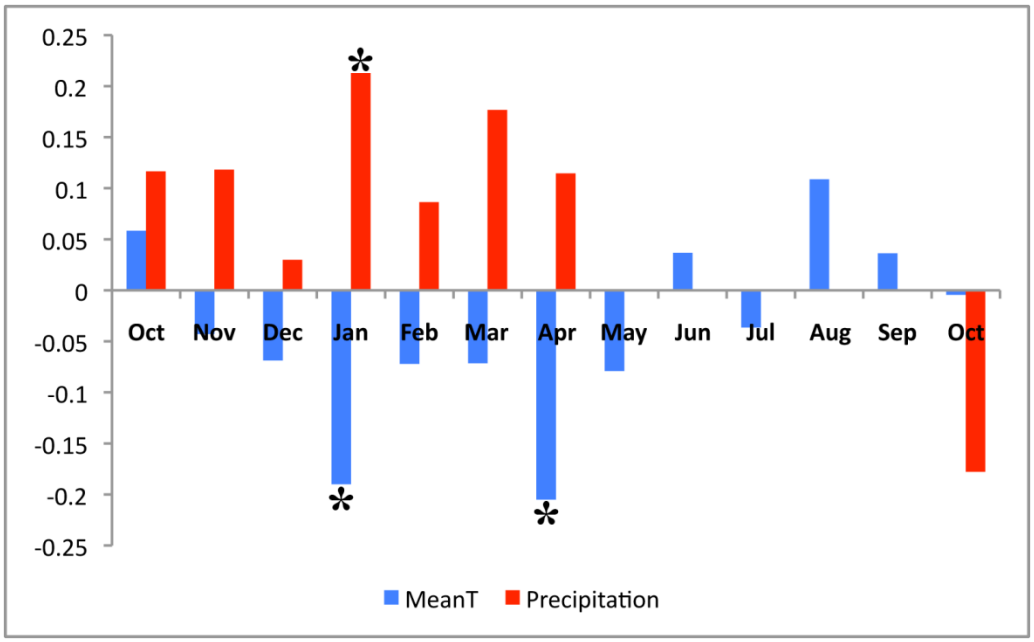

j. Israel, Judean Hills, Nes Harim, *Pinus halepensis* (NHM_PIHA)

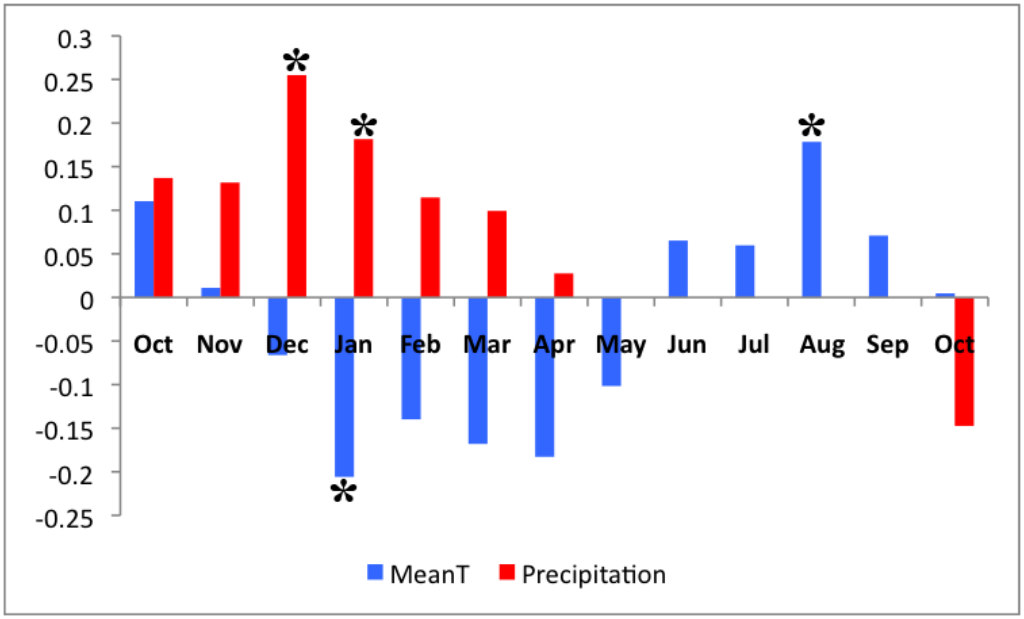

k. Israel, Judean Hills, Nes Harim, *Pinus pinea* (NHM_PIPN)

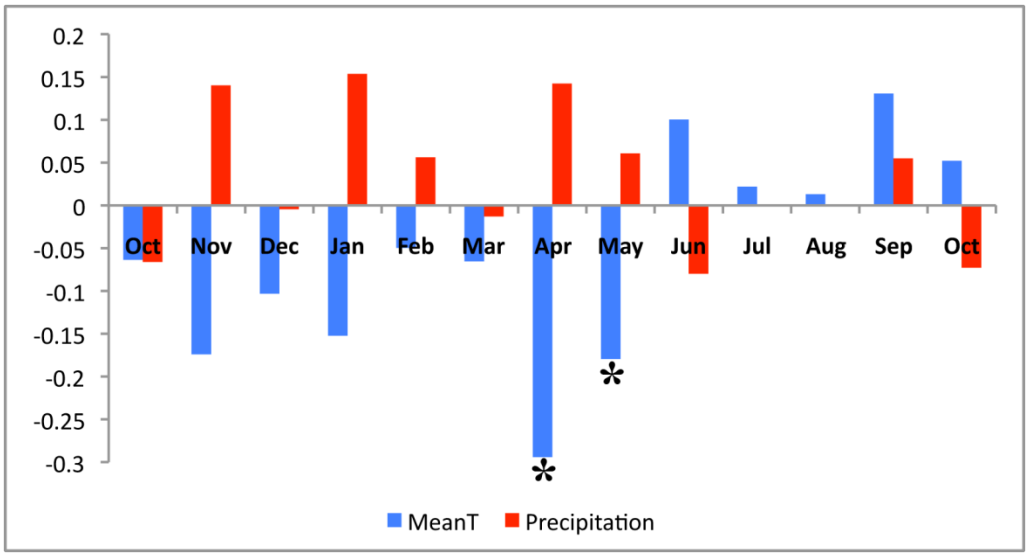

l. Israel, Rosh HaNiqra, *Pinus halepensis* (RHN_PIHA)

REFERENCES

Akkemik, Ü., 2000. Dendroclimatology of umbrella pine (*Pinus pinea* L.) in Istanbul (Turkey). *Tree-Ring Bulletin* 56: 17–20.

Al-Bashaireh, K., Hodgins, G.W.L., 2011. AMS ^{14}C dating of organic inclusions of plaster and mortar from different structures at Petra-Jordan. *Journal of Archaeological Science* 38 (3), 485-491.

Al-Eisawi, D., 1985. Vegetation in Jordan. In: Hadidi, A. (Ed.), *Studies in the History and Archaeology of Jordan 2*. Department of Antiquities of Jordan: Amman, pp. 81–93.

Allen, C.D., Macalady, A.K., Chenchouni, H., Bachelet, D., McDowell, N., Vennetier, M., Kitzberger, T., Rigling, A., Breshears, D.D., Hogg, E.H., Gonzalez, P., Fensham, R., Zhang, Z., Castro, J., Demidova, N., Lim, J.H., Allard, G., Running, S.W., Semerci, A., Cobb, N., 2010. A global overview of drought and heat-induced tree mortality reveals emerging climate change risks for forests. *Forest Ecology and Management* 259: 660–684.

Atkinson, K., Beaumont, P., 1971. The forests of Jordan. *Economic Botany* 25 (3): 305–311.

Attolini, M.R., Calvani, F., Galli, M., Nanni, T., Ruggiero, L., Schaer, E., Zuanni, F., 1990. The relationship between climatic variables and wood structure in *Pinus halepensis* Mill. *Theoretical and Applied Climatology* 41: 121-127.

Baquedano, F.J., Castillo, F.J., 2007. Drought tolerance in the Mediterranean species *Quercus coccifera*, *Quercus ilex*, *Pinus halepensis*, and *Juniperus phoenicea*. *Photosynthetica* 45 (2): 229–238.

Baruch, U., Goring-Morris, N., 1997. The arboreal vegetation of the Central Negev Highlands, Israel, at the end of the Pleistocene: evidence from archaeological charred wood remains. *Vegetation History and Archaeobotany* 6: 249-259.

Biondi, F., Waikul, K., 2004. DENDROCLIM2002: A C++ program for statistical calibration of climate signals in tree-ring chronologies. *Computers and Geosciences* 30: 303-311.

Black, E., 2011. The influence of the North Atlantic Oscillation and European circulation regimes on the daily to interannual variability of winter precipitation in Israel. *International Journal of Climatology* 32 (11): 1654–1664.

Black, E., Hoskins, B., Slingo, J., Brayshaw, D., 2011. The present-day climate of the Middle East. In: Mithen, S., Black, E. (Eds.), *Water, Life and Civilisation: Climate, Environment and Society in the Jordan Valley*. Cambridge University Press, Cambridge, pp. 13–24.

Blondel, J., Aronson, J., 1999. *Biology and Wildlife of the Mediterranean Region*. Oxford University Press, New York.

Boneh, O., 2000. Management of planted pine forests in Israel: Past, present and future. In: Ne'eman, G., Trabaud, L. (Eds.), *Ecology and Biodiversity and Management of* Pinus halepensis *and* P. brutia *Forest Ecosystems in the Mediterranean Basin*. Backhuys, Leiden, pp. 377–390.

Boydak, M., 2004. Silvicultural characteristics and natural regeneration of *Pinus brutia* Ten.–a review. *Plant Ecology* 171: 153-163.

Brewer, P. W., Sturgeon, K., Madar, L., Manning, S. W., 2010. A new approach to dendrochronological data management. *Dendrochronologia* 28: 131-134.

Bruins, H.J., 2012. Ancient desert agriculture in the Negev and climate-zone boundary changes during average, wet and drought years. *Journal of Arid Environments* 86: 28–42.

Castillo, V.M., Martínez-Mena, M., Albaladejo, J., 1997. Runoff and soil loss response to vegetation removal in a semiarid environment. *Soil Science Society of America Journal* 61: 1116–1121.

Cherubini, P., Gartner, B.L., Tognetti, R., Bräker, O.U., Schoch, W., Innes, J.L., 2003. Identification, measurement and interpretation of tree-rings in woody species from Mediterranean climates. *Biological Reviews* 78: 119-148.

Cook, E.R., 1985. *A Time Series Analysis Approach to Tree-Ring Standardization*. Unpublished Ph.D thesis, University of Arizona, Tucson.

Cook, E.R., and Kairiukstis, L.A. (editors), 1990. *Methods of Dendrochronology*. Kluwer Academic Publishers, Dordrecht.

Cook, E.R., Krusic, P., 2006. Program ARSTAN: a Tree-Ring Standardization Program Based on Detrending and Autoregressive Time Series Modeling, with Interactive Graphics. Tree-Ring Laboratory, Lamont Doherty Earth Observatory, Columbia Univ., Palisades, N.Y.

Cook, E.R., Peters, K., 1997. Calculating unbiased tree-ring indices for the study of climatic and environmental change. *The Holocene* 7: 361-370.

Cordova, C.E., 2007. *Millennial Landscape Change in Jordan: Geoarchaeology and Cultural Ecology*. University of Arizona Press, Tucson.

Cvikel, D., Kahanov, Y., 2012. The 19th-century Akko 1 Shipwreck, Israel: Hull-construction report. *The International Journal of Nautical Archaeology* 42 (1): 167–187.

Daget, P., 1977. Le bioclimat méditerranéen: Caractères généraux, modes de caractèrisation. *Vegetatio* 34: 1–20.

De Luis, M., Gričar, J., Čufar, K., Raventós, J., 2007. Seasonal dynamics of wood formation in *Pinus halepensis* from dry and semi-arid ecosystems in Spain. *IAWA Journal* 28 (4): 389–404.

De Luis, M., Novak, K., Čufar, K., Raventós, J., 2009. Size mediated climate-growth relationships in *Pinus halepensis* and *Pinus pinea*. *Trees* 23: 1065–1073.

DeMeo, T.E., Triepke, F.J., Al Smadi, E.M., Ananbeh, Y., Duran, F., 2010. Forest inventory and monitoring of Ajloun Reserve, Jordan. *Nature Areas Journal* 30 (3): 271–278.

Dufour-Dror, J., Ertaş, A., 2004. Bioclimatic perspectives in the distribution of *Quercus ithaburensis* Decne. subspecies in Turkey and in the Levant. *Journal of Biogeography* 31: 461–474.

El-Bana, M., Shaltout, K., Khalafallah, A., Mosallam, H., 2010. Ecological status of the Mediterranean *Juniperus phoenicea* L. relicts in the desert mountains of North Sinai, Egypt. *Flora* 205 (3): 171–178.

Emberger, L., 1971. *Travaux de Botanique et d'Ecologie*. Masson, Paris.

Emberger, L., 1955. Une classification biogéographique des climats. *Recherches et Travaux du Laboratoire de Botanique de la Faculté des Sciences de Montpellier* 7: 3–43.

Engel, T., 1993. Charcoal remains from an Iron Age copper smelting slag hearth at Feinan, Wadi Arabah (Jordan). *Vegetation, History and Archaeobotany* 2: 205-211.

Enzel, Y., Bookman, R., Sharon, D., Gvirtzman, H., Dayan, U., Ziv, B., Stein, M., 2003. Late Holocene climates of the Near East deduced from Dead Sea level variations and modern regional winter rainfall. *Quaternary Research* 60: 263–273.

Esteban, L.G., Martin, J.A., de Palacios, P., Fernández, F.G., López, R., 2010. Adaptive anatomy of *Pinus halepensis* trees from different Mediterranean environments in Spain. *Trees* 24: 19–30.

Fahn, A., 1953. Annual wood ring development in maquis trees in Israel. *Palestine Journal of Botany, Jerusalem Series* 6: 1–26.

Felix, J., 1968. Trees and wood in the Golan. *Teva ve'Aretz* 10: 168–178. (Hebrew)

Fish, T., Wilson, R., Edwards, C., Mills, C., Crone, A., Kirchhefer, A.J., Linderholm, H.W., Loader, N.J., Woodley, E., 2010. Exploring for senescence signals in native scots pine (*Pinus sylvestris* L.) in the Scottish Highlands. *Forest Ecology and Management* 260: 321–330.

Flexer, A., Hirsch, F., Hall, J.K., 2005. Israel: Introduction. In: Hall, J.K., Krasheninnikov, V.A., Hirsch, F., Benjamini, C., Flexer, A. (Eds.), *Geological Framework of the Levant, Volume 2: The Levantine Basin and Israel*. vol. 2. Historical Productions-Hall, Jerusalem, pp. 215–268.

Food and Agriculture Organization (FAO) of the United Nations, 2013. Country profiles: Jordan, http://www.fao.org/countryprofiles/index/en/?iso3=JOR. Accessed 13 May 2014.

Food and Agriculture Organization (FAO) of the United Nations, 2010. Global forest resources assessment 2010–country report, Jordan. FRA2010/105. FAO, Rome.

Freiwan, M., Kadioğlu, M., 2008. Spatial and temporal analysis of climatological data in Jordan. *International Journal of Climatology* 28: 521–535.

Friedman, J.H., 1984. A variable span scatterplot smoother. Laboratory for Computational Statistics, Stanford University. Technical Report 5.

Fritts, H.C., 1976. *Tree Rings and Climate*. Laboratory of Tree-Ring Research, University of Arizona, Tucson.

Galiano, L., Martínez-Vilalta, J., Lloret, F., 2011. Carbon reserves and canopy defoliation determine the recovery of Scots pine 4 yr after a drought episode. *New Phytologist* 190: 750–759.

Gaussen, 1954. *Théorie et classification des climates et microclimats*. VIIéme Congrés International de Botanique, pp. 125–130.

Gindel, J., 1947. Again on cambial activity of Aleppo pine. *Palestine Journal of Botany* 6: 23–26.

Gindel, J., 1944. Aleppo pine as a medium for tree-ring analysis. *Tree-Ring Bulletin* 11 (1): 6–8.

Goldreich, Y., 2003. *The Climate of Israel: Observation, Research, and Application*. Kluwer Academic Publishers, New York.

Griggs, C.B., Pearson, C.L., Manning, S.W., Lorentzen, B., 2014. A 250-year annual precipitation reconstruction and drought assessment for Cyprus from *Pinus brutia* (Ten.) tree-rings. *International Journal of Climatology* 34: 2702–2714.

Grissino-Mayer, H., 2001. Evaluating crossdating accuracy: a manual and tutorial for the computer program COFECHA. *Tree-Ring Research* 57 (2): 205–221.

Guiot, J., 1991. The bootstrapped response function. *Tree-Ring Bulletin* 51: 39–41.

Hijmans, R.J., Cameron, S.E., Parra, J.L., Jones, P.G., Jarvis, A., 2005. Very high resolution interpolated climate surfaces for global land areas. *International Journal of Climatology* 25: 1965–1978.

Holmes, R.L., 1983. Computer-assisted quality control in tree-ring dating and measurement. *Tree-Ring Bulletin* 43: 69–78.

Hulme, M., 1992. A 1951–80 global and precipitation climatology for the evaluation of general circulation models. *Climate Dynamics* 7: 57–72. [http://www.cru.uea.ac.uk/~mikeh/datasets/global].

Kaiser, H.F., 1992. On Cliff's formula, the Kaiser-Guttman rule, and the number of factors. *Perceptual and Motor Skills* 74: 595–598.

Kaplan, D., Gutman, M., 1999. Phenology of *Quercus ithaburensis* with emphasis on the effect of fire. *Forest Ecology and Management* 115: 61–70.

Kaplan, Y., 1984. *The Ecosystem of the Yahudia Nature Reserve with Emphasis on the Dynamics of Germination and Development of* Quercus ithaburensis *Decne*. Unpublished Ph.D. dissertation, University of Wageningen, Wageningen.

Karschon, R., 1984. Natural occurrences of Aleppo pine in the Judean Mountains in the 19th and early 20th centuries: new data. *La-Yaaran* 34: 12–13, 51–52.

Karschon, R., 1982. In defense of the Turks: A study of the destruction of Tabor oak forest in the southern plain of Sharon. *La-Yaaran* 32: 59–64.

Khammash, A., 1986. *Notes on the Village Architecture of Jordan*. University Art Museum, University of Southwestern Louisiana, Lafayette.

Khresat, S., Al-Bakri, J., Al-Tahhan, R., 2008. Impacts of land use/cover change on soil properties in the Mediterranean region of northwestern Jordan. *Land Degradation and Development* 19 (4): 397–407.

Kienast, F., Schweingruber, F.H., Bräker, O.U., Schär, E., 1987. Tree-ring studies on conifers along ecological gradients and the potential of single-year analyses. *Canadian Journal of Forestry Research* 17: 683–696.

Köppen, W., 1931. *Grundriss der Klimakunde*. Gruyter and Co., Berlin.

Lambers, H., Chapin III, F.S., Pons, T.L., 2008. *Plant Physiological Ecology*. 2nd edition. Springer, New York.

Lavi, A., Perevolotsky, A., Kigel, J., Noy-Meir, I., 2005. Invasion of *Pinus halepensis* plantations into adjacent natural habitats. *Applied Vegetation Science* 8: 85–92.

Lev-Yadun, S., 2000a. Wood structure and the ecology of annual growth ring formation in *Pinus halepensis* and *P. brutia*. In: Ne'eman, G., Trabaud, L. (Eds.), *Ecology and Biodiversity and Management of* Pinus halepensis *and* P. brutia *Forest Ecosystems in the Mediterranean Basin*. Backhuys, Leiden, pp. 67–78.

Lev-Yadun, S., Herzog, Z., Tsuk, T., 1995. Conifer beams of *Juniperus phoenica* found in the well of Tel Beer Sheba. *Tel Aviv* 22: 128-135.

Lev-Yadun, S., Liphschitz, N., Waisel, Y., 1981. Dendrochronological investigations in Israel: *Pinus halepensis* Mill.–the oldest living pines in Israel. *La Yaaran* 31 (1–4): 1–8, 49–52. (Hebrew with English abstract)

Lindner, M., Maroschek, M., Netherer, S., Kremer, A., Barbati, A., Garcia-Gonzalo, J., Seidl, R., Delzon, S., Corona, P., Kolström, M., Lexer, M.J., Marchetti, M., 2010. Climate change impacts, adaptive capacity, and vulnerability of European ecosystems. *Forest Ecology and Management* 259: 698–709.

Liphschitz, N., 2007. *Timber in Ancient Israel: Dendroarchaeology and Dendrochronology*. Monograph Series of the Institute of Archaeology of Tel Aviv University, 26. Emery and Claire Yass Publications in Archaeology, Tel Aviv.

Liphschitz, N., Biger, G., 2001. Past distribution of Aleppo pine (*Pinus halepensis*) in the mountains of Israel (Palestine). *The Holocene* 11 (4): 427–436.

Liphschitz, N., Biger, G., 2000. *Green Dress for a Country: Afforestation in Eretz-Israel, the First Hundred Years, 1850-1950*. Ariel Publishing House, Jerusalem.

Liphschitz, N., Lev-Yadun, S., 1986. Cambial activity of evergreen and seasonal dimorphics around the Mediterranean. *IAWA Bulletin* 7 (2): 145–153.

Liphschitz, N., Lev-Yadun, S., Rosen, E., Waisel, Y., 1984. The annual rhythm of activity of the lateral meristems (cambium and phellogen) in *Pinus halepensis* Mill. and *Pinus pinea* L. *IAWA Bulletin* 5 (4): 263–274.

Liphschitz, N., Mendel, Z., 1987. Comparative radial growth of *Pinus halepensis* Mill. and *Pinus brutia* in Israel. *Forêt Méditerranéenne* 9 (2): 115–117.

Liphschitz, N., Waisel, Y., 1967. Dendrochronological studies in Israel. *Quercus boissieri* of Mt. Meron. *La-Yaaran* 17: 78–90, 111–115. (Hebrew with English summary)

Maestre, F., Cortina, J., 2004. Are *Pinus halepensis* plantations useful as a restoration tool in semiarid Mediterranean areas? *Forest Ecology and Management* 198: 303–317.

Maseyk, K.S., Tongbao, L., Rotenberg, E., Grünzweig, J.M., Schwartz, A., Yakir, D., 2008. Physiology-phenology interactions in a productive semi-arid pine forest. *New Phytologist* 178: 603–616.

McDowell, N., Pockman, W.T., Allen, C.D., Breshears, D.D., Cobb, N., Kolb, T., Plaut, J., Sperry, J., West, A., Williams, D.G., Yepez, E.A., 2008. Mechanisms of plant survival and mortality during drought: why do some plants survive while others succumb to drought? *New Phytologist* 178: 719–739.

Meiggs, R., 1982. *Trees and Timber in the Ancient Mediterranean World*. Clarendon Press, Oxford.

Melzack, R.N., Grunwald, C., Schiller, G., 1981. Morphological variation in Aleppo pine (*Pinus halepensis* Mill.) in Israel. *Israel Journal of Botany* 30: 199–205.

Mitchell, T.D., Jones, P.D., 2005. An improved method of constructing a database of monthly climate observations and associated high-resolution grids. *International Journal of Climatology* 25: 693–712.

Mithen, S., Austen, P., Kennedy, A., Emberson, H., Lancaster, N., Finlayson, N., 2007. Early Neolithic woodland composition and exploitation in the southern Levant:

a comparison between archaeobotanical remains from WF16 and present-day woodland at Hammam Adethni. *Environmental Archaeology* 12: 49–70.

Mor, H., Kahanov, Y., 2006. The Dor 2001/1 Shipwreck, Israel–a summary of the excavation. *The International Journal of Nautical Archaeology* 35 (2): 274-289.

Nahal, I., 1983. Le pin brutia (*Pinus brutia* Ten. subsp. *brutia*) (première partie). *Forêt Méditerranéenne* 5: 165–172.

Nahal, I., 1981. The Mediterranean climate from a biological viewpoint. In: Di Castri, F., Goodall, D.W., Specht, R.L. (Eds.), *Mediterranean-Type Shrublands*. Elsevier Scientific Publishing, Amsterdam, pp. 63–86.

Nahal, I., 1963. *Le Pin d'Alep (*Pinus halepensis *Mill.): Etude taxonomique, phytogéographique, écologique et sylvicole*. Unpublished Ph.D. thesis, Faculté des Sciences de Montpellier.

Ne'eman, G., 1993. Variation in leaf phenology and habit in *Quercus ithaburensis*, a Mediterranean deciduous tree. *Journal of Ecology* 81 (4): 627–634.

Oppenheimer, H.R., 1945. Cambial wood production in stems of *Pinus halepensis*. *Palestine Journal of Botany* 5: 22–51.

Orni, E., 1978. *Afforestation in Israel*. 3rd edition. Ahva Press, Jerusalem.

Osborn, T.J., Briffa, K.B., Jones, P.D., 1997. Adjusting variance for sample size in tree-ring chronologies and other regional time series. *Dendrochronologia* 15:89–99.

Pantelas, V., 1985. The forests of brutia pine in Cyprus. *CIHEAM* 86 (1): 43–46.

Peel, M., Finlayson, B., McMahon, T., 2007. Updated world map of the Köppen-Geiger climate classification. *Hydrology of Earth System Sciences* 11: 1633–1644.

Penman, H.L., 1948. Natural evaporation from open water, bare soil and grass. *Proceedings of the Royal Society*, *Section A* 193: 120–145.

Piraino, S., Camiz, S., Di Filippo, A., Piovesan, G., Spada, F., 2013. Dendrochronological analysis of *Pinus pinea* L. on the Italian mid-Tyrrhenian coast. *Geochronometria* 40 (1): 77–89.

Quézel, P., 2000. Taxonomy and biogeography of Mediterranean pines (*Pinus halepensis* and *P. brutia*). In: Ne'eman, G., Trabaud, L. (Eds.), *Ecology and Biodiversity and Management of* Pinus halepensis *and* P. brutia *Forest Ecosystems in the Mediterranean Basin*. Backhuys, Leiden, pp. 1–12.

Quézel, P., Barbero, M., 1992. Le pin d'Alep et les espèces voisines: repartition et caractères écologiques généraux, sa dynamique récente en France méditerranéenne. *Forêt Méditerranéenne* 13: 158–170.

Rathgeber, C.B.K., Misson, L., Nicault, A., Guiot, J., 2004. Bioclimatic model of tree radial growth: application to the French Mediterranean Aleppo pine forests. *Trees* 19 (2): 162–176.

Rencher, A.C., 2002. *Methods of Multivariate Analysis*. 2nd edition. John Wiley and Sons, New York.

Rinn, F., 1996. TSAP (Time Series Analysis and Presentation) Version 3.0. Heidelberg, Germany.

Royal Society for the Conservation of Nature (RSCN), 2011. Protected areas. The Royal Society for the Conservation of Nature, Amman, Jordan, http://www.rscn.org/jo/orgsite/RSCN/HelpingNature/ProtectedAreas/. Accessed 12 August 2013.

Rustum, A.J., 1936. *The Royal Archives of Egypt and the Origins of the Egyptian Expedition to Syria, 1831–1841*. American Press, Beirut.

Saaroni, H., Halfon, N., Ziv, B., Alpert, P., Kutiel, H., 2010. Links between the rainfall regime in Israel and location and intensity of Cyprus lows. *International Journal of Climatology* 30: 10141025.

Sánchez-Salguero, R., Navarro-Cerrillo, R.M., Camarero, J.J., Fernández-Cancio, A.F., 2010. Drought-induced growth decline of Aleppo and maritime pine forests in south-eastern Spain. *Forest Systems* 19 (3): 458–469.

Sarris, D., Christodoulakis, D., Körner, C., 2011. Impact of recent climatic change on growth of low elevation eastern Mediterranean forest trees. *Climatic Change* 106 (2): 203–223.

Sarris, D., Christodoulakis, D. Körner, C., 2007. Recent decline in precipitation and tree growth in the eastern Mediterranean. *Global Change Biology* 13: 1187–1200.

Schiller, G., 2001. Biometeorology and recreation in east Mediterranean forests. *Landscape and Urban Planning* 57: 1–12.

Schiller, G., 2000. Ecophysiology of *Pinus halepensis* Mill. and *P. brutia* Ten. In: Ne'eman, G., Trabaud, L. (Eds.), *Ecology and Biodiversity and Management of* Pinus halepensis *and* P. brutia *Forest Ecosystems in the Mediterranean Basin*. Backhuys, Leiden, pp. 51–65.

Schiller, G., 1982. Significance of bedrock as a site factor for Aleppo pine. *Forest Ecology and Management* 4: 213–223.

Schiller, G., Cohen, Y., 1998. Water balance of *Pinus halepensis* Mill. afforestation in an arid region. *Forest Ecology and Management* 105 (1–3): 121–128.

Schiller, G., Cohen, Y., 1995. Water regime of a pine forest under a Mediterranean climate. *Agricultural and Forest Meteorology* 74: 181–193.

Schiller, G., Cohen, S., Ungar, E.D., Moshe, Y., Herr, N., 2007. Estimating water use of sclerophyllous species under East-Mediterranean climate III. Tabor oak forest sap flow distribution and transpiration. *Forest Ecology and Management* 238: 147–155.

Schiller, G., Ungar, E.D., Cohen, S., Herr, N., 2010. Water use by Tabor and Kermes oaks growing in their respective habitats in the Lower Galilee region of Israel. *Forest Ecology and Management* 259 (5): 1018–1024.

Shami, S., 1992. 19th century Circassian settlements in Jordan. In: Hadidi, A. (Ed.), *Studies in the History and Archaeology of Jordan IV*. Department of Antiquities, Amman, pp. 417–418.

Serre, F., 1976. Les rapports de la croissance et du climat chez le pin d'Alep. *Oecologia Plantarum* 11: 143–171.

Serre-Bachet, F., Tessier, L., 1990. Response function analysis for ecological study. In: Cook, E., Kairiukstis, L.A. (Eds.), *Methods of Dendrochronology: Applications in the Environmental Sciences*. Kluwer Academic Publishers, Dodrecht, pp. 247–258.

Shapiro, M., 2006. Soils of Israel. *Eurasian Soil Science* 39 (11): 1170–1175.

Singer, A., 2007. *The Soils of Israel*. Springer, New York.

Stokes, M.A., Smiley, T.L., 1996. *An Introduction to Tree-Ring Dating*. 2nd edition. University of Arizona Press, Tucson.

Strahler, A.H., Strahler, A.N., 2006. *Introducing Physical Geography*. 4th edition. John Wiley and Sons, New York.

Tal, A., 2013. *All the Trees of the Forest: Israel's Woodlands from the Bible to the Present*. Yale University Press, New Haven.

Talhouk, S.N., Zurayk, R., Khuri, S., 2001. Conservation of the coniferous forests of Lebanon: past, present and future prospects. *Oryx* 35 (3): 206–215.

Tamari, A., 1976. *Climatic Fluctuations in the Eastern Basin of the Mediterranean based on Dendrochronological Analysis*. Unpublished Ph.D. thesis, Tel Aviv University. (Hebrew)

Tessler, N., Wittenberg, L., Greenbaum, N., 2008. Soil water repellency persistence after recurrent forest fires on Mount Carmel, Israel. *International Journal of Wildland Fire* 22 (4): 515–526.

Thornthwaite, C.W., 1948. An approach toward a rational classification of climate. *Geographical Review* 38 (1): 55–94.

Touchan, R., Anchukaitis, K.J., Shishov, V.V., Sivrikaya, F., Attieh, J., Ketmen, M., Stephan, J., Mitsopoulos, I., Christou, A., Meko, D.M., 2014a. Spatial patterns of eastern Mediterranean climate influence on tree growth. *The Holocene* 24 (4): 381–392.

Touchan, R., Christou, A.K., Meko, D.M., 2014b. Six centuries of May–July precipitation in Cyprus from tree rings. *Climate Dynamics* 43: 3281–3292.

Touchan, R., Hughes, M.K., 1999. Dendrochronology in Jordan. *Journal of Arid Environments* 42: 291–303.

Touchan, R., Meko, D.M., Aloui, A., 2008. Precipitation reconstruction for Northwestern Tunisia from tree rings. *Journal of Arid Environments* 72: 1887–1896.

Touchan, R., Meko, D., Hughes, M.K., 1999. A 396-year reconstruction of precipitation in southern Jordan. *Journal of the American Water Resources Association* 35 (1): 49–59.

Touchan, R., Xoplaki, E., Funkhouser, G., Luterbacher, J., Hughes, M.K., Erkan, N., Akkemik, Ü., Stephan, J., 2005. Reconstructions of Spring/Summer Precipitation for the Eastern Mediterranean from Tree-Ring Widths and Its Connection to Large-Scale Atmospheric Circulation. *Climate Dynamics* 25: 75-98.

Triepke, F.J., DeMeo, T.E., Al-Otoum, M., Al-Azzam, L., 2012. Composition and structure of Aleppo pine (*Pinus halepensis*) communities in the Dibeen Forest Reserve, Jordan. *Natural Areas Journal* 32 (4): 356–366.

United States Naval Observatory (USNO). 2013. Duration of daylight/darkness table for one year, http://www.usno.navy.mil/USNO/astronomical-applications/data-services/duration-world. Accessed 11 July 2013.

Wade, A., Holmes, P., El Bastawesy, M., Smith, S., Black, E., Mithen, S., 2011. The hydrology of the Wadi Faynan. In: Mithen, S., Black, E. (Eds.), *Water, Life and Civilisation: Climate, Environment and Society in the Jordan Valley*. Cambridge University Press, Cambridge, pp. 157–174.

Waisel, Y., Liphschitz, N., 1968. Dendrochronological studies in Israel II: *Juniperus phoenicea* of north and central Sinai. *La-Yaaran* 8: 2–22, 63–67. (Hebrew with English summary)

Warnock, P., 2001. Wood remains. In: Bikai, P. (Ed.) *The Petra Church*. American Center of Oriental Research, Amman, pp. 398–408.

Weinstein, A., 1989. Geographic variation and phenology of *Pinus halepensis*, *P. brutia* and *P. eldarica* in Israel. *Forest Ecology and Management* 27: 99–108.

Weinstein-Evron, M., Lev-Yadun, S., 2000. Paleoecology of *Pinus halepensis* and *P. brutia* in the eastern Mediterranean in the light of archaeobotanical data. In: Ne'eman, G., Trabaud, L. (Eds.), *Ecology and Biodiversity and Management of* Pinus halepensis *and* P. brutia *Forest Ecosystems in the Mediterranean Basin*. Backhuys, Leiden, pp. 119–130.

Wigley, T.M.L., Briffa, K.R., Jones, P.D., 1984. On the average value of correlated time series, with applications in dendroclimatology and hydrometeorology. *Journal of Climate and Applied Meteorology* 23: 201–213.

Wils, T.H.G., Robertson, I., Eshetu, Z., Touchan, R., Sass-Klaassen, U., Koprowski, M., 2011. Crossdating *Juniperus procera* from North Gondar, Ethiopia. *Trees* 25: 71–82.

Zohary, M., 1973. *Geobotanical Foundations of the Middle East*. 2 vols. Gustav Fischer, Stuttgart.

CHAPTER 3:

THE LEVANTINE DIVIDE: REGIONAL VARIABILITY IN *P. HALEPENSIS* MILL. AND *P. BRUTIA* TEN. TREE-RING GROWTH AND CLIMATE RESPONSE

SUMMARY

The Levant is a bioclimatically diverse region, in which there are pronounced changes in climate and environment, particularly along latitudinal and altitudinal gradients. For the following study, tree-ring chronologies of *Pinus halepensis* Mill. and *Pinus brutia* Ten. were built from forest sites located along both latitudinal and altitudinal gradients in the Levant. Tree-ring climate responses and teleconnections are compared, in order to determine how the Levantine tree-ring record may be used for paleoclimate, dendrochronological dating, and dendroprovenancing research.

The results show that *P. brutia* and *P. halepensis* tree-rings growing in the northern and southern Levant have distinct year-to-year ring-width patterns, which result primarily from different climatic limiting factors in the two regions. Tree-ring growth in the southern Levant, which is more arid with a longer, more severe dry season, has a positive response to winter precipitation and a negative response to winter/late spring mean temperature. Tree-ring growth in the northern Levant generally has a positive response to late spring/early summer precipitation. At high-altitude sites in the northern Levant, tree-rings have a positive response to winter temperature, and precipitation becomes a less critical limiting factor. As a result, there

is generally low correlation between the northern Levant's high and low-altitude chronologies, and extremely poor (and often negative) correlation between high-altitude chronologies from the northern Levant and the southern Levant chronologies.

Consequently, it is recommended that tree-ring reference chronologies from multiple altitudinal gradients in the northern Levant and a separate reference chronology from the southern Levant be used for dating historical and archaeological timbers procured from these regions. It is also possible to identify whether historical/archaeological timber was procured from the northern or southern Levant using dendroprovenancing techniques. Tree-ring data from the southern Levant, rather than the northern Levant, should be used for reconstructing climate in the southern Levant, especially at high frequency timescales, because of the particularly marked bioclimatic differences along the East Mediterranean latitudinal gradient.

INTRODUCTION

Forest ecosystems in both the northern and southern Levant have many shared characteristics. Both are part of the Mediterranean bioclimatic zone and share many common species assemblages. Both the northern and southern Levant also have long histories of human habitation and timber exploitation that have heavily impacted present-day species abundance and richness in their forests. However, differences in coastal orientation, topography, and latitude create variability in Levantine climatic and environmental conditions. Because of such bioclimatic variability, radial growth of tree species might be regulated by different climatic variables throughout the

Levant, resulting in distinct regional year-to-year tree-ring patterns for each of these bioclimatic zones.

In the previous chapter, variability in the tree-ring records and climate responses of forest sites within the southern Levant were examined. In this chapter, I expand the study area to a larger region, by analyzing the climate responses and radial growth of two common Mediterranean pine species (*Pinus halepensis* Mill. and *Pinus brutia* Ten.) sampled from forest sites along latitudinal and altitudinal gradients in both the northern and southern Levant. The specific objectives of this study are to: 1) identify the primary climatic factors that influence radial growth of *P*. *brutia* and *P*. *halepensis* growing at different altitudes and latitudes in the Levant, 2) analyze teleconnections among *P*. *brutia* and *P*. *halepensis* tree-ring chronologies in the Levant, particularly between the northern and southern Levant, and 3) divide the study area into geographic zones in which there are coherent tree-ring signals and in which reliable dendrochronological crossdating can be made.

Since both *P*. *brutia* and *P*. *halepensis* have been used in previous dendrochronological and dendroclimatic studies (e.g., De Luis 2009; Griggs et al. 2014; Kienast et al. 1987; Sarris et al. 2007; Touchan et al. 2005; Touchan et al. 2005, 2008, 2014a, b) and are important in afforestation efforts around the Mediterranean, greater information on variability in *P*. *halepensis* and *P*. *brutia* tree-ring growth and climate response across the eastern Mediterranean is useful for regional forest management and planning. Information on the overall coherence of tree-ring growth and climate response can also help in evaluating the usefulness of these chronologies

as a climate proxy and the geographic resolution over which such tree-ring derived climate reconstructions are able to represent climatic variability.

Furthermore, as discussed in Chapter 2, both *P*. *halepensis* and *P*. *brutia* have been commonly used as low-quality firewood and building material throughout the Levant (Liphschitz 2007; Meiggs 1982). *P*. *brutia* remains one of the most economically important tree species in the northern Levant and the Aegean, particularly in Cyprus and Turkey (Boydak 2004; Ciesla 2004). Information about spatial variability in the tree-ring chronologies of both species therefore gives information for delineating the geographic area and bioclimatic zones over which their tree-ring chronologies may crossdate. This allows researchers to determine the degree to which archaeological and building samples may be provenanced using dendrochronology and if (and where) additional reference chronologies must be created for successfully dating wood material from these species.

Previous research

As discussed in Chapters 1 and 2, most dendroclimatological studies in the East Mediterranean that have used robust tree-ring standardization and response function analysis methods are relatively recent. Additionally, analysis has been restricted mostly to sites in the northeastern Mediterranean, particularly Anatolia and Cyprus. Tree-ring responses to climate in these areas have been investigated along both spatial and altitudinal gradients for a single species. Kienast et al. (1987) and most recently, Griggs et al. (2014) investigated the climate response of *Pinus brutia* Ten. tree-rings along altitudinal transects in Cyprus and used this information to reconstruct precipitation. Köse et al. (2012) investigated the climate response of *Pinus nigra* Arn.

subsp. *pallasiana* along spatial gradients in western Turkey and used the tree-ring data to reconstruct precipitation on local and regional scales (Köse et al. 2011).

Very few dendroclimatological studies have used multi-site tree-ring networks to investigate tree-ring teleconnections on a wider regional scale in the Mediterranean. Hughes et al. (2001) examined the climate responses of a multi-species network of tree-ring chronologies over a very wide study area that included sites in southern Italy, the Balkans, Anatolia (including sites in northeastern Turkey along the Black Sea), and Cyprus. They also examined April–June sea level pressure anomalies during positive and negative regional 'signature years'[1] for the chronologies, in order to identify specific large-scale circulation patterns controlling regional precipitation and affecting tree-ring growth. Nicault et al. (2008) used an even wider network of tree-ring data that included sites in Spain, Morocco, Switzerland, the Balkans, Turkey, and Cyprus, in order to build a 500-year gridded summer drought reconstruction for the Mediterranean. However, this study also did not include tree-ring data from much of the northern and southern Levant, and the authors note that reconstructions were less robust in areas where tree-ring proxy data were rare or absent (particularly the southern Levant).

Most recently, Touchan et al. (2005, 2014a) built and analyzed a multi-species network of chronologies that included a large number of sites in Lebanon, Syria, Greece, Cyprus, and Turkey. They used the tree-ring data to reconstruct regional

[1] A 'signature year' is a year in which trees at the majority of the sampled sites have narrower (a 'negative signature') or wider (a 'positive signature') rings than in the previous year (Schweingruber et al. 1990). For their study, Hughes et al. (2001) defined a regional signature year as one in which approximately 78% of the chronologies had the same signature year sign (i.e., positive or negative).

spring/summer (i.e., May–August) precipitation and examined the connection between tree-ring growth and large-scale atmospheric circulation patterns. However, these studies did not include sites from the southern Levant in their analysis. This study is, therefore, the first large-scale dendroclimatic study to investigate tree-ring teleconnections and climate responses using sites sampled along latitudinal and altitudinal gradients in both the northern and southern Levant.

Study area

The study area includes sites in the eastern Mediterranean between 37.08º–31.745ºN latitude and 30.47º–35.98ºE longitude. All of the study area is part of the Mediterranean climate zone, which is characterized by long, hot dry summers and cool, rainy winters. However, there is considerable diversity in the bioclimatic characteristics, monthly potential evapotranspiration (*PET*), and dry season length (*LDS*) and water deficits (*DSWD*) of the different sites sampled within the study area, which are summarized in Table 3.1 (see also: Appendices 2.1 and 3.1 for monthly climagrams that include monthly *PET* for sites in the study area). Differences in latitude, altitude, land-sea contrasts, and large-scale atmospheric circulation patterns all contribute to variability in precipitation and temperature throughout the study area (Lionello et al. 2006) and are summarized below.

Table 3.1. Bioclimatic characteristics of sites in the study area, which were calculated using 0.5º CRU gridded datasets (available from the Climate Research Unit at the University of East Anglia) from the northern and southern Levant, and Cypriot meteorological station data. Each CRU gridded dataset is listed according to the geographic coordinates of the grid's center. Note that climate data from Panagia Bridge and Prodromos, Cyprus, were not used in the tree-ring climate response function analysis (see: section below), but are included here to illustrate bioclimatic characteristics of low and high-altitude sites in Cyprus, respectively. Temperature data are not available from the Cypriot climate stations of Peristerona, Ag. Epifanos, and Pedoulas, which are used in the climate response function analysis, and so *DSWD* cannot be calculated for these stations. For a detailed view of the locations of the Cypriot meteorological stations used in the climate response function analysis, see: Appendix 3.2. For an explanation of the bioclimatic classification systems used here, see: Chapter 2.

Climate dataset	Station elevation (m)	Köppen bioclimatic zone	Emberger bioclimatic zone	*LDS* (months)	*DSWD* (mm)
Northern Levant:					
CRU (34.25ºN, 35.75ºE)		Csb	cool humid	5.0	-507
CRU (35.75ºN, 35.75ºE)		Csa	hot humid	5.0	-625
CRU (37.25ºN, 30.75ºE)		Csa	cool sub-humid	5.0	-427
Cyprus, Peristerona[a]	225	Csa	hot arid	7.5–8.0	
Cyprus, Panagia Bridge	440	Csa	warm semi-arid	7.0	-618
Cyprus, Ag. Epifanos[a]	605	Csa	warm semi-arid	7.0	
Cyprus, Pano Panagia	820	Csb	warm sub-humid	7.0	-606
Cyprus, Pedoulas[a]	1080	Csb	cool sub-humid	4.0–5.0	
Cyprus, Prodromos	1380	Csb	cool humid	4.5	-387
Southern Levant:					
CRU (31.75ºN, 35.25ºE)		Csa	warm semi-arid	7.0	-734
CRU (32.75ºN, 35.25ºE)		Csa	hot sub-humid	7.0	-713
CRU (33.25ºN, 35.25ºE)		Csa	hot sub-humid	6.0	-670
CRU (32.25ºN, 35.75ºE)		Csa/Csb	warm semi-arid	7.0	-683
CRU (32.75ºN, 35.75ºE)		Csa	warm semi-arid	7.0	-738

[a]Temperature data is not available from the meteorological station.

East Mediterranean climate variability

The Mediterranean region is situated in a critical climatic transition zone between the subtropical high pressure belt and midlatitude westerlies (Lionello et al. 2006; Trigo et al. 1999). During the winter months, sites in both the northern and southern areas of the study region receive rainfall primarily from midlatitude cyclones, which are produced from cold air masses of European origin that gain moisture and become unstable when they reach the warm Mediterranean waters (Black et al. 2011; Eshel and Farrell 2000; Türkeş 1996; Xoplaki et al. 2004; Ziv et al. 2006). Many of these low pressure systems ('Cyprus lows') move through, intensify, or develop around Cyprus, (Enzel et al. 2003; Goldreich 2003; Saaroni et al. 2010). These systems generally pass to the north or northeast over Turkey, Syria, and Lebanon, bringing rainfall to these areas (Alpert et al. 1990; Black et al. 2011).

The Cyprus lows bring rainfall less frequently to the southern Levant, which is located further from the typical center of cyclogenesis in the East Mediterranean, and is at the edge of the Mediterranean storm track, close to the arid subtropical high pressure zone over North Africa (Black et al. 2011; Enzel et al. 2004; Goldreich 2003). As a result, aridity generally increases from north to south (i.e., as latitude decreases) in the eastern Mediterranean basin.

Despite regional differences in total annual precipitation, year-to-year precipitation variability is fairly coherent for sites in the northern Levant and sites in the northern part of the southern Levant, largely because of the critical role that the Cyprus lows play in delivering winter precipitation (which comprises the majority of

annual precipitation) to sites throughout the region (Table 3.2). However, correlation between sites in the extreme northern and southern/southeastern parts of the study area is insignificant (p<0.05), indicating critical differences in year-to-year rainfall variability between these two areas. These differences arise from the complex interactions among large-scale atmospheric circulation patterns (which affect the trajectory and intensity of the low pressure systems producing precipitation), land-sea distances and distribution, topography, and small-scale climatic processes in the Levant, which are reviewed below.

Atmospheric circulation patterns and climate

The atmospheric circulation patterns responsible for the intensity and trajectory of low pressure systems (and thus the spatial distribution and variability of precipitation) in the East Mediterranean are highly complex. Certain atmospheric circulation regimes have been identified as closely linked with, and can explain the highest percentage of, winter precipitation variability in the Mediterranean, although it should be noted that variability in Levantine precipitation is not solely explained by the circulation regimes and associated large-scale teleconnection patterns described here.

Xoplaki et al. (2004) and Dünkeloh and Jacobheit (2003) found that (in particular) low (high) pressure anomalies over Northwest Europe and north of the Caspian Sea during winter (October–March) are associated with weaker (stronger) westerlies and produce high (low) precipitation throughout all of the Mediterranean, except the southern Levant. This climate regime is linked to, and has negative correlation with, the North Atlantic Oscillation (NAO) and East Atlantic-West Russia

Table 3.2. Correlation coefficients between normalized October–September precipitation series of the 0.5º CRU gridded datasets (available from the Climate Research Unit at the University of East Anglia) (Hulme 1992; Mitchell and Jones 2005) and Cypriot meteorological station data over a 1961–1990 baseline period. ***= p<0.001; **= p<0.01; and *= p<0.05

	31,75_35.25									
32.75_35.25	r=0.632*** p<0.001	32.75_35.25								
33.25_35.25	r=0.553*** p<0.001	r=0.923*** p<0.001	33.25_35.25							
32.25_35.75	r=0.760*** p<0.001	r=0.763*** p<0.001	r=0.702*** p<0.001	32.25_35.75						
32.75_35.75	r=0.655*** p<0.001	r=0.845*** p<0.001	r=0.856*** p<0.001	r=0.880*** p<0.001	32.75_35.75					
34.25_35.75	r=0.389** p=0.002	r=0.737*** p<0.001	r=0.863*** p<0.001	r=0.615*** p<0.001	r=0.780*** p<0.001	34.25_35.75				
35.75_35.75	r=0.145 p=0.273	r=0.420*** p<0.001	r=0.534*** p<0.001	r=0.229 p=0.082	r=0.400** p=0.002	r=0.527*** p<0.001	35.75_35.75			
37.25_30.75	r= -0.158 p=0.233	r=0.434** p=0.001	r=0.490*** p<0.001	r= -0.109 p=0.411	r=0.138 p=0.297	r=0.313* p=0.016	r=0.552*** p<0.001	37.25_30.75		
Ag. Epifanos	r=0.204 p=0.121	r=0.434*** p<0.001	r=0.490*** p<0.001	r=0.396** p=0.002	r=0.561*** p<0.001	r=0.485*** p<0.001	r=0.308* p=0.018	r=0.378** p=0.003	Ag. Epifanos	
Pedoulas	r= 0.077 p= 0.560	r= 0.425** p= 0.001	r= 0.507*** p<0.001	r= 0.269* p= 0.040	r= 0.474*** p<0.001	r= 0.577*** p<0.001	r= 0.626*** p<0.001	r= 0.516*** p<0.001	r= 0.716*** p<0.001	Pedoulas
Pano Panagia	r= 0.054 p= 0.686	r= 0.406** p= 0.001	r= 0.498*** p<0.001	r= 0.215 p= 0.102	r= 0.418*** p<0.001	r= 0.566*** p<0.001	r= 0.693*** p<0.001	r= 0.595*** p<0.001	r= 0.563*** p<0.001	r= 0.860*** p<0.001
Peristerona	r= 0.207 p= 0.116	r= 0.390** p= 0.002	r= 0.463** p<0.001	r= 0.393** p= 0.002	r= 0.480 p<0.001	r= 0.469*** p<0.001	r= 0.344** p= 0.008	r= 0.147 p= 0.266	r= 0.688*** p<0.001	r= 0.626*** p<0.001

Pano Panagia
r= 0.542*** p<0.001

(EAWR) teleconnection patterns. Thus, atmospheric circulation favoring high precipitation in the northern Levant is more likely when the NAO and EAWR are in negative phases, while a positive NAO and EAWR are more likely to contribute to low winter precipitation (Dünkeloh and Jacobheit 2003; Krichak and Alpert 2005; Xoplaki et al. 2004).

Black (2011) and Enzel et al. (2003) found that high winter precipitation in the southern Levant is generally associated with high pressure over Central/Southeast Europe, which diverts the Mediterranean storm track southwards more frequently than usual. Low pressure or a zonal ridge over Northwest-Central Europe and high pressure over southern Europe directs the Mediterranean storm track along the southern coast of Turkey (Enzel et al. 2003), and produces dry conditions in the southern Levant (Black 2011).

Atmospheric circulation regimes favoring high precipitation in the southern Levant are more common when the NAO is in its positive phase (Black 2011; Xoplaki et al. 2004). However, Black (2011) and Xoplaki et al. (2004) note that the relationship between the NAO and winter precipitation in the southern Levant is non-linear. A strong positive NAO does not always bring high rainfall to the southern Levant, and dry years in the southern Levant do not strongly correspond with negative NAO years. Black (2011) found an association between a negative EAWR and circulation regimes producing low rainfall in the southern Levant, although, like the NAO, the relationship between the EAWR and rainfall in the southern Levant is not symmetrical (i.e., there is a weak association between a positive EAWR and high rainfall). Other large-scale climate teleconnection patterns, including the North Sea-

Caspian Pattern (NCP) (Kutiel et al. 2002), and the El Niño-Southern Oscillation (ENSO) (Black 2011; Price et al. 1998; Ziv et al. 2006) have been found to influence precipitation variability in the southern Levant, although their influences are temporally, spatially, and seasonally variable.

Spring (April and May) is a period of rapid climatic change in the Mediterranean, as atmospheric pressure systems transition from their winter to summer regimes, resulting in further spatial variability in rainfall throughout the northern and southern Levant. The Cyprus lows weaken and become less frequent, leading to lower overall rainfall for the region (Black et al. 2011; Dünkeloh and Jacobheit 2003; Xoplaki et al. 2004). Storms generally move to the northeast through the northern part of the study area, bringing precipitation (albeit in smaller amounts than in winter) to the northern Levant, but do not reach the southern Levant (Alpert et al. 1990; Dünkeloh and Jacobheit 2003; Goldreich 2003).

Local-scale conditions in the northern Levant, especially local instabilities and convection, largely determine the development and intensity of rain-producing atmospheric systems during the spring and summer months, rather than large-scale atmospheric circulation patterns (Dünkeloh and Jacobheit 2003; Trigo et al. 2002). However, Touchan et al. (2014b) note that in years with abnormally low rainfall, there is generally an anomalous high pressure system over the East Mediterranean or eastern North Africa, with an anomalous strong westerly flow over the Balkans or southern Europe. During years with abnormally high precipitation in Cyprus, there is frequently anomalous low pressure over North Africa or the Mediterranean and anomalous flow from the south or southeast.

During the spring, heating of the North African continent also creates a strong temperature gradient between the warm continental landmass and the still relatively cold Mediterranean Sea. This leads to the formation of 'sharav cyclones' along the northern edge of the North African desert, typically in the lee of the Atlas Mountains. These systems move along the North African coast and bring dry desert air and sand and dust storms to the southern Levant (Alpert et al. 1990; Goldreich 2003). This contributes to a longer dry season in the southern Levant (Gaussen 1954), which lasts from April to October (Blondel and Aronson 1999; Dufour-Dror and Ertaş 2004; Goldreich 2003), while in the northern Levant, the summer dry season typically lasts from June to September (Price et al. 1999).

Land-sea interactions and climate

The varying geographic positions of land and sea in the Levant modulate atmospheric circulation and contribute to further variability in precipitation and climate in the region. The southern Levant is bordered by the arid, continental climate of the Syrio-Arabian Desert to its east; to the south by the arid Sinai Peninsula, Negev, and Southern Deserts; and to the west by the Mediterranean (Lionello et al. 2006). In the northern Levant, dry, continental landmasses (namely, Europe and Anatolia) are located to the north, and the Mediterranean is located to the south and west. Consequently, frontal depressions (associated with the low pressure systems) arriving at the southern Levant from the northwest bring moist air and rainfall from the Mediterranean. However, the amount of precipitation received from atmospheric systems arriving from the northwest can be completely opposite in the northeastern Mediterranean, particularly in southwestern Turkey and (to a lesser degree) Syria and

Cyprus. This is because air masses arriving from continental Europe from the north-northwest pass over Anatolia, resulting in dry conditions in southwestern Turkey and (to a lesser degree) Cyprus and Syria (Dünkeloh and Jacobheit 2003).

Conversely, low pressure systems with southwesterly air flows pass over the Mediterranean and bring high rainfall to the northeastern Mediterranean, especially southern Turkey (Dünkeloh and Jacobheit 2003; Türkeş 1996). However, frontal depressions with associated southerly circulation pass over dry land masses and lose their moisture, resulting in dry conditions throughout the southern Levant (Goldreich 2003; Kutiel and Paz 1998; Saaroni et al. 2010).

Storm systems with westerly air flows pass over the Mediterranean, and bring rainfall to both the northeastern Mediterranean, as well as the northern part of the southern Levant. However, in the southernmost part of the study area, westerly winds pass over North Africa and the Sinai, resulting in dry conditions in the southern half of the southern Levant (Kutiel and Paz 1998; Saaroni et al. 2010).

Additionally, land-sea distance has an important effect on climate in both the northern and southern Levant, since areas closer to the sea generally receive higher annual rainfall and are more humid even during the summer. As a result, coastal areas are less arid and potential evapotranspiration values are lower than in areas further inland or on leeward mountain slopes (Cordova 2007; Goldreich 2003; Price et al. 1999).

Topography and climate

Topographic variation creates considerable localized climate variation in the northern and southern Levant. High-altitude, windward slopes in the northern Levant

typically receive higher annual rainfall than sites at lower elevations (Price et al. 1999; Türkeş 1996). High-altitude sites also generally have cooler summers with a shorter dry season (Delipetrou et al. 2008; Türkeş 1996). Coastal and high-altitude sites in the northern Levant may also receive small amounts of summer rainfall from isolated thunderstorms, although the contribution of these systems to total annual rainfall is very small (Price et al. 1999; Türkeş 1996). In contrast, the summer months in the southern Levant are almost completely dry (Goldreich 2003).

Sites in the northern Levant located at higher altitudes also have a cooler winter thermal variant than lowland areas in the northern Levant and the majority of sites in the southern Levant (Blondel and Aronson 1999; Delipetrou et al. 2008; Emberger 1955, 1971). At high-altitude sites, minimum temperatures are often near or below freezing, and snow may cover the ground for several weeks (Pashiardis 2000; Tohmé et al. 2004). Mid-altitude sites in the northern Levant, as well as high-altitude areas in the southern Levant, may also receive snowfall during colder, wetter years (Cordova 2007; Goldreich 2003; Pashiardis 2000). However, snowfall in these areas usually remains on the ground for only a few days. In contrast, snowfall is rare in low-altitude forests in the northern Levant and most of the southern Levant (Goldreich 2003; Pashiardis 2000).

All of these variations in atmospheric circulation, geography, and topography within the eastern Mediterranean therefore create a diverse mosaic of environmental and climatic conditions, with a particularly strong contrast between the northern and southern Levant. These differences can also create variability in the primary factors limiting radial growth in the region's trees.

METHODS

Tree-ring chronologies and species

Tree-ring chronologies from 10 forest sites in the northern Levant and 8 in the southern Levant were selected for analysis (Figure 3.1). The location and elevation range of each sampled site is given in Table 3.3. The elevations of the sampled sites in the northern Levant range from 409–1646 meters a.s.l., while the elevations of the sampled sites in the southern Levant range from 106–1134 meters a.s.l. (with the majority of sites below 800 meters a.s.l.).

There is not a single tree species suitable for dendrochronology that also has a widespread native distribution throughout the entire study area. Therefore, in order to minimize variability caused by physiological differences and ecological requirements between species, two common lowland pine species–*Pinus halepensis* Mill. and *Pinus brutia* Ten.–were chosen for analysis. Of the two species, *P. halepensis* has a wider distribution around most of the Mediterranean basin from Morocco and Tunisia through Mediterranean coastal ranges in Spain, France, Italy, and the southern Balkans, along with a small eastern population in southern Lebanon, Israel/Palestine, and Jordan (Nahal 1963; Quézel 2000). The range of *P. brutia* is restricted to northern Greece, Crete, Cyprus, coastal Turkey, and the Syrian and northern Lebanese littoral (Nahal 1983; Quézel 2000; Quézel and Barbero 1992) (Figure 3.2).

Figure 3.1. Locations of the tree-ring sites (*green*) sampled in the study area. Site codes are given in Table 3.3. (For a more detailed view of the Cypriot sites sampled and meteorological stations used, see: Appendix 3.2.

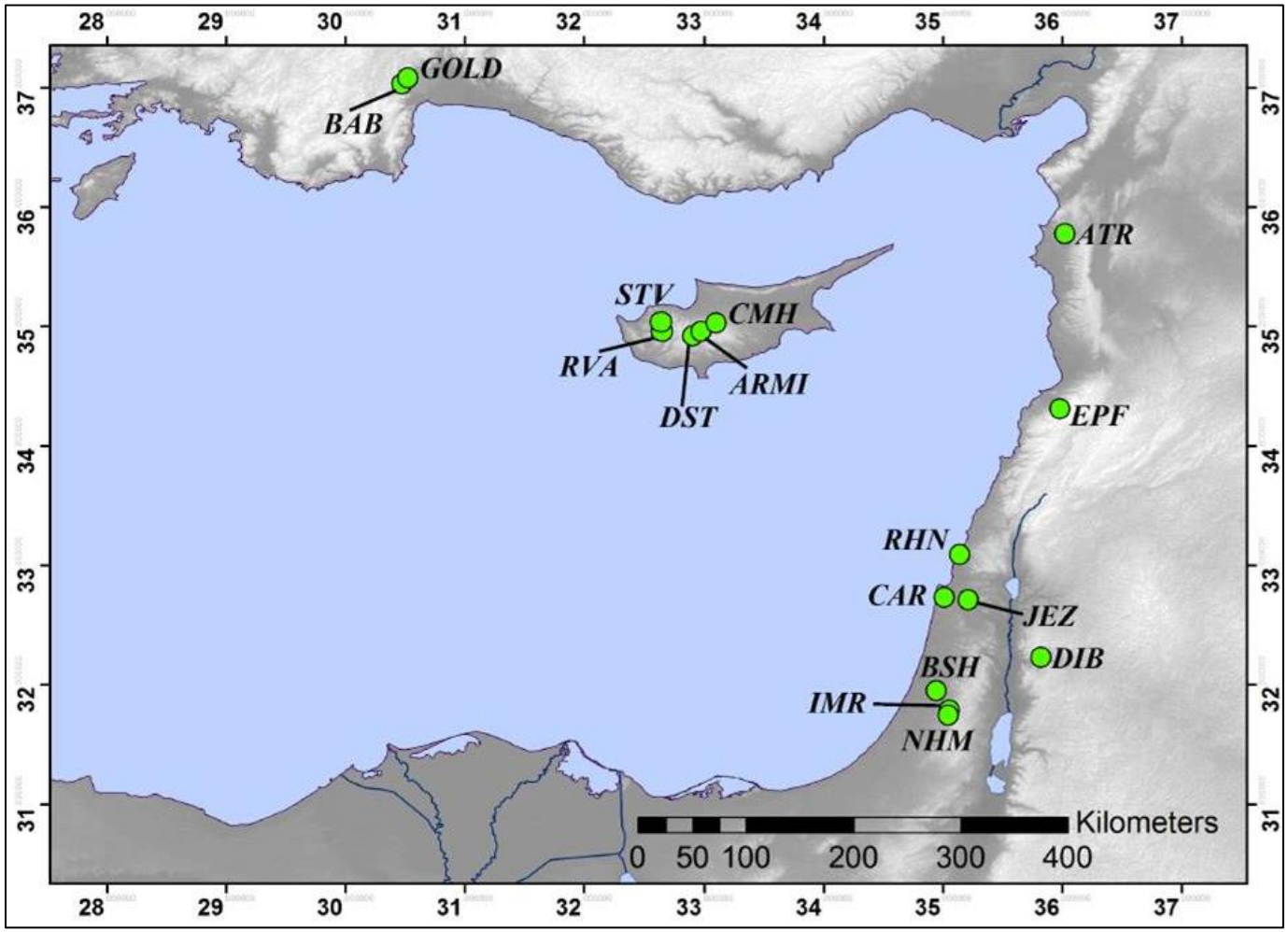

Table 3.3. Description of the northern Levant site locations and tree-ring chronologies. All tree-ring chronologies from the northern Levant were built from *Pinus brutia*. Chronologies sampled from the southern Levant were built from both *Pinus halepensis* and *Pinus brutia*. For information on the southern Levant chronologies, see: Chapter 2.

Country	Site name	Site code	Latitude ºN	Longitude ºE	Elevation range (m)	Years spanned	Total years	No. of trees	No. of cores/ radii	Author
Cyprus	Armiantos	ARMI	34.92	32.90	1483–1646	1584–2002	419	17	33	Touchan et al., 2005
	Doxa Soi o Theos	DST	34.96	32.97	1328–1403	1637–2008	372	25	41	Griggs et al, 2014
	Mitsero Hills	CMH	35.03	33.09	485–498	1776–2009	234	20	42	Griggs et al., 2014
	Roudhias Valley, Arodafna	RVA	34.96	32.65	494–860	1633–2011	379	23	40	Griggs et al., 2014
	Stavros tis Psokas	STV	35.04	32.64	860–1132	1656–2006	351	24	53	Griggs et al., 2014
Lebanon	Herch Ehden	EPF	34.31	35.98	1347–1431	1874–2010	137	18	29	Lorentzen, *this study*
Syria	Atera	ATR	35.78	36.02	409–462	1892–2001	110	7	7	Touchan et al., 2005
Turkey	Bayat Bademleri	BAB	37.03	30.47	641–754	1738–2001	264	15	15	Touchan et al., 2005
	Dumalı Dağ[a]	GOLD	37.4	30.63	887–1426	1694–2001	218	21	27	Touchan et al., 2005
	Göller[a]	GOLD	37.08	30.52	1002–1093	1695–2001	308	22	35	Touchan et al., 2005

[a] Chronologies were pooled together into a single chronology for analysis.

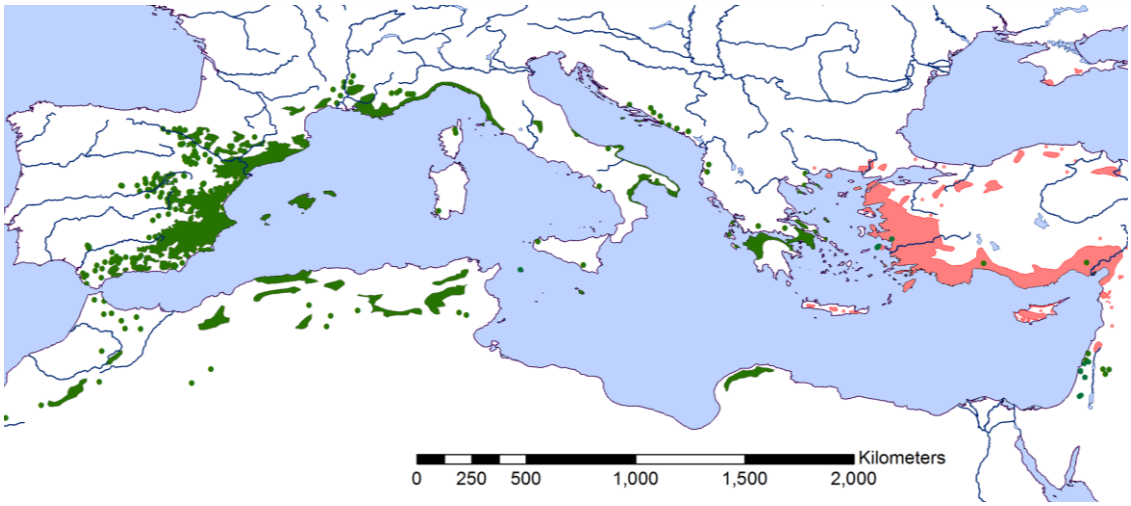

Figure 3.2. Species distributions of *Pinus halepensis* (*green*) and *Pinus brutia* (*pink*) in the Mediterranean (modified from the datasets of: EUFORGEN 2009a, b).

These two species are very closely related, so much so that *P*. *brutia* was once considered a sub-species of *P*. *halepensis* (Panetsos 1981; Quézel 2000). The wood of the two species cannot be distinguished only by their anatomical features (Akkemik and Yaman 2012; Lev-Yadun 2000; Schweingruber 1990), and their overall morphological differences are small (Richardson and Rundel 1998). These species will also naturally hybridize where their ranges overlap, and where the species have been planted near one another (Madmony et al. 2003; Panetsos 1981).

Previous research indicates that the ecological requirements of both species are similar. Both are thermophilous, although *P*. *brutia* is slightly more cold tolerant than *P*. *halepensis* (Boydak 2004; Quézel 2000). Both are also extremely drought resistant with a deep rooting zone, and although the genetic provenances of both species exhibit variability, *P*. *halepensis* is considered more drought resistant and can grow in semi-arid bioclimatic regions (Boydak 2004; Schiller 2000). Comparisons among pine chronologies–including *P*. *halepensis* and *P*. *brutia*–in the southern Levant (see:

Chapter 2) also show great coherence, in terms of both their tree-ring growth signals and climate responses. Therefore, since these two species have great physiological similarity and ecological requirements, occupy the same ecological niche, and have strong heteroconnections (that is: significant crossdating across species), it is considered appropriate to compare the two species in this study.

This study uses seven *Pinus halepensis* chronologies and one *Pinus brutia* chronology from 8 sites in Israel and Jordan (described in Chapter 2). I also analyzed 9 *Pinus brutia* tree-ring chronologies from 10 forest sites in the northern Levant (Cyprus, Lebanon, Syria, and southern Turkey). The northern Levant dataset includes tree-ring chronologies developed by Griggs et al. (2014) and Touchan et al. (2005). An additional chronology was built from *P. brutia* trees sampled from the Ehden Nature Reserve in northern Lebanon specifically for this study.

Sampling, measurement, and chronology building and analysis

The methods for sampling, measurement, and chronology building tree-ring chronologies from the Ehden site and the southern Levant chronologies are outlined in Chapter 2, while the sampling, measurement, and chronology-building methods used to develop the Turkish, Cypriot, and Syrian tree-ring chronologies (which are similar to those used in the present study) are described in Griggs et al. (2014) and Touchan et al. (2005, 2014a, b). Two of the sites in Turkey (Göller and Dumalı Dağ) were pooled together into a single site chronology because of their extremely high correlation, following Touchan et al.'s (2005) study.

Mean sensitivity was calculated from each residual site chronology in the program ARSTAN (Cook 1985; Cook and Krusic 2006). First-order autocorrelation

was also calculated in ARSTAN from each standardized site chronology, prior to the removal of significant autocorrelation from the time series in the pre-whitening process. Both of these statistical parameters were used to quantify and compare the climatic and environmental sensitivity of trees from the sites sampled in the northern and southern Levant.

Climate response functions

The relationship between tree-ring growth and climate was analyzed by determining the response function coefficients for each chronology using the DENDROCLIM2002 program (Biondi and Waikul 2004) (for a description of response function analysis, see: Chapter 2: Materials and Methods). Analysis was conducted over a common period of AD 1943–2001, so that each chronology would have adequate sample depth (SSS> 0.85) (Wigley et al. 1984), particularly in the earliest years of the chronologies, while still maximizing the number of years analyzed.

Each calculated response function includes 13 coefficients associated with mean temperature and 13 coefficients associated with monthly total precipitation variables. The monthly climate data were used as predictors and the standardized site chronologies as predictands over the 1943–2001 common period for the pine chronologies; thus, climate data from September–December of the previous year (1942) were also used. The stability of the climate signal in each of the tree-ring chronologies was also computed in DENDROCLIM by computing the response functions using a moving interval (see: Chapter 2: Materials and Methods) with varying base lengths of 52, 60, and 70 years (when sufficient climate and tree-ring

data was available). Moving interval response functions for each chronology were computed between the years 2001 and 1930 or the earliest year in which the chronology's SSS was greater than 0.85.

Monthly precipitation and temperature data were obtained from the high-resolution climate dataset CRU TS 3.1 gridded at 0.5º intervals, which are available from the Climate Research Unit at University of East Anglia (Hulme 1992; Mitchell and Jones 2005), and local meteorological station data obtained from the Cypriot, Israeli, Jordanian, and Turkish Meteorological Services. During preliminary analysis, it was found that the gridded data were generally more robust, longer, free from missing data, and had higher correlation with the tree-ring chronologies than local meteorological station data. Therefore I preferred to use the gridded dataset closest to each site.

However, the CRU gridded precipitation data were not suitable for analyzing the climate responses of the Cypriot tree-ring chronologies. The CRU precipitation grids for Cyprus were developed primarily using climate data from low-altitude, coastal sites and Nicosia, which is located roughly in the island's arid interior (Griggs et al. 2014). Climate conditions at these sites do not correspond well with those of the forest sites analyzed here. Instead I used the same meteorological datasets as Griggs et al. (2014) (for more information on the Cypriot meteorological stations, see: Appendix 3.2). Precipitation data from the Agios Epifanos meteorological station in central Cyprus was used to analyze the climate response of the Mitsero Hills (CMH) site chronology, since this climate dataset had the highest correlation and largest number of significant response functions with the CMH chronology (Griggs et al.

2014). The climate responses of the four other Cypriot chronologies (ARMI, DST, RVA, and DST) were analyzed using an average of precipitation data from the following three meteorological stations: Pano Panagia, Pedoulas, and Peristerona. The temperature responses of all of the Cypriot sites (including CMH) were analyzed using an average of the mean temperature data values from four 0.5º CRU grids covering 32.5º–33.5ºN, 32.5–33.5ºE.

Correlation among site chronologies

Variability in tree-ring growth at different sites was evaluated over the 1943–2001 common period with the same statistical analyses described in Chapter 2, i.e., Pearson correlation, hierarchical cluster analysis (HCA), and principal component analysis (PCA). HCA using Ward's linkage method was performed using all 18 chronologies as a means of exploratory analysis (Rencher 2002: 466–479). Principal component analysis was performed first for the correlation matrix of the 10 chronologies sampled from the northern Levant, in order to examine regional variability on a smaller scale. A second PCA was then performed using the correlation matrix of all 18 pine chronologies from the northern and southern Levant. The most representative principal components from the PCA, which explain most of the variance in tree-ring growth, were selected according to Kaiser's rule, where eigenvalues >1 are retained (Kaiser 1992). VARIXMAX rotation was then performed on the retained components.

Tree-ring correlation for historical/archaeological crossdating

Since *Pinus halepensis*/*brutia* timbers have been frequently found in historical and archaeological sites in the eastern Mediterranean, regional variability and tree-ring teleconnections for the two species were also examined using standard dendrochronological crossdating methods. This was performed in order to determine whether *P*. *halepensis*/*brutia* chronologies from the study area could be crossdated reliably using the other site chronologies as reference chronologies, and the geographic extent over which reliable dendrochronological crossdates could be made. In particular, I tested whether site chronologies from the southern Levant could be reliably crossdated using site chronologies from the northern Levant as reference chronologies (and vice versa), or if the two regions were dendrochronologically distinct.

Standardized site chronologies (that is: chronologies which had been 'standardized' using the variance stabilization and de-trending methods described in the previous chapter, but which had not been 'pre-whitened' using autoregressive models), which were built in ARSTAN, were used for this crossdating exercise. The quality of crossmatches between pairs of chronologies was evaluated using three different statistical tests: Gleichläufigkeit (*GL*), the Baillie-Pilcher *t*-value (t_{BP}), and the Hollstein *t*-value (t_H), using the TSAP dendrochronological software package (Rinn 1996).

The trend coefficient, or *Gleichläufigkeit* (*GL*; alternatively referred to as the *W* statistic) (Eckstein and Bauch 1969), is a simple non-parametric test that calculates the fraction of years in which two overlapping tree-ring chronologies have common

parallel increases or decreases in ring-width (Eckstein and Bauch 1969). The *GL* value is often expressed as a percentage (*%GL*). Two randomly matched tree-ring series are expected to have a *Gleichläufigkeit* of 50% with a standard deviation (*S*) of:

$$S = \left(\frac{1}{2\sqrt{n}} \right)$$

where *n* is the number of overlapping years between the two chronologies. The significance of a *GL* value is determined by calculating its *z*-score, using the formula:

$$z = \left(\frac{GL - 0.5}{S} \right)$$

The standard normal curve is then used to determine the probability that an observed or large *z*-value will occur when there is not an actual match between two chronologies (i.e., a statistical type I error). *GL* is useful in expressing high-frequency similarities between chronologies or tree-ring series. However, it does not take into account the amplitude of change in ring-width values from year to year (Jansma 1995).

The Baillie-Pilcher and Hollstein *t*-values are widely used dendrochronological crossdating statistics. They are versions of Student's *t*-test that attach probabilities to the calculated correlation coefficient (*r*) between two tree-ring chronologies (Baillie and Pilcher 1973; Hollstein 1980). Unlike the *GL*-value, the *t*-value takes into account the magnitude of year-to-year ring-width variations in the two curves being compared and also measures the significance of a match between the two curves by taking into account their length of overlap (Baillie and Pilcher 1973). Higher t_{BP} and

t_H-values indicate that a dendrochronological match between two chronologies is more likely. A *t*-value is calculated as:

$$t = \frac{r\sqrt{n-2}}{\left(1-r^2\right)}$$

where:

r= the correlation coefficient between the two chronologies

n= the number of years overlap between the two chronologies

However, the strength of agreement between chronologies (and thus the likelihood of a type I error) cannot be assessed by using confidence intervals calculated from the Student's *t* distribution. This is because the crossdating process involves sliding an undated site chronology past the reference chronology and calculating *t*-values for each placement of the two curves. This is the statistical equivalent of making multiple comparisons ('multiplicity'), which increases the likelihood of a type I error if the calculated dendrochronological *t*-value's likelihood is interpreted using the same probability attached to a *t*-value in a single comparison *t*-test (Wigley et al. 1984). Additionally, there is often naturally occurring low frequency variance and autocorrelation in the tree-ring series being compared, meaning that the data are not independent and do not have a normal distribution. This increases the likelihood of spurious dates with high *t*-values arising by chance (Munro 1984; Wigley 1987).

Different standardization techniques have been developed, in which the tree-ring series are fitted to either an autoregressive or moving-average model, so that the transformed tree-ring data have an approximately normal distribution, the dataset's

high frequency variation is emphasized, and the likelihood of a type I error is minimized (Munro 1984; Wigley et al. 1987). Accordingly, dendrochronological analysis programs like TSAP transform tree-ring data before Baillie-Pilcher and Hollstein *t*-values are calculated. Before the Baillie-Pilcher *t*-value is calculated, the tree-ring data undergo a simple transformation, in which each ring-width is converted to a percentage of the mean of the five ring-widths of which it is a center value (Baillie and Pilcher 1973). These percentage figures then undergo a natural logarithmic transformation, using the following:

$$y_i = \log\left(\frac{y_i}{y_i + 1}\right)$$

where:

y_i= the ring-width percentage value at year *i*

y_i= the tree-ring index in year y_i after the natural log transform

The Hollstein *t*-value is similar to the Baillie-Pilcher *t*-value, except that the tree-ring measurements undergo only a logarithmic transformation before the *t*-value is calculated (Hollstein 1980). Additional standardization of a dataset may be necessary to eliminate low-frequency trends due to the effects of age, stand dynamics, disturbances, and other factors that may dampen the tree-ring signal and hinder successful, secure crossdating. However, Wigley et al. (1987) note that there is no specific standardization procedure that is most effective at eliminating both type I and type II errors (that is: correct crossmatches that are not accepted, because they are associated with low correlation values).

Many dendrochronologists set an empirically derived minimum 'threshold' *t*-value (which varies depending on the study region) that will most likely indicate a secure dendrochronological crossmatch (Baillie 1982; Wigley et al. 1987). For instance, in the East Mediterranean, a *t*-value above 5.0 has been interpreted as indicating a secure dendrochronological match (e.g., Kuniholm 2000; Kuniholm et al. 2007; Kuniholm and Striker 1987). However, spurious crossdating results may still arise, even when a pair of chronologies crossdate with the minimum *t*-value (particularly in cases when the chronologies have a short overlap or low sample depth). Additionally, different dendrochronological analysis programs may calculate slightly different *t*-values when comparing the same filtered tree-ring curves (Sander and Levanič 1996). This can especially affect datasets with short overlaps and only poor to moderate correlation. However, it should be noted that crossdated datasets with high correlation and especially those with long overlaps maintain high *t*-values regardless of the statistical program and standardization methods used.

Consequently, it is recommended that dendrochronologists use multiple lines of evidence to establish secure crossmatches, including using different statistical tests (i.e., *t*-values and *GL*) and (critically) inspecting the visual fit between chronologies to verify the dating placement. The overlap between crossdated chronologies should be as long as possible (at least 50–100 years), with as much sample replication in the chronology as possible; and significant crossmatches with the same end date should be found against multiple, different reference chronologies (when they are available) (Baillie 1982; Munro 1984; Wigley et al. 1987).

In accordance with these above-mentioned guidelines, I assessed the quality of dendrochronological crossdates between pairs of chronologies by evaluating their statistical fit holistically, in which *GL* values with $p<0.05$ and t_{BP} and t_H-values above 5.0–5.5 suggest a secure fit. The visual fit between pairs of chronologies was then examined and compared with the statistical level of fit. Tree-ring chronologies were crossdated over the 1943–2001 common period, so that the overlap between chronologies would be consistent. As an additional test, I repeated the crossdating exercise over the (usually longer) period in which for each chronological pair had SSS>0.85 (calculated in ARSTAN), in order to assess how the length of overlap between chronologies affected the statistical and visual quality of the crossmatch.

RESULTS

Tree-ring chronologies

The length, number of samples, and the general statistics for each chronology are given in Tables 3.3 and 3.4. The mid-to-high-altitude sites in Turkey and Cyprus are the longest tree-ring chronologies and contain trees that are, on average, older than those from other sites in the Levant. Touchan et al.'s (2005) chronology from Armiantos (which is located at the uppermost limits of *Pinus brutia*'s ecological zone in Cyprus) is the longest *P*. *brutia*/*halepensis* chronology in the study region.

Mean sensitivity is generally lower for most of the northern Levant chronologies than for those in the southern Levant, except for the Mitsero Hills site in Cyprus, which has high mean sensitivity (MS=0.403). First-order autocorrelation is also generally higher for the chronologies from the northern Levant sites than for those

from the south, indicating greater influence on tree-ring growth in a given year by the previous year's growth conditions.

Table 3.4. Descriptive statistics for the samples and chronologies. First order autocorrelation (AC1) is calculated from the standardized chronology, while all other statistics are calculated from the residual chronologies.

Site code	Standard deviation	Skewness	Kurtosis	Mean sample segment length	Mean inter-series correlation	1st year SSS >0.85	MS	AC1
No. Levant								
ARMI-PIBR	0.160	-0.03	0.49	238	0.404	1706	0.181	0.467
ATR-PIBR	0.116	0.00	-0.25	89	0.225	1872	0.146	0.344
BAB-PIBR	0.173	-0.01	-0.07	171	0.572	1751	0.211	0.292
CMH-PIBR	0.320	-0.51	0.08	160	0.762	1820	0.403	0.436
DST-PIBR	0.200	-0.48	0.29	181	0.628	1816	0.183	0.623
EPF-PIBR	0.162	0.14	0.79	104	0.352	1902	0.192	0.345
GOLD-PIBR	0.150	-0.01	0.25	159	0.471	1793	0.172	0.336
RVA-PIBR	0.210	-0.21	0.37	235	0.606	1740	0.221	0.636
STV-PIBR	0.230	0.05	-0.05	234	0.622	1756	0.168	0.400
So. Levant								
BSH-PIBR	0.194	-0.18	-0.33	59	0.480	1933	0.258	0.251
BSH-PIHA	0.238	0.00	-0.18	75	0.478	1930	0.278	0.249
CAR-PIHA	0.016	0.01	-0.10	68	0.407	1911	0.209	0.198
DIB-PIHA	0.211	-0.14	-0.11	74	0.541	1915	0.272	0.297
IMR-PIHA	0.202	-0.05	0.02	82	0.539	1851	0.242	0.294
JEZ-PIHA	0.027	0.15	-0.13	64	0.542	1938	0.330	0.129
NHM-PIHA	0.180	0.00	-0.35	62	0.449	1943	0.231	0.247
RHN-PIHA	0.204	0.01	0.08	80	0.469	1914	0.235	0.275

Climate response function analysis

Monthly temperature and precipitation values that have significant correlation (p<0.05) with each of the tree-ring chronologies over the 1943–2001 common period, and their relative stability over the moving intervals, are given in Table 3.5 (for individual response function plots for each chronology, see: Appendices 2.3 and 3.3).

The climate responses of the southern Levant tree-ring chronologies are described and analyzed in greater detail in Chapter 2, so they are described here largely in comparison to climate responses from the northern Levant chronologies. Tree-ring growth is more responsive to monthly precipitation values in both the southern and northern Levant sites. Radial growth at all of the sampled sites generally has positive correlation with monthly precipitation values, meaning that higher (lower) monthly precipitation values correspond to wider (narrower) tree-ring widths.

However, the climatic sensitivity of tree-ring chronologies and the months in which precipitation is a significant limiting factor differ between the two regions. As mentioned in Chapter 2, significant responses between precipitation and tree-ring growth for chronologies from southern Levant sites are concentrated during the rainy season from October through April, with the most significant responses in December–January (and to a lesser degree, November and February).

While the northern Levant chronologies do have significant responses to precipitation during the earlier part of the rainy season (i.e., October–February), significant responses (that are also stable over time) are more concentrated during spring–summer months, particularly March–June, and (for DST) even August. Tree-ring chronologies from low-altitude sites are more sensitive to precipitation and yield

more months with a significant positive response to precipitation. The Mitsero Hills (CMH) chronology is the most climatically sensitive to precipitation of all the northern Levant chronologies. Chronologies from high-altitude sites like Armiantos (ARMI), Ehden (EPF), and Göller (GOLD) do not produce significant positive responses to precipitation. The Armiantos chronology has a significant negative response to February precipitation. This relationship may occur, because unusually high snowfall may increase the amount of time that the site is covered with snow, which may lengthen the amount of time that the trees are photosynthetically inactive and delay the onset of the spring growing season. Alternatively, this negative response may indicate the influence of a limiting factor that is indirectly related to precipitation. For instance, high precipitation and accompanying high cloud cover may reduce solar radiation, limiting photosynthesis (Fritts 1976).

Chronologies from southern Levant sites generally have significant negative responses to mean monthly temperature, particularly in April and December–January. This means that higher (lower) temperatures correspond to narrower (wider) tree-rings. However, many of these temperature responses are not stable over time (unlike the southern Levant precipitation responses). Temperature response is much more variable, less significant, and unstable over time for the northern Levant chronologies. High-altitude sites like Ehden and Armiantos have significant positive responses to mean monthly temperature over the common period during February–March, meaning that higher (lower) temperatures correspond to wider (narrower) tree-rings. The Mitsero Hills chronology (which is from a low-altitude site) has a significant negative response to mean temperature in December. The Göller chronology (which is a mid-

Table 3.5. Summary of significant response function coefficients of the 17 tree-ring chronologies to monthly precipitation and mean temperature over the 1943–2001 common period. A '+' signifies significant positive correlation, while a '-' signifies significant negative correlation. Months shaded in gray had significant response function coefficients throughout the moving interval analysis.

Precipitation

Site	Oct	Nov	Dec	Jan	Feb	Mar	Apr	May	Jun	Jul	Aug	Sep	Oct
No. Levant													
ARMI-PIBR					-								
ATR-PIBR			+										
BAB-PIBR						+							+
CMH-PIBR			+			+		+					
DST-PIBR								+			+		
EPF-PIBR													
GOLD-PIBR													
RVA-PIBR	+							+					
STV-PIBR	+							+	+				
So. Levant													
BSH-PIBR			**+**	**+**									
BSH-PIHA													
CAR-PIHA		**+**	**+**	**+**									
DIB-PIHA		**+**	**+**	**+**	**+**								
IMR-PIHA	**+**	**+**	**+**	**+**	**+**	**+**							
JEZ-PIHA		**+**	**+**	**+**									
NHM-PIHA				**+**									
RHN-PIHA													

Mean Temp.

Site	Oct	Nov	Dec	Jan	Feb	Mar	Apr	May	Jun	Jul	Aug	Sep	Oct
No. Levant													
ARMI-PIBR					**+**	**+**							
ATR-PIBR													
BAB-PIBR													
CMH-PIBR			**-**										
DST-PIBR													
EPF-PIBR					**+**								
GOLD-PIBR					**+**	**+**				**-**	**-**		
RVA-PIBR													
STV-PIBR													
So. Levant													
BSH-PIBR			**-**				**-**						
BSH-PIHA			**-**				**-**						
CAR-PIHA							**-**						
DIB-PIHA							**-**						
IMR-PIHA			**-**	**-**	**-**	**-**	**-**						
JEZ-PIHA				**-**									
NHM-PIHA				**-**			**-**						
RHN-PIHA							**-**	**-**					

altitude site at the northernmost part of the study area) has significant positive responses to mean temperature in February–March, and significant negative responses to mean temperature in July–August.

Correlation among site chronologies

Pearson correlation values among the different site chronologies over the 1943–2001 common period are given in Table 3.6. As was discussed in Chapter 2, there is significant correlation ($p<0.05$, and often $p<0.01$) among the southern Levant chronologies, and correlation strength is largely a function of distance. Correlation among the northern Levant chronologies (which are distributed over a broader geographic area) is more variable and is a function of both distance and elevation. Thus, high-altitude site chronologies like Armiantos and Ehden have significant correlation with one another, despite their considerable distance from one another, while Armiantos and Mitsero Hills, which are within 22 km of one another but have an altitudinal gradient of over 1000 m between them, are negatively correlated. In fact, none of the northern Levant chronologies has significant correlation with the Mitsero Hills chronology except Roudhias Valley, which is close to Mitsero Hills and includes trees sampled from the same or slightly higher (i.e., up to 360 meters higher) elevation.

Most of the northern Levant chronologies do not have significant correlation with the southern Levant chronologies. Two high-altitude site chronologies from the northern Levant (ARMI and EPF) have significant negative correlation with southern Levant chronologies from especially arid bioclimatic zones. However, the Mitsero

Table 3.6. Pearson correlation among the tree-ring chronologies for the 1943–2001 common period, and distance (km) between pairs of sites. Sites which are both in the northern or southern Levant whose correlation is significant at the $p<0.05$ level or below are shaded in green. Sites in the northern Levant whose correlation is significant at the $p<0.05$ level or below with sites in the southern Levant are shaded in blue. Sites in the northern Levant which have negative correlation that is significant at the $p<0.05$ level or below with sites in the southern Levant are shaded in pink. ***= $p<0.001$; **= $p<0.01$; and *= $p<0.05$

	ARM								
DST_PIBR	r= 0.727** 7 km	DST							
STV_PIBR	r= 0.471** 27 km	r= 0.651** 31 km	STV						
RVA_PIBR	r= 0.261* 23 km	r= 0.537** 29 km	r= 0.634** 9 km	RVA					
CMH_PIBR	r= -0.152 22 km	r= 0.230 15 km	r= 0.213 43 km	r= 0.385** 43 km	CMH				
GOLD_PIBR	r= 0.442** 332 km	r= 0.447** 332 km	r= 0.507** 307 km	r= 0.523** 314 km	r= 0.033 333 km	GOLD			
BAB_PIBR	r= 0.326* 320 km	r= 0.442** 322 km	r= 0.473** 295 km	r= 0.510** 302 km	r= 0.136 324 km	r= 0.514** 25 km	BAB		
ATR_PIBR	r= 0.100 298 km	r= 0.245 292 km	r= 0.398** 317 km	r= 0.514** 319 km	r= 0.226 278 km	r= 0.381** 513 km	r= 0.285* 515 km	ATR	
EPF_PIBR	r= 0.474** 290 km	r= 0.336** 285 km	r= 0.427** 316 km	r= 0.210 313 km	r= 0.016 276 km	r= 0.355** 586 km	r= 0.323* 582 km	r= 0.245 163 km	EPF
BSH_PIHA	r=-0.171 380 km	r= -0.147 381 km	r= -0.043 404 km	r= 0.257* 396 km	r= 0.354** 383 km	r= -0.074 710 km	r= 0.177 697 km	r= 0.071 437 km	r= -0.054 280 km
BSH_PIBR	r= -0.278* 380 km	r= -0.205 381 km	r= -0.107 404 km	r= 0.186 396 km	r= 0.409** 383 km	r= -0.136 710 km	r= 0.035 697 km	r= 0.068 437 km	r= -0.253 280 km
CAR-PIHA	r= -0.140 311 km	r= -0.058 311 km	r= -0.055 337 km	r= 0.245 329 km	r= 0.411** 311 km	r= -0.076 643 km	r= 0.124 632 km	r= 0.208 351 km	r= -0.125 197 km
IMR-PIHA	r= -0.351** 401 km	r= -0.266* 401 km	r= -0.242 424 km	r= 0.071 416 km	r= 0.344** 404 km	r= -0.108 731 km	r= -0.025 718 km	r= -0.062 452 km	r= -0.310* 293 km
JEZ-PIHA	r= -0.235 325 km	r= -0.181 324 km	r= -0.088 351 km	r= 0.143 344 km	r= 0.435** 324 km	r= -0.147 657 km	r= -0.075 646 km	r= 0.068 349 km	r= -0.179 192 km
NHM-PIHA	r= -0.205 405 km	r= -0.163 405 km	r= -0.186 428 km	r= 0.052 420 km	r= 0.282* 408 km	r= -0.087 735 km	r= -0.091 721 km	r= -0.018 457 km	r= -0.316* 298 km
RHN-PIHA	r= -0.255 290 km	r= -0.162 288 km	r= -0.204 316 km	r= 0.094 309 km	r= 0.231 287 km	r= -0.063 620 km	r= -0.127 610 km	r= -0.025 310 km	r= -0.427** 156 km
DIB-PIHA	r= -0.192 403 km	r= -0.063 402 km	r= -0.148 429 km	r= 0.203 422 km	r= 0.324* 401 km	r= -0.160 734 km	r= 0.143 723 km	r= 0.056 395 km	r= -0.286* 232 km

Table 3.6. (***continued***)

	BSH_PIHA						
BSH_PIBR	*r*= 0.826** 0 km	**BSH_PIBR**					
CAR-PIHA	*r*= 0.683** 87 km	*r*= 0.741** 87 km	**CAR_PIHA**				
IMR-PIHA	*r*= 0.675** 20 km	*r*= 0.772** 20 km	*r*= 0.616** 104 km	**IMR_PIHA**			
JEZ-PIHA	*r*= 0.607** 88 km	*r*= 0.631** 88 km	*r*= 0.747** 19 km	*r*= 0.604** 103 km	**JEZ_PIHA**		
NHM-PIHA	*r*= 0.580** 25 km	*r*=0.724** 25 km	*r*= 0.532** 109 km	*r*= 0.818** 5 km	*r*= 0.567** 108 km	**NHM_PIHA**	
RHN-PIHA	*r*= 0.336** 128 km	*r*= 0.530** 128 km	*r*= 0.589** 42 km	*r*= 0.579** 144 km	*r*= 0.499** 43 km	*r*= 0.579** 150 km	**RHN_PIHA**
DIB-PIHA	*r*= 0.699** 88 km	*r*= 0.743** 88 km	*r*= 0.649** 94 km	*r*= 0.568** 87 km	*r*= 0.585** 78 km	*r*= 0.568** 91 km	*r*= 0.496** 115 km

Hills chronology has significant correlation with all of the southern Levant chronologies except Rosh HaNiqra (which is a less climatically sensitive chronology).

The principal component analysis generates three principal components, which explain 65.4% of the variance in the original data set. The summary statistics and loadings for each individual chronology in PC1, 2, and 3 after VARIMAX rotation are given in Table 3.7 and are plotted in Figure 3.3.

Table 3.7. Summary statistics of the PCA over the 1943–2001 common period, and the rotated principal components and individual loadings for each site retained in PCA. The rotated principal component with the highest loading for each chronology is noted in bold.

Summary statistics	**PC1**	**PC2**	**PC3**
Eigenvalue	6.0389	4.0251	1.0604
Proportion variance (%)	0.355	0.237	0.062
Cumulative variance (%)	0.355	0.592	0.654
Site code			
ARMI-PIBR	0.041	**0.490**	0.408
ATR-PIBR	-0.101	0.058	**-0.607**
BAB-PIBR	0.072	**0.364**	-0.026
CMH-PIBR	0.097	-0.010	**-0.465**
DST-PIBR	0.016	**0.450**	0.089
EPF-PIBR	-0.097	**0.278**	-0.022
GOLD-PIBR	-0.014	**0.352**	-0.062
RVA-PIBR	0.059	0.286	**-0.357**
STV-PIBR	-0.058	**0.350**	-0.212
BSH-PIBR	**0.375**	-0.013	-0.047
BSH-PIHA	**0.358**	0.063	-0.014
CAR-PIHA	**0.331**	0.026	-0.132
DIB-PIHA	**0.369**	0.038	0.040
IMR-PIHA	**0.376**	-0.042	0.055
JEZ-PIHA	**0.291**	-0.062	-0.152
NHM-PIHA	**0.373**	0.003	0.129
RHN-PIHA	**0.278**	-0.068	0.003

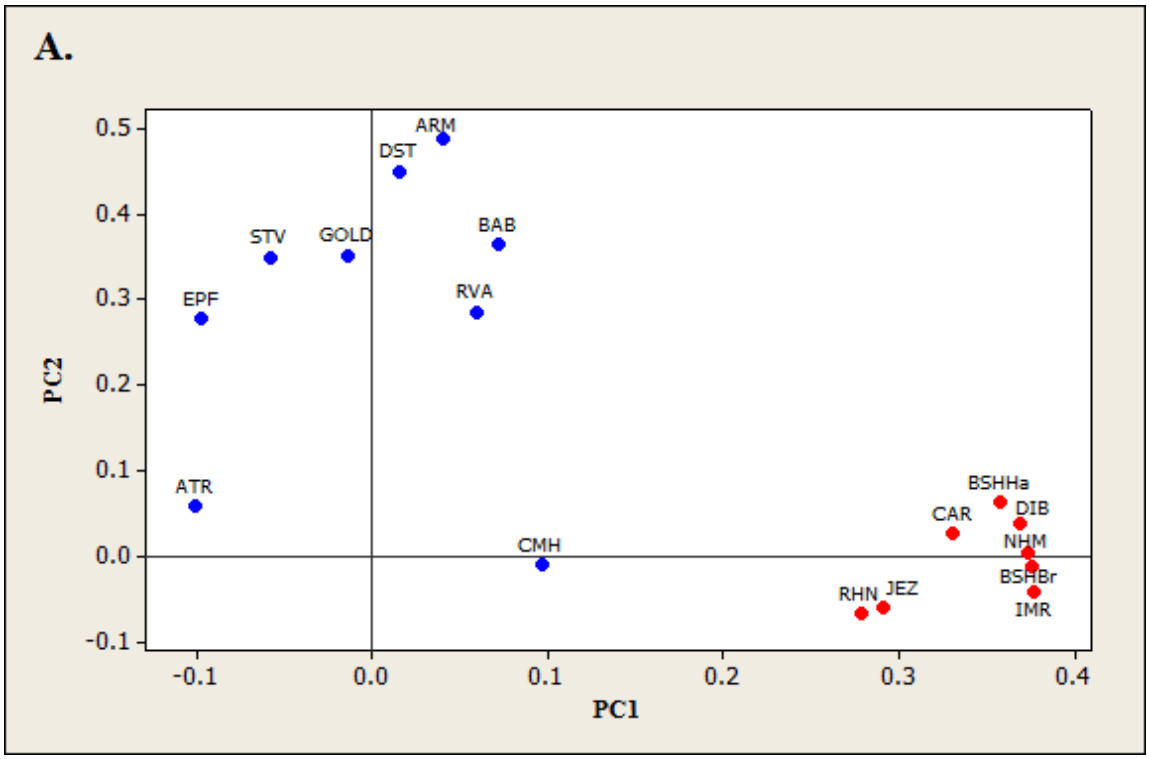

Figure 3.3. Biplots showing the relationship among the different tree-ring chronologies (labeled by site code) for the common period 1943–2001 in terms of their individual loadings in: a. PC1 (*x*-axis) and PC2 (*y*-axis), b. PC1 (*x*-axis) and PC3 (*y*-axis), and c. PC2 (*x*-axis) and PC3 (*y*-axis). Southern Levant site chronologies are marked in red, and northern Levant site chronologies are marked in blue.

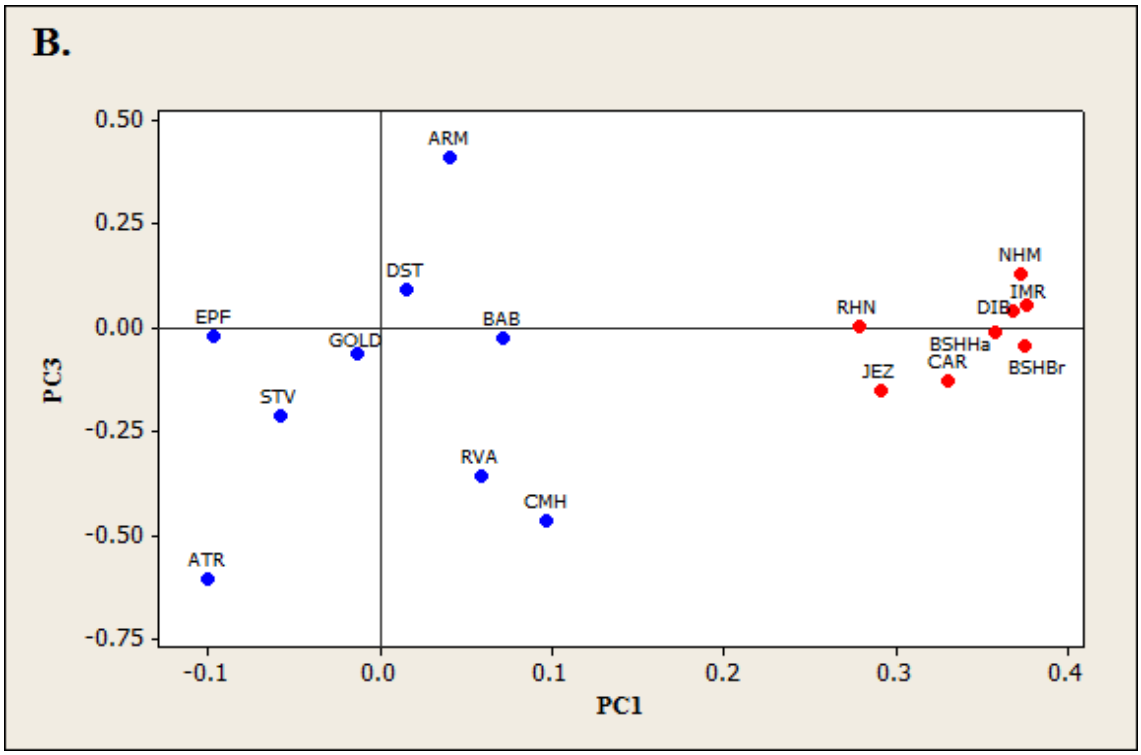

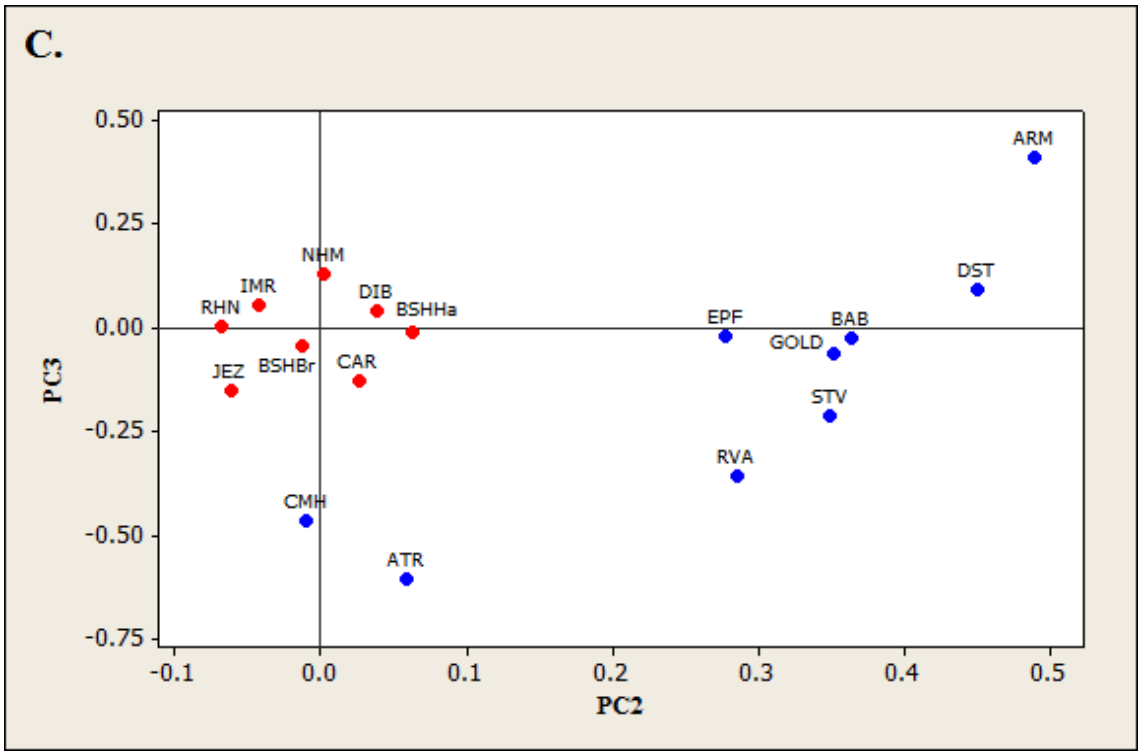

Figure 3.3. (***continued***)

These results clearly separate the northern and southern Levant sites. All of the southern Levant chronologies have the highest loading (all positive) in PC1 and loadings near zero in PC2 and PC3. The groupings in PC2 and 3 are not as clearly defined geographically, although generally, higher elevation sites (ARMI, DST, EPF, and STV) or the Turkish sites at the northwestern boundary of the study area (BAB and GOLD) have the highest loading in PC2. Lower elevation sites in the northern Levant (ATR, CMH, and RVA) have the highest, negative loading in PC3. However, three of the sites have loadings that are more evenly distributed across PC 2 and 3. ARMI has a high positive loading in PC3, while STV has a high negative loading in PC3. RVA also has a high positive loading in PC2.

Hierarchical cluster analysis of all 18 chronologies from the Levant over the 1943–2001 common period yields two main groups and four main sub-groups (Figure 3.4). The 'southern Levant' and the Mitsero Hills pine chronologies are placed in 'Group 1,' while the remainder of the 'northern Levant' chronologies are placed in 'Group 2.'

The distance between these two groups is considerable. Within 'Group 1,' Mitsero Hills (CMH) is placed in its own distinct sub-group, while the 'southern Levant' chronologies are placed in the second sub-group. Within 'Group 2,' the sites are divided largely by site elevation. Chronologies from five sites (GOLD, BAB, STV, RVA, and ATR), which are located at mid-to-low altitudes, are placed into a sub-group. Chronologies from three sites (ARMI, DST, and EPF), which are located at high altitudes (and close to the upper altitudinal limit of *P. brutia*), comprise the

second sub-group, in which EPF has the furthest correlation distance from the other two chronologies.

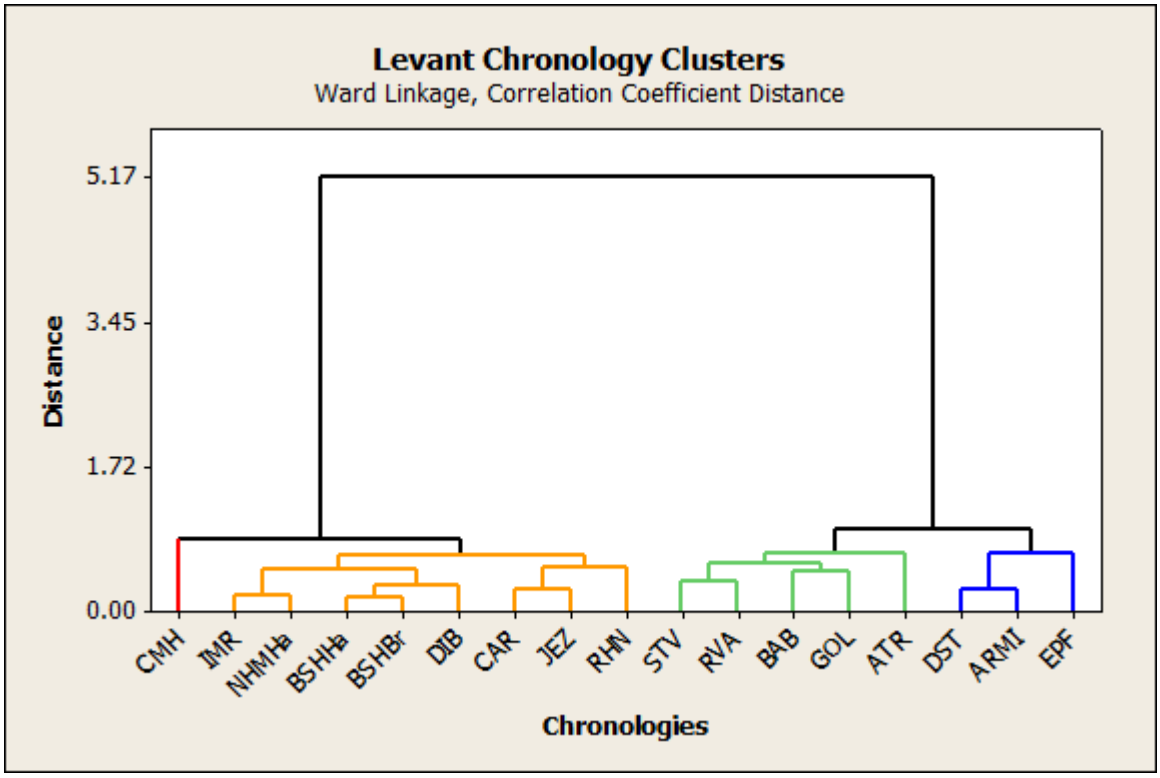

Figure 3.4. Dendrogram resulting from the cluster analysis of the tree-ring chronologies over the 1943–2001 common period.

Tree-ring correlation for historical/archaeological crossdating

The crossdating statistics for the northern and southern Levant chronologies are given in Table 3.8. The results are similar to the Pearson correlation analysis, although there are fewer significant matches between sites because of the stricter correlation criteria. All of the southern Levant chronologies yield significant crossdates with one another, except for the Nes Harim and Rosh HaNiqra chronologies (which are both somewhat noisy chronologies that still have near-significant correlation and are at the southern and northern extremes, respectively, of the southern

Levantine pine chronologies). None of the southern Levant chronologies has significant crossdates with the northern Levant chronologies.

There is greater variability in the northern Levant in site-to-site correlation, which is dependent on differences in altitude and distance between sites. High-altitude sites like Armiantos and Ehden yield significant crossdates with one another, as do low- to mid-altitude sites like Roudhias Valley, Göller, and Atera (despite their considerable distances from one another). Similarly, of the Cypriot chronologies (which are located along an altitudinal transect), the mid-altitude sites (STV, RVA, and DST) all crossdate significantly, but Armiantos (ARMI), which is located at the highest elevation, correlates only with Doxa Soi o Theos (DST), which is closest in elevation and in distance. Mitsero Hills (CMH), which is at the bottom of the transect in the rain shadow of the Troodos Massif, does not yield significant crossdates with any of the other site chronologies in the northern Levant, including ARMI and DST, which are less than 25 km away. In fact, the Mitsero Hills chronology has stronger correlation with the more distant southern Levant chronologies, although it does not crossdate significantly with these site chronologies.

If the length of overlap is increased, and the entire length of the chronologies in which SSS> 0.85 is used (Wigley et al. 1984), there are more significant crossdates among mid-altitude and low-to-mid-altitude chronologies from the northern Levant (e.g., ATR, GOLD, BAB, STV, RVA) (Table 3.9). The number of significant crossdates between chronologies from high-altitude sites in Cyprus and Lebanon (e.g., ARMI, DST, and EPF) and those from mid-altitude sites in Turkey and Cyprus (e.g., GOLD, RVA, and STV) also increases. However, there are no significant crossdating

results between site chronologies from the northern Levant (including Mitsero Hills) with site chronologies from the southern Levant. Likewise, there are no significant dendrochronological crossdates between the Mitsero Hills chronology and other chronologies from the northern Levant, except for Roudhias Valley (RVA).

Table 3.8. Crossdating statistics (calculated in TSAP) among the site chronologies over the 1943–2001 common period, and distance (km) between pairs of sites. Chronologies from sites in the northern Levant which crossdate significantly with one another are shaded in green. Chronologies from sites in the southern Levant which crossdate significantly with one another are shaded in pink. t_{BP}= Baillie-Pilcher *t*-value; t_H= Hollstein *t*-value; *GL= Gleichläufigkeit* (trend coefficient) values and their associated *p*-values; *n*= years overlap between the two pairs of chronologies. For the *GL p*-values, ***= $p<0.001$; **= $p<0.01$; and *= $p<0.05$.

	ARMI	DST	STV	RVA	CMH	GOLD
DST_PIBR	t_{BP}= 8.3 t_H= 8.1 *GL*= 87*** 7 km					
STV_PIBR	t_{BP}= 4.2 t_H= 3.8 *GL*= 77*** 27 km	t_{BP}= 8.0 t_H= 7.6 *GL*= 85*** 31 km				
RVA_PIBR	t_{BP}= 1.5 t_H= 1.5 *GL*= 67** 23 km	t_{BP}= 5.2 t_H= 5.2 *GL*= 78*** 29 km	t_{BP}= 7.4 t_H= 6.9 *GL*= 81*** 9 km			
CMH_PIBR	t_{BP}= 1.6 t_H= 1.8 *GL*= 40 22 km	t_{BP}= 1.9 t_H= 2.2 *GL*= 55 15 km	t_{BP}= 2.1 t_H= 1.9 *GL*= 60 43 km	t_{BP}= 3.8 t_H= 4.9 *GL*= 60 43 km		
GOLD_PIBR	t_{BP}= 3.7 t_H= 3.1 *GL*= 65* 332 km	t_{BP}= 4.9 t_H= 4.0 *GL*= 66** 332 km	t_{BP}= 6.0 t_H= 5.2 *GL*= 73*** 307 km	t_{BP}= 5.9 t_H= 5.0 *GL*= 69** 314 km	t_{BP}= 0.9 t_H= 0.5 *GL*= 48 333 km	
BAB_PIBR	t_{BP}= 2.4 t_H= 2.2 *GL*= 66** 320 km	t_{BP}= 4.8 t_H= 3.9 *GL*= 70** 322 km	t_{BP}= 4.8 t_H= 3.8 *GL*= 69** 295 km	t_{BP}= 4.7 t_H= 3.7 *GL*= 58 302 km	t_{BP}= 2.8 t_H= 1.2 *GL*= 53 324 km	t_{BP}= 5.3 t_H= 4.2 *GL*= 74*** 25 km

Table 3.8. (*continued*)

	ARMI	DST	STV	RVA	CMH	GOLD	BAB		
ATR_PIBR	t_{BP}= 0.5 t_H= 0.1 *GL*= 54 298 km	t_{BP}= 2.8 t_H= 1.5 *GL*= 61* 292 km	t_{BP}= 4.8 t_H= 3.2 *GL*= 62* 317 km	t_{BP}= 7.3 t_H= 5.0 *GL*= 66** 319 km	t_{BP}= 2.3 t_H= 1.6 *GL*= 50 278 km	t_{BP}= 5.2 t_H= 4.1 *GL*= 75*** 513 km	t_{BP}= 4.1 t_H= 1.5 *GL*= 64* 515 km		
EPF_PIBR	t_{BP}= 5.1 t_H= 4.7 *GL*= 78*** 290 km	t_{BP}= 4.0 t_H= 3.7 *GL*= 79*** 285 km	t_{BP}= 4.7 t_H= 4.0 *GL*= 78*** 316 km	t_{BP}= 1.7 t_H= 1.5 *GL*= 61* 313 km	t_{BP}= 0.6 t_H= 0.3 *GL*= 55 276 km	t_{BP}= 2.9 t_H= 3.0 *GL*= 69** 586 km	t_{BP}= 3.9 t_H= 3.0 *GL*= 67** 582 km	**ATR** t_{BP}= 2.5 t_H= 1.0 *GL*= 61 163 km	
BSH_PIHA	t_{BP}= 2.4 t_H= 2.7 *GL*= 41 380 km	t_{BP}= 2.3 t_H= 2.4 *GL*= 42 381 km	t_{BP}= 1.4 t_H= 1.7 *GL*= 41 404 km	t_{BP}= 1.7 t_H= 1.2 *GL*= 57 396 km	t_{BP}= 2.3 t_H= 2.6 *GL*= 64* 383 km	t_{BP}= 0.4 t_H= 1.3 *GL*= 47 710 km	t_{BP}= 0.2 t_H= 0.8 *GL*= 49 697 km	t_{BP}= 0.5 t_H= 0.3 *GL*= 55 437 km	**EPF** t_{BP}= 2.5 t_H= 3.3 *GL*= 34 280 km
BSH_PIBR	t_{BP}= 3.3 t_H= 3.3 *GL*= 34 380 km	t_{BP}= 2.4 t_H= 2.6 *GL*= 41 381 km	t_{BP}= 1.5 t_H= 2.2 *GL*= 43 404 km	t_{BP}= 1.6 t_H= 1.2 *GL*= 57 396 km	t_{BP}= 2.8 t_H= 2.9 *GL*= 69** 383 km	t_{BP}= 1.1 t_H= 1.5 *GL*= 44 710 km	t_{BP}= 0.1 t_H= 0.8 *GL*= 47 697 km	t_{BP}= 1.0 t_H= 0.5 *GL*= 57 437 km	t_{BP}= 2.3 t_H= 3.3 *GL*= 35 280 km
CAR-PIHA	t_{BP}= 2.3 t_H= 2.7 *GL*= 38 311 km	t_{BP}= 1.4 t_H= 1.6 *GL*= 47 311 km	t_{BP}= 0.4 t_H= 1.0 *GL*= 52 337 km	t_{BP}= 1.9 t_H= 1.7 *GL*= 59 329 km	t_{BP}= 3.2 t_H= 3.2 *GL*= 59 311 km	t_{BP}= 0.2 t_H= 0.4 *GL*= 56 643 km	t_{BP}= 1.4 t_H= 0.1 *GL*= 51 632 km	t_{BP}= 1.9 t_H= 1.5 *GL*= 60 351 km	t_{BP}= 1.2 t_H= 2.0 *GL*= 39 197 km
IMR-PIHA	t_{BP}= 3.3 t_H= 2.8 *GL*= 34 401 km	t_{BP}= 2.9 t_H= 2.7 *GL*= 38 401 km	t_{BP}= 1.8 t_H= 2.2 *GL*= 46 424 km	t_{BP}= 1.0 t_H= 0.3 *GL*= 56 416 km	t_{BP}= 2.3 t_H= 2.1 *GL*= 61* 404 km	t_{BP}= 0.9 t_H= 1.3 *GL*= 50 731 km	t_{BP}= 0.3 t_H= 0.6 *GL*= 48 718 km	t_{BP}= 0.0 t_H= 1.0 *GL*= 51 452 km	t_{BP}= 2.9 t_H= 2.6 *GL*= 34 293 km
JEZ-PIHA	t_{BP}= 2.7 t_H= 2.9 *GL*= 43 325 km	t_{BP}= 1.8 t_H= 1.7 *GL*= 47 324 km	t_{BP}= 1.4 t_H= 1.5 *GL*= 45 351 km	t_{BP}= 0.9 t_H= 1.2 *GL*= 52 344 km	t_{BP}= 3.8 t_H= 3.8 *GL*= 59 324 km	t_{BP}= 0.9 t_H= 1.1 *GL*= 49 657 km	t_{BP}= 0.4 t_H= 1.1 *GL*= 58 646 km	t_{BP}= 0.2 t_H= 0.7 *GL*= 50 349 km	t_{BP}= 2.6 t_H= 3.6 *GL*= 35 192 km
NHM-PIHA	t_{BP}= 2.2 t_H= 2.2 *GL*= 38 405 km	t_{BP}= 2.1 t_H= 2.1 *GL*= 44 405 km	t_{BP}= 1.6 t_H= 1.6 *GL*= 43 428 km	t_{BP}= 0.7 t_H= 0.2 *GL*= 55 420 km	t_{BP}= 2.0 t_H= 2.2 *GL*= 59 408 km	t_{BP}= 0.5 t_H= 1.0 *GL*= 53 735 km	t_{BP}= 0.6 t_H= 0.2 *GL*= 54 721 km	t_{BP}= 0.4 t_H= 1.3 *GL*= 47 457 km	t_{BP}= 2.2 t_H= 2.7 *GL*= 34 298 km
RHN-PIHA	t_{BP}= 3.2 t_H= 3.1 *GL*= 34 290 km	t_{BP}= 2.4 t_H= 2.1 *GL*= 41 288 km	t_{BP}= 1.9 t_H= 2.0 *GL*= 48 316 km	t_{BP}= 1.1 t_H= 2.1 *GL*= 50 309 km	t_{BP}= 1.9 t_H= 2.6 *GL*= 55 287 km	t_{BP}= 0.1 t_H= 0.5 *GL*= 49 620 km	t_{BP}= 0.3 t_H= 0.3 *GL*= 51 610 km	t_{BP}= 0.7 t_H= 0.7 *GL*= 53 310 km	t_{BP}= 3.0 t_H= 3.7 *GL*= 34 156 km
DIB-PIHA	t_{BP}= 2.5 t_H= 2.6 *GL*= 36 403 km	t_{BP}= 1.5 t_H= 1.5 *GL*= 41 402 km	t_{BP}= 2.0 t_H= 2.3 *GL*= 43 429 km	t_{BP}= 1.2 t_H= 1.0 *GL*= 52 422 km	t_{BP}= 2.6 t_H= 2.8 *GL*= 66** 401 km	t_{BP}= 1.1 t_H= 1.4 *GL*= 46 734 km	t_{BP}= 0.9 t_H= 0.4 *GL*= 47 723 km	t_{BP}= 0.8 t_H= 0.3 *GL*= 57 395 km	t_{BP}= 2.4 t_H= 3.5 *GL*= 35 232 km

Table 3.8. (***continued***)

	BSH_PIHA						
BSH_PIBR	t_{BP}= 14.2 t_H= 15.0 *GL*= 84*** 0 km	**BSH_PIBR**					
CAR-PIHA	t_{BP}= 9.0 t_H= 9.1 *GL*= 78*** 87 km	t_{BP}= 9.5 t_H= 9.5 *GL*= 76*** 87 km	**CAR_PIHA**				
IMR-PIHA	t_{BP}= 9.8 t_H= 9.3 *GL*= 78*** 20 km	t_{BP}= 9.8 t_H= 9.7 *GL*= 73*** 20 km	t_{BP}= 8.0 t_H= 7.0 *GL*= 73*** 104 km	**IMR_PIHA**			
JEZ-PIHA	t_{BP}= 8.8 t_H= 9.1 *GL*= 81*** 88 km	t_{BP}= 7.0 t_H= 7.9 *GL*= 74*** 88 km	t_{BP}= 11.5 t_H= 12.0 *GL*= 86*** 19 km	t_{BP}= 7.1 t_H= 5.3 *GL*= 78*** 103 km	**JEZ_PIHA**		
NHM-PIHA	t_{BP}= 8.9 t_H= 8.7 *GL*= 71*** 25 km	t_{BP}= 7.2 t_H= 7.0 *GL*= 76*** 25 km	t_{BP}= 5.8 t_H= 5.5 *GL*= 69** 109 km	t_{BP}= 12.3 t_H= 12.9 *GL*= 77*** 5 km	t_{BP}= 5.7 t_H= 5.4 *GL*= 77*** 108 km	**NHM_PIHA**	
RHN-PIHA	t_{BP}= 6.6 t_H= 5.1 *GL*= 64* 128 km	t_{BP}= 6.5 t_H= 5.6 *GL*= 66** 128 km	t_{BP}= 8.0 t_H= 8.0 *GL*= 76*** 42 km	t_{BP}= 6.1 t_H=4.1 *GL*= 66** 144 km	t_{BP}= 6.7 t_H= 7.2 *GL*= 73*** 43 km	t_{BP}= 6.1 t_H= 4.5 *GL*= 72*** 150 km	**RHN_PIHA**
DIB-PIHA	t_{BP}= 8.1 t_H= 8.2 *GL*= 84*** 88 km	t_{BP}= 8.7 t_H= 10.1 *GL*= 84*** 88 km	t_{BP}= 7.1 t_H= 7.1 *GL*= 83*** 94 km	t_{BP}= 7.0 t_H= 6.5 *GL*= 78*** 87 km	t_{BP}= 7.2 t_H= 7.5 *GL*= 81*** 78 km	t_{BP}= 4.3 t_H= 4.6 *GL*= 67** 91 km	t_{BP}= 5.8 t_H= 5.6 *GL*= 72*** 115 km

Table 3.9. Crossdating statistics among the site chronologies for the period in which SSS> 0.85 for each chronology, and distance (km) between pairs of sites. Chronologies from sites in the northern Levant which crossdate significantly with one another are shaded in green. Chronologies from sites in the southern Levant which crossdate significantly with one another are shaded in pink. t_{BP}= Baillie-Pilcher *t*-value; t_H= Hollstein *t*-value; *GL= Gleichläufigkeit* (trend coefficient) values and their associated *p*-values; *n*= years overlap between the two pairs of chronologies. For the *GL p*-values, *= *p*<0.001; **= *p*<0.01; and *= *p*<0.05.**

	ARMI	DST	STV	RVA	CMH	GOLD	BAB	ATR
DST_PIBR	t_{BP}= 11.9 t_H= 10.6 *GL*= 72*** *n*= 187 7 km							
STV_PIBR	t_{BP}= 8.8 t_H= 9.2 *GL*= 72*** *n*= 247 27 km	t_{BP}= 9.1 t_H= 8.9 *GL*= 67*** *n*= 191 31 km						
RVA_PIBR	t_{BP}= 5.4 t_H= 5.0 *GL*= 64*** *n*= 263 23 km	t_{BP}= 8.0 t_H= 7.1 *GL*= 69*** *n*= 192 29 km	t_{BP}= 15.1 t_H= 13.5 *GL*= 71*** *n*= 251 9 km					
CMH_PIBR	t_{BP}= 2.9 t_H= 2.2 *GL*= 57 *n*= 182 22 km	t_{BP}= 3.4 t_H= 3.5 *GL*= 58* *n*= 188 15 km	t_{BP}= 3.6 t_H= 2.3 *GL*= 54 *n*= 187 43 km	t_{BP}= 7.8 t_H= 7.5 *GL*= 68*** *n*= 190 43 km				
GOLD_PIBR	t_{BP}= 6.0 t_H= 5.3 *GL*= 60** *n*= 209 332 km	t_{BP}= 5.9 t_H= 5.0 *GL*= 59** *n*= 186 332 km	t_{BP}= 8.2 t_H= 7.1 *GL*= 63*** *n*= 209 307 km	t_{BP}= 8.5 t_H= 6.8 *GL*= 64*** *n*= 209 314 km	t_{BP}= 2.9 t_H= 1.7 *GL*= 54 *n*= 182 333 km			
BAB_PIBR	t_{BP}= 4.5 t_H= 3.7 *GL*= 63*** *n*= 251 320 km	t_{BP}= 6.9 t_H= 5.8 *GL*= 67*** *n*= 186 322 km	t_{BP}= 7.4 t_H= 6.4 *GL*= 62*** *n*= 246 295 km	t_{BP}= 7.5 t_H= 7.1 *GL*= 62*** *n*= 251 302 km	t_{BP}= 3.7 t_H= 2.3 *GL*= 55 *n*= 182 324 km	t_{BP}= 11.2 t_H= 10.2 *GL*= 72*** *n*= 209 25 km		
ATR_PIBR	t_{BP}= 3.2 t_H= 3.2 *GL*= 62* *n*= 93 298 km	t_{BP}= 4.7 t_H= 4.0 *GL*= 62** *n*= 93 292 km	t_{BP}= 6.9 t_H= 5.2 *GL*= 66*** *n*= 93 317 km	t_{BP}= 9.1 t_H= 7.1 *GL*= 70*** *n*= 93 319 km	t_{BP}= 3.5 t_H= 2.5 *GL*= 54 *n*= 93 278 km	t_{BP}= 6.0 t_H= 5.2 *GL*= 76*** *n*= 93 513 km	t_{BP}= 4.8 t_H= 2.6 *GL*= 68*** *n*= 93 515 km	
EPF_PIBR	t_{BP}= 5.5 t_H= 5.3 *GL*= 75*** *n*= 101 290 km	t_{BP}= 3.5 t_H= 3.6 *GL*= 65*** *n*= 106 285 km	t_{BP}= 6.4 t_H= 6.5 *GL*= 77*** *n*= 105 316 km	t_{BP}= 3.3 t_H= 3.8 *GL*= 65*** *n*= 109 313 km	t_{BP}= 0.3 t_H= 0.1 *GL*= 57 *n*= 108 276 km	t_{BP}= 3.1 t_H= 3.8 *GL*= 66*** *n*= 100 586 km	t_{BP}= 3.6 t_H= 3.2 *GL*= 63** *n*= 100 582 km	t_{BP}= 3.3 t_H= 2.5 *GL*= 61* *n*= 93 163 km

Table 3.9. (*continued*)

	ARMI	DST	STV	RVA	CMH	GOLD	BAB	ATR	EPF
BSH_PIHA	t_{BP}= 3.1 t_H= 3.0 *GL*= 38 *n*= 73 380 km	t_{BP}= 2.1 t_H= 2.0 *GL*= 51 *n*= 78 381 km	t_{BP}= 1.7 t_H= 1.7 *GL*= 41 *n*= 77 404 km	t_{BP}= 1.5 t_H= 0.9 *GL*= 58 *n*= 72 396 km	t_{BP}= 2.5 t_H= 2.0 *GL*= 64** *n*= 80 383 km	t_{BP}= 0.7 t_H= 1.4 *GL*= 44 *n*= 72 710 km	t_{BP}= 2.9 t_H= 3.2 *GL*= 64 *n*= 71 697 km	t_{BP}= 0.2 t_H= 0.0 *GL*= 50 *n*= 72 437 km	t_{BP}= 2.9 t_H= 3.9 *GL*= 33 *n*= 80 280 km
BSH_PIBR	t_{BP}= 4.0 t_H= 3.5 *GL*= 35 *n*= 70 380 km	t_{BP}= 2.2 t_H= 2.3 *GL*= 50 *n*= 75 381 km	t_{BP}= 2.1 t_H= 2.1 *GL*= 44 *n*= 74 404 km	t_{BP}= 1.5 t_H= 1.3 *GL*= 59 *n*= 77 396 km	t_{BP}= 2.8 t_H= 3.2 *GL*= 68*** *n*= 77 383 km	t_{BP}= 2.0 t_H= 1.8 *GL*= 43 *n*= 69 710 km	t_{BP}= 3.6 t_H= 3.3 *GL*= 61 *n*= 68 697 km	t_{BP}= 0.1 t_H= 0.1 *GL*= 54 *n*= 69 437 km	t_{BP}= 3.1 t_H= 3.6 *GL*= 38 *n*= 77 280 km
CAR-PIHA	t_{BP}= 1.9 t_H= 2.3 *GL*= 53 *n*= 91 311 km	t_{BP}= 0.5 t_H= 1.0 *GL*= 51 *n*= 97 311 km	t_{BP}= 0.3 t_H= 0.2 *GL*= 55 *n*= 96 337 km	t_{BP}= 2.6 t_H= 2.9 *GL*= 61* *n*= 101 329 km	t_{BP}= 4.5 t_H= 4.4 *GL*= 65** *n*= 99 311 km	t_{BP}= 0.6 t_H= 0.1 *GL*= 55 *n*= 91 643 km	t_{BP}= 1.7 t_H= 2.3 *GL*= 47 *n*= 90 632 km	t_{BP}= 3.0 t_H= 1.7 *GL*= 57 *n*= 91 351 km	t_{BP}= 1.8 t_H= 1.1 *GL*= 48 *n*= 100 197 km
IMR-PIHA	t_{BP}= 2.1 t_H= 2.2 *GL*= 45 *n*= 152 401 km	t_{BP}= 0.7 t_H= 0.9 *GL*= 52 *n*= 157 401 km	t_{BP}= 0.9 t_H= 0.4 *GL*= 55 *n*= 155 424 km	t_{BP}= 3.2 t_H= 2.2 *GL*= 58* *n*= 159 416 km	t_{BP}= 3.6 t_H= 3.0 *GL*= 58* *n*= 159 404 km	t_{BP}= 0.4 t_H= 0.1 *GL*= 51 *n*= 151 731 km	t_{BP}= 0.5 t_H= 0.2 *GL*= 52 *n*= 151 718 km	t_{BP}= 2.3 t_H= 0.5 *GL*= 59* *n*= 93 452 km	t_{BP}= 2.4 t_H= 2.8 *GL*= 36 *n*= 108 293 km
JEZ-PIHA	t_{BP}= 2.1 t_H= 2.3 *GL*= 45 *n*= 65 325 km	t_{BP}= 1.1 t_H= 0.9 *GL*= 55 *n*= 70 324 km	t_{BP}= 1.6 t_H= 1.3 *GL*= 42 *n*= 69 351 km	t_{BP}= 0.3 t_H= 1.3 *GL*= 50 *n*= 71 344 km	t_{BP}= 3.0 t_H= 4.1 *GL*= 58 *n*= 71 324 km	t_{BP}= 1.1 t_H= 0.9 *GL*= 52 *n*= 64 657 km	t_{BP}= 0.0 t_H= 0.6 *GL*= 59 *n*= 64 646 km	t_{BP}= 0.2 t_H= 0.4 *GL*= 53 *n*= 64 349 km	t_{BP}= 3.6 t_H= 3.2 *GL*= 40 *n*= 71 192 km
NHM-PIHA	t_{BP}= 2.9 t_H= 2.9 *GL*= 38 *n*= 60 405 km	t_{BP}= 1.5 t_H= 1.3 *GL*= 53 *n*= 65 405 km	t_{BP}= 2.0 t_H= 1.9 *GL*= 44 *n*= 64 428 km	t_{BP}= 0.9 t_H= 1.3 *GL*= 58 *n*= 67 420 km	t_{BP}= 2.7 t_H= 2.9 *GL*= 60 *n*= 67 408 km	t_{BP}= 0.7 t_H= 1.0 *GL*= 54 *n*= 59 735 km	t_{BP}= 0.1 t_H= 0.1 *GL*= 55 *n*= 59 721 km	t_{BP}= 0.2 t_H= 1.5 *GL*= 47 *n*= 59 457 km	t_{BP}= 2.8 t_H= 2.3 *GL*= 35 *n*= 67 298 km
RHN-PIHA	t_{BP}= 4.1 t_H= 3.6 *GL*= 36 *n*= 89 290 km	t_{BP}= 2.7 t_H= 2.6 *GL*= 41 *n*= 94 288 km	t_{BP}= 0.9 t_H= 1.5 *GL*= 49 *n*= 93 316 km	t_{BP}= 1.7 t_H= 1.5 *GL*= 51 *n*= 97 309 km	t_{BP}= 3.6 t_H= 3.9 *GL*= 57 *n*= 96 287 km	t_{BP}= 0.0 t_H= 0.5 *GL*= 49 *n*= 88 620 km	t_{BP}= 0.1 t_H= 0.0 *GL*= 51 *n*= 88 610 km	t_{BP}= 0.8 t_H= 0.4 *GL*= 49 *n*= 88 310 km	t_{BP}= 2.7 t_H= 3.7 *GL*= 40 *n*= 97 156 km
DIB-PIHA	t_{BP}= 2.8 t_H= 2.0 *GL*= 67 *n*= 87 403 km	t_{BP}= 0.0 t_H= 0.3 *GL*= 54 *n*= 93 402 km	t_{BP}= 0.7 t_H= 0.9 *GL*= 46 *n*= 92 429 km	t_{BP}= 2.3 t_H= 2.3 *GL*= 56 *n*= 97 422 km	t_{BP}= 4.0 t_H= 4.2 *GL*= 71*** *n*= 95 401 km	t_{BP}= 1.7 t_H= 1.7 *GL*= 48 *n*= 87 734 km	t_{BP}= 2.3 t_H= 1.9 *GL*= 59 *n*= 86 723 km	t_{BP}= 2.0 t_H= 0.7 *GL*= 58 *n*= 87 395 km	t_{BP}= 2.3 t_H= 2.6 *GL*= 37 *n*= 96 232 km

Table 3.9. (***continued***)

	BSH_PIHA						
BSH_PIBR	t_{BP}= 14.0 t_H= 12.1 *GL*= 84*** *n*= 77 0 km	**BSH_PIBR**					
CAR-PIHA	t_{BP}= 6.7 t_H= 5.5 *GL*= 74*** *n*= 80 87 km	t_{BP}= 8.4 t_H= 8.1 *GL*= 71*** *n*= 77 87 km	**CAR_PIHA**				
IMR-PIHA	t_{BP}= 9.9 t_H= 9.0 *GL*= 76*** *n*= 80 20 km	t_{BP}= 9.0 t_H= 10.2 *GL*= 71*** *n*= 77 20 km	t_{BP}= 7.8 t_H= 7.2 *GL*= 71*** *n*= 99 104 km	**IMR_PIHA**			
JEZ-PIHA	t_{BP}= 7.7 t_H= 7.7 *GL*= 78*** *n*= 71 88 km	t_{BP}= 6.5 t_H= 8.1 *GL*= 70*** *n*= 71 88 km	t_{BP}= 10.3 t_H= 10.4 *GL*= 86*** *n*= 71 19 km	t_{BP}= 5.4 t_H= 5.5 *GL*= 73*** *n*= 71 103 km	**JEZ_PIHA**		
NHM-PIHA	t_{BP}= 7.8 t_H= 4.9 *GL*= 71*** *n*= 67 25 km	t_{BP}= 7.7 t_H= 6.8 *GL*= 77*** *n*= 67 25 km	t_{BP}= 6.3 t_H= 5.8 *GL*= 68** *n*= 67 109 km	t_{BP}= 12.0 t_H= 11.1 *GL*= 78*** *n*= 67 5 km	t_{BP}= 4.5 t_H= 5.1 *GL*= 73*** *n*= 66 108 km	**NHM_PIHA**	
RHN-PIHA	t_{BP}= 7.2 t_H= 5.4 *GL*= 68*** *n*= 80 128 km	t_{BP}= 5.7 t_H= 5.6 *GL*= 64** *n*= 77 128 km	t_{BP}= 7.7 t_H= 6.4 *GL*= 73*** *n*= 97 42 km	t_{BP}= 6.3 t_H= 5.1 *GL*= 64** *n*= 96 144 km	t_{BP}= 4.7 t_H= 6.2 *GL*= 67** *n*= 71 43 km	t_{BP}= 4.7 t_H= 4.0 *GL*= 71*** *n*= 67 150 km	**RHN_PIHA**
DIB-PIHA	t_{BP}= 8.6 t_H= 6.2 *GL*= 83*** *n*= 80 88 km	t_{BP}= 9.5 t_H= 10.3 *GL*= 80*** *n*= 77 88 km	t_{BP}= 7.1 t_H= 7.1 *GL*= 75*** *n*= 97 94 km	t_{BP}= 7.6 t_H= 7.1 *GL*= 77*** *n*= 95 87 km	t_{BP}= 6.5 t_H= 7.5 *GL*= 75*** *n*= 71 78 km	t_{BP}= 5.3 t_H= 5.9 *GL*= 69*** *n*= 67 91 km	t_{BP}= 5.1 t_H= 5.1 *GL*= 62** *n*= 96 115 km

DISCUSSION

Tree-ring chronologies

The age distributions of the trees sampled here indicate that there are long-lived *P*. *halepensis* and *P*. *brutia* forests in the study region, but that they are still relatively rare. This is likely the result of heavy anthropogenic disturbance and deforestation in the region. However, natural disturbances, particularly wildfires and insect outbreaks, also have had a significant impact on the structure and composition of these pine

forests (although in many cases, humans are also responsible for these disturbances) (Boydak 2004). Since *P*. *brutia* and *P*. *halepensis* are both thermophilous species that generally grow in the 'thermo-Mediterranean' and 'meso-Mediterranean' life zones (Blondel and Aronson 1999; Quézel and Médail 2003), they are most commonly found at lower altitudes. This also means that these species grow in more accessible locations and are therefore particularly vulnerable to deforestation.

The major deforestation events of the 19th and early 20th century that were described in Chapter 2–namely, cutting of forest timbers for Mehmet Ali's navy, building of railroads, and fuel and railways during World War I–greatly affected forests in Syria and Lebanon as well as the southern Levant (Mikesell 1969; Rustum 1936; Talhouk et al. 2001)[2]. Low-altitude forests also have been cleared for agriculture throughout the study area, and heavy grazing or over-grazing has inhibited forest regeneration in many of these areas (McNeill 1992; Mikesell 1969; Thirgood 1987).

In Lebanon, even high elevation areas were cleared, terraced, and cultivated, so that old growth forests survive only in fragmentary stands that were usually protected as part of religious sites (Mikesell 1969; Talhouk et al. 2001). Travel accounts from the mid-19th century (Hepper 2001; Porter 1871), just prior to the time when the oldest pine samples from Ehden germinated, describe the area around Ehden as a densely cultivated and settled area. Consequently, Talhouk et al. (2001) have argued that many of the *P*. *halepensis* and *P*. *brutia* stands in Lebanon, including the Ehden pine

[2] However, as recent geoarchaeological and dendrochronological studies have shown (e.g., Akkemik et al. 2012), these events are only the most recent of several waves of deforestation in Turkey and elsewhere in the Levant and Cyprus.

forest, contain relatively young trees that re-colonized former agricultural terraces, farmlands, and degraded deciduous and cedar forests. The relatively young ages of the pines from Ehden studied here support this argument.

Elsewhere in Cyprus and Turkey, large numbers *P*. *brutia* trees were tapped for resin, their bark stripped for tanning, and their wood and branches cut for fuel and building material (Ciesla 2004; Thirgood 1987). The Anatolian timber trade intensified during the 19th century, when vast quantities of timber, including pine, were shipped to Egypt and the Levant (Beaufort 1818; McNeill 1992; Mikhail 2011). However, many forest areas in the Troodos Massif in Cyprus and in the Taurus Mountains in Anatolia remained largely inaccessible for large-scale logging operations (Ciesla 2004; McNeill 1992; Thirgood 1987). It is perhaps not surprising, then, that the oldest *Pinus brutia* trees in this study area are located at high-altitude sites (i.e., ARMI, DST, GOLD, RVA, STV) in Cyprus and Turkey, since these locations were difficult for loggers to access.

Climate response function analysis

The significant limiting factors identified for each site by the response function analysis vary with respect to site bioclimatic characteristics, rather than by species. The results of the response function analysis for the chronologies from Cyprus, Turkey, and Syria also corroborate the findings of Griggs et al. (2014) and Touchan et al. (2005, 2014a, b).

Overall, radial growth of *P*. *brutia* Mitsero Hills in the northern Levant and of *P*. *halepensis* and *P*. *brutia* from the southern Levant sites is especially sensitive to water availability, as demonstrated by the significant responses of radial growth to

precipitation at these sites. This is likely because these sites are situated at the more arid extremes of the study area's altitudinal and latitudinal gradients. As was also noted in Griggs et al. (2014), the Mitsero Hills site has significant or near-significant positive responses to monthly precipitation throughout the Cypriot rainy season that are generally stable over time. Consequently, the Mitsero Hills tree-ring data give a clear record of local annual precipitation.

While Touchan et al.'s (2005) Atera pine chronology is from a low-altitude site, it is not particularly sensitive to climate and does not have a consistent significant response to either temperature or precipitation. This may be because unlike the Mitsero Hills pines, the Atera trees grow on the windward side of the Syrian mountains close to the coast and receive on average greater annual precipitation and experience overall humid conditions during even the dry summer months because of on-shore air transport (which lowers potential evapotranspiration). Since this site chronology has a small sample size with comparatively low inter-series correlation, it would be useful to determine if the same response function results can be obtained using a more robust dataset from Atera with greater sample depth.

At high-to-mid-altitude sites, cold winter temperatures during November–March inhibit photosynthesis and radial growth. As a result, high-to-mid-altitude site chronologies most commonly have significant positive responses to spring precipitation (i.e., March–May) after temperatures rise and in early autumn months when soil moisture content for the growing season begins to be replenished. Additional (although much less common) precipitation is possible from local convection at the cooler high-altitude sites even during summer, which has a

significant positive impact on tree-ring growth in years when it occurs. However, many of these precipitation responses are not stable over time, and most of the high-altitude sites have few significant growth responses to precipitation (and in some cases, none). This indicates that precipitation during one particular month or group of months is not a major limiting factor (especially compared to sites at lower latitudes and altitudes), and that low precipitation during one particular month can generally be offset by higher precipitation during other months of the growing season. In contrast, in the southern Levant–where there is also a shorter growing season and lower total annual rainfall–trees are consistently dependent on winter rainfall to replenish water.

High-to-mid-altitude sites in the northern Levant also have a positive response to winter temperature that contrast with the negative winter temperature responses found at low-altitude and low-latitude (i.e., southern Levant) sites. This is likely because during abnormally cold winters at high-to-mid-altitude sites, low temperatures inhibit photosynthesis and cambial activity. Warmer than average temperatures allow trees at mid-to-high-altitude sites to resume photosynthesis and radial growth at an earlier date. The limiting effect of cold winter temperatures is particularly pronounced at sites that are at *P. brutia*'s upper altitudinal limit (e.g., ARMI and EPF). Some of the pine samples analyzed from Ehden even had frost damage ('frost rings') (Schweingruber 1996), which is uncommon at the other sampled sites. Alternatively, high temperatures at or just below freezing may produce snowfall with higher moisture content than snow produced under colder temperatures. Warmer air and surface temperatures at or just above freezing may also cause winter snowpack to melt

more gradually, allowing water to penetrate the soil rather than flowing away from the site as runoff after rapid snowmelt.

During the warmer spring and summer months, higher temperatures raise *PET*, limit water availability, and lower water use efficiency, so the relationship between high temperatures and radial growth at high-to-mid-altitude sites is then negative. In contrast, at low altitudes in the northern Levant and particularly throughout the southern Levant, warmer winter temperatures can limit water availability and lower water use efficiency even during the coldest months of the year, creating a significant limiting factor to radial growth.

Correlation among site chronologies

The gradients of altitude, latitude, and land-sea distance, which cause bioclimatic variation and differences in the key limiting factors determined in the response function analysis, largely explain the spatial and altitudinal groups identified for the tree-ring chronologies studied here. The largest difference in tree-ring growth is between chronologies from the northern and southern Levant. This "Levantine divide" largely results from several critical bioclimatic differences between the two regions that change the key factors limiting radial growth.

Two of the most important bioclimatic differences between sites in the northern and southern Levant are the southern Levant's longer dry season and greater aridity because of its proximity to the low latitude desert belt. Trees growing at sites in the southern Levant must endure a dry season in which there is little to no rainfall and which is on average two months longer than in the northern Levant. As is shown in the response function analysis, spring rainfall (i.e., May–June), while still

comparatively lower than winter rainfall totals, has a significant impact on tree-ring growth for sites in the northern Levant, while in the southern Levant, these months are more consistently dry. The dry season length has also been cited in biogeographical studies (e.g., Blondel and Aronson 1999; Dufour-Dror and Ertaş 2004; Quézel and Médail 2003) as a critical difference between Anatolia/the northern Levant and the southern Levant. At the northern and southern extremes of the study area the differences in aridity, dry season length, and atmospheric circulation are especially marked, such that interannual variability in precipitation and the tree-ring signal for these two areas also differ significantly.

The chronology from Mitsero Hills, which is in the rain shadow of the Troodos Massif, is an exception to the north-south Levant tree-ring dichotomy. The area around Mitsero Hills has a longer dry season than the other sites in the northern Levant and receives lower annual precipitation. Winter precipitation has a significant impact on the radial growth of the pines at Mitsero Hills and of the pines in the southern Levant. Winter precipitation in the southern Levant and at Mitsero Hills largely originates from mid-latitude cyclones, which have a regional-scale impact on precipitation, in contrast to the local-scale impact of spring-summer precipitation in the northern Levant. It is notable that the CRU gridded datasets from the southern Levant (i.e., those above 32.25ºN latitude) whose annual precipitation variability has significant correlation with those from the Agios Epifanos meteorological station in Cyprus (near Mitsero Hills) correspond to the locations of site chronologies in the southern Levant that have strongest correlation with the Mitsero Hills chronology.

However, radial growth of the Mitsero Hills pines also has a significant response to May precipitation, unlike the southern Levant pine chronologies. This suggests that the Mitsero Hills pines still receive May rainfall from local-scale convection over Cyprus (that also affects sites in the Troodos) (Griggs et al. 2014), unlike the southern Levant sites. The difference in May precipitation between Mitsero Hills and the southern Levant is likely a critical source of variability between tree-ring datasets from these areas.

Topographic variation creates further variability in the tree-ring record within the northern Levant. Cooler temperatures and orographic effects mean that the high-altitude sites in the northern Levant are less water stressed, reducing the effect of precipitation as a significant limiting factor. Instead, the sustained, cold winter temperatures at the high-altitude sites become a significant limiting factor, so that sites at high and low altitudes have opposite responses to temperature. Therefore, an unusually cold winter will result in narrower ring growth at high-altitude sites, while it will contribute to wider ring growth at lower altitudes and latitudes. In this way, opposite patterns of tree-ring growth may be produced at the extremes of the altitudinal gradient. This explains the significant negative Pearson correlation observed between high-altitude tree-ring chronologies (e.g., ARMI, DST, and EPF) from the northern Levant, which have a significant positive winter temperature response, and chronologies from sites at the lower latitudinal limit of *P*. *halepensis* in the southern Levant (e.g., BSH and IMR), where there is an especially significant negative winter temperature response.

Higher-altitude sites (including sites sampled in the Western and Eastern Highlands for this study) receive more rainfall and have cooler winters than low-altitude sites in the southern Levant. However, the southern Levant's Western and Eastern Highlands are generally lower in elevation than the mountain ranges further north. Additionally, because of the lower latitude, there is still greater aridity and fewer days at or below freezing even at high-altitude sites in the southern Levant. The dry season is also longer than in the northern Levant even at higher altitudes, and winter precipitation remains the major limiting factor to radial growth. Consequently, there is a shift in the vegetation 'life zones' found along Mediterranean altitudinal gradients as latitude decreases. Therefore 'thermo-Mediterranean' species assemblages (including *P. halepensis*/*brutia*) of the northern Levant are found even at high altitudes in the southern Levant (Blondel and Aronson 1999; Quézel and Médail 2003).

Meanwhile, the southern Levant's low-altitude, inland sites in the rain shadow of the highlands (like the Rift Valley) are so arid that they do not support Mediterranean vegetation and instead contain steppe or desert vegetation (Cordova 2007; Zohary 1973). However, as mentioned in Chapter 2, the high-altitude sites of Mt. Meron and Mt. Kena'an in the southern Levant have unique microclimates with shorter dry seasons, higher annual rainfall, and colder winters. Trees growing at high altitudes at these sites may therefore produce unique tree-ring signals, and these sites

should be investigated further for dendrochronological analysis, if an adequate number of suitable samples can be found[3].

The Lebanese coastal plain around 34–34.25ºN latitude is the likely transition zone between the southern and northern Levant tree-ring groups (Figure 3.7). Annual precipitation values increase dramatically in this area and dry season length decreases, since this location is closer to the main route of East Mediterranean pressure systems and further away from the low latitude desert belt (Alpert et al. 1990; Black et al. 2011). The steep Lebanon-Anti Lebanon mountain chain (which is an extension of the southern Levant's Western and Eastern Highlands) also curves close to the coast, leading to a sharp altitudinal gradient that results in high rainfall from orographic effects. This area is also where the ranges of *P*. *halepensis* and *P*. *brutia* overlap (Abi-Saleh and Safi 1998; Talhouk et al. 2001), although (as was mentioned in Chapter 1) these species distributions may also be influenced by anthropogenic impacts.

Further sampling of forests in this area (if an adequate number of samples can be found) may improve our understanding of precisely where and how tree-ring growth and climate responses change in this critical transition zone. Additional variation in the pine tree-ring signal likely exists along altitudinal gradients and different slope exposures in Lebanon, especially since the Ehden pine chronology has poor heteroconnections with Touchan et al.'s (2005) cedar chronology, which he sampled from higher altitudes at Ehden (t_{BP}= 2.1; t_H= 2.4; and *GLK*= 57, in which *n*=

[3] Attempts were made to sample pine (*P*. *halepensis* and *P*. *brutia*) and prickly juniper (*Juniperus oxycedrus* L.) from Mt. Meron and Mt. Kena'an for this study. However, most of the trees in these areas were extremely short-lived, and anthropogenic impacts in these areas are high, creating idiosyncratic ring growth with poor inter-series correlation among samples.

100 years) (Touchan et al. 2005). Thus, dendrochronological variability should be explored along these bioclimatic gradients.

Additionally, as discussed in the previous chapter for the southern Levant, site characteristics play an important role in modulating the effects of climate on tree-ring growth among and within the sites sampled in the northern Levant. For instance, in the Troodos Massif, where four of the sampled sites (ARMI, DST, STV, and RVA) are located, there is considerable heterogeneity in bedrock lithology, which greatly affects site water availability. Bedrock in the Troodos Massif is largely dominated by an ophiolite complex comprised of dunites, hazburgites, serpentinites, gabbros, sheeted dyke complexes, and pillow lavas (Boronina et al. 2003; Delipetrou et al. 2008; Dünkeloh 2005; Mederer 2005). The Mitsero Hills site is situated on pillow lavas that are peripheral to the central core of the Troodos Ophiolite Complex (Griggs et al. 2014). Gabbros, sheeted dykes, and pillow lavas have relatively high permeability, and overlying soils (generally non-calcareous eutric lithosols and cambiosols) have low to medium field capacity. Consequently, there is relatively little surface runoff, even along steep slopes. However, water storage is low in these areas, since there is relatively fast discharge of precipitation into the groundwater. Serpentinites have lower permeability than other bedrock types in the ophilite complex, which raises water retention for plants growing in these areas, although more precipitation is lost as surface runoff, particularly areas with steep slope gradients (Dünkeloh 2005; Maderer 2005).

Dünkeloh (2005) also notes that slope aspect has a critical effect on temperature within the Troodos, where southerly and westerly exposed slopes receive greater solar

radiation and therefore experience higher temperatures than northerly and easterly exposures at a similar elevation. Higher winter temperatures along southerly and westerly exposures would therefore prove advantageous growth conditions for pines in the high-altitude sites sampled in the Troodos (and similarly for pines growing in the high-altitude forest at Ehden in Lebanon) by extending the number of growing degree days. Conversely, higher solar irradiance and temperatures along these exposures during spring and summer raises *PET*, lowers the water use efficiency of pines, and inhibits radial growth, particularly at those sites in the northern Levant growing in xeric, low-altitude environments (e.g., sites like ATR, BAB, and CMH).

Use in Dendrochronological Dating and Provenancing Research

The dendochronological crossdating statistics further illustrate that *Pinus halepensis* and *Pinus brutia* chronologies from the southern Levant are part of a dendrochronological zone whose tree-ring signal is distinct from the *Pinus brutia* chronologies from the northern Levant (Figure 3.7). Within the southern Levant, *P. brutia* and *P. halepensis* chronologies have strong teleconnections with one another and even strong heteroconnections with other pine and oak species (see: Chapter 2). Thus, the *P. halepensis* chronologies developed for this study can be combined into a single regional reference chronology for the southern Levant for dating historical/archaeological timbers that were culled from forests in this region. However, northern Levant *P. brutia* chronologies cannot be used to date historical/archaeological timbers procured from southern Levant forests.

These results indicate that it is possible to provenance tree-ring chronologies of historical/archaeological *P. brutia*/*halepensis* timbers from eastern Mediterranean sites

to either the southern or northern Levant by comparing their visual and statistical fits against the East Mediterranean network of *P*. *brutia* and *P*. *halepensis* reference chronologies. This has important applications for research on timber trade and the environmental history of the Levant, particularly during the Ottoman Period. Liphschitz and Biger (2000, 2001) have argued that *P*. *halepensis* grew only in fragmented stands during the Ottoman Period in the southern Levant. Consequently, they have argued that *P*. *brutia*/*halepensis* timbers found in the southern Levant in Ottoman-era buildings (e.g., Biger and Liphschitz 1991a,b) and shipwrecks (e.g., Cvikel and Kahanov 2012) from the Ottoman Period and earlier (e.g., Barkai and Kahanov 2007; Mor and Kahanov 2006) are actually *P*. *brutia* timber that was imported from Anatolia. Dendrochronological dating and provenancing of these timbers can therefore help determine whether local or imported pine timber was being used during these periods.

Within the northern Levant, there are teleconnections over a larger geographic area than in the southern Levant, such that similarities in *P*. *brutia* tree-ring chronologies depend on both distance and elevation differences between sites. Thus, strong crossmatches between historical/archaeologicalchronologies with north Levantine *P*. *brutia* chronologies may indicate that the historical/archaeological timbers were cut either from trees close to, or at a similar elevation to, a given reference chronology. Further *P*. *brutia* reference chronologies should therefore be collected across altitudinal, as well as spatial, gradients in the northern Levant, in order to improve success in dating historical/archaeological timbers, as has been recommended for other regions in Europe where there is similar altitude-dependent

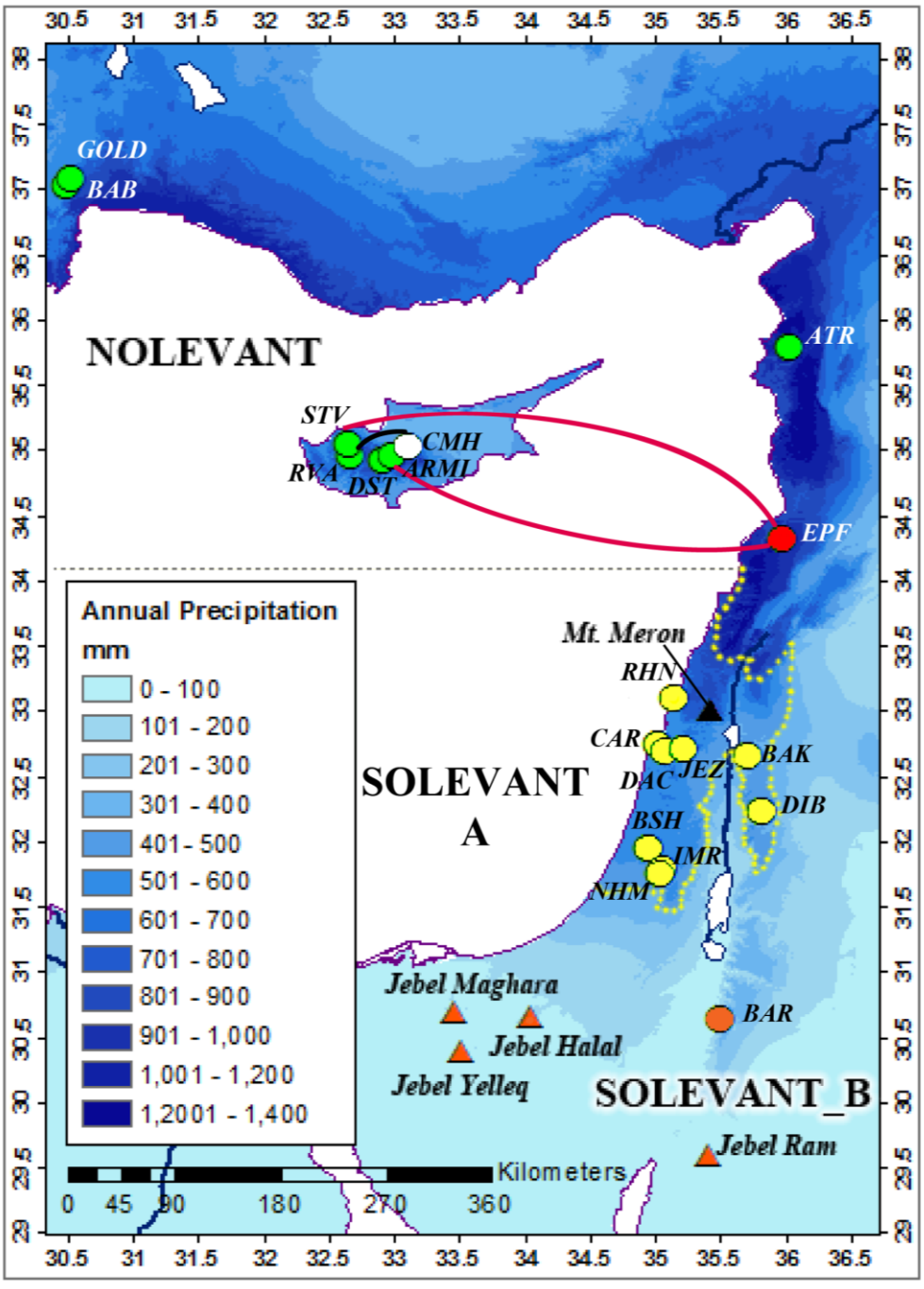

Figure 3.5. Levantine dendrochronological zones and annual precipitation distribution (Hijmans et al. 2005). In zone 'NoLevant', the EPF chronology (*red*) has teleconnections only with STV and ARMI (*connected with red lines*). The CMH chronology (*white*) has teleconnections only with RVA (*connected with a black line*). All other 'NoLevant' zone chronologies (*green*) crossdate. 'SoLevant_A' sites and boundaries are marked in yellow. The 'SoLevant_B' zone site (BAR) is marked in orange; the 'SoLevant_B' zone also likely includes relict juniper populations in the Sinai Peninsula (*orange triangles*).

tree-ring variability (e.g., Dittmar et al. 2012; Domínguez-Delmás et al. 2013; Levanič et al. 2001).

While historical/archaeological timbers can be provenanced to a less specific geographic location in the northern Levant than in the southern Levant, the strong (especially high-altitude) teleconnections are useful, since, in some cases, they widen the number of reference chronologies available for crossdating historical timbers. For instance, historical timber culled from high-altitude sites in Lebanon, where the pine reference chronologies are shorter, can also be crossdated using the much longer, high elevation chronology from Armiantos in Cyprus, thereby improving chances of dating the timber successfully and building long reference chronologies in the region for dating even older wood samples. Similarly, mid-altitude site chronologies (e.g., RVA, STV, and GOLD) may act as 'bridging' reference chronologies, which can be used to date timber from both low-altitude and high-altitude sites successfully. Further development of pine chronologies from the hypothesized Lebanese transition zone between the northern and southern Levant may also create a suitable 'bridging' chronologies between the two zones.

Relationship with large-scale circulation patterns

A detailed examination of the effects of large-scale atmospheric circulation patterns and teleconnections on Levantine precipitation and tree-ring growth is beyond the scope of this study, but will be mentioned briefly here with regard to the results of dendrochronological analysis presented above. As described in previous sections, large-scale circulation indices (particularly the NAO and EAWR) are linked to atmospheric circulation patterns that affect the frequency and trajectory of cyclones

largely responsible for bringing precipitation to the Levant and therefore the region's spatial and temporal climatic variability–and, by extension, tree-ring teleconnections. However, previous analyses of meteorological and tree-ring data (e.g., Black 2011; Black et al. 2011; Dunkelöh and Jacobheit 2003; Griggs et al. 2014; Touchan et al. 2005, 2014c) suggest that caution must be exercised when extrapolating the current relationships between circulation indices and tree-rings from the Levantine study area for long-term climate reconstructions.

As Touchan et al. (2014c) note, using tree-ring chronologies from the northern Levant–especially those from mid-to-high-altitudes–to reconstruct large-scale climate indices like the NAO, EAWR, or ENSO is complicated. This is because (as this study corroborates) May–June precipitation is the dominant climate variable that affects tree-ring growth and that may be derived from tree-ring proxy data from these sites. As discussed above, spring and summer precipitation in the East Mediterranean largely results from local convection and instabilities, rather than regional circulation patterns linked to large-scale climate modes like the NAO, EAWR, or ENSO. Touchan et al. (2014c) demonstrate that both the spring NAO and spring ENSO lack a clear and stable association with May–June precipitation throughout the northern and southern Levant

Within the northern Levant, Touchan et al.'s (2005) study of tree-rings and large-scale circulation indices did not find a strong, consistent link between the NAO and tree-ring records (which includes the *P. brutia* chronologies also analyzed here). Significant correlation was found between the tree-ring record and another large-scale climate mode, the East Atlantic-Jet pattern (EA-Jet). However, this relationship is not

stable over time, and the authors caution against using East Mediterranean tree-rings to reconstruct this circulation index (Touchan et al. 2005). Similarly, Touchan et al. (2008) did not find a strong consistent link between the NAO and *P. halepensis* tree-ring data to the southwest of the study area in Tunisia. Griggs (2006) found temporally stable, significant relationships between the May NAO index and oak tree-ring growth further north of the study area along the Black Sea coast of northern Turkey and Greece. However, she notes that this association is marginally significant and temporally unstable.

Large-scale atmospheric circulation patterns and climate indices (especially the NAO) have a much stronger link with winter precipitation than with spring or summer precipitation in the study area. Thus, tree-ring datasets from low altitude sites in the northern Levant (like that from Mitsero Hills) and from sites in the southern Levant, which have an annual or winter precipitation signal, may have greater potential for reconstructing atmospheric circulation patterns than tree-ring data from mid-to-high-altitude sites in the northern Levant. However, previous research (e.g., Black 2011; Jones et al. 2003) demonstrates that the teleconnection between large-scale climate modes and atmospheric circulation patterns affecting East Mediterranean winter precipitation are also temporally unstable, creating a critical challenge for reconstructing large-scale climate modes from tree-ring data. An additional complication is that the locations of the NAO's two centers of action (the Icelandic low and the Azores high) move on decadal time scales, changing the spatial extent of the NAO's influence over Europe and the Eastern Mediterranean (Jung et al. 2003; Wang et al. 2012).

Griggs et al. (2014) did not find significant high-frequency correlation between the NAO or EAWR indices with the Mitsero Hills chronology, but they do note that periods of drought reconstructed from Cypriot tree-ring data and from meteorological data correspond to winters in which the NAO and EAWR were in positive phase. They also argue that periods of extended drought in the early 19th century (1806–1808 and 1819–1824), which they reconstructed from the tree-ring record, occurred when the NAO was in positive phase. This would support Cook et al.'s NAO reconstruction for the early 19th century, but contradicts the winter NAO reconstruction of Luterbacher et al. (1999), who argue that the NAO was negative from ca. 1805–1820.

As mentioned above, years with high annual precipitation in the southern Levant are more likely when the NAO is in positive phase (which is opposite to the effect of the NAO in western Europe and the northern Levant) (Black 2011; Xoplaki et al. 2004), but the winter NAO's link with precipitation and tree-ring growth in the southern Levant is also complex. A positive NAO leading to circulation favoring high precipitation can certainly impact tree-ring growth, since the results from this study demonstrate the important effect of winter precipitation on tree-ring growth throughout the southern Levant. However, a strong positive NAO does not always bring high rainfall to the southern Levant, and dry years in the southern Levant do not always correspond to, and are not significantly correlated with, negative NAO years (Black 2011).

Yakir et al. (1996) analyzed the relationship between the ENSO index and rainfall in Israel from 1975–1995, and its effects on tree-ring growth. They found that a strong positive ENSO index results in high rainfall and wide tree-rings, and it should

be noted that the tree-ring pattern from their study matches that of the southern Levant chronologies studied here. However, both they and Black (2011) point out that the relationship between ENSO and precipitation in Israel is significant only for the past 20 years; thus long-term, high-frequency reconstructions of ENSO from tree-rings would not be robust.

Despite the clearly complex influences of multiple large-scale climate modes on precipitation and tree-ring growth in the East Mediterranean, atmospheric circulation patterns certainly impact the region's precipitation patterns and can be responsible for spatial variability in precipitation in the northern and southern Levant that contributes to the contrasting tree-ring patterns in these two areas. As Touchan et al. (2014c) suggest, the spatial patterns observed from large-scale climate reconstructions using tree-ring data may still give critical evidence or "fingerprints" of large-scale climate modes influencing regional climate systems in the past.

Further research is necessary to understand more clearly the effects of atmospheric circulation patterns and large-scale climate modes on climate and tree-ring growth in the study region over both high and low-frequency timescales. Tree-ring data from low-altitude sites in the northern Levant and those from the southern Levant, including those analyzed here, may provide a valuable contribution for this work, because, unlike high-altitude sites, they provide a record of winter precipitation.

A network of tree-ring data (which have a winter precipitation signal) with a wide spatial distribution across the East Mediterranean and southern Europe (rather than tree-ring data from only one or two site) will be necessary to provide spatially robust climate proxy data for analyzing changes in climate and the potential impacts of

changes in atmospheric circulation on a regional scale (Luterbacher et al. 1999; Touchan et al. 2014c). Tree-ring chronologies from dendrochronological zones with winter precipitation responses must also be extended further back in time using historical and archaeological timbers, in order to examine long-term (and especially low-frequency) changes in climate and large-scale atmospheric circulation. Using the dendroprovenancing methods described in the previous section will be critical in identifying wood materials from these dendrochronological zones. In the southern Levant, it will be necessary to build such long chronologies using other species, such as *Quercus macrolepis* and *Juniperus phoenicea*, which may have longer tree-ring sequences and be more ubiquitous in the southern Levant's historical and archaeological sites than *Pinus halepensis* (for further details, see: Chapter 2).

CONCLUSIONS

The results of this study demonstrate that bioclimatic variation along the Levant's latitudinal and altitudinal gradients changes the primary climatic factors limiting radial growth, particularly for species with wide ecological amplitudes, like the *Pinus halepensis* and *Pinus brutia* populations studied here. In turn, the bioclimatic diversity and changes in limiting factors over these gradients creates distinct groups of tree-ring data. There is a particularly clear divide between the northern and southern parts of the Levant, as well as across altitudinal gradients in the northern Levant.

The tree-ring chronologies from the northern Levant forests extend further back in time, which theoretically makes them more useful for climate reconstruction. However, for *Pinus brutia* and *Pinus halepensis* in the Levant, the results indicate that

the most climatically sensitive trees are those from more arid locations, either at low altitudes or low latitudes, rather than trees from high altitudes. Trees sampled from these more water-stressed areas more likely provide annual, rather than sub-annual, precipitation records. It is also these low-altitude sites, like Mitsero Hills in the northern Levant, and particularly the low latitude *P. halepensis* sites in the southern Levant, which are most vulnerable to projected changes in climate in the eastern Mediterranean (Lindner et al. 2010).

These varying latitudinal and altitudinal growth responses have an important impact on the climate data that can be reconstructed from tree-ring records and the spatial scale over which such reconstructions may be applied. Most of the chronologies from the northern Levant examined here provide sub-annual records of late spring (May–June) precipitation, which constitutes only a small percentage of total annual precipitation in the northern Levant. Since the principal growing season length is different for the southern Levant (where May and June are consistently months of water deficit), proxy data from the northern Levant may not give an accurate representation of the climatic conditions that have a critical impact on vegetation growth in the southern Levant.

Chronologies can be pooled together and their principal components extracted to provide a sub-annual, or even annual, climate signal for a broader region (e.g., Touchan et al. 2005). However, with this approach, some of the spatial climatic variability in the Levant (which, for precipitation, can be especially heterogeneous) is lost, particularly if chronologies over a large, bioclimatically diverse area are pooled together. Local-scale dendroclimatic reconstructions–like that which Griggs et al.

(2014) built with the Mitsero Hills chronology–can give a useful, accurate record of drought severity, year-to-year variability, and effects of precipitation or temperature on vegetation (and human populations) of a given area. As Köse et al. (2011) demonstrate, when tree-ring data have a common climate signal, comparing local reconstructions from several different sites allows one to identify regions or areas in which climatic events like drought are most severe and assess more precisely how changes in climate impacted human populations and vegetation in these locations.

In addition to their differing dry season lengths and dendrochronological climate signals, it was also demonstrated that there is low correlation in year-to-year precipitation between meteorological data from the northern Levant and the southernmost part of the 'SoLevant_A' dendrochronological zone. Therefore, dendroclimatic reconstructions from the northern Levant should not be used to reconstruct climate at high-frequency timescales in the southern Levant, particularly for these southernmost locations. Instead, Touchan et al.'s (1999) *Juniperus phoenicea* chronology in the 'SoLevant_B' zone, which has better correlation with the 'SoLevant_A' zone (particularly its southern area that includes the area around Jerusalem) gives a much more accurate indication of climate conditions and plant growth for this area. The 'SoLevant_B' zone *Juniperus phoenicea* chronologies, and (ideally) pine or oak chronologies from 'SoLevant_A' should be developed further and extended back in time, in order to provide the southern Levant with appropriate local climate proxy data.

This study's results also have important implications for the spatial scale over which tree-ring reference chronologies may be used for dendrochronological dating

and provenancing in the Levant. Since trees in the 'SoLevant_A' zone have their own distinct tree-ring signal, it is necessary to continue lengthening the separate network of reference chronologies for the southern Levant built in this study. This new network of southern Levant tree-ring chronologies will allow historical/archaeological timbers culled from this region to be dated successfully. In the northeastern Mediterranean, further reference chronologies should also be built across an even broader region from sites throughout *P*. *brutia*'s natural distribution in Turkey, mainland Greece, and the Greek islands to determine if there are other teleconnections among *P*. *brutia* sites at even greater distances.

The latitudinal zonation of tree-ring chronologies is useful for dendroprovenancing, since it allows researchers to identify whether timbers were procured from the northern or southern Levant. Within the northern Levant, the vertical zonation of chronologies gives information on the altitude from which timbers were procured. Such new dendroprovenancing information can be used together with geoarchaeological, palynological, and other paleoenvironmental data, as well as textual information (when available) to reconstruct changes in human usage of local vs. regional forest resources and their relationship with deforestation in the region.

Dendrochronology is a valuable tool for studying climate variability and human-environmental interactions in the Levant. Levantine tree-ring records provide high-precision proxy data for reconstructing climate and for dating when the region's archaeological/historical timbers were cut. They can also source the forest region from which these materials were procured. The new chronologies built from this study and new information on tree-ring teleconnections and climate response therefore

open several new avenues of climate, environmental, and cultural heritage research in this bioclimatically diverse and historically rich region.

APPENDIX 3.1

Climate diagrams showing mean monthly temperatures (*black line*), average monthly precipitation total (*dark gray bars*), and average monthly potential evapotranspiration (*light gray bars, shown as negative values*) calculated from each of the gridded CRU datasets and the Cypriot meteorological stations in the study area. Climate diagrams for sites in the southern Levant are given in Appendix 2.1 of Chapter 2.

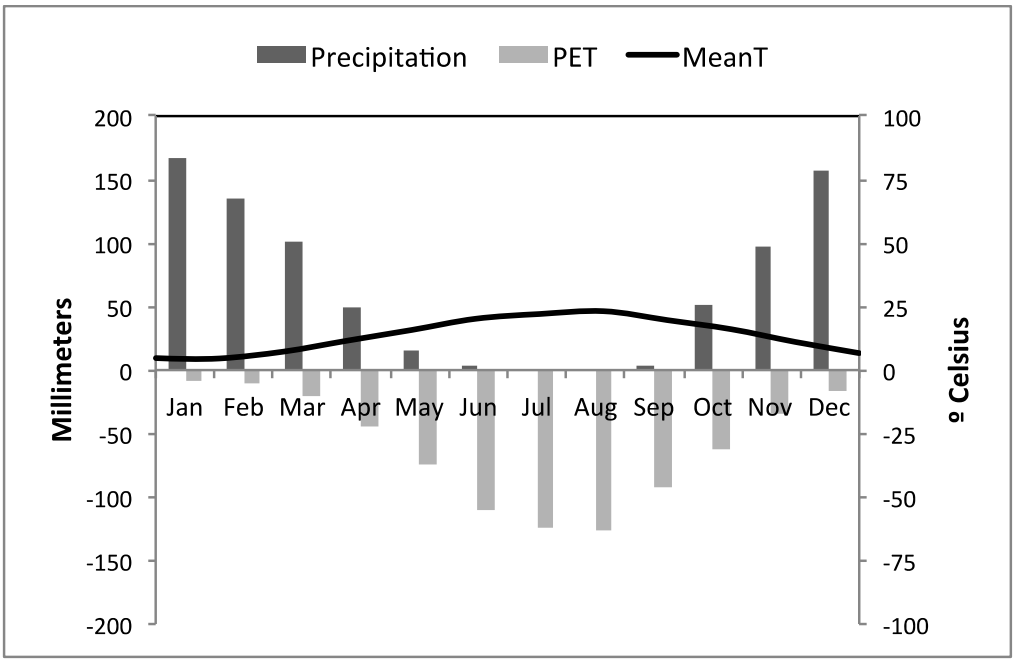

a. CRU (34.25ºN, 35.75ºE)

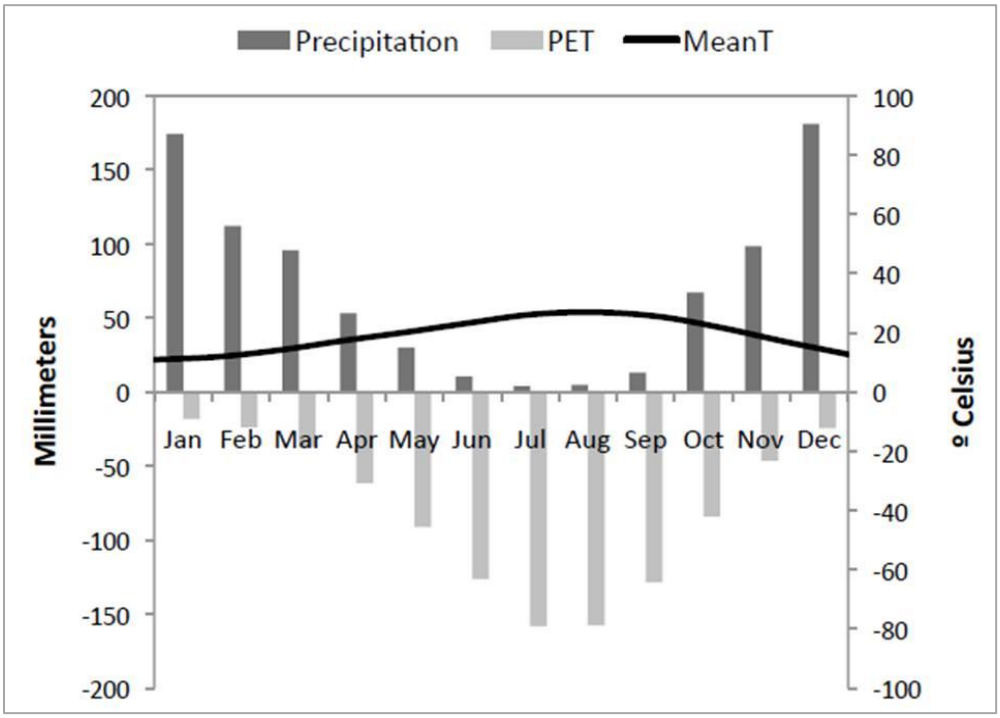

b. CRU (35.75ºN, 35.75ºE)

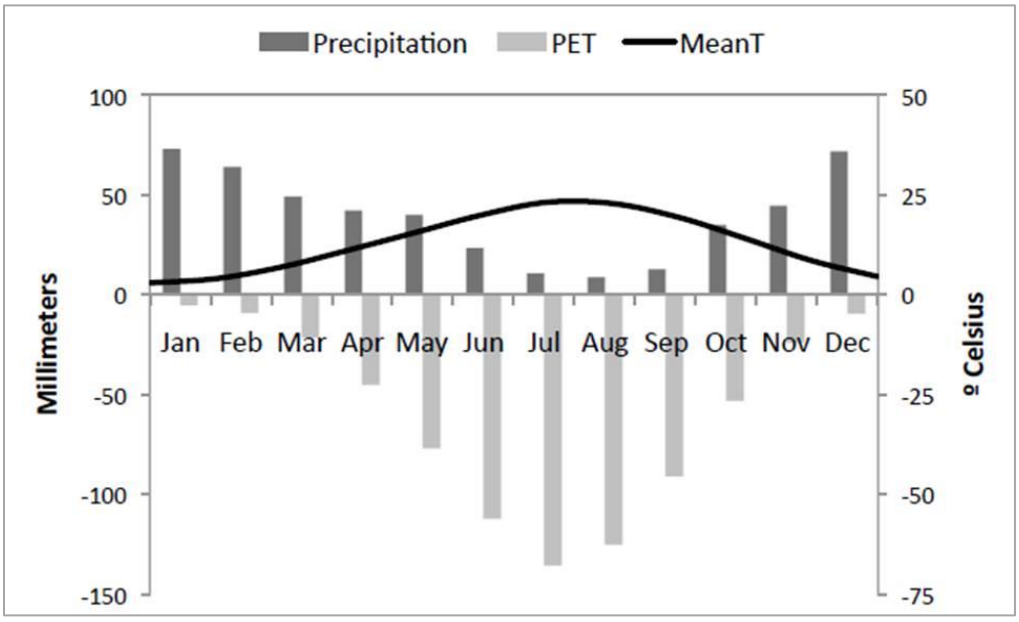

c. CRU (37.25ºN, 30.25ºE)

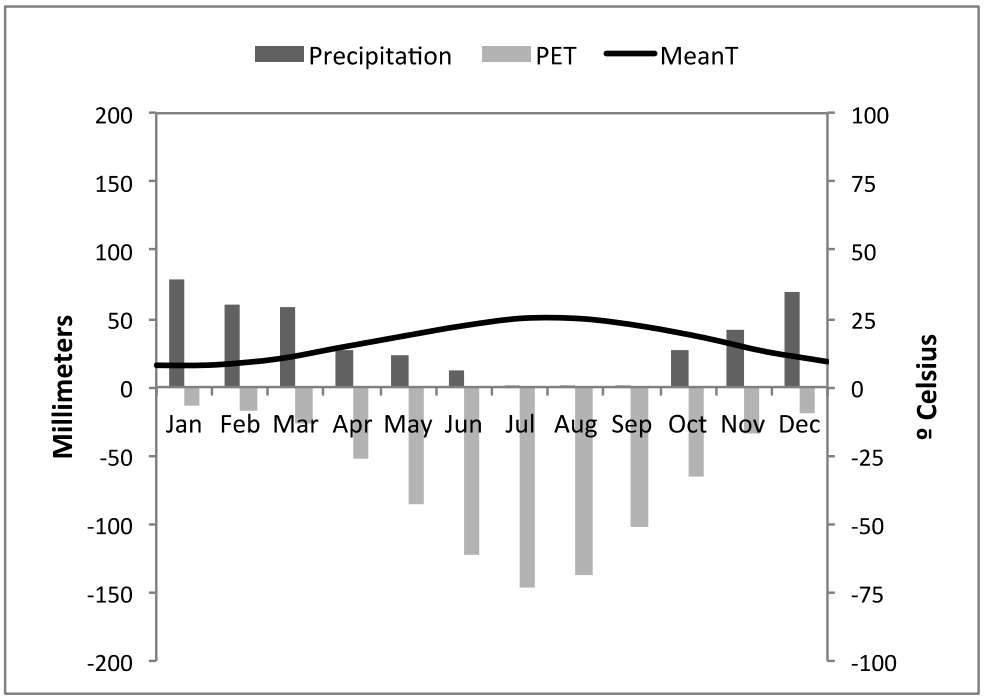

d. Cyprus, Panagia Bridge

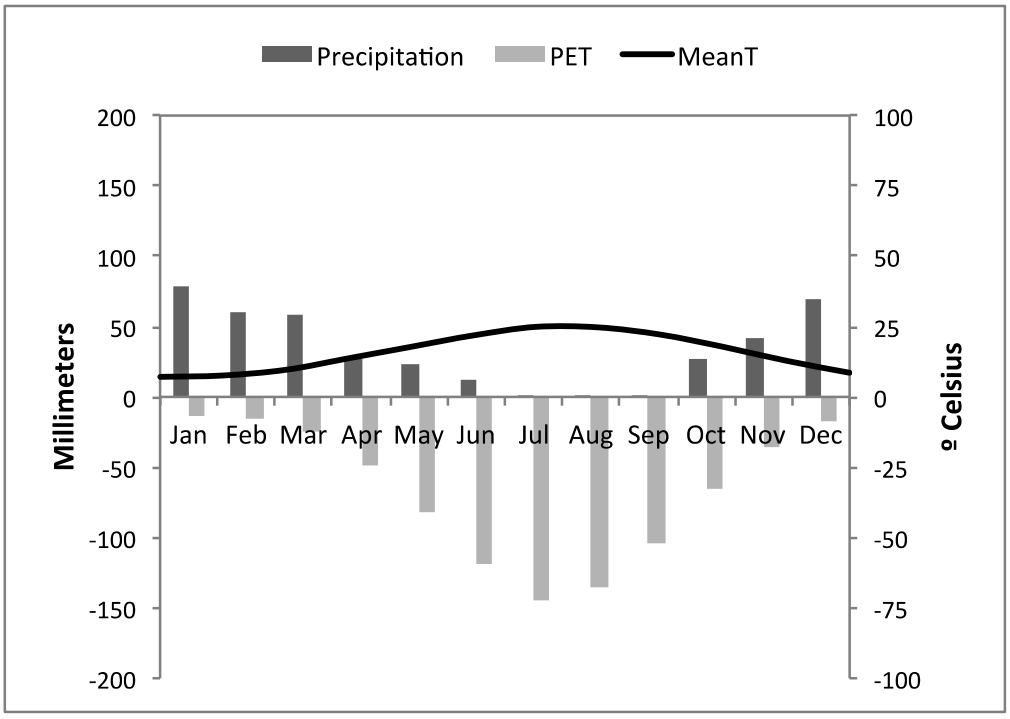

e. Cyprus, Pano Panagia

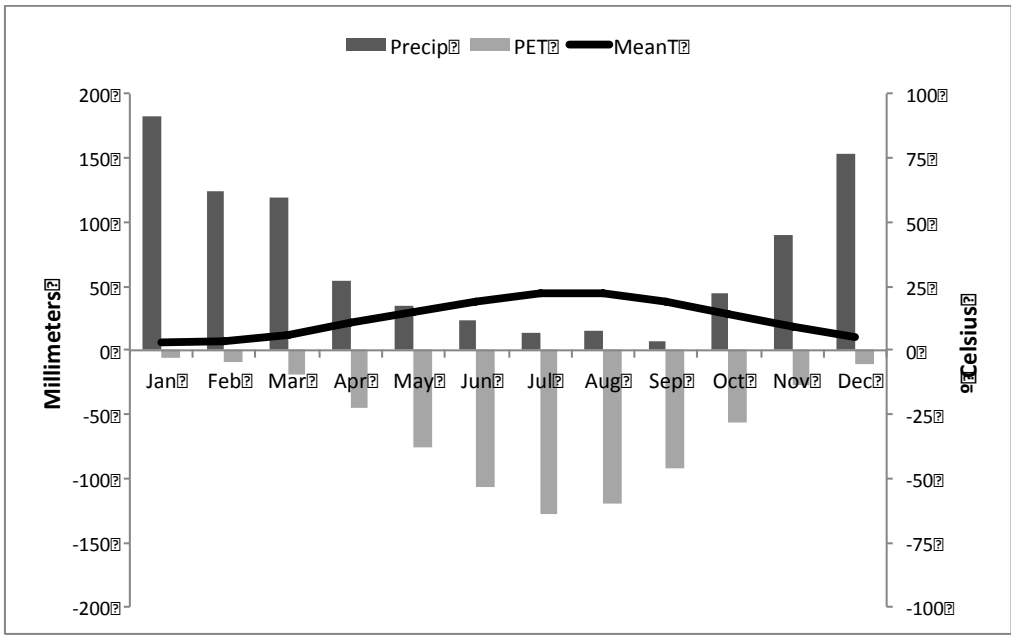

f. Cyprus, Prodromos

APPENDIX 3.2

Locations of forest sites (*green*) sampled in Cyprus and meteorological stations (*red triangles*) used in the climate response function analysis. Site codes are given in Table 3.3.

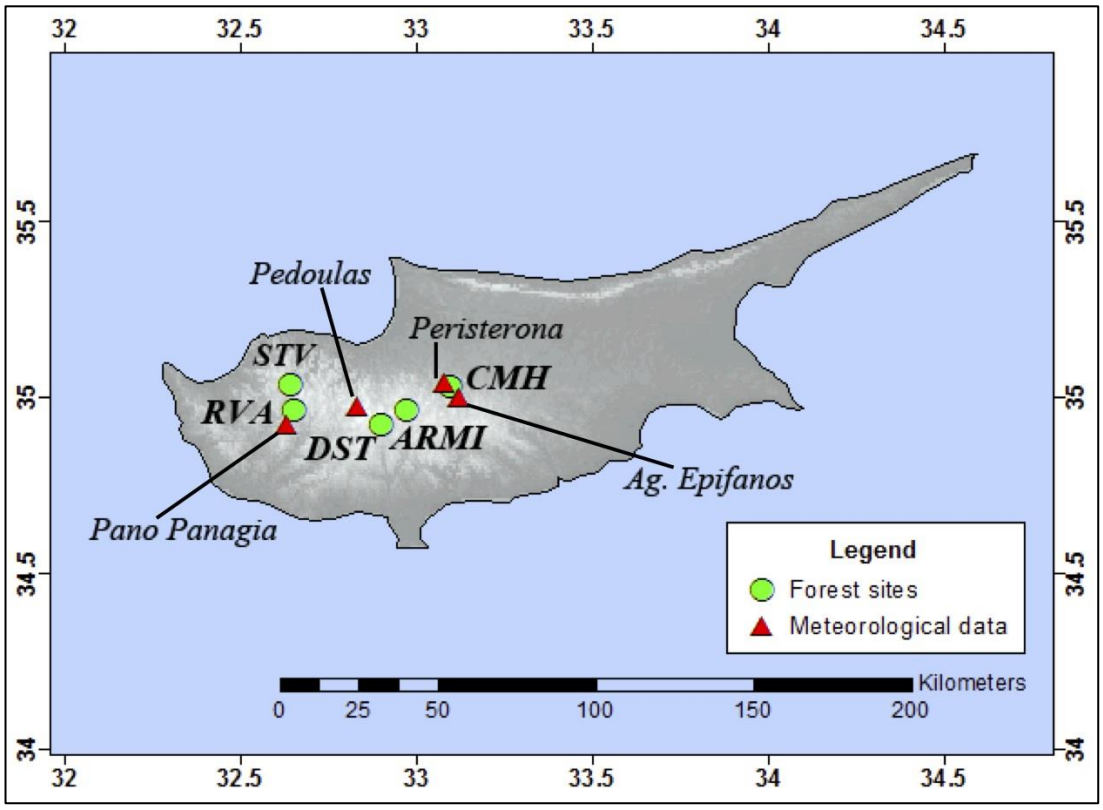

APPENDIX 3.3

Response function plots showing response function coefficients (*y*-axis) for tree-ring growth at each site in the study area against mean temperature (*blue*) and precipitation (*red*) values for each month (*x*-axis). An '*' = significant response function coefficient ($p<0.05$) for a given month. Response function plots for sites in the southern Levant are given in Appendix 2.3 of Chapter 2.

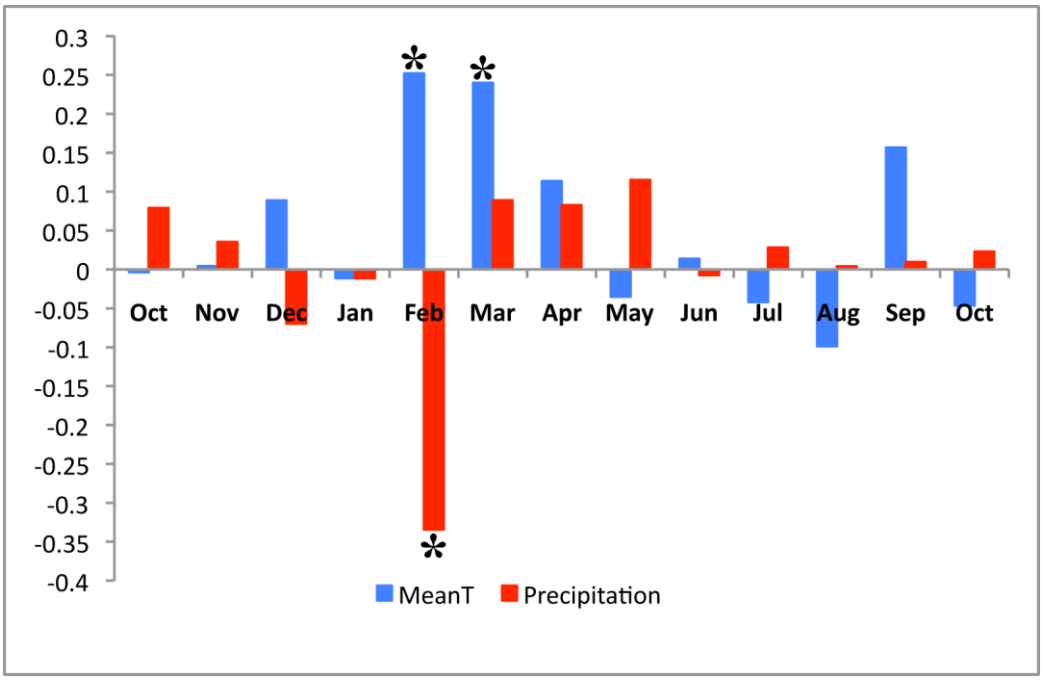

a. Cyprus, Armiantos, *Pinus brutia* (ARMI_PIBR)

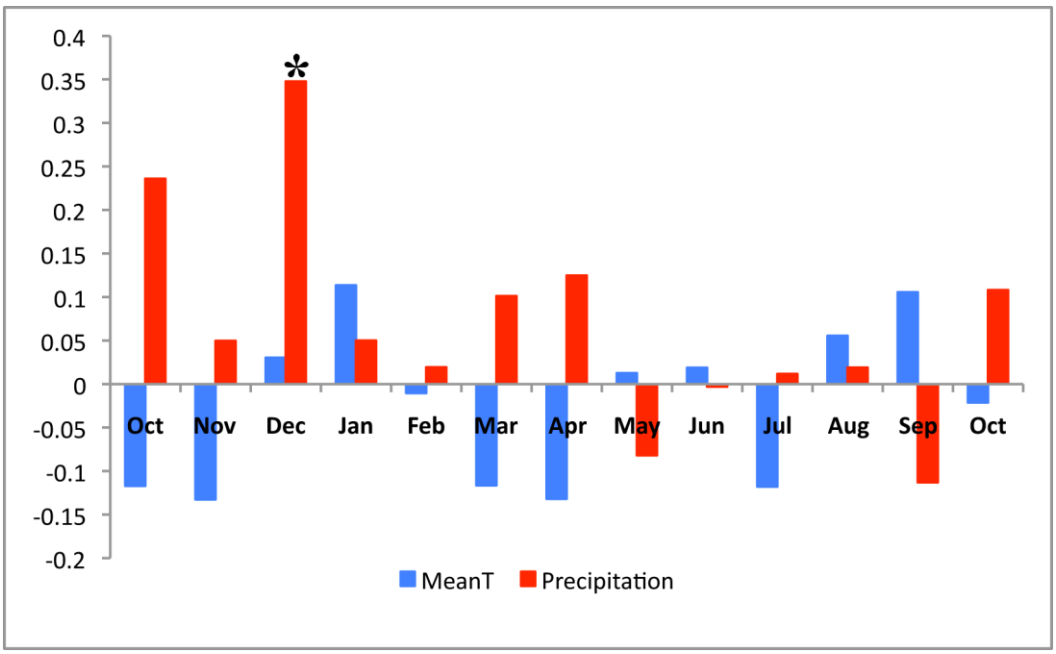

b. Syria, Atera, *Pinus brutia* (ATR_PIBR)

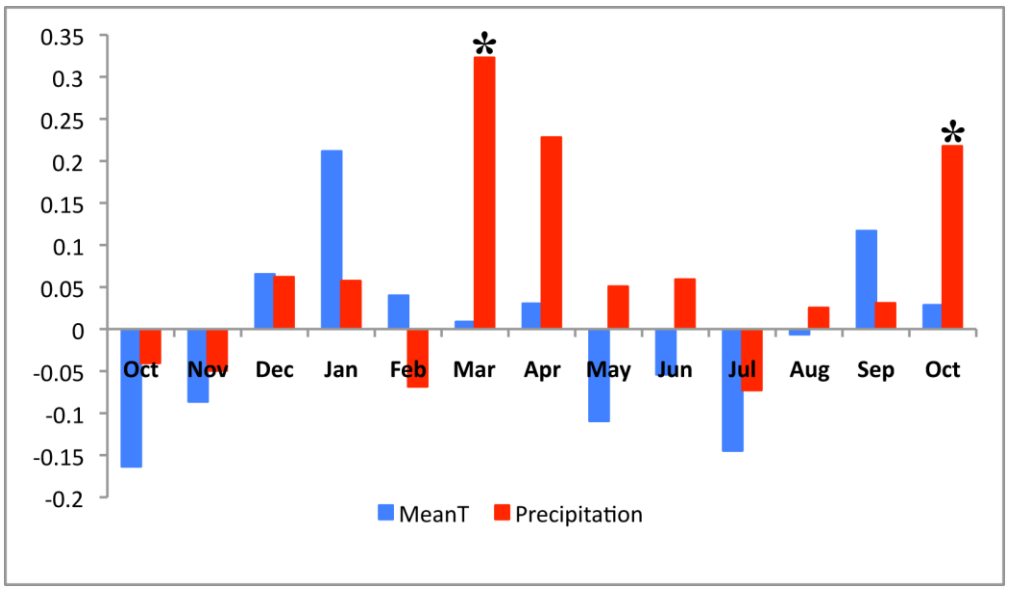

c. Turkey, Bayat Bademleri, *Pinus brutia* (BAB_PIBR)

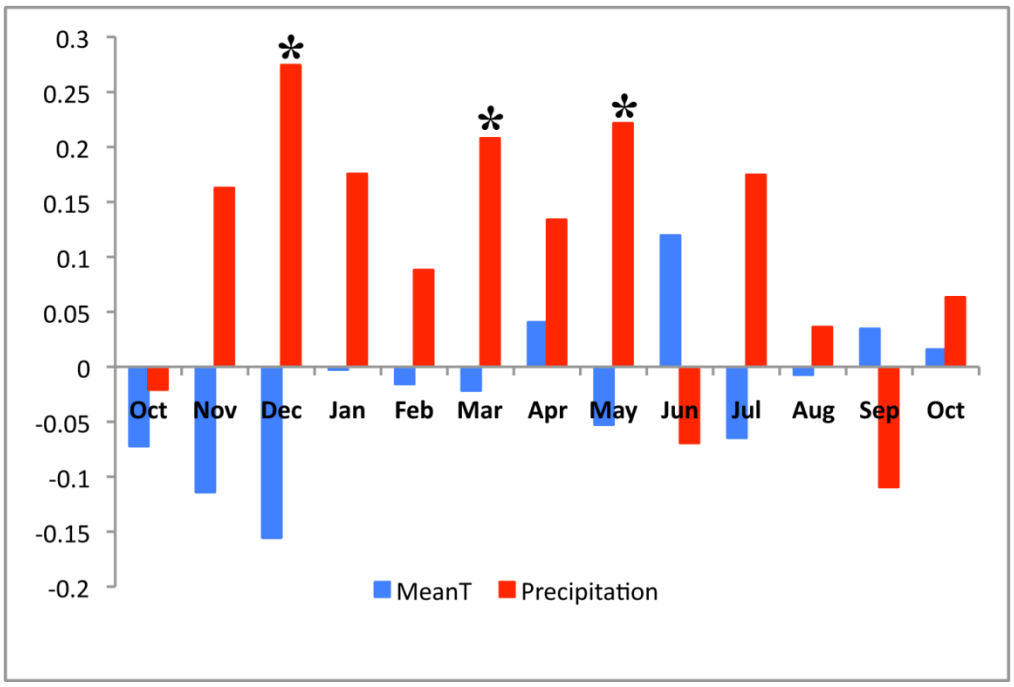

d. Cyprus, Mitsero Hills, *Pinus brutia* (CMH_PIBR)

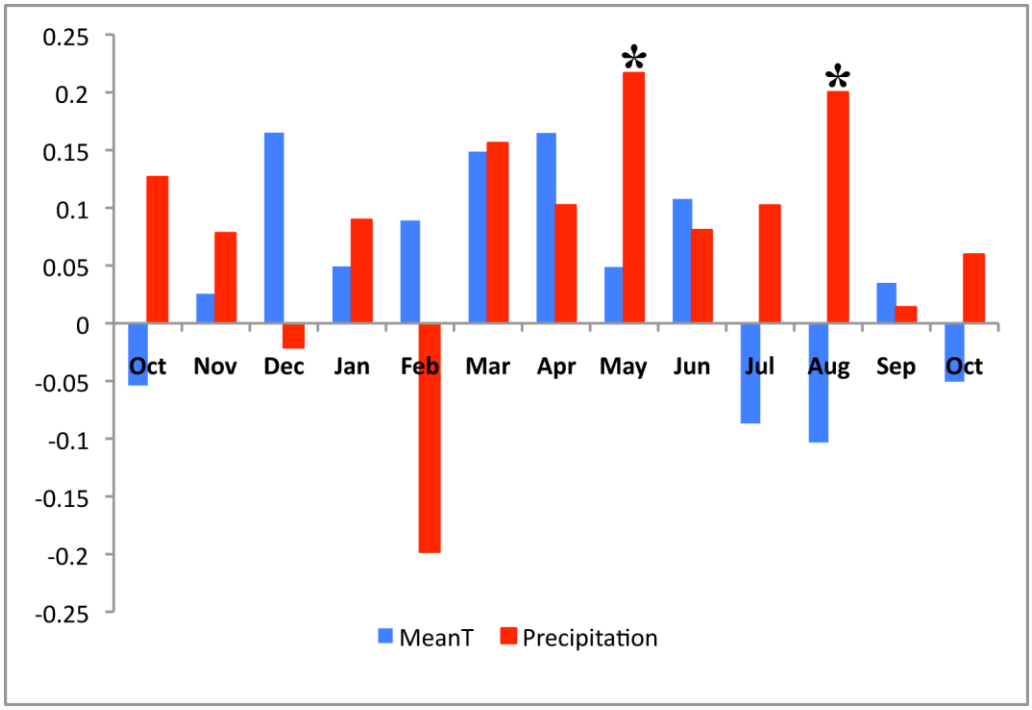

e. Cyprus, Doxa Soi o Theos, *Pinus brutia* (DST_PIBR)

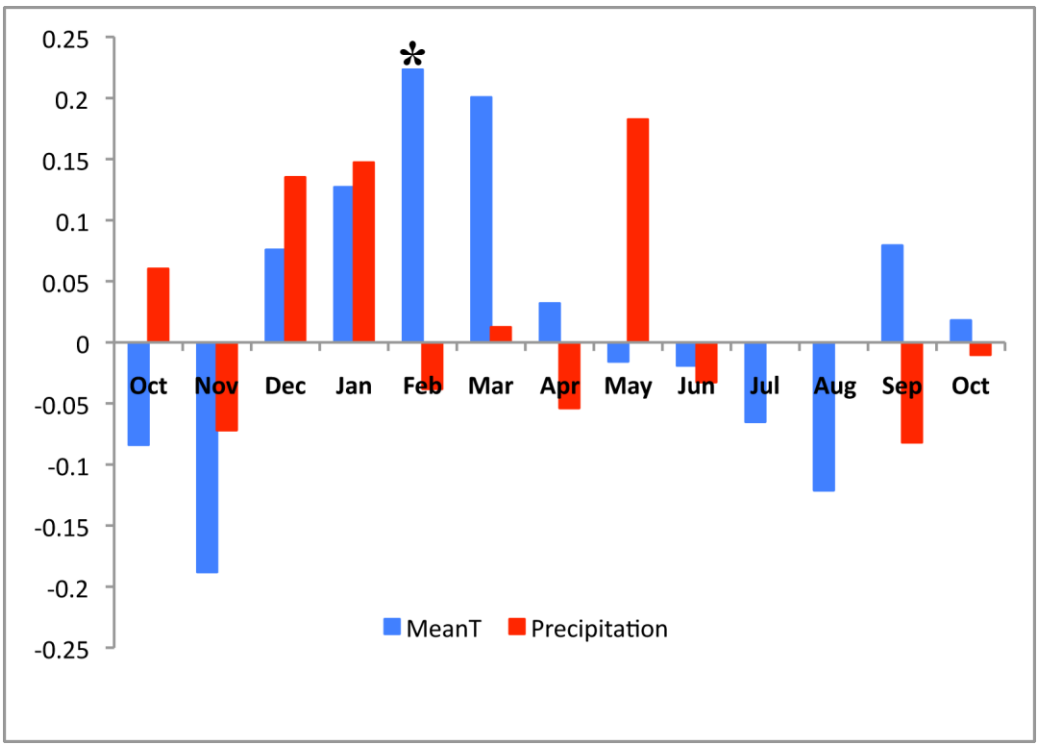

f. Lebanon, Herch Ehden, *Pinus brutia* (EPF_PIBR)

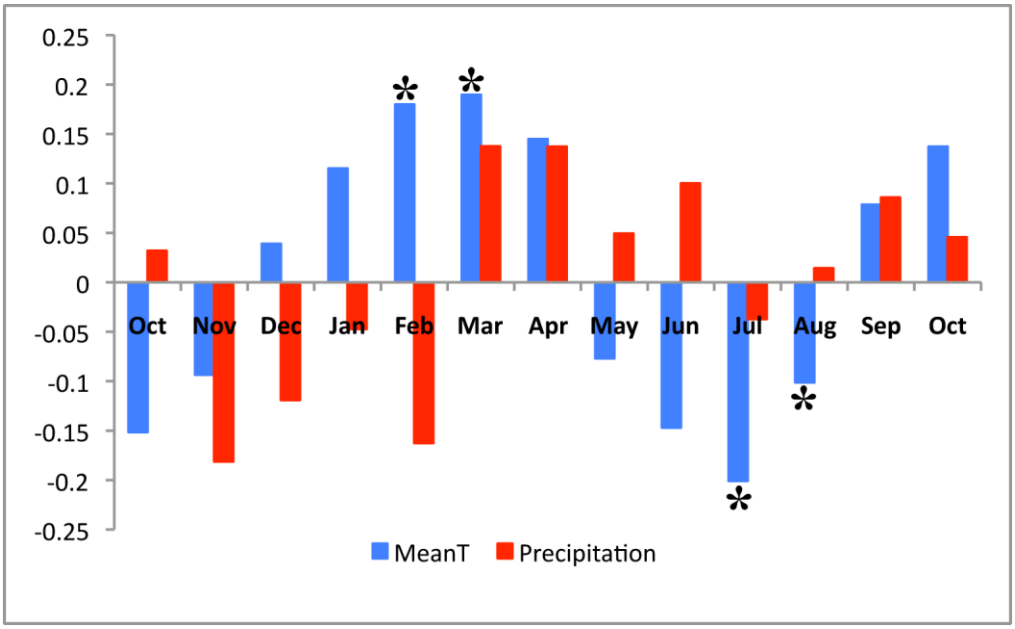

g. Turkey, Göller-Dumalı Dağ, *Pinus brutia* (GOLD_PIBR)

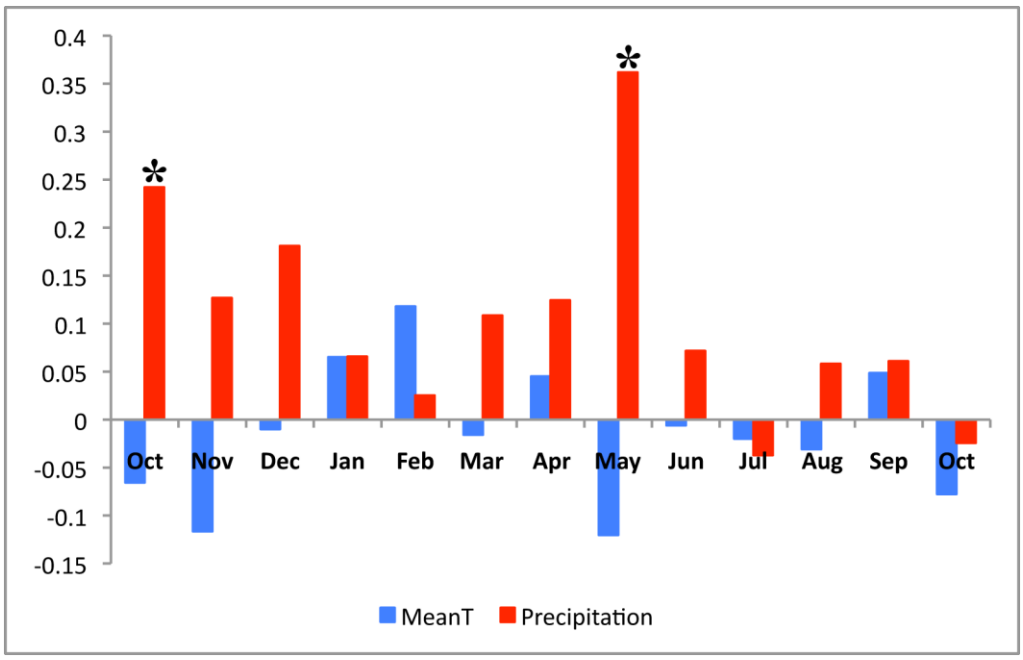

h. Cyprus, Roudhias Valley Arodafna, *Pinus brutia* (RVA_PIBR)

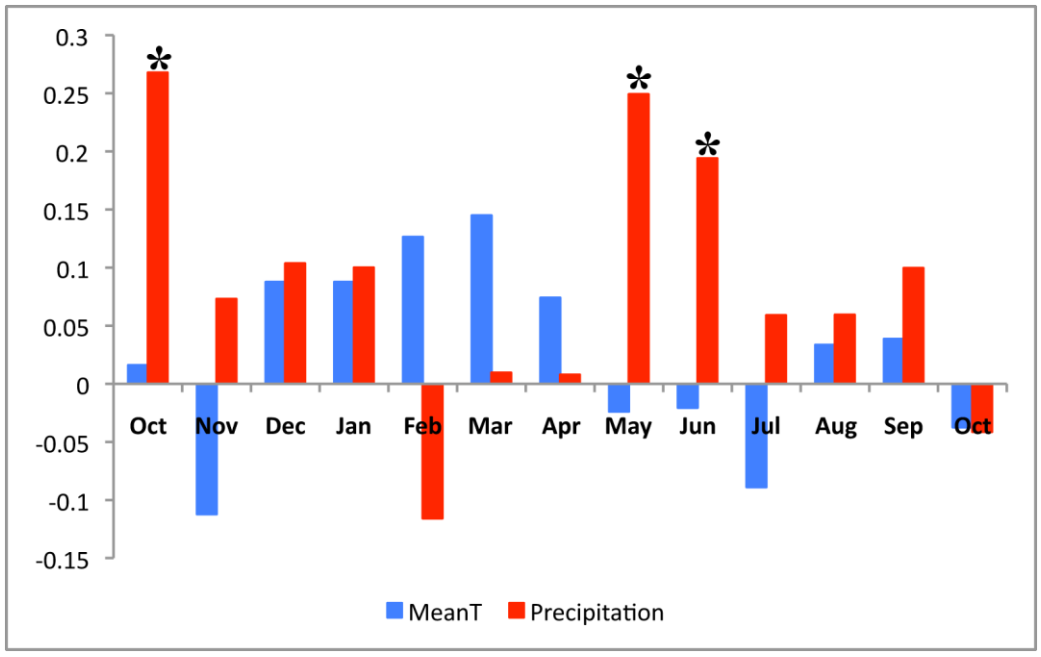

i. Cyprus, Stavros tis Psokas, *Pinus brutia* (STV_PIBR)

REFERENCES

Abi-Saleh, B., Safi, S., 1998. Carte de la vegetation du Liban. *Ecologia Mediterranea* XIV (1/2): 123–141.

Akkemik, Ü., Caner, H., Conyers, G.A., Dillon, M.J., Karlıoğlu, N., Rauh, N.K., Theller, L.O., 2012. The archaeology of deforestation in south coastal Turkey. *International Journal of Sustainable Development and World Ecology*, doi: 10.1080/13504509.2012.684363.

Akkemik, Ü., Yaman, B., 2012. *Wood Anatomy of Eastern Mediterranean Species*. Verlag Kessel, Remagen-Oberwinter.

Alpert, P., Neeman, B., Shay-El, Y., 1990. Intermonthly variability of cyclone tracks in the Mediterranean. *Journal of Climate* 3: 1474–1478.

Baillie, M.G.L., 1982. *Tree-Ring Dating and Archaeology*. University of Chicago Press, Chicago.

Baillie, M.G.L., Pilcher, J.R., 1973. A simple crossdating program for tree-ring research. *Tree-Ring Bulletin* 33: 7-14.

Barkai, O., Kahanov, Y., 2007. The Tantura F shipwreck, Israel. *The International Journal of Nautical Archaeology* 36 (1): 21–31.

Beaufort, F., 1818. *Karamania*. R. Hunter, London.

Biger, G., Liphschitz, N., 1991a. Regional dendrohistory and timber analysis: The use of wood in the buildings of nineteenth-century Jaffa. *Mediterranean Historical Review* 6 (1): 86–104.

Biger, G., Liphschitz, N., 1991b. Historical geography and botany: Timber in the nineteenth century Old City of Jerusalem. *Palestine Exploration Quarterly* 123: 4–18.

Biondi, F., Waikul, K., 2004. DENDROCLIM2002: A C++ program for statistical calibration of climate signals in tree-ring chronologies. *Computers and Geosciences* 30: 303–311.

Black, E., 2011. The influence of the North Atlantic Oscillation and European circulation regimes on the daily to interannual variability of winter precipitation in Israel. *International Journal of Climatology* 32 (11): 1654–1664.

Black, E., Hoskins, B., Slingo, J., Brayshaw, D., 2011. The present-day climate of the Middle East. In: Mithen, S., Black, E. (Eds.), *Water, Life and Civilisation: Climate, Environment and Society in the Jordan Valley*. Cambridge University Press, Cambridge, pp. 13–24.

Blondel, J., Aronson, J., 1999. *Biology and Wildlife of the Mediterranean Region*. Oxford University Press, New York.

Boronina, A., Renard, P., Balderer, W., Christodoulides, A., 2003. Groundwater resources in the Kouris catchment (Cyprus): data analysis and numerical modeling. *Journal of Hydrology* 271: 130–149.

Boydak, M., 2004. Silvicultural characteristics and natural regeneration of *Pinus brutia* Ten.–a review. *Plant Ecology* 171: 153–163.

Ciesla, W.M., 2004. Forests and forest protection in Cyprus. *The Forestry Chronicle* 80 (1): 107–113.

Cook, E.R., 1985. *A Time Series Analysis Approach to Tree-Ring Standardization*. Unpublished Ph.D thesis, University of Arizona, Tucson.

Cook, E.R., D'Arrigo, R., Briffa, K.R., 1998. A reconstruction of the North Atlantic Oscillation using tree-ring chronologies from North America and Europe. *The Holocene* 8: 9–17.

Cook, E.R., Krusic, P., 2006. Program ARSTAN: a Tree-Ring Standardization Program Based on Detrending and Autoregressive Time Series Modeling, with Interactive Graphics. Tree-Ring Laboratory, Lamont Doherty Earth Observatory, Columbia Univ., Palisades, N.Y.

Cordova, C.E., 2007. *Millennial Landscape Change in Jordan: Geoarchaeology and Cultural Ecology*. University of Arizona Press, Tucson.

Cullen, H.M., Kaplan, A., Arkin, P.A., Demenocal, P.B., 2002. Impact of the North Atlantic Oscillation on Middle Eastern climate and streamflow. *Climatic Change* 55: 315–338.

Cvikel, D., Kahanov, Y., 2012. The 19th-century Akko 1 Shipwreck, Israel: Hull-construction report. *The International Journal of Nautical Archaeology* 42 (1): 167–187.

Delipetrou, P., Makhzoumi, J., Dimopoulos, P., Georghiou, K., 2008. Cyprus. In: Vogiatzakis, I., Pungetti, G., Mannion, A. (Eds.), *Mediterranean Island Landscapes: Natural and Cultural Approaches*. Landscape Series, vol. 9. Springer Science, Dordrecht, pp. 170–203.

De Luis, M., Gričar, J., Čufar, K., Raventós, J., 2007. Seasonal dynamics of wood formation in *Pinus halepensis* from dry and semi-arid ecosystems in Spain. *IAWA Journal* 28 (4): 389–404.

Dittmar, C., Eißing, T., Rothe, A., 2012. Elevation-specific tree-ring chronologies of Norway spruce and silver fir in southern Germany. *Dendrochronologia* 30: 73–83.

Domínguez-Delmás, M., Alejano-Monge, R., Ważny, T., García-González, I., 2013. Radial growth variations of black pine along an elevation gradient in the Cazorla Mountains (south of Spain) and their relevance for historical and environmental studies. *European Journal of Forest Research* 132: 635–652.

Dufour-Dror, J., Ertaş, A., 2004. Bioclimatic perspectives in the distribution of *Quercus ithaburensis* Decne. subspecies in Turkey and in the Levant. *Journal of Biogeography* 31: 461–474.

Dünkeloh, A., 2005. Water budget of the Upper Diarizos Catchment, Troodos, Cyprus. *Hydrogeologie und Umwelt* 33 (15) supplement: 1–24.

Dünkeloh, A., Jacobheit, J., 2003. Circulation dynamics of Mediterranean precipitation variability, 1948–98. *International Journal of Climatology* 23: 1843–1866.

Eckstein, D., Bauch, J., 1969. Ein Beitrag zur Rationalisierung eines dendrochronologischen Verfahrens und zur Analyse seiner Aussagesicherheit. *Forstwissenschaftliches Centralblatt* 88: 230–250.

Emberger, L., 1971. *Travaux de Botanique et d'Ecologie*. Masson, Paris.

Emberger, L., 1955. Une classification biogéographique des climats. *Recherches et Travaux du Laboratoire de Botanique de la Faculté des Sciences de Montpellier* 7: 3–43.

Enzel, Y., Bookman, R., Sharon, D., Gvirtzman, H., Dayan, U., Ziv, B., Stein, M., 2003. Late Holocene climates of the Near East deduced from Dead Sea level variations and modern regional winter rainfall. *Quaternary Research* 60: 263–273.

Eshel, G., Farrell, B., 2000. Mechanisms of Eastern Mediterranean rainfall variability. *Journal of Atmospheric Sciences* 57: 3219–3232.

EUFORGEN, 2009a. Distribution map of Calabrian pine (*Pinus brutia*). EUFORGEN 2009. Online database, http://www.euforgen.org. Accessed 2 May, 2013.

EUFORGEN, 2009b. Distribution map of Aleppo pine (*Pinus halepensis*). EUFORGEN 2009. Online database, http://www.euforgen.org. Accessed 2 May, 2013.

Freiwan, M., Kadıoğlu, M., 2008. Spatial and temporal analysis of climatological data in Jordan. *International Journal of Climatology* 28: 521–535.

Fritts, H.C., 1976. *Tree Rings and Climate*. Laboratory of Tree-Ring Research, University of Arizona, Tucson.

Gaussen, 1954. *Théorie et classification des climates et microclimats*. VIIéme Congrés International de Botanique, pp. 125–130.

Goldreich, Y., 2003. *The Climate of Israel: Observation, Research, and Application*. Kluwer Academic Publishers, New York.

Griggs, C.B., Pearson, C.L., Manning, S.W., Lorentzen, B., 2014. A 250-year annual precipitation reconstruction and drought assessment for Cyprus from *Pinus brutia* (Ten.) tree-rings. *International Journal of Climatology* 34: 2702–2714.

Griggs, C.B., DeGaetano, A.T., Kuniholm, P.I., Newton, M.W., 2007. A regional reconstruction of May-June precipitation in the north Aegean from oak tree-rings, AD 1089–1989. *International Journal of Climatology* 27: 1075–1089.

Griggs, C.B., 2006. *Tale of Two: Reconstructing Climate from Tree-Rings in the North Aegean, AD 1089-1989, and Late Pleistocene to Present Dendrochronology in Upstate New York*. Unpublished Ph.D. thesis, Cornell University.

Haneca, K., Ważny, T., Van Acker, J, Beeckman, H., 2005. Provenancing Baltic timber from art historical objects: success and limitations. *Journal of Archaeological Science* 32: 261–271.

Hepper, F.N., 2001. The Bcharrê cedars of Lebanon as seen by travelers. *Archaeology and History in Lebanon* 14: 96–106.

Hijmans, R.J., Cameron, S.E., Parra, J.L., Jones, P.G., Jarvis, A., 2005. Very high resolution interpolated climate surfaces for global land areas. *International Journal of Climatology* 25: 1965–1978.

Hollstein, E., 1980. *Mitteleuropäische Eichenchronologie: Trierer dendrochronologische Forschungen zur Archäologie und Kunstgeschichte*. Trierer Grabungen und Forschungen 11. P. von Zabern, Mainz am Rhein.

Hulme, M., 1992. A 1951–80 global and precipitation climatology for the evaluation of general circulation models. *Climate Dynamics* 7: 57–72. [http://www.cru.uea.ac.uk/~mikeh/datasets/global].

Hughes, M.K., Kuniholm, P.I., Eischeid, J.K., Garfin, G., Griggs, C.B., Latini, C., 2001. Aegean tree-ring signature years explained. *Tree-Ring Research* 57 (1): 67–73.

Jansma, E., 1995. Remember*RINGS: The development and application of local and regional tree-ring chronologies of oak for the purposes of archaeological and historical research in the Netherlands*. Ph.D. thesis, University of Amsterdam.

Jones, P.D., Osborn, T.J., Briffa, K.R., 2003. Pressure-based measures of the North Atlantic Oscillation (NAO): A comparison and an assessment of changes in the strength of the NAO ands its influence on surface climate parameters. In: Hurrell, J.W., Kushnir, Y., Ottersen, G., Visbeck, M. (Eds.), *The North Atlantic Oscillation: Climate Significance and Environmental Impacts*. American Geophysical Union, Washington DC, pp. 51–62.

Jung, T., Hilmer, M., Ruprecht, E., Kleppek, S., Gulev, K., Zolina, O., 2003. Characteristics of the recent eastward shift of interannual NAO variability. *Journal of Climatology* 16 (20): 3371–3382.

Kaiser, H.F., 1992. On Cliff's formula, the Kaiser-Guttman rule, and the number of factors. *Perceptual and Motor Skills* 74: 595–598.

Kienast, F., Schweingruber, F.H., Bräker, O.U., Schär, E., 1987. Tree-ring studies on conifers along ecological gradients and the potential of single-year analyses. *Canadian Journal of Forestry Research* 17: 683–696.

Köse, N., Akkemik, Ü., Dalfes, H., Özeren, M.S., Tolunay, D., 2012. Tree-ring growth of *Pinus nigra* Arn. subsp. *pallasiana* under different climate conditions throughout western Anatolia. *Dendrochronologia* 30: 295–301.

Köse, N., Akkemik, Ü., Dalfes, N.D., Özeren, M.S., 2011. Tree-ring reconstructions of May-June precipitation for western Anatolia. *Quaternary Research* 75: 438–450.

Krichak, S.O., Alpert, P., 2005. Signatures of the NAO in the atmospheric circulation during wet winter months over the Mediterranean region. *Theoretical and Applied Climatology* 82: 27–39.

Kuniholm, P.I., 2000. Dendrochronologically dated Ottoman monuments. In: Baram, U., Carroll, L. (Eds.), *A Historical Archaeology of the Ottoman Empire: Breaking New Ground*. Plenum Press, New York, pp. 93–136.

Kuniholm, P.I., Griggs, C.B., Newton, M.W. 2007. Evidence for early timber trade in the Mediterranean. In: Belke, K., Kisslinger, E.A.K., Stassinopoulou, M.A. (Eds.), *Byzantina Mediterranea: Festschrift für Johannes Koder zum 65. Geburtstag*. Böhlau Verlag, Vienna, pp. 365–385.

Kuniholm, P.I., Striker, C.L., 1987. Dendrochronological investigations in the Aegean and neighboring regions, 1983–1986. *Journal of Field Archaeology* 14: 385-398.

Kutiel, H., Benaroch, Y., 2002. North Sea-Caspian Pattern (NCP)–An upper level atmospheric teleconnection affecting the Eastern Mediterranean: identification and definition. *Theoretical and Applied Climatology* 71: 17–28.

Kutiel, H., Paz, S., 1998. Sea level pressure departures in the Mediterranean and their relationship with monthly rainfall conditions in Israel. *Theoretical and Applied Climatology* 60 (1–4): 93–109.

Levanič, T., Pignatelli, O., Čufar, K., 2001. A regional larch chronology of trees and historical buildings from Slovenia and Northern Italy. *Dendrochronologia* 19: 221–229.

Lev-Yadun, S., 2000. Wood structure and the ecology of annual growth ring formation in *Pinus halepensis* and *P. brutia*. In: Ne'eman, G., Trabaud, L. (Eds.), *Ecology and Biodiversity and Management of* Pinus halepensis *and* P. brutia *Forest Ecosystems in the Mediterranean Basin*. Backhuys, Leiden, pp. 67–78.

Lindner, M., Maroschek, M., Netherer, S., Kremer, A., Barbati, A., Garcia-Gonzalo, J., Seidl, R., Delzon, S., Corona, P., Kolström, M., Lexer, M.J., Marchetti, M., 2010. Climate change impacts, adaptive capacity, and vulnerability of European ecosystems. *Forest Ecology and Management* 259: 698–709.

Lionello, P., Malanotte-Rizzoli, P., Boscolo, T., Alpert, P., Artale, V., Li, L., Luterbacher, J., May, W., Trigo, R., Tsimplis, M., Ulbrich, U., Xoplaki, E., 2006. The Mediterranean climate: an overview of the main characteristics and issues. In: Lionello, P., Malanotte-Rizzoli, P., Boscolo, R. (Eds.), *Mediterranean Climate Variability*. Elsevier, Amsterdam, pp. 1–27.

Liphschitz, N., 2007. *Timber in Ancient Israel: Dendroarchaeology and Dendrochronology*. Monograph Series of the Institute of Archaeology of Tel Aviv University, 26. Emergy and Claire Yass Publications in Archaeology, Tel Aviv.

Liphschitz, N., Biger, G., 2001. Past distribution of Aleppo pine (*Pinus halepensis*) in the mountains of Israel (Palestine). *The Holocene* 11 (4): 427–436.

Liphschitz, N., Biger, G., 2000. *Green Dress for a Country: Afforestation in Eretz-Israel, the First Hundred Years, 1850-1950*. Ariel Publishing House, Jerusalem.

Luterbacher, J., Schmutz, C., Gyalistras, D., Xoplaki, E., Wanner, H. 1999. Reconstruction of monthly NAO and EU indices back to AD 1675. *Geophysical Research Letters* 26: 2745–2748.

Madmony, A., Schiller, G., Moshe, Y., Tsabary, G., Mendel, Z., Riov, J., 2003. Controlled and open pollination between *Pinus brutia* (Ten.) and *Pinus halepensis* (Mill.) in Israel and hybrid performance. *Israel Journal of Plant Sciences* 51: 213–222.

McNeill, J.R., 1992. *The Mountains of the Mediterranean World*. Cambridge University Press, Cambridge.

Mederer, J., 2005. Groundwater resources of the Limnatis Catchment in Cyprus: Application of the water balance modeling program MODBIL in an area of irrigation. *Hydrogeologie und Umwelt* 33 (4): 1–13.

Meiggs, R., 1982. *Trees and Timber in the Ancient Mediterranean World*. Clarendon Press, Oxford.

Melzack, R.N., Grunwald, C., Schiller, G., 1981. Morphological variation in Aleppo pine (*Pinus halepensis* Mill.) in Israel. *Israel Journal of Botany* 30: 199–205.

Michaelides, S.C., Tymvios, F.S., Michaelidou, T., 2009. Spatial and temporal characteristics of the annual rainfall frequency distribution in Cyprus. *Atmospheric Research* 94: 606–615.

Mikesell, M., 1969. The deforestation of Mount Lebanon. *Geographical Review* 59 (1): 1–28.

Mikhail, A., 2011. *Nature and Empire in Ottoman Egypt: An Environmental History*. Cambridge University Press, Cambridge.

Mitchell, T.D., Jones, P.D., 2005. An improved method of constructing a database of monthly climate observations and associated high-resolution grids. *International Journal of Climatology* 25: 693–712.

Mor, H., Kahanov, Y., 2006. The Dor 2001/1 Shipwreck, Israel–a summary of the excavation. *The International Journal of Nautical Archaeology* 35 (2): 274–289.

Munro, M.A.R., 1984. An improved algorithm for crossdating tree-ring series. *Tree-Ring Bulletin* 44: 17–27.

Nahal, I., 1983. Le pin brutia (*Pinus brutia* Ten. subsp. *brutia*) (première partie). *Forêt Méditerranéenne* 5: 165–172.

Nicault, A., Alleaume, S., Brewer, S., Carrer, M., Nola, P., Guiot, J., 2008. Mediterranean drought fluctuation during the last 500 years based on tree-ring data. *Climate Dynamics* 31 (2–3): 227–245.

Panetsos, K.P., 1981. Monograph of *Pinus halepensis* (Mill.) and *P. brutia* (Ten.). *Annales Forestales* 9: 39–77.

Pashiardis, S., 2000. *Trends of precipitation in Cyprus rainfall analysis for agricultural planning*. Internal report 1418, Meteorological Service, Nicosia, Cyprus.

Pearson, C.L., Griggs, C.B., Kuniholm, P.I., Brewer, P.W., Ważny, T., Canady, L., 2012. Dendroarchaeology of the mid-first millennium AD in Constantinople. *Journal of Archaeological Science* 39: 3402–3414.

Porter, J.L., 1871. *The Giant Cities of Bashan and Syria's Holy Places*. Thomas Nelson and Sons, New York.

Price, C, Michaelides S, Pashiardis S, Alperta, P., 1999. Long term changes in diurnal temperature range in Cyprus. *Atmospheric Research* 51 (2): 85–98.

Price, C., Stone, L., Huppert, A., Rajagopalan, B., Alpert, P., 1998. A possible link between El Niño and precipitation in Israel. *Geophysical Research Letters* 25 (21): 3963–3966.

Quézel, P., Médail, F., 2003. *Écologie et Biogéographie des Forêts du Bassin Méditerranéen*. Elsevier, Paris.

Quézel, P., 2000. Taxonomy and biogeography of Mediterranean pines (*Pinus halepensis* and *P. brutia*). In: Ne'eman, G., Trabaud, L. (Eds.), *Ecology and Biodiversity and Management of* Pinus halepensis *and* P. brutia *Forest Ecosystems in the Mediterranean Basin*. Backhuys, Leiden, pp. 1–12.

Quézel, P., Barbero, M., 1992. Le pin d'Alep et les espèces voisines: repartition et caractères écologiques généraux, sa dynamique récente en France méditerranéenne. *Forêt Méditerranéenne* 13: 158–170.

Rencher, A.C., 2002. *Methods of Multivariate Analysis*. 2nd edition. John Wiley and Sons, New York.

Richardson, D.M., Rundel, P.W., 1998. Ecology and biogeography of *Pinus*: An introduction. In: Richardson, D.M. (Ed.), *Ecology and Biogeography of* Pinus. Cambridge University Press, Cambridge, pp. 3–46.

Rinn, F., 1996. TSAP (Time series Analysis and Presentation) Version 3.0. Heidelberg, Germany.

Rustum, A.J., 1936. *The Royal Archives of Egypt and the Origins of the Egyptian Expedition to Syria, 1831–1841*. American Press, Beirut.

Saaroni, H., Halfon, N., Ziv, B., Alpert, P., Kutiel, H., 2010. Links between the rainfall regime in Israel and location and intensity of Cyprus lows. *International Journal of Climatology* 30: 1014–1025.

Sander, C., Levanič, T., 1996. Comparison of *t*-values calculated in different dendrochronological programmes. *Dendrochronologia* 14: 269–272.

Sarris, D., Christodoulakis, D. Körner, C., 2007. Recent decline in precipitation and tree growth in the eastern Mediterranean. *Global Change Biology* 13: 1187–1200.

Schiller, G., 2000. Ecophysiology of *Pinus halepensis* Mill. and *P. brutia* Ten. In: Ne'eman, G., Trabaud, L. (Eds.), *Ecology and Biodiversity and Management of* Pinus halepensis *and* P. brutia *Forest Ecosystems in the Mediterranean Basin*. Backhuys, Leiden, pp. 51–65.

Schweingruber, F.H., 1996. *Tree Rings and Environment Dendroecology*. Verlag Paul Haupt, Bern.

Schweingruber, F.H., 1990. *Anatomy of European Woods*. Verlag Paul Haupt, Bern.

Schweingruber, F.H., Eckstein, D., Serre-Bachet, F., Bräker, O.U., 1990. Identification, presentation and interpretation of event years and pointer years in dendrochronology. *Dendrochronologia* 8: 9–38.

Talhouk, S.N., Zurayk, R., Khuri, S., 2001. Conservation of the coniferous forests of Lebanon: Past, present and future prospects. *Oryx* 35 (3): 206–215.

Thirgood, J.V., 1987. *Cyprus: A Chronicle of Its Forests, Lands, and People*. University of British Columbia Press, Vancouver.

Touchan, R., Akkemik, Ü., Hughes, M.K., Erkan, N., 2007. May–June precipitation reconstruction of southwestern Anatolia, Turkey, during the last 900 years from tree-rings. *Quaternary Research* 68: 196–202.

Touchan, R., Anchukaitis, K.J., Shishov, V.V., Sivrikaya, F., Attieh, J., Ketmen, M., Stephan, J., Mitsopoulos, I., Christou, A., Meko, D.M., 2014a. Spatial patterns of eastern Mediterranean climate influence on tree growth. *The Holocene* 24 (4): 381–392.

Touchan, R., Christou, A.K., Meko, D.M., 2014b. Six centuries of May–July precipitation in Cyprus from tree rings. *Climate Dynamics* 43: 3281–3292.

Touchan, R., Hughes, M.K., 1999. Dendrochronology in Jordan. *Journal of Arid Environments* 42: 291–303.

Touchan, R., Meko, D.M., Aloui, A., 2008. Precipitation reconstruction for northwestern Tunisia from tree rings. *Journal of Arid Environments* 72: 1887–1896.

Touchan, R., Meko, D.M., Anchukaitis, K.J., 2014c. Dendroclimatology in the eastern Mediterranean. *Radiocarbon/Tree-Ring Research* 56 (4): S61–S68.

Touchan, R., Xoplaki, E., Funkhouser, G., Luterbacher, J., Hughes, M.K., Erkan, N., Akkemik, Ü., Stephan, J., 2005. Reconstructions of spring/summer precipitation for the eastern Mediterranean from tree-ring widths and its connection to large-scale atmospheric circulation. *Climate Dynamics* 25: 75–98.

Trigo, I.F., Bigg, G.R., Davies, T.D., 2002. Climatology of cyclogenesis mechanisms in the Mediterranean. *Monthly Weather Review* 130 (3): 549–569.

Türkeş, M., 1996. Spatial and temporal analysis of annual rainfall variations in Turkey. *International Journal of Climatology* 16: 1057–1076.

Wang, Y.H., Magnusdottir, G., Stern, H., Tian, Z., Yu, Y., 2012. Decadal variability of the NAO: Introducing an augmented NAO index. *Geophysical Research Letters* 39: 1–5.

Wigley, T.M.L., Briffa, K.R., Jones, P.D., 1984. On the average value of correlated time series, with applications in dendroclimatology and hydrometeorology. *Journal of Climate and Applied Meteorology* 23: 201–213.

Wigley, T.M.L., Jones, P.D., Briffa, K.R., 1987. Cross-dating methods in dendrochronology. *Journal of Archaeological Science* 14: 51–64.

Xoplaki, E., González-Rouco, J.F., Luterbacher, J., Wanner, H., 2004. Wet season Mediterranean precipitation variability: influence of large-scale dynamics and trends. *Climate Dynamics* 23 (1): 63–78.

Yakir, D., Lev-Yadun, S., Zangvil, A., 1996. El Niño and tree growth near Jerusalem over the last 20 years. *Global Change Biology* 2: 97–101.

Ziv, B., Dayan, U., Kushnir, Y., Roth, C., Enzel, Y., 2006. Regional and global atmopheric patterns governing rainfall in the southern Levant. *International Journal of Climatology* 26: 55–73.

Zohary, M., 1973. *Geobotanical Foundations of the Middle East*. 2 vols. Gustav Fischer, Stuttgart.

CHAPTER 4:

DENDROCHRONOLOGICAL AND ^{14}C EVIDENCE FOR OVER A MILLENNIUM OF LONG-DISTANCE TIMBER TRADE TO AL-AQSA MOSQUE, JERUSALEM

SUMMARY

Al-Aqsa mosque is one of Jerusalem's most prominent buildings. Because of its religious and political significance, the mosque has a dynamic history of over a millennium since its construction in the late 7th century AD. This study investigates timbers removed from the mosque's southeast area during its 1968–1983 renovations, using a combination of dendrochronology and ^{14}C wiggle-matching, in order to date more precisely when the timbers were cut and determine the forests from which they were procured. The results reveal a complex building history, in which old timbers were repurposed, and new, high-quality timbers were imported, including cedar from the eastern Mediterranean, larch from the Italian Alps in the 14th century AD, and oak from western Anatolia during the 18th century AD.

Tree-ring and ^{14}C data from previous studies on al-Aqsa's timbers–which concluded that the mosque contained wood re-used from assorted Iron Age through Byzantine-era buildings–are also re-evaluated. It is instead argued that while some of al-Aqsa's wooden panels were re-used from earlier Byzantine-era wood, many of its earliest cedar timbers likely date to the late 7th–early 8th century AD, around the mosque's construction date, or later, during the late 8th century AD.

INTRODUCTION

The al-Aqsa mosque (Arabic: *Masjid al-Aqsa*, or 'the Farthest Mosque') is one of the most important and prominent religious buildings in Jerusalem. Al-Aqsa is considered the third most holy site in Islam, and is, according to the Muslim faith, the location to which the Prophet Muhammad was transported during the Night Journey from Mecca to Jerusalem. The mosque is at the heart of Jerusalem's Old City on top of the Temple Mount, or *al-Haram al-Sharif* (Arabic: 'the Noble Sacred Enclosure'), next to the Dome of the Rock and upon the remains of the First and Second Jewish Temples (Figure 4.1). This area is considered sacred to Jews, Christians, and Muslims alike, giving the mosque a dynamic history of over 1,000 years.

In the following study, timbers from the southeast part of al-Aqsa (recovered from its 1969–1983 restorations), as well as a previously collected sample from the north part of the mosque (recovered from the 1938 renovations), are analyzed using dendrochronology and ^{14}C wiggle-matching, in order to date when the timbers were felled, determine possible timber sources, and to fit these remains into both Jerusalem's and the region's histories. Results from previous analyses of a different group of roof timbers (Lev-Yadun 1992; Lev-Yadun et al. 1984) and carved wooden panels and beams (Liphschitz et al. 1997) from the mosque are also reviewed and reevaluated based on this new information.

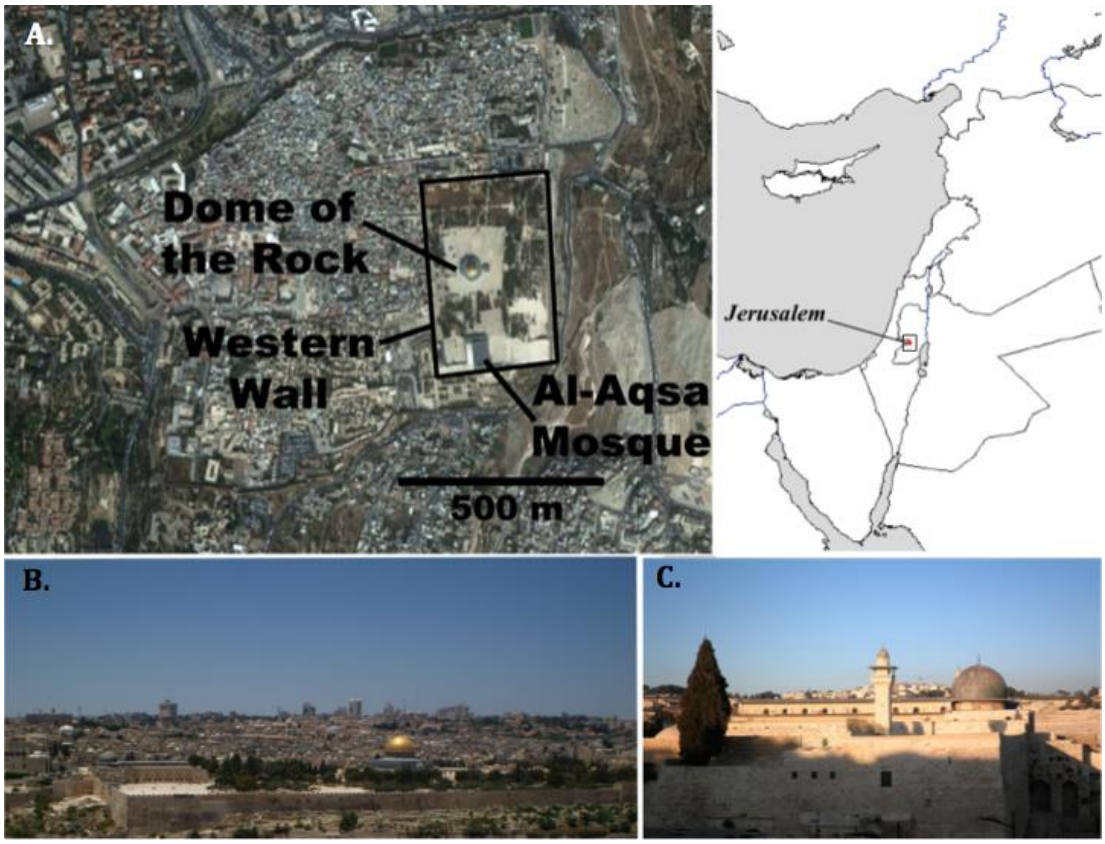

Figure 4.1. Overhead from Google Images (A) of al-Aqsa on the *Haram al-Sharif* (*outlined in black*) in Jerusalem's Old City, and panoramic views of the mosque from the east (B) and the southwest (C). ***Photo credit: Brita Lorentzen***

Site

Detailed accounts about al-Aqsa's building history and architecture are available in Creswell (1958), Hamilton (1949), and Le Strange (1965), so only a brief summary is given here. Al-Aqsa's present configuration is 83 x 56 m; the mosque is a seven bay hypostyle hall with additional smaller halls on the southeastern and southwestern sides of the building. There is a lead-sheeted dome and minbar at the southern end of the mosque, and ornate carved and painted wooden tie-beams span the central nave and connect the columns lining the nave's arcades (Creswell 1958; Hamilton 1949).

The Umayyad caliph ‘Abd al-Malik (685–705 AD) began construction of al-Aqsa toward the end of the 6th century AD. It is thought that Al-Aqsa replaced a smaller wooden building constructed by the Rashidun caliph ‘Umar (634–644 AD) (Creswell 1958; Hamilton 1949), which was in existence by at least 679 AD (Rosen-Ayalon 1989). Since then, the mosque has undergone several reconstructions and renovations. The building sits upon the rubble of at least 5,000 years of settlement on the Temple Mount in a tectonically active region adjacent to the Dead Sea Transform fault system, which has meant that al-Aqsa is at great risk from, and has frequently sustained, earthquake damage (Hamilton 1949; Marco et al. 2003). Earthquakes in 749, 774, and 1033 AD all caused severe damage that required extensive renovation and repair, changing the mosque’s structure and dimensions (Creswell 1958; Hamilton 1949; Marco et al. 2003).

Al-Aqsa reached its present form in the middle of the fourteenth century AD under the Mamluk Sultan Aybak al-Miṣri (Hamilton 1949), although repairs (particularly to the roof) continued under the Ottomans (Heyd 1960; St. Laurent and Riedlmayer 1993). During the 20th century, the mosque underwent renovations in 1938 and 1942 to repair damage from earthquakes in 1927 and 1937 (Hamilton 1949). A fire in the mosque on August 21, 1969, destroyed large parts of the southeastern wing of the mosque, including the dome, minbar, and roof. The building underwent large-scale restoration from 1969–1983, which led to the removal of several structural timbers that were decaying or had sustained fire damage (Serageldin 1989).

Previous Dendrochronological and ^{14}C Research

Lev-Yadun et al. (1984) investigated a group of 140 roof beams removed from the southeast part of al-Aqsa during the 1969–1983 renovations. This assemblage included beams that they identified as cedar of Lebanon (*Cedrus libani* A. Rich.), Turkey oak (*Quercus cerris* L.), cypress (*Cupressus sempervirens* L.), poplar (*Populus* sp.), and plane (*Platanus* sp.). They crossdated 23 cedar timbers and used 19 of these to build a 231-year chronology (referred to here as 'AQS_cedar1'). The inner rings of the earliest sample component of the chronology (sample #2, whose outermost ring dates to relative year 192 of the 231-year chronology) and the outer rings of another sample (sample #1, which dates to relative year 202 of the 231-year master chronology) were dated using conventional ^{14}C counting techniques. The outer rings of sample #2 dated to 1340 ±250 years BP (Lev-Yadun 1984), which Liphschitz et al. (1997) later calibrated to 516 ±250 AD (at 68.2% probability). The inner rings of sample #1 dated to 1670 ±50 years BP (Lev-Yadun 1984), from which Liphschitz et al. (1997) calculated a calibrated date of 506 ±50 AD for the sample's outer rings (at 69.2% probability).

Lev-Yadun et al. (1984) were unable to crossdate and build chronologies for the oak and the cypress samples, but single samples of the outer rings of five of these timbers were dated using conventional ^{14}C counting techniques. Their results, which have been recalibrated using the IntCal09 curve (Reimer et al. 2009), are shown in Table 4.1. Lev-Yadun et al.'s (1984) analysis produced surprisingly old dates for two individual samples. The outer rings of an oak (*Quercus cerris*) were dated to 2860 ±180 years, which dated in terms of the IntCal09 radiocarbon calibration curve

(Reimer et al. 2009) is 1516–555 BC at 95.4% probability. The outer rings of a cypress timber were dated to 2610 ±170 years, which, when calibrated with IntCal09, dates to 1253–378 BC at 95.4% probability.

Table 4.1. ^{14}C dates and available metadata for samples studied by Lev-Yadun et al. (1984). The calibrated dates are calculated (when possible) for the sample's outer rings against IntCal09 (Reimer et al. 2009) for the present study. It is assumed that the uncalibrated ^{14}C ages reported are conventional ^{14}C ages that have been corrected for sample δ^{13}C fractionation (Stuiver and Polach 1977), but this information was not available either from the publication or from the records of the Weizmann Institute ^{14}C Laboratory in Rehovot, Israel, which performed the analysis.

Species	^{14}C age (BP)	Calibrated age BC/AD (68.2%)	Calibrated age BC/AD (95.4%)	Notes
Quercus cerris	2860 ±180	1264–839 BC	1516–555 BC	outer rings dated
Cupressus sempervirens	2610 ±170	968–421 BC	1253–378 BC	outer rings dated
Cupressus sempervirens	1460 ±250	266–870 AD	5–1119 AD	center of the tree dated; sample had 50 rings
Quercus cerris	760 ±150	1051–1391 AD	975–1444 AD	outer part of the tree dated
Quercus cerris	220 ±210	1518–1952 AD	1330–… AD	center of the tree dated (no ring count given)

From this information, they concluded that the cedar timbers had been cut and previously used during the Byzantine Period, and that the al-Aqsa builders had also re-used the timbers from other, older buildings (Lev-Yadun 1992; Lev-Yadun et al. 1984; Liphschitz et al. 1997). Similarly, Liphschitz et al. (1997) argued that oak timber was reused from an Iron Age building during the time of the First Jewish Temple. Unfortunately, additional sample metadata and the individual ring measurements for these samples were never published.

More recently, Liphschitz et al. (1997) analyzed a group of 21 decorated panels and beams that were removed from al-Aqsa's central nave and tie-beams and are now on display in the Rockefeller Museum in East Jerusalem. Their analysis included wood species identification and sampling the outer rings of six timbers for AMS ^{14}C analysis. All of the timbers analyzed were cut from *Cedrus libani* or *Cupressus sempervirens*. Their samples' AMS dates, which have been recalculated using IntCal09 (Reimer et al. 2009), are given in Table 4.2 (modified from: Liphschitz et al. 1997: Table 2). From this information, they concluded that the timbers were cut during the Byzantine and Roman Periods, predating the mosque's late seventh century AD construction date. They therefore argued that the timbers were taken from earlier constructions on or near the Temple Mount and were reused to build the mosque.

Table 4.2. ^{14}C data for carved wooden panels analyzed in Liphschitz et al. (1997: Table 2). The calibrated dates have been recalculated for the present study using the IntCal09 calibration curve (Reimer et al. 2009).

Lab ID	Catalogue #	Species	Conventional ^{14}C age (BP)	Calibrated age BC/AD (68.2%)	Calibrated age BC/AD (95.4%)
ETH-8252	53.10	*Cupressus sempervirens*	2110 ±35	182–60 BC	346–43 BC
ETH-8253	53.12	*Cedrus libani*	1670 ±35	339–420 AD	256–527 AD
ETH-8254	53.19	*Cupressus sempervirens*	2190 ±35	357–198 BC	376–171 BC
ETH-8255	53.26	*Cedrus libani*	1565 ±40	434–540 AD	411–582 AD
ETH-9477	53.2	*Cupressus sempervirens*	1505 ±50	443–621 AD	433–642 AD
ETH-9478	53.5	*Cedrus libani*	1915 ±50	20–135 AD	37 BC–224 AD

Additionally, in 1986, Kuniholm (*unpublished data*) analyzed three roof timbers removed from the northern part of al-Aqsa during the 1938 renovations. This

assemblage consists of one cedar (*Cedrus libani*) core, one oak (*Quercus* section *Cerris*) section, and one poplar (*Populus* sp.) section (Table 4.3). Only the oak section was measured, since it was the only sample suitable for dendrochronology. (Poplar does not produce clear annual rings, while the cedar sample's rings were 'complacent,' meaning that there is little year-to-year ring-width variability.) Unfortunately, Kuniholm's oak sample did not crossdate with any oak reference chronologies available at the time.

The following study aims to improve upon this work by analyzing a new group of timbers from al-Aqsa using dendrochronology (and a larger collection of tree-ring reference chronologies from the eastern Mediterranean and Europe than was available for the previous studies) and, for some samples, ^{14}C wiggle-matching. The radiocarbon dates reported for Lev-Yadun et al.'s (1984) *Cedrus libani* chronology have also been recalculated against the IntCal09 calibration curve (Reimer et al. 2009) using Bayesian analysis techniques (Bayliss 2007; Bronk Ramsey 2009a). These methods provide a narrower, more precise date or date range for when the timbers were cut. Dendroprovenancing techniques and wood anatomical analyses are also used, and the historical record consulted, to determine the geographic region where the timbers were procured and improve the overall interpretation of the results.

MATERIALS AND METHODS

Materials and Collection

Because al-Aqsa's location on the Temple Mount/ *Haram al-Sharif* is an extremely politically sensitive and highly restricted area, it was not possible to sample from the building directly. Instead, fifteen sections were sampled from a group of roof

timbers removed from the southeastern corner of the mosque during 1960–1983 restorations to the mosque's dome. The timbers are currently in the private collection of Mr. Ze'ev Ehrlich, who purchased a portion of the removed timbers in 1983.

The collection includes four decorated Mediterranean cypress (*Cupressus sempervirens* L.) and two decorated cedar of Lebanon (*Cedrus libani* A.Rich.) timbers. The timbers are carved with floral motifs similar to the decorated timbers described in Hamilton (1949) (Figure 4.2A,B), and the carved timbers in the Rockefeller Museum that Liphschitz et al. analyzed (1997). Both Creswell (1958) and Hamilton (1949) dated this type of carving stylistically to the Abbasid Period, and argued that they were created during Caliph al-Mahdi's renovations to the mosque in 780 AD. However, more recent scholarship has argued that the carvings are in fact Umayyad, probably from the time of Caliph al-Walid I (705–715 AD) (St. Laurent, pers. comm., 2013; Talgam 2004). A Kufic inscription, which stylistically dates to the 10th century AD, containing the words *Bayt al-Maqdis* (Arabic: "the Temple," another name for Jerusalem) and *al-Masjid* (Arabic: "the mosque") (transl. David Powers) is carved on one cypress timber (Figure 4.2C), and was possibly added to the timber at a later period.

Most of these timbers have fewer than 50 tree-rings with little year-to-year variability in width (i.e., complacency), or, in the case of cypress, are a species that can form multiple rings, sometimes with unclear boundaries, in a given year (Liphschitz et al. 1981; Schweingruber 1993). Thus these samples are not suitable for dendrochronological analysis. A section was cut from one cedar timber (AQS-6) with

a suitable ring count (Figure 4.2B). The remaining samples were taken from undecorated timbers (labeled AQS-7–20) from the mosque roof.

Figure 4.2. Timbers decorated with Umayyad/Abbasid floral motifs in the collection analyzed for this study (A). One decorated *Cedrus libani* timber (AQS-6) was sampled for analysis (B). Another *Cupressus sempervirens* timber has an inscription in Kufic (C). *Photo credit: Brita Lorentzen*

In addition to the samples in Mr. Ehrlich's collection, a small section of cedar timber was recovered from the ^{14}C laboratory at the Weizmann Institute of Science in Rehovot, Israel. This sample (labeled AQS-4) was a subsection of a timber that Lev-Yadun et al. (1984) had previously analyzed and sent to the Institute for radiocarbon analysis. This sample was therefore included in this study and re-analyzed, as was Kuniholm's previously studied oak section (labeled AQS-2).

Timber Identification, Measurement, and Dendrochronological Crossdating

Before measurement and crossdating, transverse, radial, and tangential microsections were taken from the timber samples, in order to identify the species of each timber. The microsections were then inspected under an Olympus Bx41 binocular microscope at magnifications up to x100, and were compared with archaeological and modern wood reference collections, standard reference texts (Akkemik and Yaman 2012; Fahn et al. 1986; Schweingruber 1990), and the InsideWood anatomical database (InsideWood 2004–onwards).

The rest of the timber section was then sanded and polished, so that the tree-rings and cell anatomy were clearly visible for dendrochronological analysis. Each sample's tree-ring widths were then measured to the nearest 0.01 mm on a measurement table under a dissecting microscope, using the Tellervo TRiDaS (Brewer et al. 2010) and TSAP (Rinn 1996) dendrochronological analysis packages. Notable anatomical features were also marked and described for each ring using the same programs. The oak (*Quercus* sp.) timbers were examined to determine if any sapwood was present, since an accurate estimation of an oak timber's felling date is often possible when sapwood is preserved (Hillam et al. 1987; Hughes et al. 1981; Miles 2005; Ważny 1990).

The measured tree-ring series were cross-matched with other samples belonging to the same species, and the synchronized sample measurements for each year were then averaged together to create composite site chronologies for each species present at the site, using standard dendrochronological methods (Cook and Kairiukstis 1990). The site chronologies and individual tree-ring sequences were

compared and crossdated against absolutely dated reference chronologies built from sites of the same species in the eastern Mediterranean and Europe, as well as dendrochronologically dated site chronologies from historical buildings and wooden objects from these areas.

Crossdating between the al-Aqsa chronologies and reference chronologies was performed in the TSAP program (Rinn 1996). Each potential cross-match was evaluated using two different statistical tests: the *t*-value and Gleichläufigkeit (*GL*) (Eckstein and Bauch 1969) (described in: Chapter 3). Since different algorithms (which use different tree-ring de-trending functions) used to calculate *t*-values can produce different results (see: Chapter 3), the Baillie-Pilcher *t*-value (t_{BP}) (Baillie and Pilcher 1973) is used here, although *t*-values calculated using the Hollstein algorithm (t_H) (Hollstein 1980) were also calculated for comparison. The t_{BP}-value was chosen, in order to compare results with those of other studies (e.g., Bebber 1990; Bernabei and Bontadi 2012; Levanič et al. 2001) whose chronologies were used to date al-Aqsa and which used the t_{BP}-value for crossdating.

In this study, a t_{BP}-value above 5.0 is indicative of a correct cross-match, following standard practice in East Mediterranean dendrochronology (Kuniholm 2000a; Kuniholm et al. 2007; Kuniholm and Striker 1987). However, for tree-ring series and chronologies built from cedar of Lebanon, whose tree-ring growth is more responsive to local environmental conditions (thereby introducing greater 'noise into the tree-ring pattern), t_{BP}-values higher than 5.5 are indicative of a correct cross-match (see also: Chapter 5). Cross-matches with *GL* values above 50% were checked for their statistical significance (*p*-value) in TSAP. It was also required that crossdated

chronologies overlap one another by at least 50–100 years (thereby lessening the possibility of random correlation between tree-ring patterns), in order for a dendrochronological crossmatch to be considered secure. For particularly 'noisy' species like cedar of Lebanon, a longer overlap of at least 100 years or more was preferred. All statistical matches in TSAP were visually checked and verified.

Radiocarbon Wiggle-Matching

Four samples (AQS-6, 9, 14, and 18) were selected for radiocarbon wiggle-matching (Bayliss 2007; Bayliss and Tyers 2004; Bronk Ramsey et al. 2001; Galimberti et al. 2004), because they are from a decorated timber (AQS-6); form a sequence in a long chronology that does not dendrochronologically crossdate against current reference chronologies (AQS-9 and AQS-14); or are an individual sequence that had significant crossdates against reference chronologies, but required independent dating confirmation (AQS-18). Twenty decadal-length segments (three from AQS-6; six from AQS-9 and 14; and five from AQS-18) (see also: Appendix 4.1), whose relative position to one another on each sample is known from exact ring counts and dendrochronological crossdating, were dissected and sent to the Heidelberg Radiocarbon Laboratory for analysis. Decadal, rather than sub-decadal, sections were chosen for wiggle-matching, because most of the samples include periods of extremely narrow ring growth. Thus taking decadal sections allowed sufficient amounts of material to be sampled for dating while gaining adequate dating precision against a calibration curve that was also developed primarily from ^{14}C measurements of decadal tree-ring sections (Reimer et al. 2009).

The series of radiocarbon dates for each sample was wiggle-matched using OxCal 4.1 (Bronk Ramsey 2009a, 1995; Bronk Ramsey et al. 2001) and compared against the IntCal09 radiocarbon calibration curve (Reimer et al. 2009) with curve resolution set at 1 year. Each radiocarbon date is treated as dating the center-point of the dated rings (e.g., the date for rings 1001-1010 is treated as ring 1005.5). Since the wiggle-matched al-Aqsa tree-ring sequences do not dendrochronologically crossdate with one another, they were treated as independent series in a single model, in which there is no prior assumption about which sample was older/younger.

The timber species distributions (Akkemik and Yaman 2012; Schweingruber 1990), dendrochronological crossdates, and supporting historical evidence (see: Results and Discussion) all indicate that the wiggle-matched al-Aqsa timbers were imported to Jerusalem from either the north Aegean or (in some cases) possibly the northern Levant. Current available data (Manning and Kromer 2012; Manning et al. 2010) indicate that regional offsets between the radiocarbon calibration curve and the samples' radiocarbon content should be small to negligible, so no allowance was made for possible regional ^{14}C variation ($\Delta R = 0$).

Neither of the two wiggle-matched oak samples (AQS-9 and AQS-18) contains sapwood. Thus a minimum number of additional rings–based on the average number of sapwood rings for oaks in the timbers' likely area of origin–was added to the wiggle-matched date of each sample's final ring count, in order to determine a minimum felling date for the trees. Since all available dendrochronological, botanical, and historical data indicate that the oaks were imported from the Aegean, sapwood estimates were calculated using data from a multi-species group of 167 oaks growing

in northern Turkey and Greece (Griggs, pers. comm., 2012; modified from: Griggs et al. 2007, 2009). Sapwood estimates for larch are taken from Bernabei and Bontadi's data (2012) for Italian Alpine larch. Reliable sapwood estimates for the other remaining wiggle-matched and/or dendrochronologically dated cedar timbers analyzed here are not available.

Bayesian Analysis of Previous ^{14}C and Dendrochronological Data

New minimum cutting dates for the roof timbers in Lev-Yadun et al.'s (1984) cedar chronology ('AQS_cedar1') were calculated with a Bayesian analytical model in OxCal (Bayliss 2007; Bronk Ramsey 2001) and compared against the IntCal09 radiocarbon calibration curve (Reimer et al. 2009). This model uses the two reported radiocarbon dates that they obtained from samples (samples #1 and 2) that crossdate one another in the AQS_cedar1 chronology (described above). Since the dendrochronological crossdating gives a relative sequence, in which the exact number of years by which one radiocarbon date precedes the other is known, this information can be incorporated into the dating model to narrow the probability ranges of the two ^{14}C dates and calculate a more precise minimum date range for when timbers in the chronology were cut.

The exact number of rings that were extracted from the samples for each radiocarbon date in Lev-Yadun et al.'s (1984) study is not given. However, since the samples were dated using conventional counting ^{14}C, a large amount of material would have been required for analysis. Therefore three versions of the model (labelled 'a, b, and c') were created, which assumed that: a) ten rings; b) twenty rings; or c) forty rings were extracted from each sample for radiocarbon dating. This means (like the

assumptions given in the wiggle-matching model above) that the radiocarbon date obtained for each sample is treated as dating the center point of the number of rings extracted for analysis. For instance, the radiocarbon date reported for the outer rings of AQS_cedar1's sample #1 (whose final extant ring dates to relative year 202 of the chronology) is treated as dating relative year: a) 197.5, b) 192.5, or c) 182.5 in the three versions of the dating model.

The model was used to calculate probability distributions dating relative years 202, 231, and 244 in the AQS_cedar1 chronology. Relative year 202 is the outermost extant ring of sample #1; the final extant rings of many of the samples in the chronology also cluster around relative year 202 (Lev-Yadun et al. 1984: Table 1). Relative year 231 is the date of the final extant ring of the final published version of the chronology. However, Lev-Yadun et al. (1984) also report an additional sample, whose placement is less secure and whose final extant ring dates to relative year 244. Since none of the samples in this chronology had the bark or vascular cambium present, the dates calculated in this new model provide only a *terminus post quem* date range for when the timbers were cut and used in the mosque roof construction.

RESULTS

Of the 17 samples examined for the present study, one is European larch (*Larix decidua* Mill.); seven are cedar of Lebanon (*Cedrus libani* A.Rich.); and nine are oak (*Quercus* sp.). None of these species is native to Israel/Palestine, so all of the timbers were clearly imported to Jerusalem from abroad. A full list of sample metadata is given in Table 4.3, and the results are given below by species. All of the samples showed clear signs of mild to heavy decay, so the dates given below should all be

interpreted as a *terminus post quem* for the timber cutting dates, since many of the trees' outer (and inner) rings have been lost from decay as well as the timber cutting process. The new dating model of the AQS_cedar1 chronology follows the results from the more recent material.

Larch Sample

One sample (AQS-15) is a section of European larch (*Larix decidua* Mill.) with 188 rings (and one partial, unmeasured ring). The timber was clearly imported to Jerusalem, since larch does not grow in the eastern Mediterranean and is instead native to the central European Alps and Carpathian Mountains (EUFORGEN 2009) (Figure 4.3).

The AQS-15 sequence was crossdated against multiple larch reference chronologies built from forests and historical buildings in Italy (Bebber 1990; Bernabei and Bontadi, *unpublished*), Austria (Nicolussi et al. 2009), and France (Serre 1979). The sequence was also compared against historical larch chronologies from the Church of the Nativity in Bethlehem (Bernabei and Bontadi 2012); Hg. Paraskevi in Chalkis, Greece (Kuniholm et al. 2007); and St. George's Church in Piran, Slovenia (Levanič et al. 2001) (Figure 4.3).

Crossmatching is particularly strong between AQS-15 and the Church of the Nativity (Figure 4.4), Nicolussi's (2009) Austrian Alpine larch, and Bernabei and Bontadi's (2012) and Bebber's (1990) NE Italian Alps chronologies. The al-Aqsa larch overlaps and correlates extremely well with the oldest segment of Bebber's chronology (1990), which includes samples from medieval churches and buildings around Venice and the Trentino-Alto Adige region in northern Italy. Visual and

Figure 4.3. Map of the Mediterranean basin showing the forest (*green triangles*) and historical (*yellow squares*) reference chronologies used to date samples, and sites listed in the historical record that shipped larch timber to Jerusalem for the mosque. The current species distribution of *Larix decidua* is shaded in green.

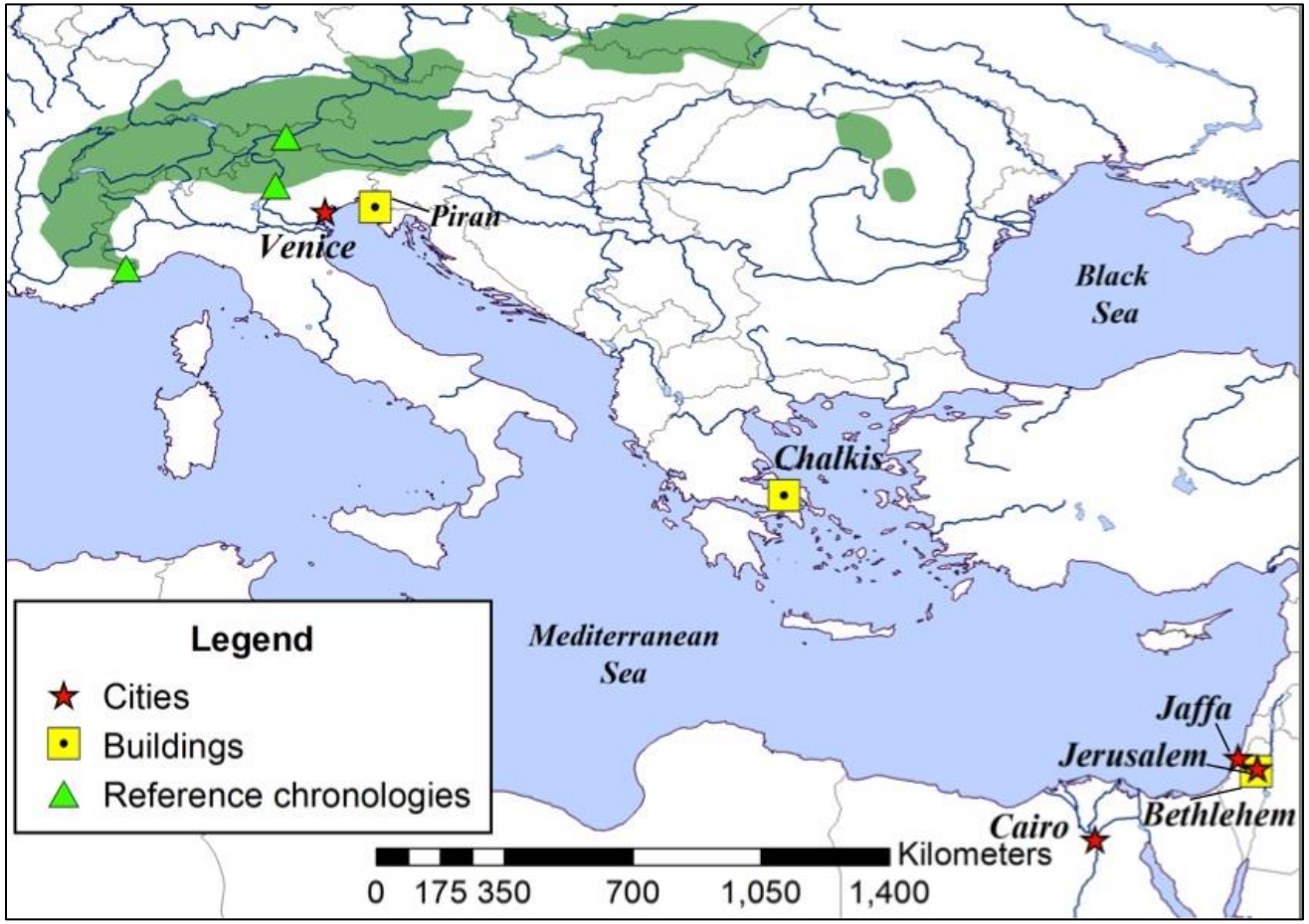

Table 4.3. Metadata for the sampled timbers from al-Aqsa.

Sample	Species	Shape	Dimensions (cm)	Pith present?	# of measured rings
AQS-1	*Cedrus libani*	unknown (core)	unknown[a]	No	Not measured (<50 rings)
AQS-2	*Quercus* section *Cerris*	squared beam from whole section	23x 20.5[b]	Yes	99
AQS-3	*Populus* sp.	squared beam from whole section	20.2x 19.7[b]	Yes	Not measured (unsuitable species)
AQS-4	*Cedrus libani*	unknown	6.5x 5[a]	No	59
AQS-6	*Cedrus libani*	squared beam from whole section	107x 22x 22	Yes	54
AQS-7	*Quercus* sect. *Quercus*	squared beam from whole section	71x 18.5x 18	Yes	88
AQS-8	*Cedrus libani*	half section	30.5x 24.1x 15.2	Yes	79
AQS-9	*Quercus* sect. *Cerris*	squared beam from whole section	149x 17x 21	No	106
AQS-10	*Quercus* sect. *Quercus*	squared beam from whole section	111x 13.2x 24	Yes	117
AQS-11	*Cedrus libani*	whole section	*l*=126, *d*= 19	Yes	59
AQS-12	*Quercus* sect. *Quercus*	squared beam from half section	142x 18.2x 21.8	Near	110
AQS-13	*Cedrus libani*	whole section	148x 20x 19.5	Yes	80
AQS-14	*Cedrus libani*	third section	*l*=160, *d*= 15	No	173
AQS-15	*Larix decidua*	squared beam from half section	194x 16.1x 24.6	Yes	188
AQS-16	*Cedrus libani*	three-quarters section	164x 13x 15.7	Near	83
AQS-17	*Quercus* sect. *Quercus*	squared beam from quarter section	153x 14.6x 18.5	No	64
AQS-18	*Quercus* sect. *Quercus*	beam straightened on one side	125x 15.1x 20.4	No	178
AQS-19	*Quercus* sect. *Cerris*	squared beam from half section	105x 14.2x 21	Near	78
AQS-20	*Quercus* sect. *Quercus*	squared beam from two-thirds section	150x 18x 15	Yes	63

[a]Sampled from a timber with unknown dimensions
[b]Section sampled from a timber with unknown length

Table 4.4. Crossdating statistics for sample AQS-15 at 1082–1269 AD against the *Larix decidua* reference chronologies. Significant crossdates are marked in bold. t_{BP}= Baillie-Pilcher *t*-value; t_H= Hollstein *t*-value; *GL*= *Gleichläufigkeit* values and their associated *p*-values.

Reference chronology	t_{BP}	t_H	*GL*	Overlap (years)	Author
Bethlehem, Church of the Nativity	**13.7**	**13.7**	**72*****	**188**	Bernabei and Bontadi, 2012
NE Italian Alps	**10.0**	**9.0**	**71*****	**188**	Bebber, 1990, *corrected*[a]
Tyrol, Austrian Alps	**8.3**	**7.4**	**64*****	**188**	Nicolussi et al., 2009
Greece, Chalkis, Hg. Paraskevi	**7.9**	**7.2**	**64*****	**141**	Kuniholm et al., 2007
NE Italian Alps	**7.0**	**7.0**	**69*****	**188**	Bernabei and Bontadi, *unpublished*
French Alps, Les Mervailles	**5.1**	**5.3**	**59****	**188**	Serre, 1979
Slovenia, Piran, St. George's Church	4.2	3.8	61**	183	Levanič et al., 2001

[a] The chronology was adjusted by removing two excessive ring-width measurements from the published chronology (*see text below*).
'*' = statistical significance of *GL* at p< 0.001; '**' = p< 0.01; '*' = p< 0.05**

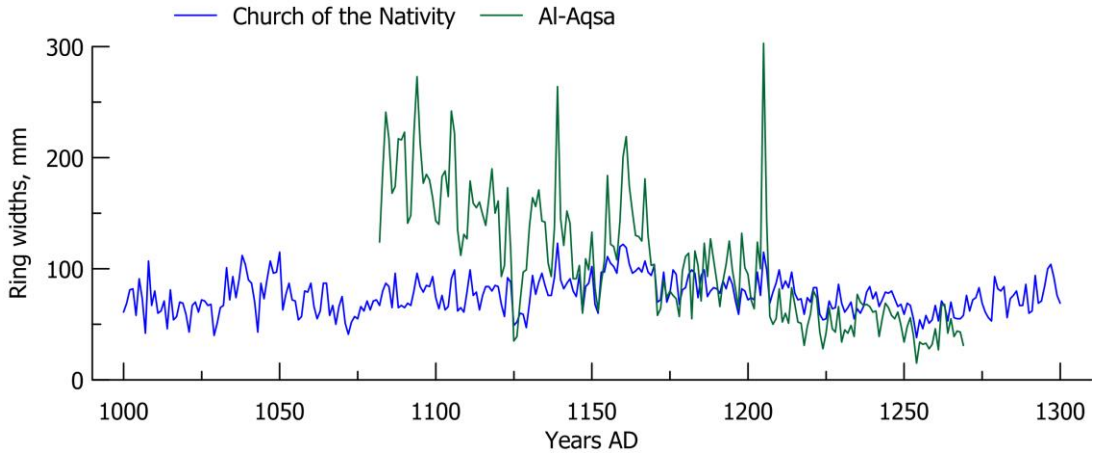

Figure 4.4. Plot showing the crossmatch between the al-Aqsa (*green*) and Church of the Nativity (*blue*) raw larch chronologies.

statistical correlation between AQS-15 and Bebber's chronology is improved if two excessive rings are removed from the poorly replicated part of the Bebber chronology between 1370 and 1390, following the recommendations of Nicolussi (1995) and Nola and Motta (1996).

Good teleconnections exist for larch in the Alpine region, and often larch chronologies from sites that are geographically distant but at similar altitudes have greater correlation than those from neighboring sites at different altitudes (Bebber 1990; Levanič et al. 2001; Nola and Motta 1996). Thus the strong correlation between al-Aqsa and the Church of the Nativity, NE Italian Alps, and Austrian Alpine larch chronologies suggests that the wood originated from a similar location or altitude.

Cedar Samples

Six of the samples–plus the two additional samples previously analyzed by Kuniholm (*unpublished data*) and Lev-Yadun et al. (1984)–are cedar of Lebanon (*Cedrus libani* A. Rich). Cedar of Lebanon is not native to Israel/Palestine; its forests grow today in fragmentary stands extending across the Taurus Mountains of southern Turkey down through the coastal mountains of Cilicia, Syria, and Lebanon (Boydak 2003; Hajar et al. 2010; Quézel and Médail 2003). A subspecies, *Cedrus libani* subsp. *brevifolia* (Hook.f.) Meikle, grows in a small area in western Cyprus (Ciesla 2004). Therefore this material was imported to Jerusalem from one of these areas.

Of the eight cedar samples, only two (AQS-14 and 16) crossdate with one another in a 173-year chronology (plus one partial, unmeasured ring). Both timbers were cut from trees with narrow, sensitive rings. This chronology ('AQS_cedar2')

does not yield any significant dendrochronological crossdates with available East Mediterranean cedar reference chronologies from forest or historical sites.

In order to provide an absolute date range for the AQS_cedar2, four decadal sections were sampled from the chronology's longest and most recent sequence, AQS-14, for ^{14}C wiggle-matching. An initial run of the model in OxCal produced two outliers (rings 1020–1029 and 11100–1109) using Bronk Ramsey's General Outlier model (2009b) that had poor agreement with the other modeled dates (see: Appendices 4.1 and 4.2). Since these two outliers are likely the result of laboratory instrument error, these samples were re-measured. A new model was run in OxCal using the new dates and excluding the outliers. The resulting probability distributions, which are calculated in terms of their fit on the IntCal09 radiocarbon calibration curve (Reimer et al. 2009), are shown in Figure 4.5. OxCal places the date of the chronology's final extant ring (which serves as a *terminus post quem* for the tree's cutting date) at 1229–1241 AD (10.6% probability) or 1250–1278 AD (84.8% probability) (Figure 4.6). This dating model produces an analysis with a good OxCal agreement index ($A_{model}68>60$) and no outliers using Bronk Ramsey's General Outlier model (2009b).

There are several possible reasons why the remaining cedar sections do not crossdate with one another or with existing reference chronologies. It is possible that these sequences predate the time period covered by current Mediterranean cedar chronologies (1370 AD to present), or that the timbers were cut from a forest (or forests) whose regional chronological signal is not well-represented by the current cedar tree-ring data. These remaining undated al-Aqsa cedar sections are also generally short sequences (<100 rings) and often rounded sections containing juvenile

rings (meaning that they were either cut from young trees, or the outermost rings were removed during the timber shaping process). Juvenile ring sequences in cedar generally have a low Estimated Population Signal (EPS) (Wigley et al. 1984), meaning that their combined ring sequences are noisy and do not contain a strong enough common tree-ring growth signal to represent a whole population or crossdate securely. Many also have complacent ring sequences (where there is little year-to-year ring-width variation), suggesting they were cut from trees growing in an environment with favorable growth conditions.

Sample AQS-6 was also cut from the center of a tree stem and had a relatively short ring sequence (*n*= 55, plus one partial, unmeasured ring) with complacent, juvenile rings. However, since it was taken from a timber carved with Umayyad or Abbasid-era decorations, three decadal sections were sampled for ^{14}C wiggle-matching, in order to determine a more precise absolute date for the timber.

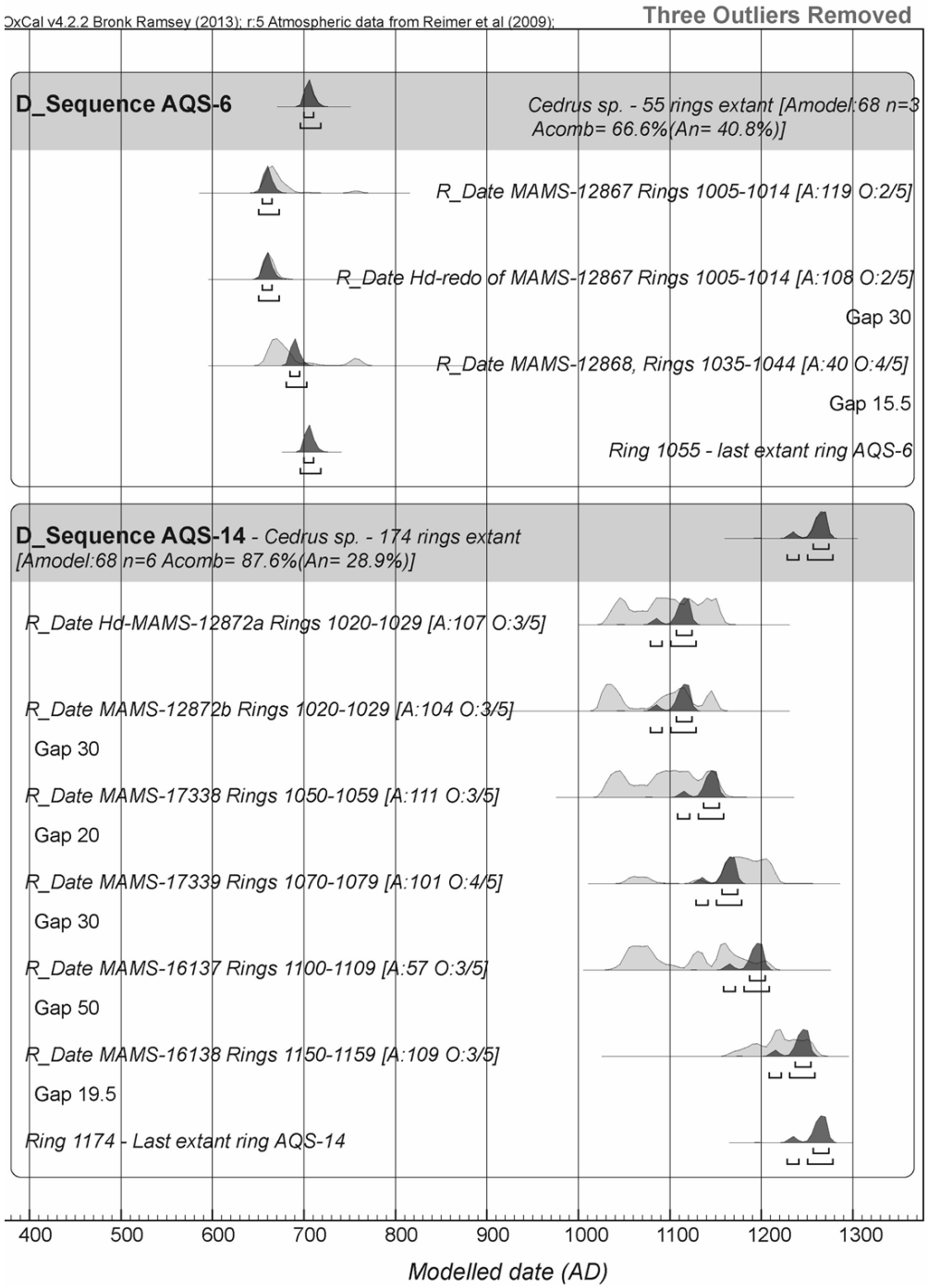

Figure 4.5. Modeled probability distributions of the calibrated ^{14}C data for AQS-6 and AQS-14. A values are the OxCal agreement values for the individual samples; a satisfactory value is ≥60. O values are the posterior values from the General Outlier Model (Bronk Ramsey, 2009b); values >5 are outliers. These models exclude one outlier from AQS-6 and two outliers from AQS-14.

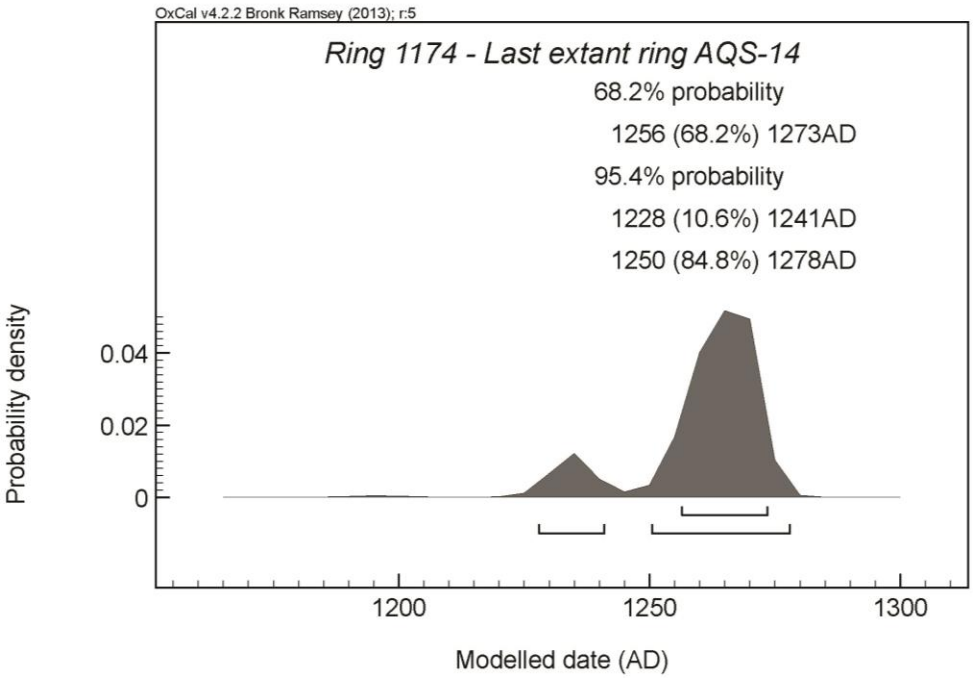

Figure 4.6. The modeled probability distribution for the date of the last extant tree-ring on sample AQS-14 at 68.2% and 95.4% probabilities, which provides a minimum date range for when the timber was cut.

An initial run of the model in OxCal produced one outlier (rings 1025–1034) using Bronk Ramsey's General Outlier model (2009b) that had poor agreement with the other modeled dates (see: Appendices 4.1 and 4.2). If this outlier is removed and a new model run, including a new ^{14}C date that was re-run in the Heidelberg Laboratory (Figure 4.5), this produces a dating model with good overall agreement ($A_{model}68>60$) and no outliers using the General Outlier model (Bronk Ramsey 2009b). OxCal places the final extant ring for AQS-6 at 696–718 AD at 95.4% probability (Figure 4.7). Since the sample does not have bark, and additional rings were likely removed from the sample due to decay, this date also serves as a *terminus post quem* for when the tree was cut.

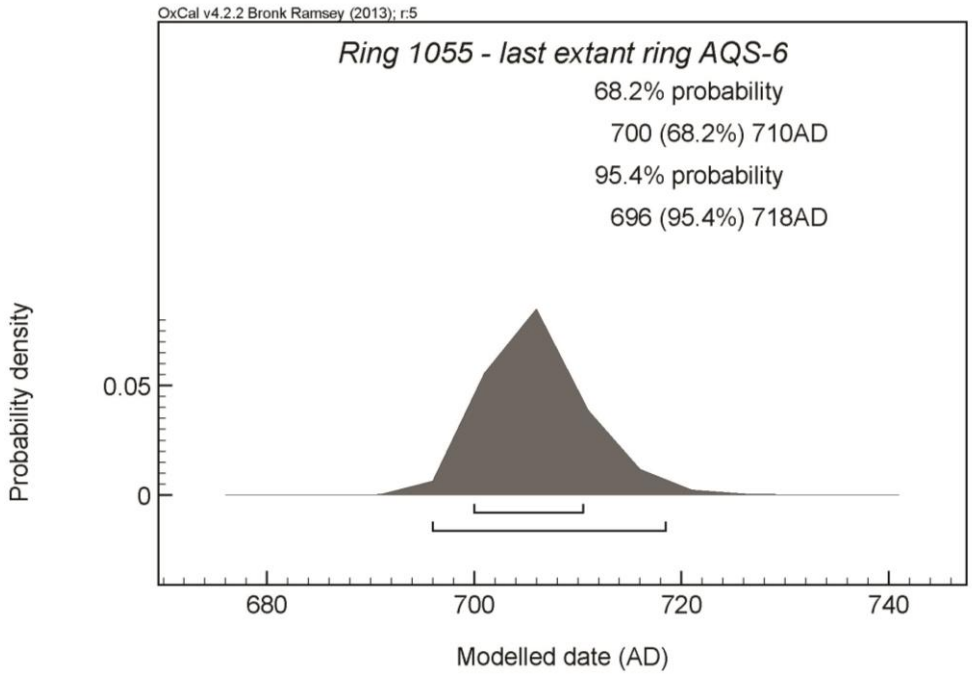

Figure 4.7. The modeled probability distribution for the date of the last extant tree-ring on sample AQS-6 at 68.2% and 95.4% probabilities, which provide a minimum date range for when the timber was cut.

Oak Samples

Identifying European and Mediterranean oak wood at the species level is not possible based on wood anatomy alone; thus wood identifications are given only at section level, following the recommendations of Akkemik and Yaman (2012) and Schweingruber (1990). Of the eight oak samples, three (including Kuniholm's previously analyzed sample) were cut from oaks (*Quercus*) belonging to the section *Cerris* (red oaks), which in Europe and the Mediterranean includes the common species *Quercus cerris* L. Six samples were cut from oaks belonging to the section *Quercus* (white oaks), which in Europe and the Mediterranean includes the common species *Quercus petraea* (Mattuschka) Liebl., *Quercus pubescens* Willd., *Quercus robur* L., and *Quercus frainetto* L.

The oak species listed above are not native to Israel/Palestine, with the exception of a small, scattered population of *Quercus cerris* growing on Mt. Hermon in the very north (Zohary 1973). The combined species distributions of oaks in section *Quercus* stretches from the Black Sea and southwest coasts of Anatolia westward throughout most of Europe and the British Isles (Akkemik and Yaman 2012; Ducousso and Bordacs 2003). The species distributions of oaks in section *Cerris* extend from south central and southeastern Europe, through Anatolia and Levant to the southernmost extension of the Lebanon/Anti-Lebanon mountain chain (Akkemik and Yaman 2012; Quézel and Médail 2003; Zohary 1973). Thus the al-Aqsa oak timbers must have been imported to Jerusalem.

None of the al-Aqsa oak samples crossdate with one another. It is possible that this is because at least some of the samples belong to different time periods, or are from different geographic areas with distinct tree-ring chronological signals. Samples AQS-7 and 10, in particular, have prominent injuries, which greatly distort ring growth and create idiosyncratic growth. Most of the timbers were cut from juvenile trees with ring counts less than 100. Both timber shaping and more recent decay have also removed or destroyed additional rings on both the outsides and insides of the samples.

Sample AQS-18 is an oak (*Quercus* section *Quercus*), which, based on the lack of both pith and sapwood, and ring curvature, was cut from the intermediate to outer part of the tree stem. The sample's 178-year ring sequence yields significant crossdates against Griggs et al.'s (2007) northwest Turkey oak reference chronology, which excludes a long historical chronology from Bekdemir on the Black Sea further

to the east in north-central Turkey (Kuniholm 2000). AQS-18 also has moderately good statistical correlation with an oak timber from the substructure of an Ottoman well (Bostan Kuyusu) found during the recent Marmaray excavations in Istanbul (Kuniholm et al., *in press*; Pearson et al. 2012). Additionally, AQS-18 has moderately good statistical correlation with Griggs et al.'s North Greece oak reference chronology (2007) (Table 4.5). The crossmatches consistently place the AQS-18 sequence at 1550–1727 AD; the sample has one additional, unmeasured partial ring on its outermost edge, which, when added, dates the last extant ring to 1728 AD.

Since AQS-18 is a single sample sequence, which has significant, but not extremely significant (t_{BP} >7.0) correlation with only one reference chronology, four decadal sections were sampled for ^{14}C wiggle-matching to provide independent dating confirmation. The modeled probability distributions of the decadal sections from AQS-18 are shown in terms of their calculated placements on the IntCal09 calibration curve (Reimer et al. 2009) in Figure 4.8. OxCal places the final extant ring for AQS-18 at 1721–1729 AD at 95.4% probability (Figure 4.9), which supports the 1727 AD dendrochronological date.

There is no sapwood present on the sample. According to Griggs' (pers. comm., 2012; modified from: Griggs 2009; Griggs et al. 2007) north Aegean oak sapwood data (which includes the reference chronologies used to date AQS-18), oaks in the 176–225 year age class have, on average, 25.32 ±6.122 sapwood rings. Since AQS-18 is from a tree that was at least 178 years old (plus an additional unknown number of rings from the center of the tree that were removed during the timber shaping process), the sample fits comfortably within this age class. If the average

number of sapwood rings is added to the date of the last extant ring, this places the tree's minimum cutting date at 1753 AD (1747–1759 AD within 1σ). Even if it is assumed that several heartwood rings are missing and one uses the sapwood estimate for the >226 year age class (which has an average of 27.24 ± 7 rings), this would alter results by only three years at most.

Table 4.5. Crossdating statistics for sample AQS-18 at 1550–1727 AD against the oak reference chronologies. Significant crossdates are marked in bold. t_{BP}= Baillie-Pilcher *t*-value; t_H= Hollstein *t*-value; *GL*= *Gleichläufigkeit* values and their associated *p*-values.

Reference chronology	t_{BP}	t_H	*GL*	Overlap (years)	Author
Northwest Turkish oak (without Bekdemir)	**5.8**	**4.5**	**68*** **	**178**	Griggs et al., 2007
Istanbul, Marmaray, Bostan Kuyusu	4.6	5.2	64***	149	Kuniholm et al., *forthcoming*
North Turkish oak (with Bekdemir)	4.6	4.0	62***	178	Griggs et al., 2007
North Greece oak	3.5	2.8	59*	178	Griggs et al., 2007
Bekdemir	2.7	2.2	60**	178	Kuniholm, 2000a

'*' = statistical significance of *GL* at p< 0.001; '**' = p< 0.01; '*' = p< 0.05**

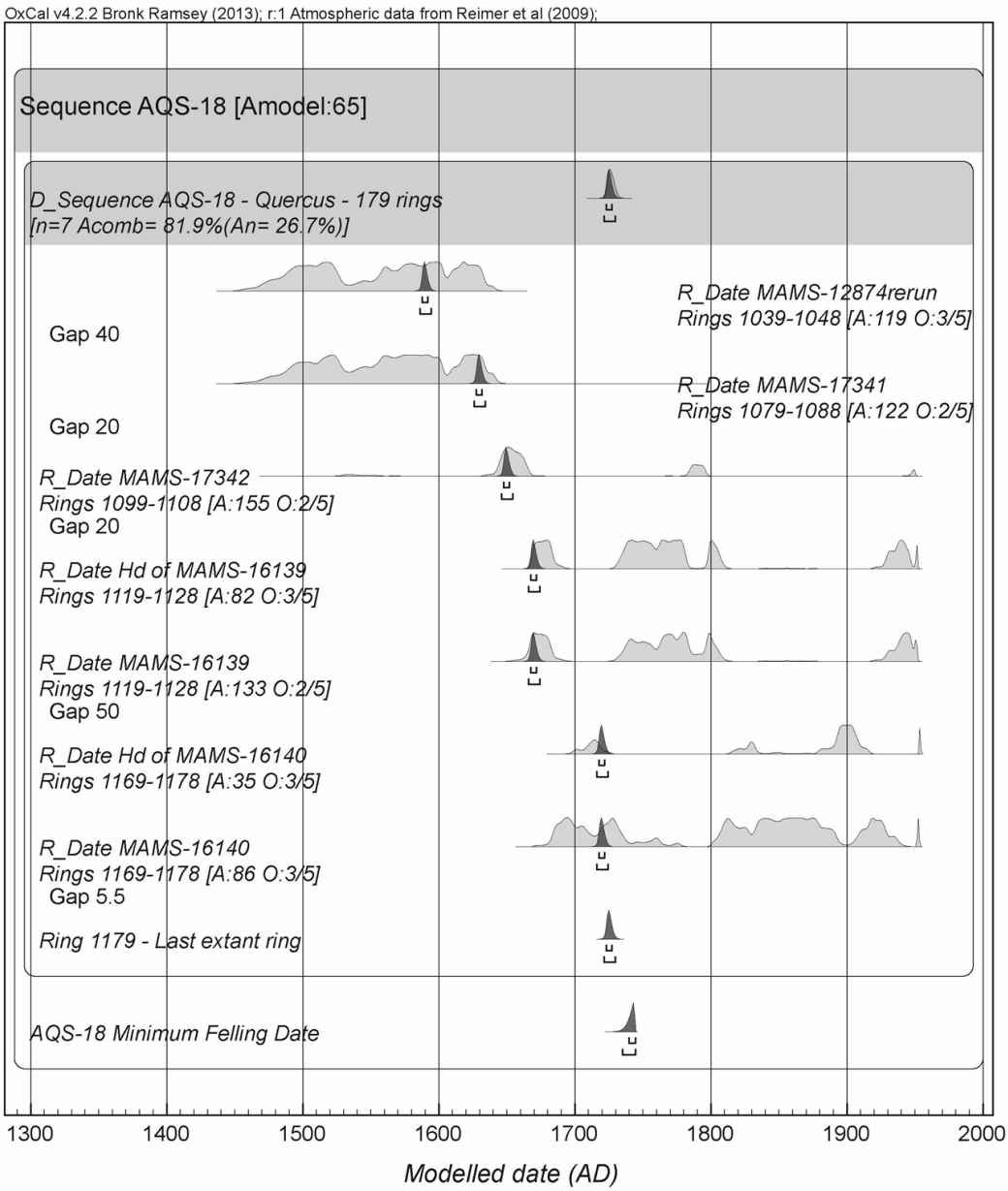

Figure 4.8. Modeled probability distributions of the calibrated ^{14}C data in OxCal for the AQS-18. The A values are the OxCal agreement values for the individual samples; a satisfactory value is ≥60. The O values are the posterior values from the General Outlier Model (Bronk Ramsey, 2009b); values >5 are outliers. The model has good overall agreement ($A_{model}65>60$) and no flagged outliers, indicating that it is robust.

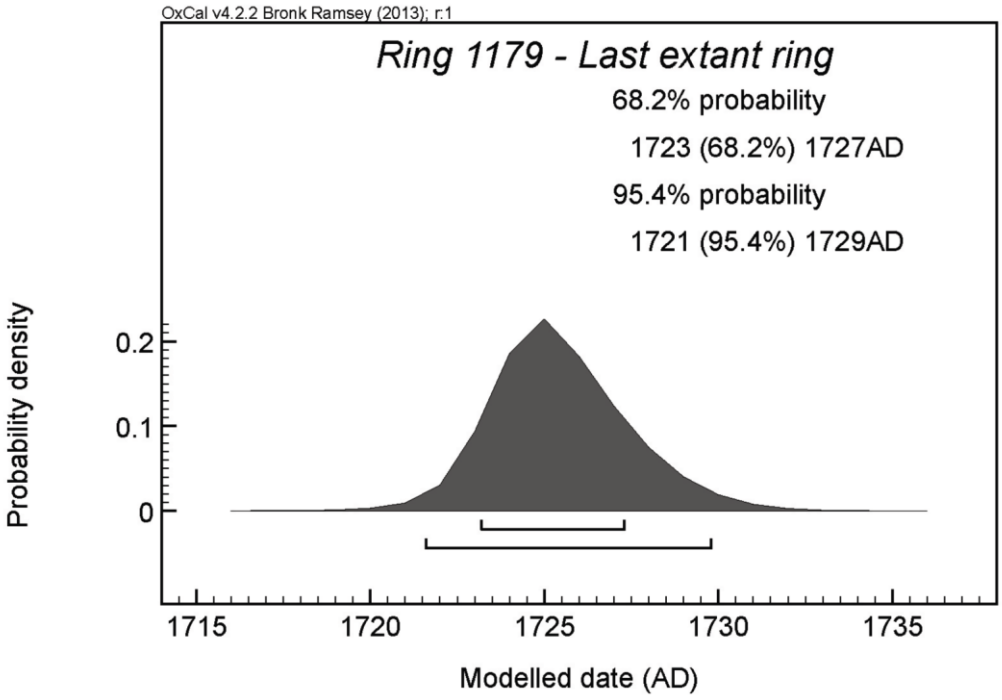

Figure 4.9. The modeled probability distribution for the date of the last extant tree-ring on sample AQS-18 at 68.2% and 95.4% probabilities (not including the estimated number of missing sapwood rings).

Sample AQS-9, which was cut from an oak in *Quercus* section *Cerris*, has 106 rings (plus one partial, unmeasured ring). The sample sequence did not yield any significant dendrochronological crossdates. Since it is the longest section *Cerris* timber sampled, four decadal sections were taken from AQS-9 for ^{14}C wiggle-matching, in order to determine if the timber's cutting date was contemporaneous with that of AQS-18.

The modeled probability ranges of the decadal sections used in the wiggle-match, which are calculated in terms of their fit on the IntCal09 radiocarbon calibration curve (Reimer et al. 2009), are given in Figure 4.10. Their calculated placements are shown in terms of their fit on the IntCal09 radiocarbon calibration curve (Reimer et al. 2009) in Figure 4.11. OxCal places the sample's last extant ring

at 1736–1744 AD at 95.4% probability (Figure 4.12A). Since AQS-9 has at least 107 rings, plus an unknown number of additional rings on the outer edge of the sample and a smaller number of rings missing from the inner part of the sample that were lost to decay (likely <10, based on ring curvature), it was most likely cut from a tree in Griggs' 75–125 years age class for north Aegean oak sapwood, which have an average of 20.13 ± 4.43 sapwood rings (pers. comm., modified from Griggs 2009; Griggs et al. 2007). Thus, if the partial unmeasured ring and the average sapwood estimate is added to the dating model with the ^{14}C data from the wiggle-match, OxCal calculates an estimated minimum cutting date of 1751–1764 AD at 95.4% probability (Figure 4.12B).

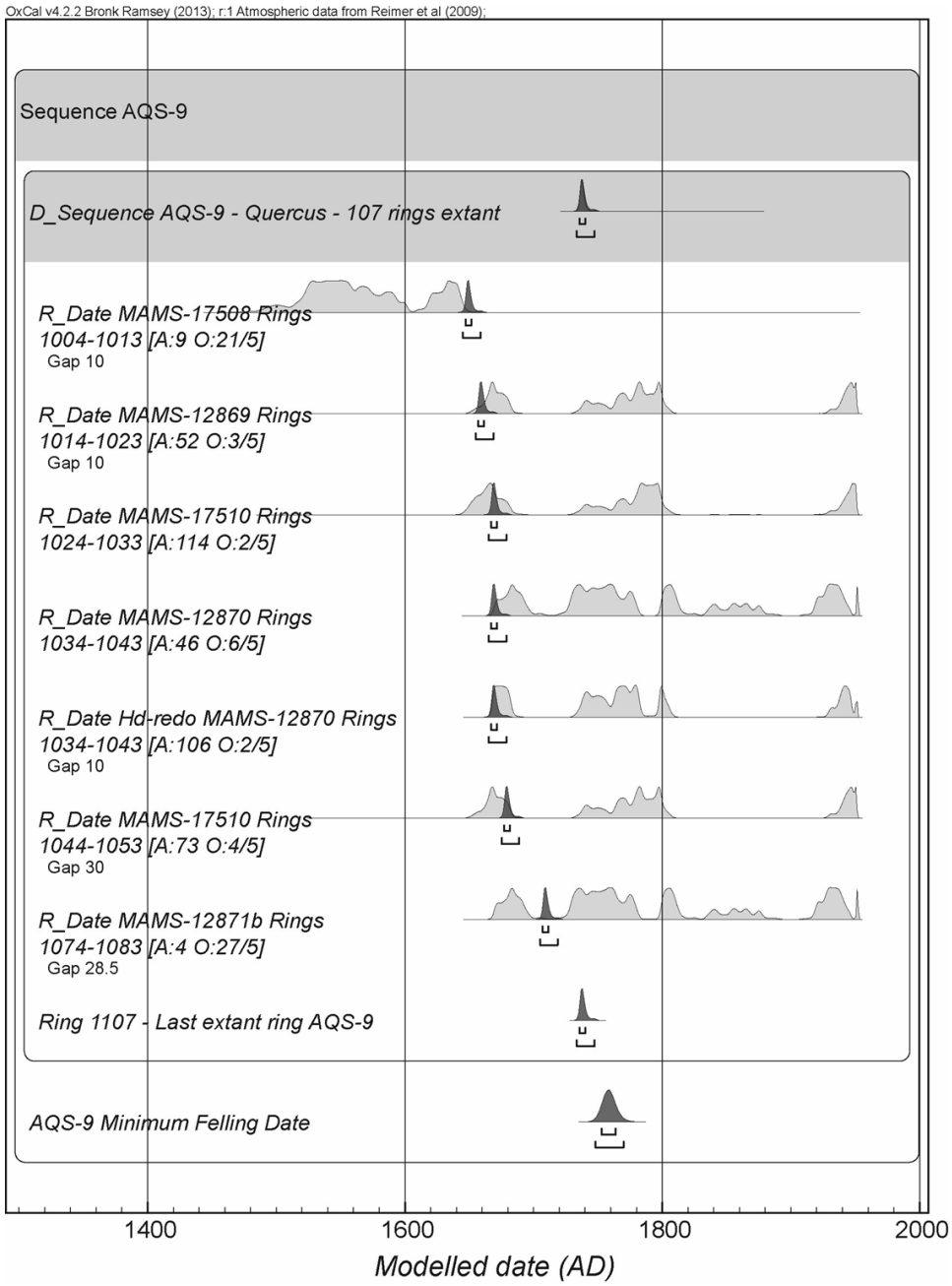

Figure 4.10. Modeled probability distributions of the calibrated ^{14}C data in OxCal for AQS-9. The A values are the OxCal agreement values for the individual samples; a satisfactory value is ≥60. The O values are the posterior values from the General Outlier Model (Bronk Ramsey, 2009b); values >5 are outliers.

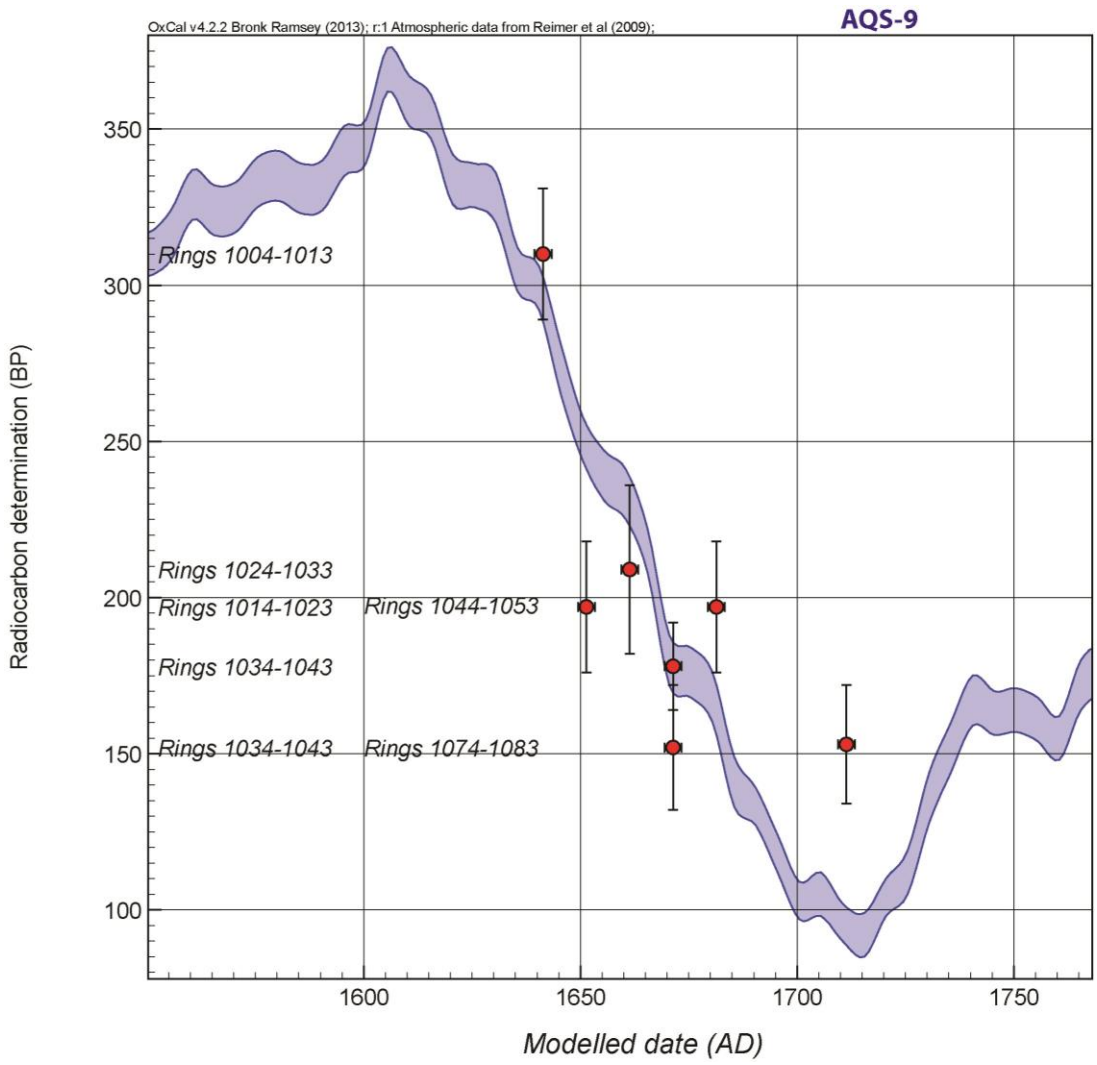

Figure 4.11. The placement of the ^{14}C data in the AQS-9 wiggle-match from Figure 4.10 against the IntCal09 (Reimer et al. 2009) radiocarbon calibration curve (±1σ). The ^{14}C data are shown as the μ±σ of the modeled ranges in Figure 4.10 on the *x* axis (calendar date scale), and as the ^{14}C age BP (±1σ) on the *y* (^{14}C years) axis.

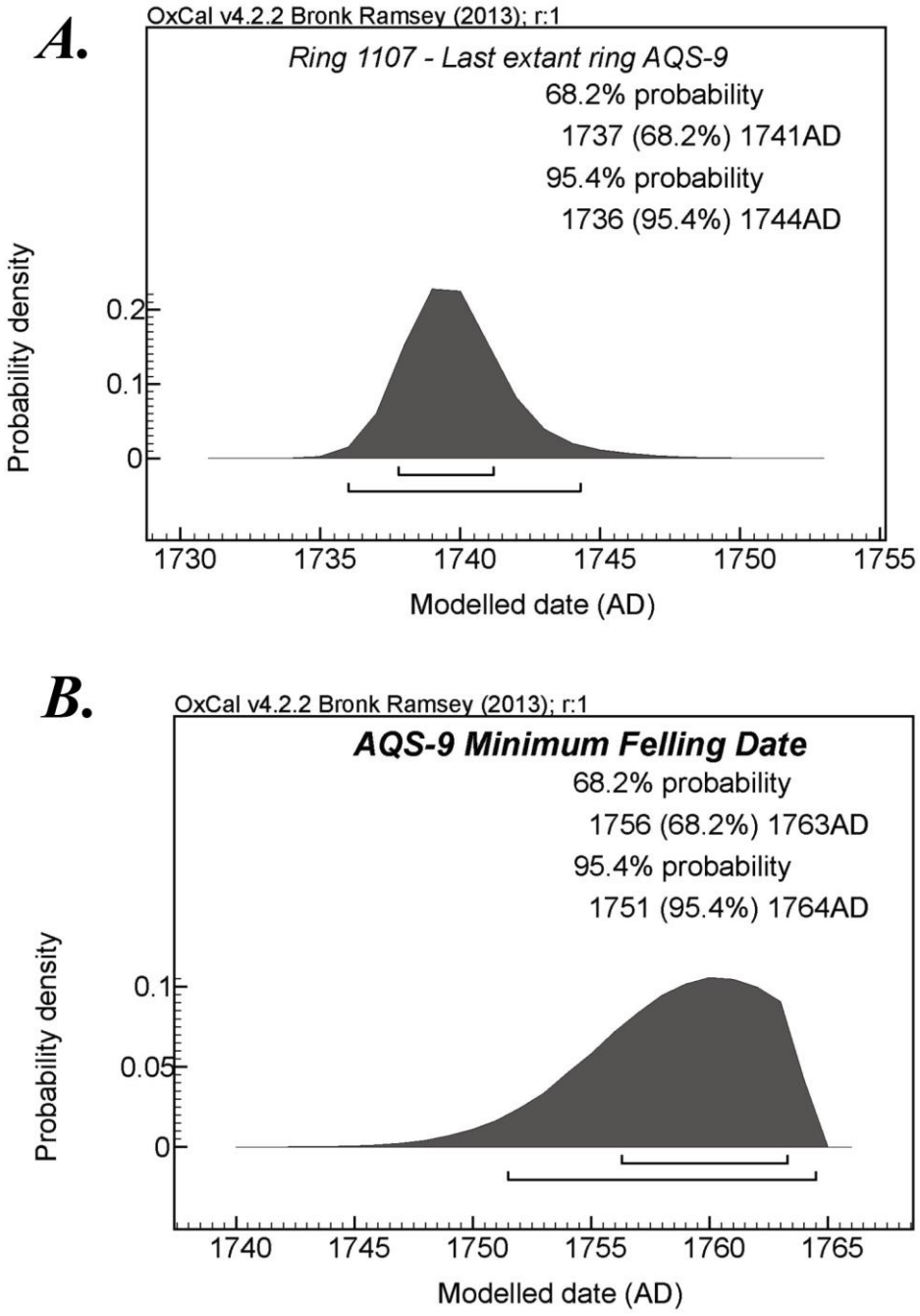

Figure 4.12. The modeled probability distribution for the date of the last extant tree-ring on sample AQS-9 at 68.2% and 95.4% probabilities (A); and the modeled probability distribution for the minimum date when the tree was felled when the sapwood estimate is included in the dating model (B).

Re-analysis of the AQS_cedar1 chronology

The three versions of the modeled probability distributions (labeled 'a, b, c' for models assuming 10, 20, and 40 extracted rings, respectively) for the ^{14}C dates in Lev-Yadun et al.'s cedar chronology ('AQS_cedar1') in terms of their fit against the IntCal09 calibration curve are shown in Figure 4.13. The calculated date ranges for relative years 202, 231, and 244 of the chronology (labeled '1, 2, and 3,' respectively) at 68.2% and 95.4% probabilities for each model (a, b, or c) are given in Table 4.6.

Table 4.6. Date ranges calculated by the Bayesian model in OxCal at 68.2% and 95.4% probabilities for: (1) relative year 202; (2) relative year 231; and (3) relative year 244 of Lev-Yadun et al.'s (1984) 'AQS_cedar1' chronology. Three different models were run to calculate each date, assuming that: (a) 10 rings; (b) 20 rings; and (c) 40 rings were extracted from each sample for ^{14}C dating. Model 2a (which dates the final extant ring of the 231-year chronology and assumes that 10 rings were extracted from each of the samples for ^{14}C dating) is the preferred model. It is shaded in gray and the date ranges are marked in bold.

Model	Calibrated age AD 68.2%		Calibrated age AD 95.4%	
1a	753	835	634	856
1b	750	830	629	851
1c	740	821	620	841
2a	783	867	661	885
2b	**777**	**861**	**657**	**880**
2c	766	850	648	870
3a	795	880	675	897
3b	791	875	670	893
3c	778	863	660	883

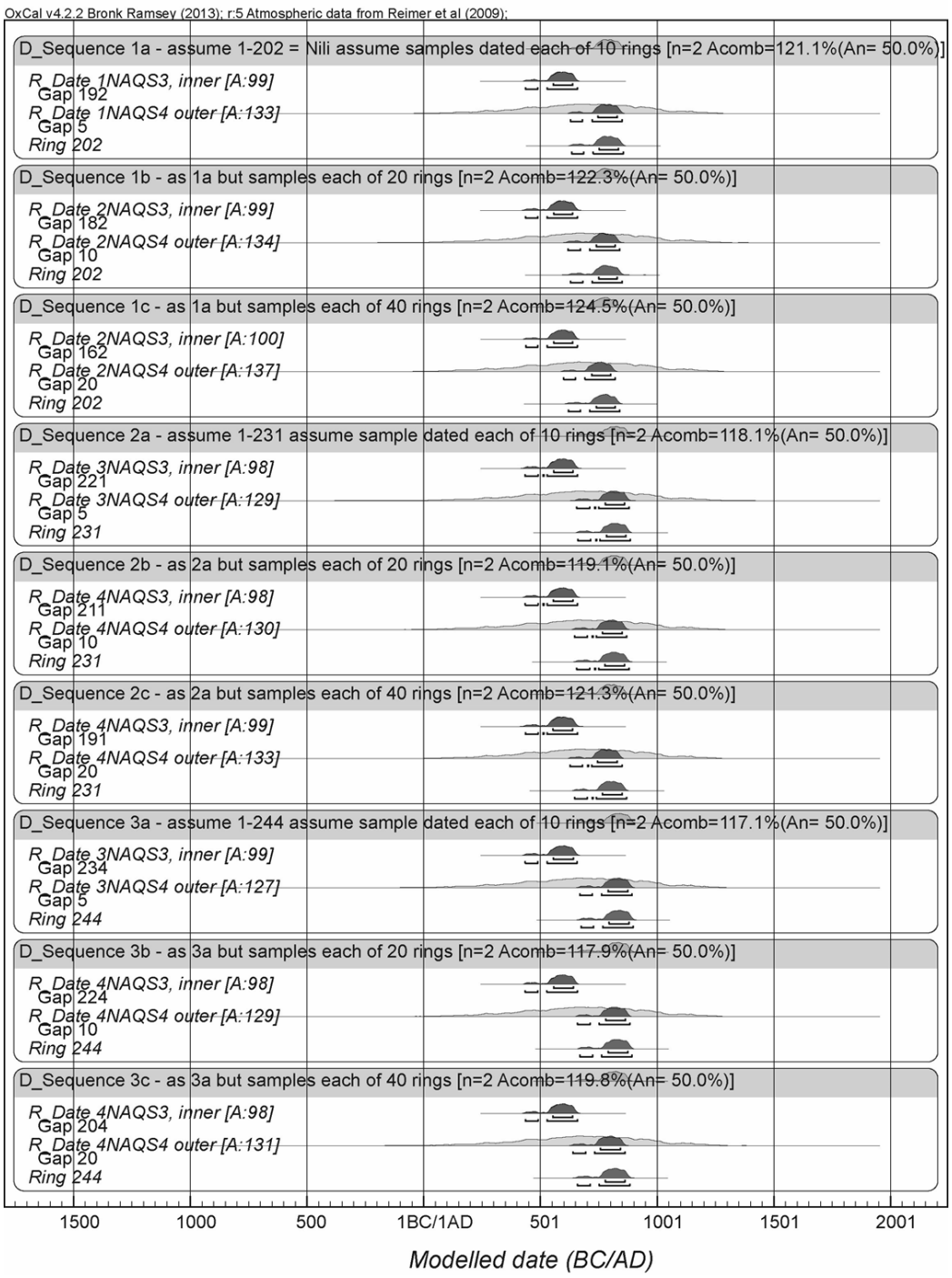

Figure 4.13. Modeled probability ranges for the ^{14}C dates from Lev-Yadun et al.'s (1984) AQS_cedar1 chronology samples and the calculated dates for: (1) relative year 202; (2) relative year 231; and (3) relative year 244 in the chronology. Three different models were run to calculate each date, assuming that: (a) 10 rings; (b) 20 rings; and (c) 40 rings were extracted from each sample for ^{14}C dating.

The calculated date ranges for these models are not as precise as those for the more recently analyzed wiggle-matched material analyzed in this study, largely because of the large error ranges of the older radiocarbon dates for the samples in AQS_cedar1 (particularly for sample #2). However, this model does provide a more precise *terminus post quem* for the timber cutting dates than single, unmodeled ^{14}C dates. The model calculates a more recent *terminus post quem* date range than those calculated and reported in Lev-Yadun (1992) or Liphschitz et al. (1997). In fact, according to the new dating model, the last extant ring of the 231-year chronology dates no earlier than 648 AD, even if it is assumed that an extremely large number of rings (i.e., 40) were extracted for analysis.

DISCUSSION

Abbasid (750–969 AD), Umayyad (661–750 AD), and Pre-Islamic Timber

The earliest reported dates for timbers from al-Aqsa are those from the studies of Lev-Yadun et al. (1984) and Liphschitz et al. (1997), which include material that they dated to the Iron Age, as well as the Hellenistic, Roman, and Byzantine Periods, all of which pre-date the mosque's late 7th century AD construction. They suggested that the timbers in al-Aqsa, including those comprising the AQS_cedar1 chronology, were taken from the ruins of older buildings, like the Byzantine Nea Maria church, the Roman Temple of Aphrodite, or the Herodian Temple, in and around the Temple Mount (Lev-Yadun 1992; Lev-Yadun et al. 1984; Liphschitz et al. 1997). This argument has been repeated more recently (Reuven 2013), who argued that the al-Aqsa timbers include material from the Herodian Temple (or structures around it),

based on comparisons that Reuven made between the measurements of the decorated timbers from Mr. Ehrlich's collection and the Herodian Temple.

Lev-Yadun et al.'s (1984) dates for the earliest timbers from al-Aqsa–the "Iron Age" oak and also the oldest cypress timber dating between the thirteenth through fourth centuries BC (95.4% probability)–should be viewed with skepticism. Timbers from the Iron Age and even earlier periods have been preserved in the archaeological record in the Near East[1]. However, in these cases, the timbers were preserved, because they had become carbonized (since charcoal is relatively inert and therefore resistant to decay) (see: samples discussed in Liphschitz 2007: chapters 5 and 6), were buried underwater in an anoxic environment (see: samples listed in Lev-Yadun 2007), or were in a dry, desert environment and often sealed under debris in caves or tels (e.g., Gale et al. 2000; Liphschitz and Lev-Yadun 1989; Werker 1988).

Lev-Yadun (2007) has argued that the al-Aqsa timbers were preserved in this type of dry environment, but there are critical differences between environmental conditions in the al-Aqsa building and sites that have preserved dry archaeological wood, like Masada (Liphschitz and Lev-Yadun 1989), Nahal Hemar (Werker 1988), the Egyptian desert (Gale et al. 2000), or even the Gordion tumulus (Blanchette et al. 1991; Kuniholm 1978). Although the al-Aqsa building is roofed, and the timbers are in part shielded from rain and temperature fluctuations, the timbers were not sealed in a low-oxygen, dry air environment. Jerusalem is in a less arid climate zone than the

[1] A full list of wood remains in the Near East from the Iron Age and earlier periods is far too extensive to list here. For a partial list of archaeological wood remains found in the southern Levant and Egypt, see: Gale et al. 2000, Lev-Yadun 2008, and Liphschitz 2007.

Dead Sea Rift, Negev, and Egyptian desert (see: Chapters 1 and 2), where these other well-preserved archaeological dry timbers have been found (with the exception of the Gordion wood, which was in a sealed tumulus). Thus the al-Aqsa timbers were exposed to greater humidity (and changes in humidity) than these steppe and desert environments, thereby promoting their decay. It is thus extremely unlikely that any of the al-Aqsa timbers were reused from the time of the First Jewish Temple.

It is more likely that the Iron Age dates from al-Aqsa are the result of laboratory error (probably contamination or poor or pre-modern sample pretreatment) and have a much more recent date. Since the samples were also dated using traditional ^{14}C gas-counting and have extremely large, imprecise date ranges, they should be re-dated using wiggle-matching techniques with sapwood estimates to test their accuracy and improve precision. The tree-ring sequence for Lev-Yadun et al.'s (1984) oak sample should also be re-examined against Aegean and European oak reference chronologies to determine if it can be dated dendrochronologically.

There is evidence that al-Aqsa's builders re-used timbers from earlier buildings to some extent. Two decorated cypress beams in the Rockefeller Museum, which Creswell (1958), Hamilton (1949), and Liphschitz et al. (1997) analyzed, have Greek inscriptions, one of which, Avi Yonah notes (1942), mentions the patriarch of Jerusalem and therefore dates the inscription (and gives a *terminus ante quem* for the beam's cutting) of 524–552 AD. A second beam has a Greek inscription dated epigraphically also to the 6th century AD (Schwabe 1949), and a third beam has a rosette decoration (later covered upon its reuse) similar to those on beams in the Church of the Nativity, which Rosen-Ayalon (1989) dates stylistically to the early to

mid-6th century AD. As both Hamilton (1949) and Liphschitz et al. (1997) also note, many of the beams display old joints and decorations, indicating re-use (although, of course, some of this reworking likely occurred during the Abbasid Period and later, to accommodate changes in the mosque's dimensions).

It is important to note, though, that of those three timbers which, based on their inscriptions and decorations, Liphschitz et al. (1997) identify as early to mid-6th century AD (and which give a *terminus ante quem* for the timber cutting dates), the outer rings of all three yield ^{14}C dates that range (depending on the probable date ranges) from 300–900 years prior to the 6th century AD (Table 4.2). While it is of course possible that these Byzantine timbers were also re-used from earlier periods, it should be noted that all but one of the decorated timbers that Liphschitz et al. (1997) analyzed contain the innermost part (and therefore the least recent rings) of the tree stems. Much of the outermost part of the tree stem was likely removed when the panels were cut; even more tree-rings were likely removed when they were carved; and still more were removed if the timbers were repurposed and re-cut at some point during the mosque's many restorations.

Additionally, both cedar and cypress can be long-lived and reach ages of 600 and 900 years, respectively (Kuniholm 2000b; Ważny, *unpublished data*), so the inner rings of very heavily-shaped timbers, like the decorated al-Aqsa panels, may yield dates that greatly precede the year when the timbers were actually cut. Even the panel not cut from the tree's interior, whose outer rings likely date from AD 256–527 (95.4% probability) (Table 4.2), has slow-growing, narrow rings, so the timber cutting and shaping process could easily have removed a few centuries of tree-ring growth.

Thus, a late 7th–early 8th century AD date for Liphschitz et al.'s samples 53.2 and 53.12 (Table 4.2), which matches their Umayyad-style carvings and the time of al-Aqsa's initial construction, is not out of the question.

Based on the new dating model produced in this study, it is also likely that the roof timbers in Lev-Yadun et al.'s (1984) AQS_cedar1 chronology were cut for al-Aqsa's initial construction, an Abbasid restoration, or (at the very earliest) were re-used from part of a previous Rashidun Period structure. If we use the preferred dating model (Model 2a), which assumes that only 10 rings were extracted for radiocarbon from each of samples #1 and #2 from the 'AQS_cedar1' chronology, the last extant ring of the chronology dates to 657–885 AD at 95.4% probability. If the dating placement of the sample whose last ring dates to relative year 244 of 'AQS_cedar1' is correct, then the date of the chronology's last extant ring (using Model 3b) is even later at 670–895 AD (95.4% probability). Even if it is assumed that some of the timbers (which cluster around relative year 202 in the chronology) were cut as part of an earlier building phase, Model 1a still places their minimum cutting date at 634–856 AD at 95.4% probability. All of these date ranges fall within the early Islamic Period (during either the Rashidun, Umayyad, or the Abbasid caliphates), and not the Byzantine Period.

Furthermore, since bark was not present on any of these samples, these date ranges provide only a *terminus post quem* for the actual cutting date(s) of the timber. Many of the cedar beams contain the pith and innermost rings of the tree trunk, were squared, and showed signs of insect damage, meaning that the tree's outermost rings have been removed (Lev-Yadun et al. 1984). Even if the earliest dating estimates

from the OxCal model are used, only 40–70 small rings would need to have been removed from the samples during the timber cutting and shaping process, in order for the actual cutting date to have occurred during the mosque's original Umayyad construction in the late 7th century AD.

Lev-Yadun et al.'s (1984) cedar chronology also has overall high series intercorrelation, and the sample sequences share a period of narrow ring growth in the middle of the chronology, which, as Lev-Yadun (1992) argues, is likely the result of a local disturbance or forest stand dynamics. The final rings of the individual series in the chronology also cluster together within a period of fifty years (with most of the group clustering even more closely). This evidence all suggests that the timbers were culled from the same forest region (and in the case of some sequences, likely even from the same tree stem) around the same time, making the scenario where the timbers were pulled from several different buildings in Jerusalem (whose timbers would have been cut at different times, possibly using material from different forests) even less plausible.

The wiggle-matched cedar timber (AQS-6) from the present study is also likely from the early period of al-Aqsa's building history. ^{14}C wiggle-matching gives sample AQS-6 a likely minimum cutting date of 696–718 AD at 95.4% probability, meaning that the timber dates at least to the Umayyad Period, and certainly is not from the Herodian Temple, as Reuven has suggested (2013). If the timber's minimum cutting date is at the earlier part of this date range, and very few of the tree's outer rings were removed during the timber shaping and carving process, then it is possible that the AQS-6 is from al-Aqsa's early 8th century AD construction under the Umayyad Caliph

al-Walid. However, since the sample was cut from the center of the tree, is heavily shaped and carved, and the wood decayed, it is more likely that a larger number of the tree's outer rings were removed and the timber is from a later Abbasid renovation, like al-Mansur's in 771 AD, or al-Mahdi's in 780 AD (Hamilton 1949).

Since it was not possible to obtain a dendrochronological crossdate for AQS 6, and the measurements from the AQS_cedar 1 chronology are not available for analysis, it is not currently possible to use dendroprovenancing techniques to determine the region from which the cedar timbers were imported. Lev-Yadun (1992) proposed that the early al-Aqsa cedars were imported from Lebanon, because Lebanon was closer (making transportation easier and cheaper) and was the traditional source of timber imported to Israel and Egypt in antiquity (Kuniholm et al. 2007; Meiggs 1982; Mikesell 1969). This is certainly possible, since 7th and 8th century documents do indicate that the Lebanese forests were used for construction projects (Mikesell 1969).

However, the caliphs did not limit themselves to exploiting forests only in Lebanon. Mikesell (1969) notes that when the Abbasid capital was moved to Samarra in 836 AD, wood imported from "Antioch and all the littoral of Syria" was used as building material, showing that Early Islamic Period timber sources extended far beyond the Lebanese mountains. In addition to the consideration of proximity, forests that could produce an adequate *volume* of timber for a building project were needed, and since the mosque was an important religious site and cedar a valued timber, the caliphs may have been willing to search for timber at greater distances from

Jerusalem. Therefore the cedar forests beyond Lebanon should not be discounted as a potential source until more conclusive scientific evidence is available.

Mamluk Period: 1250-1517 AD

The larch sample AQS-15 has a minimum cutting date of 1270 AD, meaning that the timber was procured when the Mamluk sultanate, based in Cairo, ruled Jerusalem. There are two recorded renovations to the mosque during the late 13th–early 14th century to which this timber might belong: in 1280–1290 AD, Sultan Al-Mansur Qalawun ordered the partial reconstruction of the mosque roof (Burgoyne 1987); and in 1327–1328 AD, Sultan Al-Nasir Muhammad repaired the mosque's southeastern wall, installed new windows, and restored the dome (Burgoyne 1987; Rivoira 1918).

Based on wood anatomical evidence, the latter restoration date is more likely. As evidenced by the pith on the timber's radial section, the AQS-15 timber was cut from the interior of its tree trunk, which was heavily shaped during the cutting process, removing the tree stem's outermost rings, including the entire sapwood region. According to Bernabei and Bontadi (2012), mature larch trees (which AQS-15 most certainly was, since it was at least 191 years old, when all of the measured and unmeasured rings are included) have on average 30–50 sapwood rings. If this minimum number of missing rings is added, this gives the timber a minimum cutting date of 1300–1320 AD (plus an unknown number of missing heartwood rings), postdating Al-Mansur Qalawun's restoration but corresponding well with that of Al-Nasir Muhammad. It is also significant that the Al-Nasir Muhammad restoration occurred in the southeastern part of the mosque, from which this timber was collected,

and none of the other reported Mamluk renovations to the mosque later in the 14th century included the mosque's southern side (Burgoyne 1987).

The strong dendrochronological crossdates between AQS-15 and the larch reference chronologies from the eastern Alps indicate that the timber came from a high altitude site in this region. From historical records, it is known that the Mamluk sultans were close trading partners with the Republic of Venice, which at the time dominated maritime trade in the eastern Mediterranean, Black Sea, and beyond in the Far East (Howard 1991, 2007). Venetian traders maintained trading bases in Alexandria, Cairo, and several other Mediterranean cities (including in Crete, Cyprus, Constantinople, and Jaffa) (Howard 2007, 1991; Tolkowsky 1924), spoke Arabic, and traded both with local merchants and the Mamluk sultans. Trade relations between the Venetians and Mamluks were particularly strong during Al-Nasir Muhammad's reign (Howard 2007).

Timber was one of the valuable items that the Venetians traded (Howard 2007). Larch was considered a high-quality building timber in central Europe, because the wood is durable and resistant to decay (Levanič et al. 2001). It is significant that the historical buildings whose chronologies correlate strongly with the AQS-15 sequence all are connected to the Venetians. Hg. Paraskevi is a Frankish church whose larch timbers include clear Venetian-style woodwork and imagery (Kuniholm et al. 2007). Several historical sources (Bacci et al. 2012) record how Venetian carpenters and wood-carvers, under the sponsorship of the Duke of Burgundy, and with the approval of the Pope and Mamluk sultan (Bernabei and Bontadi 2012), brought timber from the Alps to the Church of the Nativity and repaired its roof in 1479 AD. It is therefore

entirely plausible–especially given the close Mamluk-Venetian relationship at the time–that Sultan Al-Nasir Muhammad would have similarly requested Venetian timber and perhaps even Venetian carpenters to help renovate al-Aqsa. Correlation between the Church of the Nativity and al-Aqsa chronologies is so strong, that it is likely that their timbers even came from the same forest.

The Papacy greatly disapproved of the close Venetian-Mamluk trade and was particularly interested in ending Venetian export of timber and metals to the Mamluk Empire. From 1320–1344 AD, Pope John XXII instituted a ban on all trade with Muslims, and by 1326 AD, Venetian traders were forced to accept this order, or face excommunication (Howard 2007). Venetian tradesmen could have violated this ban to provide the sultan with the timber for al-Aqsa or traded indirectly through Crete or Cyprus (and there is historical evidence that this happened) (Howard 2007), although providing timber to the sultan for such a high profile building would have been difficult to conceal. It is perhaps more likely, then, that the timber was ordered, shipped, and cut just prior to the papal embargo, especially given that additional time for transport, seasoning, and shaping the timber would be needed before it could be used for the building project.

The historical context of the AQS-14 and 16 cedars is more ambiguous. ^{14}C wiggle-matching places their most likely minimum cutting dates at 1250–1278 AD at 84.8% probability, or 1229–1241 AD at 10.6% probability, although since neither sample has bark preserved, and both show signs of shaping and decay, it is likely that many of the tree's outer rings were removed. Unfortunately, unlike the oak and larch samples, a clear estimate of missing outer rings cannot be given, so the number of

missing rings is unknown. The AQS-16 sample begins near the pith at the center of the tree, and both AQS-14 and 16 were sampled from slow-growing trees, meaning that even a small amount of timber removed could contain decades (or even possibly a century or more) of wood.

Based on the provided minimum cutting dates and available historical records, these timbers may belong to Al-Mansur Qalawan's 1280 AD restoration, or (like AQS-15) Al-Nasir Muhammad's 1327–1328 AD restoration. Like the earlier Umayyad and Abbasid-era cedars, it is not possible to determine conclusively the timbers' exact provenance(s) beyond cedar's natural distribution in the Mediterranean, without additional dendrochronological, scientific, or historical information. AQS-14 and 16 were cut from slow-growing trees, indicating that they were growing in an environment with less favorable growing conditions, and unlike the cedars that Lev-Yadun analyzed (1992), these timbers are neither complacent, nor are they lacking traumatic resin ducts that show signs of mechanical injury.

Historical records do not give any explicit mention about the Mamluks importing cedar to either Egypt or Jerusalem. The Mamluk sultans controlled the Levantine coastal mountain forests in which cedar grows and from which they could have exported cedar (Hajar et al. 2010; Quézel and Médail, 2003), including the forest around Mt. Lebanon and those further north in the an-Nusayriyah and Amanus Mountains (Lapidus 1967; Mikesell 1969).

It is less likely that the cedar would have come from the Taurus in southern Anatolia, since southeastern Anatolia was under the control of the Mamluks' enemies, the Mongol Ilkhanate (1256–1265 AD) and the Armenian kingdom of Cilicia (1198–

1375 AD) (Amitai 2007). However, despite these hostilities, there are records of trade in wood from eastern Anatolia and Cilicia, and the 1323 AD peace treaty between Sultan al-Nasir Muhammad and the Mongols improved trade relations between the Mamluks and Anatolia (Amitai 2007). Additionally, both the Bey of Menteşe, who controlled the southwestern Taurus, and the Kingdom of Cyprus (which was also hostile to the Mamluks) traded with the Venetians (Fleet 2013). Therefore, there is also the possibility that the Mamluks could have procured Anatolian cedars through their Venetian trading partners.

Lev-Yadun et al. (1984) also dated an oak timber (identified as *Quercus cerris*) with ^{14}C that was potentially imported to Jerusalem during the Mamluk Period. However, the radiocarbon date obtained for the sample has a very wide probability distribution (AD 975–1444 at 95.4% probability) (Table 4.1), and they do not report the presence or absence of sapwood for this sample. Therefore the timber could equally be part of the mosque's 1187 AD Ayyubid renovation by Saladin, or Suleyman's renovations to the mosque after the Ottomans conquered Jerusalem in 1517 AD (Heyd 1960).

Ottoman Period: 1517–1921

^{14}C wiggle-matching and dendrochronological dating place the cutting dates of oak sequence AQS-18 in the mid-18th century and AQS-9 in the mid-18th to late 19th century, during the period of Ottoman rule in Jerusalem. Ottoman archival sources detail restorations to al-Aqsa during the 18th century in the following four years: 1720–21, 1742, 1753–54, and 1780 (Göyünç 1983; St. Laurent and Riedlmayer 1993). The dendrochronological crossdate (which the ^{14}C wiggle-matching supports), plus the

north Aegean sapwood estimate, places the AQS-18 cutting date at 1747–1759 AD, so it is most likely that the timber was cut for the 1753–54 restoration, particularly since the outer edge of the timber is only minimally shaped and was therefore probably cut close to the heartwood-sapwood boundary. Meanwhile, ^{14}C wiggle-matching and the north Aegean sapwood estimate places the most likely minimum cutting date for AQS-9 between 1751–1764 (95.4% probability), so this timber is likely part of the 1780 restoration, especially since this timber was more heavily shaped and more heartwood rings likely removed along with the sapwood.

Lev-Yadun et al. (1984) also report another oak sample (also *Quercus cerris*) from al-Aqsa that likely dates to the Ottoman Period (Table 4.1), but additional metadata for the sample, such as sapwood, is not available, nor are the ring-width measurements published and available to compare with the oaks studied here. Like the other samples from their study, there is a wide date range that covers the entire period of Ottoman rule (plus part of the Mamluk and post-Ottoman Periods). Additionally, the center of the section (and therefore the younger tree-rings) was sampled for radiocarbon, but the authors did not give the number of rings in the sample, making estimates of the tree's cutting date even less precise.

Detailed records of the import, transport, and processing of timber for the 18th century restorations to al-Aqsa are available in the Ottoman archives (Göyünç 1983). The governor of the Jerusalem province and other local Ottoman administrative and religious officials (including the *kadı* and the *müfti*) assessed what repairs were needed for the mosque and then sent a detailed request to the sultan in Istanbul. The lumber was procured from forests near İzmit and along the western Black Sea coast near

İğneada, Ağva, Akçasar, Çakraz, and İnebolu (Figure 4.14). The lumber was brought to İzmit and then to the Imperial Dockyards in Istanbul, along with pieces of glass, wire, and marble procured from the İzmir region. The lumber and supplies, along with parts for assembling ox-carts, were then shipped to Jaffa. The ox-carts were assembled in Jaffa, and the lumber was then transported to Jerusalem in the supply wagons. A master foreman sent from Istanbul oversaw the construction, and once the renovations were completed, a report was sent to Istanbul, and unused materials were inventoried and placed in storage. According to Göyünç (1983), the procedures for obtaining supplies and carrying out repairs are nearly identical for each restoration.

The significant crossdates between AQS-18, Griggs' (2006) northwest Turkish oak chronology, and the Bostan Kuyusu sequence from the Marmaray excavations (Kuniholm et al., *in press*) fit well with the historical information about the Ottoman al-Aqsa timbers' forest sources. The chronologies that comprise the northwest Turkey chronology during the 1550–1727 AD timeframe are from historical buildings in Üveçik (Çanakkale province) and the Bilecik province, and the timbers from both these buildings (Kuniholm 2000a), as well as that from the Bostan Kuyusu in Istanbul, likely came from forests in the Marmara (which includes İzmit) and western Black Sea regions. In contrast, the crossmatch between AQS-18 and Kuniholm's (2000a) long oak chronology from the wooden mosque at Bekdemir, which is further to the east on the Black Sea, has only moderate correlation. This gives further evidence that the AQS-18 timber came from western Turkey.

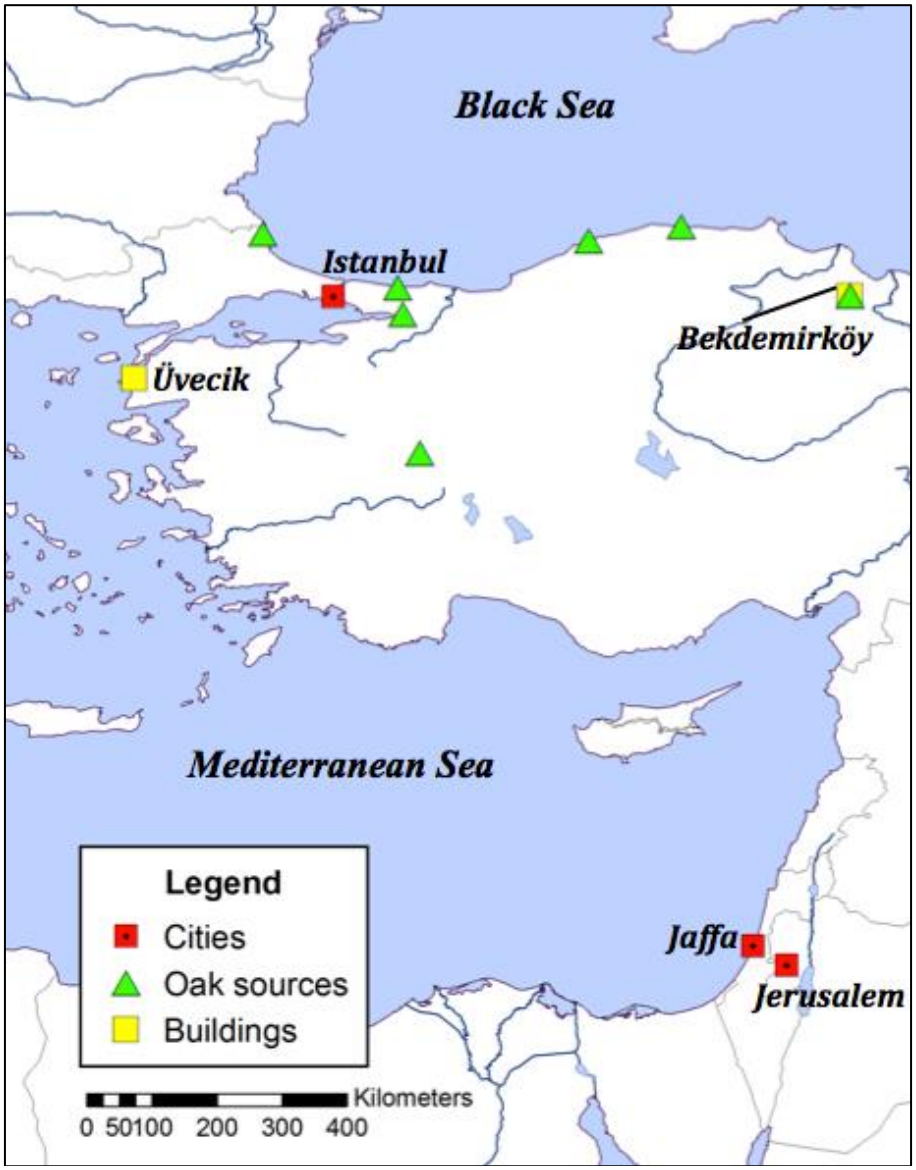

Figure 4.14. Map of the eastern Mediterranean showing the oak forests (*green triangles*) that supplied timbers for al-Aqsa via the Imperial dockyards in Istanbul. Sample AQS-18's tree-ring sequence had low correlation with Kuniholm's (2000a) oak chronology from the mosque at Bekdemirköy (*yellow*) and instead had good correlation with Griggs et al.'s (2007) Black Sea oak chronology, which included forest chronologies from northwest Turkey and historical chronologies like that from Üvecik (*yellow*) in Çanakkale province. Therefore AQS-18 likely came from one of the more western forest locations shown on the map here.

Since sample AQS-9 did not crossdate with any of the north Aegean oak chronologies, it is not possible to give a more definite provenance to the timber beyond the natural distribution of *Quercus* section *Cerris* using dendrochronological evidence. Since the timber was probably part of the 1780 restorations, it also very likely came from one of the areas on the Black Sea coast or western Turkey named in the Ottoman archives. The lack of significant dendrochronological crossdates may indicate that the AQS-9 timber is from a forest whose chronological signal is not well-represented by the current reference chronologies. Oaks generally have good teleconnections and are able to crossdate over extensive distances in the north Aegean (Griggs 2006; Griggs et al. 2009, 2007; Kuniholm and Striker 1987). However, the 18th century AD is a period where sample replication in the Aegean oak reference chronologies is low (Griggs et al. 2007; Griggs 2006), so there is greater possibility of more localized variations in climate, environment, or anthropogenic disturbance (which differ from the AQS-9 sequence or the other, undated oak sequences from al-Aqsa) influencing the reference chronology's overall signal.

It is also unlikely that samples AQS-18 and AQS-9, despite being roughly contemporaneous, do not crossdate simply because they were cut from different oak species. Studies in both the Aegean (e.g., Griggs 2006; Griggs et al. 2009, 2007; Kuniholm and Striker 1987; Ważny 2009) and Europe (Cedro 2007; Cherubini et al. 2003; Haneca et al. 2009; Ważny 2009; Ważny et al. 2011) have demonstrated that oaks crossdate well across species (including between oaks in sections *Quercus* and *Cerris*). The relatively short overlap between AQS-9 and 18, combined with the fact

that both are individual sequences (rather than an average chronology that reduces localized ring-width variation), is the more likely cause.

Table 4.7. Overview of dated timber samples from al-Aqsa mosque and the likely restoration to which they belong. Minimum date estimates include unmeasured extant rings and sapwood estimates. For all samples, there is also an unknown number of additional years ('UNY') that were removed from the timbers and that must be added to the minimum date.

Sample/ chronology	Dating technique	Tree species	Minimum Date	Time period	Notes
AQS-6	^{14}C wiggle-matching	*Cedrus libani*	696–718 AD +UNY (95.4%)	Umayyad/ Abbasid	likely from the mosque's construction
AQS_cedar 1	^{14}C wiggle-matching/ dendro-chronology	*Cedrus libani*	657–880 AD +UNY (95.4%)	Umayyad/ Abbasid	measured by Lev-Yadun et al. (1984) and modeled/re-calculated for this study; likely from the mosque's construction, or the 771 or 780 AD restorations (more likely)
AQS_cedar 2	^{14}C wiggle-matching/ dendro-chronology	*Cedrus libani*	1229–1241 AD +UNY (10.6%); 1250–1278 AD +UNY (84.8%)	Mamluk	likely from the 1280 or 1370 AD restoration
AQS-15	dendro-chronology	*Larix decidua*	1300–1320 AD +UNY	Mamluk	Alpine provenance; likely from the 1327 AD restoration
AQS-18	^{14}C wiggle-matching/ dendro-chronology	*Quercus* section *Quercus*	1747–1759 AD +UNY	Ottoman	western Anatolia provenance; likely from the 1753–54 AD restoration
AQS-9	^{14}C wiggle-matching	*Quercus* section *Cerris*	1751–1764 AD +UNY	Ottoman	likely from the 1753–54 or 1780 AD restoration

CONCLUSIONS

Dendrochronological, ^{14}C wiggle-matching, and botanical analysis of the al-Aqsa roof timbers, along with information from historical records, reveals a complex history of renovation and long-distance timber trade to Jerusalem spanning over 1,000 years since the mosque's initial construction (Table 4.7). Al-Aqsa is therefore an architectural palimpsest, in which old timbers were replaced with new material, or timbers were reworked, re-cut, and even redecorated to accommodate larger changes to the mosque's dimensions or function. Reconstructing this history requires high-precision dates using dendrochronological or (when needed) ^{14}C wiggle-matching methods, and careful interpretation of this data that also considers available botanical, art historical, and textual information. In particular, the possibility and number of likely outer rings removed from the building's timbers and wooden panels must be considered when interpreting their dendrochronological and ^{14}C-derived dates.

Although some of the wood in al-Aqsa was likely re-used from earlier Byzantine and Early Islamic materials, particularly the decorated panels and boards (Liphschitz et al. 1997), re-examination of the earlier timber dating studies (e.g., Lev-Yadun 1992; Lev-Yadun et al. 1984; Liphschitz et al. 1997) indicates that the earliest cedar and cypress timbers preserved from al-Aqsa mosque were more likely cut during the late 7th–early 8th century AD by the Umayyads for the mosque's construction. Additional decorated cedar, like that analyzed from new material in the present study, and also most likely Lev-Yadun et al.'s (1984) undecorated cedar roof timbers, were added to the mosque in the late 8th century AD under the Abbasid caliphate. The remainder of the dated timbers from the present study was cut for later renovations during the

Mamluk and Ottoman Periods, and demonstrates, as St. Laurent and Riedlmayer (1993) also note, that active upkeep to the mosque continued during these periods.

Lev-Yadun et al.'s (1984) 'Iron Age' dates for timbers from al-Aqsa most likely derive from contamination or poor or pre-modern sample pretreatment methods. Both these timbers, as well as timber in their cedar chronology, should be re-tested using the ^{14}C wiggle-matching techniques employed in this study to date the material more precisely and accurately. These same timbers should also be compared to the current European and eastern Mediterranean reference chronologies, to determine if dendrochronologically-derived dates and provenances can be found. Similarly, the longer tree-ring sequences of the decorated panels that Liphschitz et al. (1997) analyzed should be measured (likely using minimally destructive to non-destructive tree-ring measurement techniques, such as *in situ* measurement or scanning) to determine if the boards were cut from the same tree or forest region, and also if they can be dendrochronologically dated and provenanced.

Most of the timbers analyzed here and in earlier studies were cut from imported tree species (e.g., *Cedrus libani*, *Larix decidua*, and deciduous *Quercus* sp.). Only the *Platanus* sp., *Cupressus sempervirens*, and *Populus* sp. timbers may have been cut from native forests, since these species grow in Israel/Palestine (Zohary 1962). With dendroprovenancing techniques and historical records, a more exact origin of the larch and oak timbers can be determined, revealing that al-Aqsa's renovators accessed long-distance timber trading networks to import wood from not only Anatolia and the eastern Mediterranean, but also the Italian Alps. While the cedars' forest source(s) cannot be more precisely provenanced at this time, development of new cedar

reference chronologies that extend beyond their current limits of 1370 AD in Anatolia (Kuniholm 2000b) and 1382 AD in Lebanon (Touchan et al. 2005) may eventually provide a more precise, dendrochronologically-derived date and provenance.

Transporting the oak and larch timbers from Anatolia and Italy to Jaffa and then inland to Jerusalem was neither an easy nor an inexpensive task. Timbers had to be brought to port (usually by floating logs downriver) and then shipped across the Mediterranean to Jaffa. From there, the wood had to be pulled in wagons, either by teams of oxen (Göyünç 1983) or camels (Bacci et al. 2012), to Jerusalem. This required considerable labor, since the trek from Jaffa to Jerusalem required pulling several tons of lumber for 60 kilometers on an uphill gradient of about 750 meters (Cuinet 1896). The wood itself was also clearly a valuable item, no doubt, in large part because the area around Jerusalem lacked tall, straight timber for monumental buildings (Liphschitz and Biger 1991; Meiggs 1982). This is evident from the high degree of governmental control over timber importation (Howard 2007; Lapidus 1967; Mikesell 1969) and available records of monetary sums paid for the mosque's timbers (Göyünç 1983).

The amount of time, labor, and expenditure invested in al-Aqsa's furnishing and upkeep attests to the continued importance of the mosque, the *Haram al-Sharif*, and Jerusalem from the Umayyad Period to the present. Although Jerusalem was not always considered a major financial or political center (especially during the Mamluk and Ottoman sultanates) the upkeep of al-Aqsa and other holy sites in Jerusalem was a constant priority, in order to demonstrate (among other reasons) political legitimacy and prestige in the Islamic world, centralize administrative control in the Levant, and

maintain authority over potential competing religious groups and foreign powers within Jerusalem (Burgoyne 1987; Duri 1999; St. Laurent and Riedlmayer 1993). The caliphs and sultans ruling Jerusalem were therefore willing to seek out high-quality resources–which included their forests and those of their trading partners–to procure material befitting one of the most important Islamic holy sites.

The al-Aqsa timbers therefore provide a valuable resource for understanding the mosque's history and it and the *Haram*'s role in the history of Jerusalem and the Near East. Recording and analyzing this material is particularly important, because many of the timbers removed from the renovations have been sold and remain undocumented, and some have decayed and been destroyed because of poor storage conditions. Unfortunately, one of the major difficulties in analyzing the timbers removed during these renovations–including the assemblage studied here, and that which Lev-Yadun et al. (1984) studied–is that the timbers' exact locations in the mosque often have not been recorded. Therefore, (as this study demonstrates) while these timbers can still give important historical information, their contextual data, which would greatly enrich their interpretation and that of the mosque's building history, has been lost. Thus, it is important that other still-existing timbers removed from the mosque be analyzed and the results recorded, before additional valuable historical information is lost forever. Future studies should also include (if possible) timbers whose exact provenience in the mosque is known, in order to add much-needed contextual information and greatly enhance our knowledge of this building, whose dynamic history is a valuable part of Jerusalem's cultural heritage.

APPENDIX 4.1

^{14}C data from AQS-6, AQS-9, AQS-14, and AQS-18 samples employed in ^{14}C wiggle-matching. Samples in italics are flagged outliers using the General Outlier Model in OxCal (Bronk Ramsey 2009b) and are therefore excluded from the dating models.

Lab ID	Relative rings (each sample)	^{14}C age (BP)	SD
AQS-6			
MAMS-12867	1005–1014	1343	21
Hd-MAMS-12867	1005-1014	1354	13
MAMS-17337	*1025–1034*	1471	21
Hd-MAMS-12868	1035–1044	1328	21
AQS-9			
MAMS-17508	1004–1013	310	21
MAMS-12869	1014–1023	197	21
MAMS-17509	1024-1033	209	27
MAMS-12870	1034-1043	152	20
Hd-MAMS-12870	1034-1043	178	14
MAMS-17510	1044-1053	181	22
MAMS-12871a	*1074-1083*	*-11*	*19*
MAMS-12871b	1074-1083	153	19
AQS-14			
MAMS-12872a	*1020–1029*	*833*	*20*
Hd-MAMS-12872a	1020–1029	935	16
MAMS-12872b	1020–1029	964	21
MAMS-17338	1050–1059	943	22
MAMS-17339	1070–1079	872	21
MAMS-16137	1100-1109	898	20
MAMS-12873	*1100-1109*	*781*	*22*
MAMS-16138	1150-1159	827	21
AQS-18			
MAMS-12874	*1039-1048*	*378*	*22*
MAMS-12874 rerun	1039-1048	342	20
MAMS-17341	1079-1088	334	21
MAMS-17342	1099-1108	250	21
Hd-MAMS-16139	1119-1128	170	15
MAMS-16139	1119-1128	183	20
Hd-MAMS-16140	1169-1178	73	14
MAMS-16140	1169-1178	122	20

APPENDIX 4.2

The placement of the ^{14}C data in the AQS-6 and AQS-14 wiggle-matches against the IntCal09 (Reimer et al. 2009) radiocarbon calibration curve (±1σ). The ^{14}C data are shown as the μ±σ of the modeled ranges on the *x*-axis (calendar date scale), and as the ^{14}C age BP (±1σ) on the *y*-axis (^{14}C years). The wiggle-match has three outliers (*green circles*) (1 from AQS-6 and 2 from AQS-14), which are likely from instrument error in the radiocarbon laboratory and were re-tested.

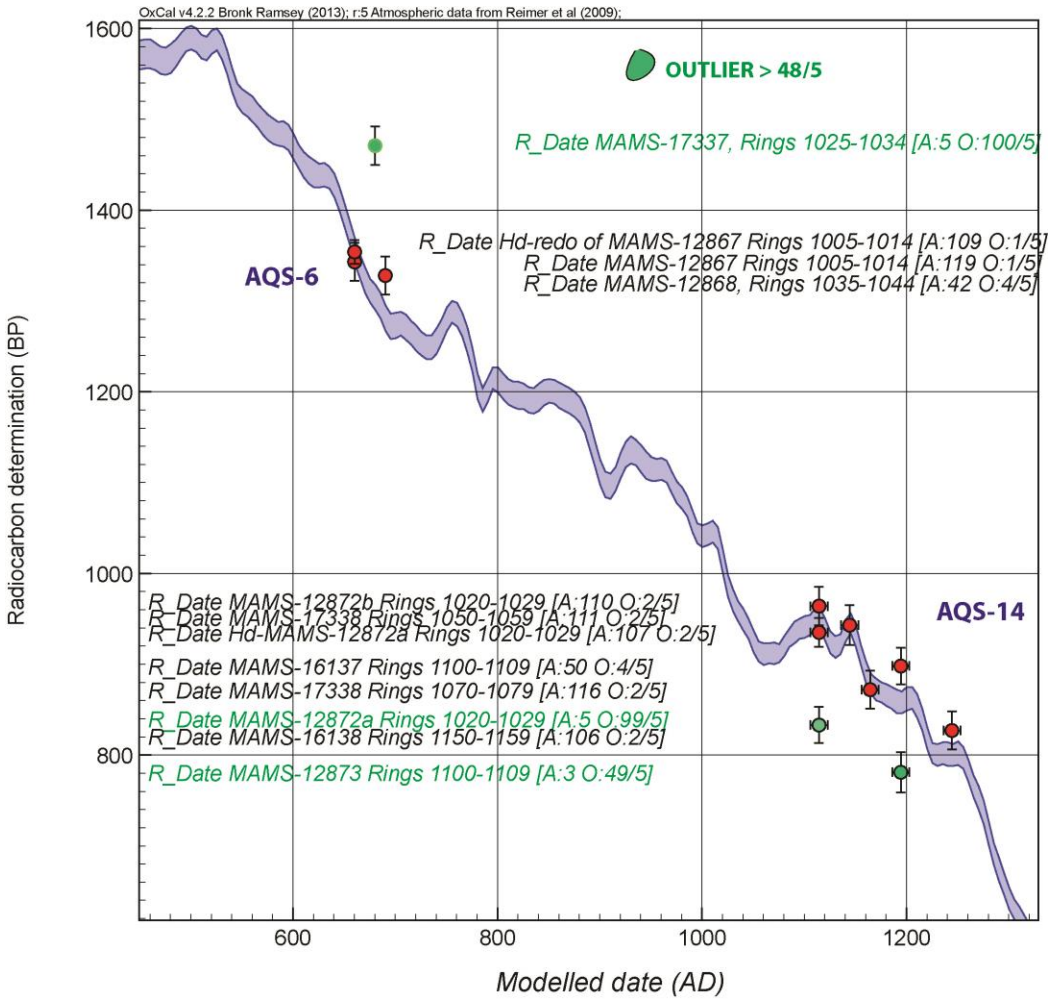

APPENDIX 4.3

The placement of the ^{14}C data in the AQS-6 and AQS-14 wiggle-matches against the IntCal09 (Reimer et al. 2009) radiocarbon calibration curve (±1σ). The ^{14}C data are shown as the μ±σ of the modeled ranges on the *x*-axis (calendar date scale), and as the ^{14}C age BP (±1σ) on the *y*-axis (^{14}C years). The three outliers (1 from AQS-6 and 2 from AQS-14) have been excluded from this model.

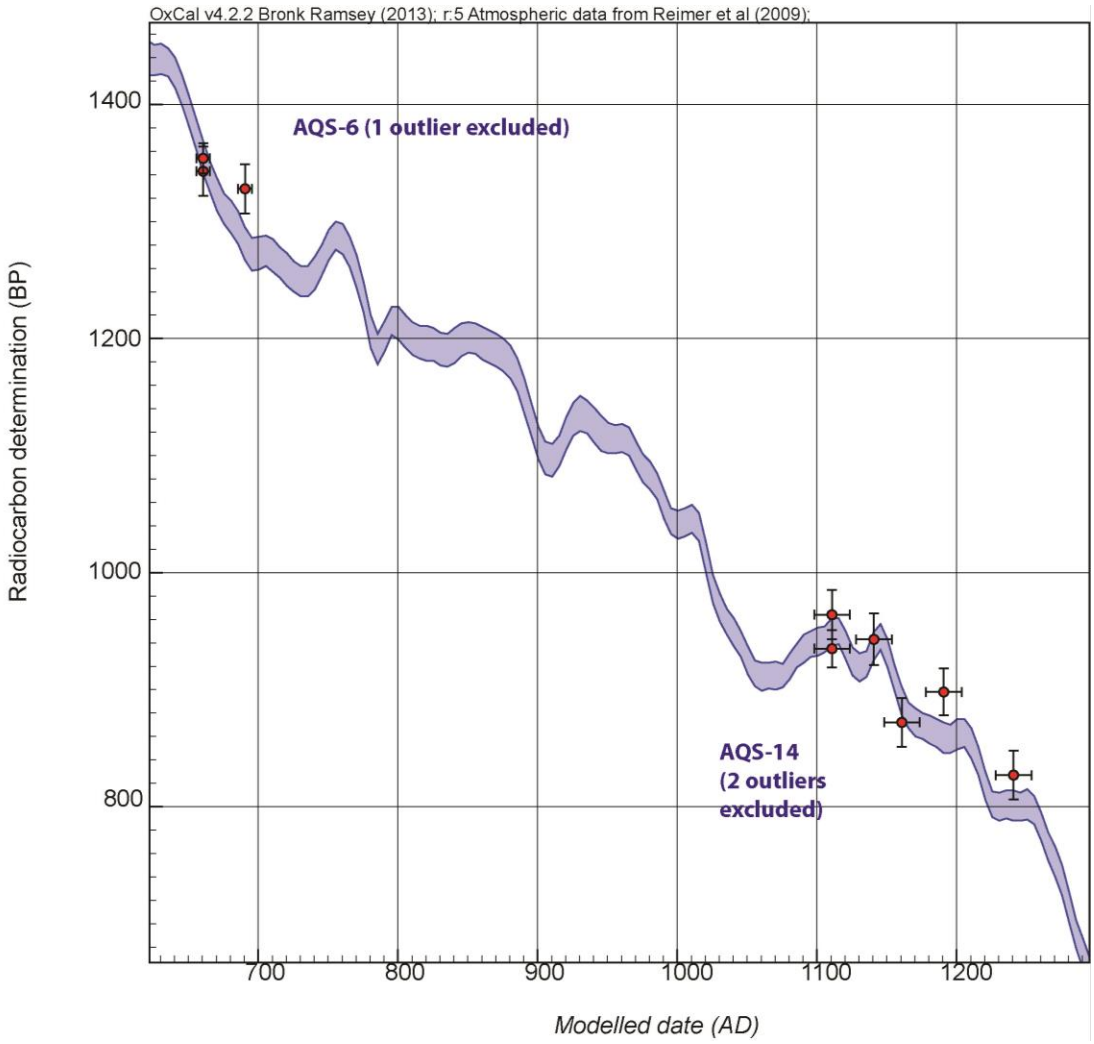

APPENDIX 4.4

The placement of the ^{14}C data in the `AQS-18 wiggle-match against the IntCal09 (Reimer et al. 2009) radiocarbon calibration curve (±1σ). The ^{14}C data are shown as the μ±σ of the modeled ranges on the *x*-axis (calendar date scale), and as the ^{14}C age BP (±1σ) on the *y*-axis (^{14}C years).

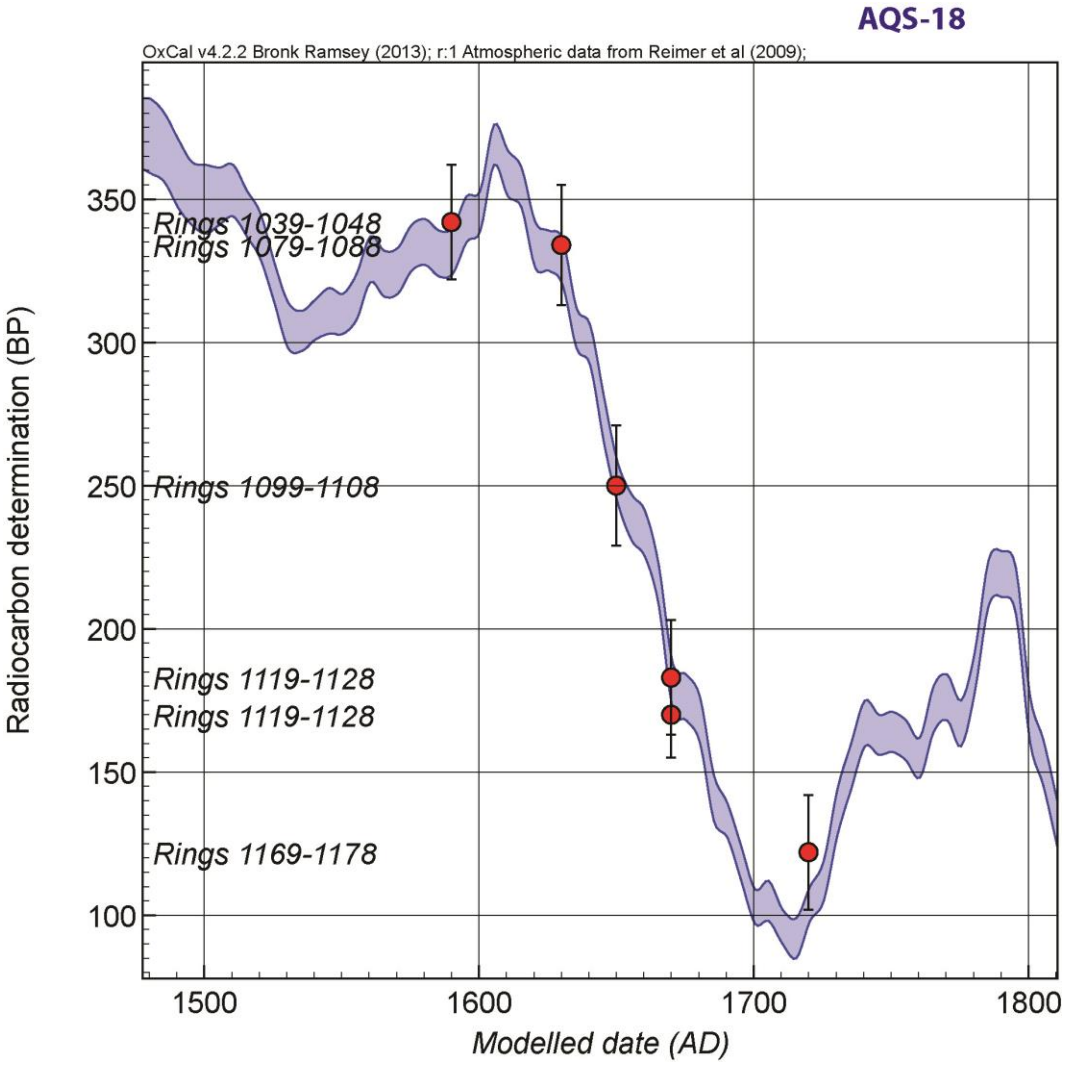

REFERENCES

Akkemik, Ü., Yaman, B., 2012. *Wood Anatomy of Eastern Mediterranean Species*. Verlag Kessel, Remagen-Oberwinter.

Amitai, R., 2007. *Mongols in the Islamic Lands: Studies in the History of the Ilkhanate*. Ashgate, Burlington.

Avi Yonah, M., 1942. Greek inscriptions from Ascalon, Jerusalem, Baisan and Hebron. *The Quarterly of the Department of Antiquities in Palestine* 10 (3): 162–165.

Bacci, M., Bianchi, G., Campana, S., Fichera, G., 2012. Historical and archaeological analysis of the Church of the Nativity. *Journal of Cultural Heritage* 13 (4) supplement: e5–e26.

Baillie, M.G.L., and Pilcher, J.R., 1973. A simple crossdating program for tree-ring research. *Tree-Ring Bulletin* 33: 7–14.

Bayliss, A., 2007. Bayesian buildings: an introduction for the numerically challenged. *Vernacular Architecture* 38: 75–86.

Bayliss A., Tyers, I., 2004. Interpreting radiocarbon dates using evidence from tree rings. Radiocarbon 46 (2), 957–964.

Bebber, A. 1990. Una cronologia del larice (*Larix decidua* Mill.) delle Alpi Orientali Italiane. *Dendrochronologia* 8: 119–139.

Bernabei, M., Bontadi, J., 2012. Dendrochronological analysis of the timber structure of the Church of the Nativity in Bethlehem. *Journal of Cultural Heritage* 13 (4) supplement: e54–e60.

Blanchette, R.A., Cease, K.R., Abad, A.R., 1991. An evaluation of different forms of deterioration found in archaeological wood. *International Biodeterioration* 28: 3–22.

Brewer, P. W., Sturgeon, K., Madar, L., Manning, S. W., 2010. A new approach to dendrochronological data management. *Dendrochronologia* 28: 131–134.

Bronk Ramsey, C., 2009a. Bayesian analysis of radiocarbon dates. *Radiocarbon* 51 (1): 337–360.

Bronk Ramsey, C., 2009b. Dealing with outliers and offsets in radiocarbon dating. Radiocarbon 51 (3): 1023–1045.

Burgoyne, M.H., 1987. *Mamluk Jerusalem: An Architectural Study*. British School of Archaeology in Jerusalem, Jerusalem.

Cedro, A., 2007. Tree-ring chronologies of downy oak (*Quercus pubescens*), pedunculate oak (*Q. robur*) and sessile oak (*Q. petraea*) in the Bielinek Nature Reserve: Comparison of the climatic determinants of tree-ring width. *Geochronometria* 26: 39–45.

Cherubini, P., Gartner, B.L., Tognetti, R., Bräker, O.U., Schoch, W., Innes, J.L., 2003. Identification, measurement and interpretation of tree rings in woody species from mediterranean climates. *Biological Reviews* 78: 119–148.

Cook, E.R., Kairiukstis, L.A. (Eds.), 1990. *Methods of Dendrochronology*. Kluwer Academic Publishers, Dordrecht.

Creswell, K.A.C., 1958. *A Short Account of Early Muslim Architecture*. Penguin Books, London.

Cuinet, V., 1896. *Syrie, Liban et Palestine: Gèographie Administrative, Statistique, Descriptive et Raisonnée*. E. Leroux, Paris.

Duri, A.A., 1999. Jerusalem in the Early Islamic Period, 7th–11th centuries AD. In: Asali, K.J. (Ed.), *Jerusalem in History: 3000 BC to the Present Day*. 2nd edition. Kegan Paul International, London, pp. 105–129.

EUFORGEN, 2009. Distribution map of European larch (*Larix decidua*). EUFORGEN 2009. Online database, http://www.euforgen.org. Accessed 15 January, 2012.

Eckstein, D., Bauch, J., 1969. Ein Beitrag zur Rationalisierung eines dendrochronologischen Verfahrens und zur Analyse seiner Aussagesicherheit. *Forstwissenschaftliches Centralblatt* 88: 230–250.

Fahn, A., Werker, E., Baas, P., 1986. *Wood Anatomy and Identification of Trees and Shrubs from Israel and Adjacent Regions*. Israel Academy of Sciences and Humanities, Jerusalem.

Fleet, K., 2013. Turks, Mamluks, and Latin merchants: Commerce, conflict, and cooperation in the Eastern Mediterranean. In: Harris, J., Holmes, C., Russell, E. (Eds.), *Byzantines, Latins, and Turks in the Eastern Mediterranean World after 1150*. Oxford University Press, Oxford, pp. 327–345.

Gale, R., Gasson, P., Hepper, N., Killen, G., 2000. Wood. In: Nicholson, P.T., Shaw, I. (Eds.), *Ancient Egyptian Materials and Technology*. Cambridge University Press, Cambridge, pp. 340–341.

Göyünç, N., 1983. The procurement of labor and materials in the Ottoman Empire (16th and 18th centuries). In: Bacqué-Grammont, J.L., Dumont, P. (Eds.), *Économie et Sociétés dans L'Empire Ottoman (Fin du XVIII-Début du XX siècle)*. Centre National de la Recherche Scientifique, Paris, pp. 327–334.

Griggs, C.B., 2006. *Tale of Two: Reconstructing Climate from Tree-Rings in the North Aegean, AD 1089-1989, and Late Pleistocene to Present Dendrochronology in Upstate New York*. Unpublished Ph.D. thesis, Cornell University.

Griggs, C.B., DeGaetano, A.T., Kuniholm, P.I., Newton, M.W., 2007. A regional reconstruction of May-June precipitation in the north Aegean from oak tree-rings, AD 1089–1989. *International Journal of Climatology* 27, 1075–1089.

Griggs, C.B., Kuniholm, P.I., Newton, M.W., Watkins, J.D. and Manning, S.W., 2009. A 924-year regional oak tree-ring chronology for north central Turkey. In: Manning, S.W., Bruce, M.J. (Eds.), *Tree-Rings, Kings and Old World Archaeology and Environment Papers Presented in Honor of Peter Ian Kuniholm*. Oxbow Books, Oxford, pp. 71–79.

Hajar, L., François, L., Khater, C., Jomaa, I., Déqué, M., Cheddadi, R., 2010. *Cedrus libani* (A. Rich.) distribution in Lebanon: Past, present and future. *C.R. Biologies* 333: 622–630.

Hamilton, R.W. 1949. *The Structural History of the Al-Aqsa Mosque*: *A Record of Archaeological Gleaning from the Repairs of 1938-1942*. Oxford University Press, London.

Haneca, K., Čufar, K., Beeckman, H., 2009. Oaks, tree-rings and wooden cultural heritage: a review of the main characteristics and applications of oak dendrochronology in Europe. *Journal of Archaeological Science* 36: 1–11.

Heyd, U., 1960. *Ottoman Documents on Palestine, 1552–1615: A Study of the Firman According to Mühimme Defteri*. Clarendon Press, Oxford.

Hillam, J., Morgan, R.A., Tyers, I., 1987. *Sapwood Estimates and the Dating of Short Ring Sequences*. In: BAR International Series, vol. 333.

Howard, D., 2007. The Mamluks. In: Carboni, S. (Ed.), *Venice and the Islamic World, 828-1797*. Metropolitan Museum of Art, New York, pp. 73–89.

Howard, D., 1991. Venice and Islam in the Middle Ages: some observations on the question of architectural influence. *Architectural History* 34: 59–74.

Hughes, M.K., Milsom, S.J., Leggett, P.A., 1981. Sapwood estimates in the interpretation of tree-ring dates. *Archaeological Science* 8: 381–390.

InsideWood, 2004-onwards. InsideWood. Online database, http://insidewood.lib.ncsu.edu/search. Accessed 12 August, 2011.

Kuniholm, P.I., Pearson, C.L., Ważny, T., Griggs, C.B., *in press*. A 2367-year oak tree-ring chronology from 98 sites for the Aegean, East Mediterranean, and Black Seas: the Marmaray contribution. Peeters, Leuven.

Kuniholm, P.I., 2000a. Dendrochronologically dated Ottoman monuments. In: Baram, U., Carroll, L. (Eds.), *A Historical Archaeology of the Ottoman Empire: Breaking New Ground*. Plenum Press, New York, pp. 93–136.

Kuniholm, P.I., 2000b. International Tree-Ring Databank. IGBP PAGES/World Data Center for Paleoclimatology Data Contribution Series #noaa-tree-3797. NOAA/NCDC Paleoclimatology Program, Boulder, Colorado, USA.

Kuniholm, P.I., 1978. *Dendrochronology at Gordion and on the Anatolian Plateau*. Unpublished Ph.D thesis, University of Pennsylvania.

Kuniholm, P.I., Griggs, C.B., Newton, M.W. 2007. Evidence for early timber trade in the Mediterranean. In: Belke, K., Kislinger, E.A.K., Stasinopoulou, M.A. (Eds.), *Byzantina Mediterranea: Festschrift für Johannes Koder zum 65. Geburtstag*. Böhlau Verlag: Vienna, pp. 365–385.

Kuniholm, P.I., Striker, C.L., 1987. Dendrochronological investigations in the Aegean and neighboring regions, 1983–1986. *Journal of Field Archaeology* 14: 385-398.

Lapidus, I.M., 1967. *Muslim Cities in the Later Middle Ages*. Harvard University Press, Cambridge.

Le Strange, G., 1965. *Palestine Under the Moslems: A Description of Syria and the Holy Land from A.D. 650 to 1500*. Khayats, Beirut.

Levanič, T., Pignatelli, O., Čufar, K., 2001. A regional larch chronology of trees and historical buildings from Slovenia and Northern Italy. *Dendrochronologia* 19: 221–229.

Lev-Yadun, S., 2008. Wood remains from archaeological excavations: A review with a Near Eastern perspective. *Israel Journal of Earth Sciences* 56: 139–162.

Lev-Yadun, S. 1992. The origin of the cedar beams from al-Aqsa Mosque: Botanical, historical and archaeological evidence. *Levant* 24: 201–208.

Lev-Yadun, S., Liphschitz, N., Waisel, Y., 1984. Ring analysis of *Cedrus libani* beams from the roof of al-Aqsa mosque. *Eretz Israel* 17: 4–5, 92–96. (Hebrew with English summary)

Liphschitz, N., 2007. *Timber in Ancient Israel: Dendroarchaeology and Dendrochronology*. Monograph Series of the Institute of Archaeology of Tel Aviv University, 26. Emery and Claire Yass Publications in Archaeology, Tel Aviv.

Liphschitz, N., Biger, G. 1991. Cedar of Lebanon: *Cedrus libani* in Eretz Israel during antiquity. *Israel Exploration Journal* 41: 167–175.

Liphschitz, N., Biger, G.,Bonani, G., Wolfli, W., 1997. Comparative dating methods: botanical identification and ^{14}C dating of carved panels and beams from the al-Aqsa Mosque in Jerusalem. *Journal of Archaeological Science* 24: 1045–1050.

Liphschitz, N., Lev-Yadun, S., 1989. The botanical remains from Masada: Identification of the plant species and the possible origin of the remnants. *Bulletin of the American Schools of Oriental Research* 274: 27–32.

Liphschitz, N., Lev-Yadun, S., Rosen, E., Waisel, Y., 1981. The annual rhythm of activity of the lateral meristems (cambium and phellogen) in *Cupressus sempervirens* L. *Annals of Botany* 47: 485–496.

Manning, S.W., Kromer, B., 2012. Considerations of the scale of radiocarbon offsets in the east Mediterranean, and considering a case for the latest (most recent) likely date for the Santorini eruption. *Radiocarbon* 54 (3–4): 449–474.

Manning, S.W., Kromer, B., Bronk Ramsey, C., Pearson, C.L., Talamo, S., Trano, N., Watkins, J.D., 2010. ^{14}C record and wiggle-match placement for the Anatolian (Gordion area) juniper tree-ring chronology ~1729 to 751 cal BC, and typical Aegean/Anatolian (growing season related) regional ^{14}C offset assessment. *Radiocarbon* 52 (4): 1571–1597.

Meiggs, R., 1982. *Trees and Timber in the Ancient Mediterranean World*. Clarendon Press, Oxford.

Mikesell, M.W., 1969. The deforestation of Mount Lebanon. *The Geographical Review* 58: 1–28.

Miles, D.H., 2005. *New Developments in the Interpretation of Dendrochronology as Applied to Oak Building Timbers*. Unpublished Ph.D. dissertation, Oxford University, Oxford.

Nicolussi, K., 1995. Dendrochronologische Untersuchungen zur mittelalterlichen Baugeschichte von Schloss Tirol. *Tiroler Heimat* 59: 19–43.

Nicolussi, K., Kaufmann, M., Melvin, T., van der Plicht, J., Schießling, P., Thurner, A., 2009. A 9111 year long conifer tree-ring chronology for the European Alps: A base for environmental and climatic investigations. *The Holocene* 19 (6): 909–920.

Nola, P., Motta, R., 1996. Una cronologia plurisecolare di larice (*Larix decidua* Mill.) per l'Alta Valmalenco (Sondrio, Italia). *Dendrochronologia* 14: 31–42.

Pearson, C.L., Griggs, C.B., Kuniholm, P.I., Brewer, P.W., Ważny, T., Canady, L., 2012. Dendroarchaeology of the mid-first millennium AD in Constantinople. *Journal of Archaeological Science* 39: 3402–3414.

Quézel, P., Médail, F., 2003. *Écologie et Biogéographie des Forêts du Bassin Méditerranéen*. Elsevier, Paris.

Reimer P.J., Baillie, M.G.L., Bard, E., Bayliss, A., Beck, J.W., Blackwell, P.G., Bronk Ramsey, C., Buck, C.E., Burr, G.S., Edwards, R.L., Friedrich, M., Grootes, P.M., Guilderson, T.P., Hajdas, I., Heaton, T.J., Hogg, A.G, Hughen, K.A, Kaiser, K.F., Kromer, B., McCormac, F.G., Manning, S.W., Reimer, R.W., Richards, D.A., Southon, J.R., Talamo, S., Turney, C.S.M., van der Plicht, J., Weyhenmeyer, C.E., 2009. IntCal09 and Marine09 radiocarbon age calibration curves, 0–50,000 years cal BP. *Radiocarbon* 51 (4): 1111–1158.

Reuven, P., 2013. Wooden beams from Herod's Temple Mount: do they still exist? *Biblical Archaeology Review* 39 (3): 40–48.

Rinn, F., 1996. TSAP (Time series Analysis and Presentation) Version 3.0. Heidelberg.

Rivoira, G.T., 1918. *Moslem Architecture: Its Origins and Development*. Translated by G. McN. Rushforth. H. Milford, Oxford University Press, London.

Rosen-Ayalon, M. 1989. *The Early Islamic Monuments of Al-Haram al-Sharif*: *An Iconographic Study*. *Qedem* Monographs of the Institute of Archaeology, 28. Institute of Archaeology, Hebrew University of Jerusalem, Jerusalem.

Schwabe, M., 1949. Note on the graffiti shown in Plate XLVIII. In: Hamilton, R.W., *The Structural History of the Al-Aqsa Mosque*: *A Record of Archaeological Gleaning from the Repairs of 1938-1942*. Oxford University Press, London, pp. 93–95.

Schweingruber, F.H., 1993. *Trees and Wood in Dendrochronology: Morphological, Anatomical, and Tree-Ring Analytical Characteristics of Trees Frequently Used in Dendrochronology*. Springer-Verlag, Berlin.

Schweingruber, F.H., 1990. *Anatomy of European Woods*. Verlag Paul Haupt, Bern.

Serageldin, I., 1989. The restoration of the Al-Aqsa Mosque. In: Serageldin, I. (Ed.), *Space for Freedom*. Butterworth Architecture, London, pp. 119–131.

Serre, F. 1979. The dendroclimatological value of the European larch (*Larix decidua* AMill.) in the French Maritime Alps. *Tree-Ring Bulletin* 38: 25–34.

St. Laurent, B., Riedlmayer, A., 1993. Restorations of Jerusalem and the Dome of the Rock and their political significance. *Muqarnas* 10: 76–84.

Stuiver, M., Polach, H.A., 1977. Discussion: reporting on ^{14}C data. *Radiocarbon* 19 (3): 355–363.

Talgam, R., 2004. *The Stylistic Origins of Umayyad Sculpture and Architectural Decoration*. Vol. 1. Harrassowitz Verlag, Wiesbaden.

Tolkowsky, S., 1924. *The Gateway of Palestine: A History of Jaffa*. George Routledge and Sons, London.

Touchan, R., Xoplaki, E., Funkhouser, G., Luterbacher, J., Hughes, M.K., Erkan, N., Akkemik, Ü., Stephan, J., 2005. Reconstructions of Spring/Summer Precipitation for the Eastern Mediterranean from Tree-Ring Widths and Its Connection to Large-Scale Atmospheric Circulation. *Climate Dynamics* 25: 75–98.

Ważny, T., 2009. Is there a separate tree-ring pattern for Mediterranean oak? In: Manning, S.W., Bruce, M.J. (Eds.), *Tree-rings, Kings, and Old World Archaeology and Environment Papers Presented in Honor of Peter Ian Kuniholm*. Oxbow Books, Oxford, pp. 41-50.

Ważny, T., 1990. Aufbau und Anwendung der Dendrochronologie für Eichenholz in Polen. Unpublished Ph.D. thesis, Hamburg University.

Ważny, T., Akkemik, Ü., Boltryk, Y., Günar, T., Köse, N., Kyncl, J., Leshtakov, K., Lorentzen, B., Nechita, C., Popa, I., Sagaydak, S., Vasileva, J., 2011. *Bridging the Gaps in Tree-Ring Records: Creating a High-Resolution Dendrochronological Network for South-Eastern Europe for Dating of Historical Objects and Evalution of Regional Climate Patterns*. Unpublished report for National Geographic.

Werker, E., 1988. Nahal Hemar Cave: botanical identification of worked wood remains. *'Atiqot* 18: 73–75.

Wigley, T.M.L., Briffa, K.R., Jones, P.D., 1984. On the average value of correlated time series, with applications in dendroclimatology and hydrometeorology. *Journal of Climate and Applied Meteorology* 23: 201–213.

Zohary, M., 1973. *Geobotanical Foundations of the Middle East*. Vol. 2. Gustav Fischer Verlag, Stuttgart.

Zohary, M., 1962. *Plant Life of Palestine: Israel and Jordan*. Ronald Press, New York.

CHAPTER 5:

DENDROCHRONOLOGICAL DATING AND PROVENANCING OF LATE OTTOMAN BUILDINGS IN JAFFA, ISRAEL

SUMMARY

The port of Jaffa (now on the southern edge of modern Tel Aviv, Israel) was an important center for maritime commerce throughout antiquity and experienced great urban development during the latter half of the 19th century under Ottoman rule. This increase in building activity required importation of large quantities of timber from the eastern Mediterranean and Europe, since the southern Levant lacked adequate high-quality building timbers. In this study, timbers were sampled from two late 19th-century buildings in Jaffa–the Ottoman *Qishle* (prison) complex and the French Sisters of St. Joseph School–for dendrochronological dating and provenancing.

The results, combined with information from historical records and dendrochronological data from other Ottoman sites in the eastern Mediterranean, demonstrate that these buildings used cedar of Lebanon (*Cedrus libani* A.Rich.) timbers that were imported from southwestern Anatolia, and that Jaffa was connected to a far-reaching maritime and overland timber trading network. The use of spruce (*Picea abies* (L.) H. Karst.) wood in the Sisters of St. Joseph School, in addition to the cedar and cypress (*Cupressus sempervirens* L.), indicates that the school's builders used available timber brought from both the eastern Mediterranean and Europe for the

construction. The results from this study also highlight the great potential for further dendroprovenancing research at Jaffa and other historical ports in the southern Levant.

INTRODUCTION

During the latter half of the 19th century, the port of Jaffa (then part of Ottoman-ruled Palestine) experienced an increase in building activity that required large-scale importation of lumber from more timber-rich areas. As Palestine's main port, Jaffa was in a prime position to receive timber from a variety of trading partners in the eastern Mediterranean and Europe. The following study uses the dendrochronological dating and dendroprovenancing methods described in previous chapters to determine more precisely the construction dates of, and the timber sources used to build, two Late Ottoman buildings in Jaffa, and provide greater information on Jaffa's position in timber trading networks during this time period.

Jaffa (located on the south side of modern Tel Aviv in Israel) has been used as a port since at least the Middle Bronze Age (Burke 2011). Jaffa's rise to prominence was due to its key position as a port along the southern Levant maritime route connecting Cyprus, Egypt, Anatolia, and Lebanon, and its role as the "gateway" to roads connecting the Mediterranean coast with settlements in the central hill country, most notably Jerusalem (Burke 2011).[1]

The port experienced a period of decline after the Crusaders were expelled from the city in 1268, the Mamluks razed the harbor during the late 13th and 14th

[1] For a more detailed account of the history of Jaffa, see: Chapters 6-12 of Peilstöcker and Burke (2011) and Tolkowsky (1924). A full account of Jaffa's more recent history during the 16th–20th centuries can be found in Kark (1984) and Avitzur (1972).

centuries, and frequent attacks by pirates and Bedouins made the area insecure for trade. Although the port suffered a setback during Napoleon's siege and a subsequent outbreak of the bubonic plague in 1799, the 18th through 19th centuries were largely a period of economic and urban renewal in Jaffa, as the Ottoman government installed more fortifications and soldiers to protect the harbor and main trade routes in Palestine, and the city developed a thriving citrus industry (Kark 1984, 2011).

By the 1870s, the area around Jaffa was secure enough that the city's fortifications were removed, and the city rapidly expanded beyond its original confines (Kark 1984; Tolkowsky 1924). The development of newer, faster trade routes, such as the Suez Canal in 1869, and the building of new railroads at the end of the 19th century–including the railroad linking Jaffa and Jerusalem in 1892–increased the flow of goods through Jaffa and brought greater prosperity to the port, which by then had become the most important port in Palestine and a major trading center in the eastern Mediterranean (Avitzur 1972; Bonine 1998). As security and transportation improved, increasing numbers of foreigners, largely from Europe, set up consulates in the port. Religious groups (largely Christian) began establishing new churches, schools, hospitals, and even small religious colonies in Jaffa and Palestine. Groups of pilgrims passed through the port at the beginning of their tours of the region's religious sites, so lodging was also constructed to accommodate the growing number of travelers (Kark 1984).

Many of the new Europeans living in Jaffa constructed buildings using traditional European building techniques, which used large amounts of timber. Local inhabitants and Ottoman officials in the Jaffa municipality likewise began using more

timber for constructing government, religious, and commercial structures. Local forest resources were inadequate for satisfying the rapidly growing city's demands, so timber was imported from Europe and the other areas of the Mediterranean in increasing amounts until the beginning of World War I (Avitzur 1972; Biger and Liphschitz 1991a).

A previous botanical survey by Biger and Liphschitz (1991a) of the timber species used in Ottoman buildings in the Old City of Jaffa and its surrounding villages and colonies confirms the predominant use of imported timber. They found that, based on current species distributions and available historical documentation, the vast majority of timbers were cut from a variety of imported tree species from Turkey or Lebanon in the Mediterranean, particularly cedar of Lebanon (*Cedrus libani*), and–in smaller numbers–Austrian pine (*Pinus nigra*), Calabrian pine (*Pinus brutia*),[2] and Cilician fir (*Abies cilicica*). Tree species native to Europe were also present, including Norway spruce (*Picea abies*), Scots pine (*Pinus sylvestris*), silver fir (*Abies alba*), unspecified "European" oak (*Quercus* sp., probably *Quercus petraea*, *Quercus pubescens*, or *Quercus robur*), and European larch (*Larix decidua*). The buildings constructed by American pilgrims in 1866 as part of an attempted religious settlement (the 'American Colony' in Jaffa) even included timbers imported from the northeast and western United States, such as eastern hemlock (*Tsuga canadensis*) and Douglas fir (*Pseudotsuga menziesii*) (Biger and Liphschitz 1993). However, the authors were

[2] It is also possible that some or all of these timbers were *Pinus halepensis*, since the species cannot be distinguished from *Pinus brutia* by wood anatomy alone (Lev-Yadun 2000; Schweingruber 1990).

not able to specify the timbers' areas of origin more precisely beyond their extensive species ranges.

In another study, Liphschitz and Biger (1988) were able to produce successful dendrochronological dates for timbers in late 19th century rural settlements near Jaffa and slightly further north near Haifa, which they sourced to southeastern France, based on historical documentation and dendrochronological data. They also dated and provenanced imported North American tree species in the American Colony in Jaffa (Biger and Liphschitz 1993), but until now, successful dendrochronological dating and provenancing of historical timbers from Mediterranean tree species used in sites in Israel has not been achieved.

Accordingly, in the present study, timbers were sampled for dendrochronological analysis from two Ottoman-era buildings in Jaffa–the *Qishle* (prison) complex and the Sisters of St. Joseph School–not only to assist in dating parts of the buildings, but also to provenance the timbers and gain greater information on forest exploitation and Jaffa's place in Late Ottoman timber trade networks.

MATERIALS AND METHODS

Sites

Both the *Qishle* complex and the French Sisters of St. Joseph School are located in the area outside the old city walls of Jaffa (Figure 5.1). Recently, this area has been part of an urban renewal project, and the Israel Antiquities Authority excavated the areas in and around both buildings (Arbel 2009).

Qishle Complex

The *Qishle* complex is located at the northern entrance of Jaffa on the coast in *Sakinat al-Dawla* (Arabic: 'The Neighborhood of the State'). The complex consists of three orthogonal two-story buildings and two yards (Arbel 2009) and was built on the site of the northeastern corner of the city walls and bastions, which were dismantled during the 1870s and early 1880s, as part of the defortification of Jaffa (Kark 1984; Shaham, *forthcoming*). Shaham (*forthcoming*) proposes a construction date of 1886/7 for the building. This is based on an inscription over the gate to the complex that glorifies the Sultan Abdul Hamid II (r. 1876–1909) on the construction of the new compound in the year 1304 after the *Hijra* (equivalent to 1886/7).

According to Shaham (*forthcoming*), the style of the buildings suggests that European, possibly German, engineers were involved in the planning, although the rounded windows in the *Qishle* corridor are clearly Ottoman (Yoav Arbel, pers. comm., 2011).

Under Ottoman rule, the *Qishle* complex was used as a prison and a military base (Shaham, *forthcoming*). During the late 1890s–early 1900s, the *Qishle* and the neighboring al-Mahmudiyya mosque became incorporated into a new square, which also featured a new government palace (*saray*) and clock tower, and marked the entrance to the city from the port (Kark 1984). The *Qishle* continued to serve as a prison and police station under the British Mandate and the modern state of Israel. The Israeli police abandoned the site in 2005 and sold it to private investors, who plan to refurbish the buildings and use them as a hotel (Shaham, *forthcoming*).

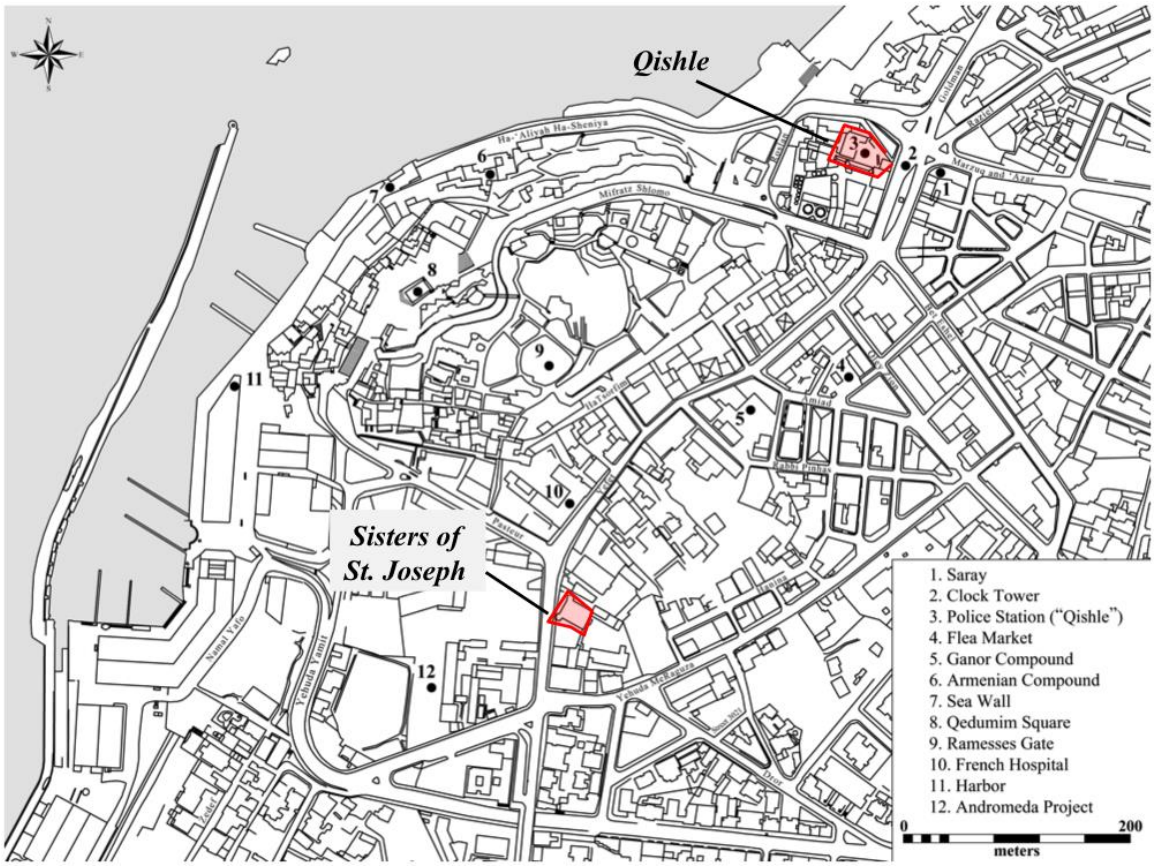

Figure 5.1. Locations of the *Qishle* complex and Sisters of St. Joseph School (*shaded in red*) in the historic center of Jaffa. (*Image courtesy of the Jaffa Cultural Heritage Project*)

Twelve sections were cut for dendrochronological analysis from floorboards in the second-story corridor, entryway, and rooms in the southeastern building of the *Qishle* complex (above excavation area D) (Figure 5.2; Table 5.1), since the excavators suspected that these timbers were part of the original structure and were easily accessible.

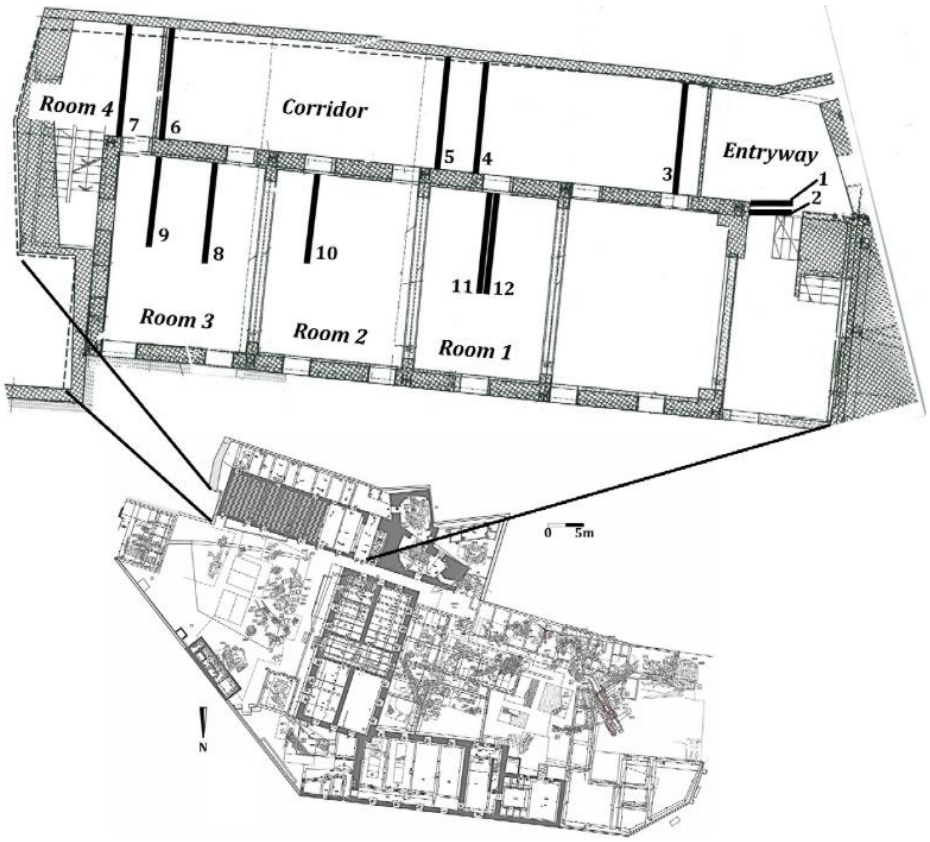

Figure 5.2. Plan of the second floor of the southwest building in the Jaffa *Qishle* complex showing the location from which each timber section was sampled. (*Adapted from an image courtesy of the Jaffa Cultural Heritage Project*)

Table 5.1. Location and dimensions of the Jaffa *Qishle* timbers.

Sample #	Location	Length (cm)	Width (cm)	Thickness (cm)
1	entryway	186	26	3
2	entryway	186	25	2
3	corridor	178	25	3
4	corridor	178	23	2
5	corridor	178	22	3
6	corridor	178	26	3
7	room 4	178	27	2
8	room 3	200	24	3
9	room 3	181	24	3
10	room 2	201	24	3
11	room 1	201	23	3
12	room 1	201	21	2

Sisters of St. Joseph School

The school of the Sisters of St. Joseph is located at 25 Yefet Street, which was one of the major commercial streets running through Jaffa, connecting the port to Gaza and cities further south (Kark 1984; Tolkowsky 1924). The French Catholic Sisters of St. Joseph of the Apparition, who had established themselves in Jaffa in the 1870s, opened the building as a school for girls in 1882 (Kark 1984; Or et al. 1988). The building was used as a school until 2008, and as of 2012, was being renovated, so that it can be converted to a boutique hotel. The school was one of the buildings analyzed in the study by Biger and Liphschitz (1991a), who identified the timbers as European in origin and concluded that timbers were brought from France specifically for the building's construction.

The building's roof has four trusses. Each of the truss components has a series of tick marks carved into it whose number corresponds to a specific truss. Thus all components of the first, westernmost truss are inscribed with one tick mark, all timbers in the second truss have two tick marks, and so on (Figure 5.3). These 'assembly marks' are a common feature in roofs from France, Belgium, and central Europe from the 12th century onwards. In west/central European building traditions, roof trusses were provisionally assembled on the ground, and the assembly marks helped identify each beam's position and the order in which the roof elements were to be put in place once the roof was assembled (Hoffsummer 2009). The struts and rafters have an additional, smaller 'lateralization mark' set at an angle, which allowed carpenters to distinguish which timbers were to be attached on the right and left sides of the roof truss.

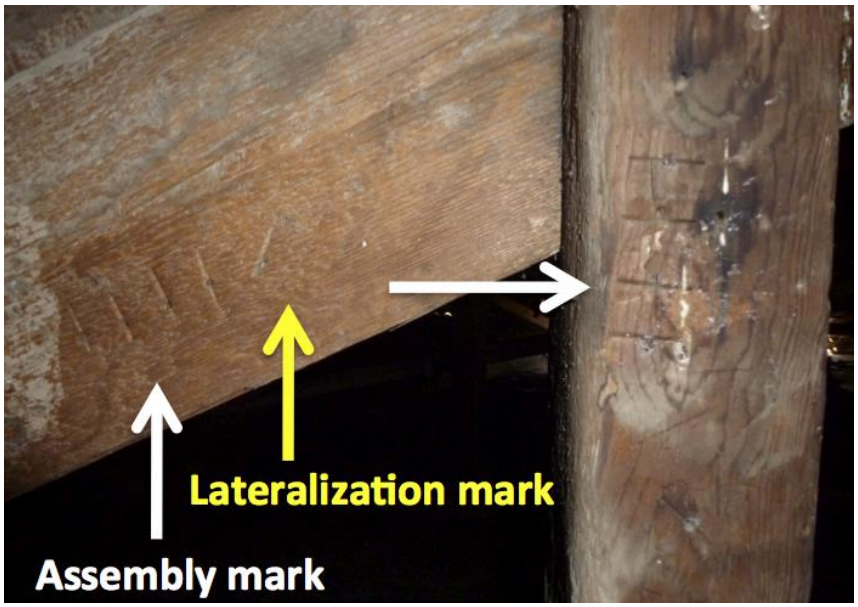

Figure 5.3. Assembly (*white arrows*) and lateralization (*yellow arrow*) marks on a post and rafter from truss IIII of the Sisters of St. Joseph roof. ***Photo credit: Brita Lorentzen***

Ten sections were cut from the roof timbers in the attic of the Sisters of St. Joseph School (Figure 5.4; Table 5.2).

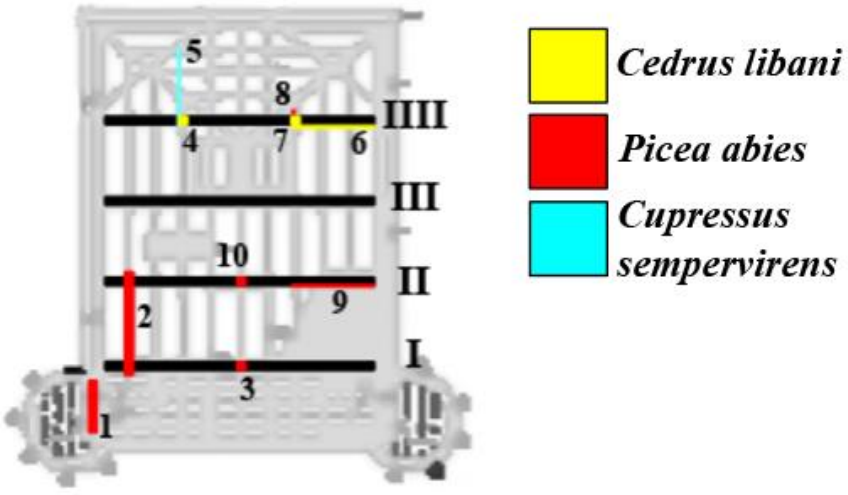

Figure 5.4. Plan of the main building of the Sisters of St. Joseph School showing the location from which each timber section was sampled and its species. Roman numerals indicate the assembly mark truss numbers. (*Adapted from an image courtesy of the Jaffa Cultural Heritage Project*)

Table 5.2. Location, species, and dimensions of the Sisters of St. Joseph timbers.

Sample #	Species	Roof element	Location	Length (cm)	Width (cm)	Height (cm)
1	*Picea abies*	rafter	north tower	355	5.5	12
2	*Picea abies*	rafter	between Truss I and II	262	6.5	3.5
3	*Picea abies*	king post	Truss I	100	15	15
4	*Cedrus libani*	post	north Truss IIII	167	20.5	10
5	*Cupressus sempervirens*	tie beam	Truss IIII	244	12	7
6	*Cedrus libani*	tie beam	Truss IIII	255	12	5.5
7	*Cedrus libani*	post	south Truss IIII	165	20	10
8	*Picea abies*	purlin cleat	south Truss IIII	41	12.5	8
9	*Picea abies*	tie beam	between Truss I and II	720	17.5	14.5
10	*Picea abies*	king post	Truss II	100	15	15

Timber Identification, Measurement, and Crossdating

Before measurement and crossdating, transverse, radial, and tangential microsections were taken from the timber samples, in order to identify the species of each timber. The microsections were then inspected under an Olympus Bx41 binocular microscope at magnifications up to x100, and were compared with archaeological and modern wood reference collections, standard reference texts (Fahn et al. 1986; Schweingruber 1990), and the InsideWood anatomical database (InsideWood 2004-onwards).

The rest of the timber section was then sanded and polished, so that the tree-rings and cell anatomy were clearly visible for dendrochronological analysis. Each sample's tree-ring widths were then measured to the nearest 0.01 mm on a

measurement table under a dissecting microscope, using the Tellervo ring measurement program (Brewer et al. 2010). Notable anatomical features were also marked and described for each ring using the same program. On 4 of the samples from the *Qishle* complex (labeled JOK 3, 4, 7, and 8), it was possible to measure 2 separate radii, which were then averaged together to form a single, composite measurement sequence for the sample.

The measured tree-ring series were cross-matched with other samples belonging to the same species, and the synchronized sample measurements for each year were then averaged together to create composite site chronologies for each species present at the site, using standard dendrochronological methods (Cook and Kairiukstis 1990).

The site chronologies were crossdated against absolutely dated reference chronologies built from sites of the same species in the eastern Mediterranean and Europe, as well as dendrochronologically dated site chronologies from historical buildings and wooden objects from these areas. Crossdating was evaluated by visually matching similar growth patterns between the Jaffa building chronologies and reference chronologies, and by evaluating their correlation using several different statistical tests: the the Hollstein *t*-value (t_H) (Hollstein 1980), Baillie-Pilcher *t*-value (t_{BP}) (Baillie and Pilcher 1973), and Gleichläufigkeit (*GL*) (Eckstein and Bauch 1969) (for a description of each statistical test, see: Chapter 3).

In East Mediterranean dendrochronology, an empirically-derived *t*-value of 5.00 is frequently used as a minimum for a statistically reliable crossmatch (e.g., Kuniholm 2000a; Kuniholm et al. 2007), provided that the suggested crossmatch also

has a significant corresponding *GL* value and (most importantly) can be visually verified. It is also recommended that the undated site and dated reference chronologies overlap by at least 50–100 years, with a larger overlap preferred, in order to lessen the possibility of spurious dates resulting from random high correlation between short tree-ring patterns.

However, since many of the timbers from the *Qishle* and the Sisters of St. Joseph School were cut from a species (cedar of Lebanon) that is more responsive to its local environment (introducing greater 'noise' into the tree-ring pattern), in this case, an overlap with the reference chronologies of at least 100 years or more was required to date the *Qishle* and Sisters of St. Joseph cedar chronologies securely. Additionally, experiments in crossdating known-age 100–200-year segments of different modern and historical cedar chronologies and reference chronologies indicate that a slightly more conservative set of minimum *t*-values be adopted for cedar. Therefore in this study, *t*-values between 4.5 and 5.0 indicate a possible match, and *t*-values higher than 5.0–5.5 are a clear indication of a correct dating position. The suggested dendrochronological dates were then cross-checked and verified against the match's corresponding *GL* value (and its statistical significance) and visual fit. Significant visual and statistical correlation between the Jaffa chronologies and multiple reference chronologies at the same point in time (so that the last ring consistently dated to the same year) was also required to indicate a reliable dating placement.

Dendroprovenancing

Once the Jaffa site chronologies had been securely dated, statistical matches were calculated between the Jaffa site chronologies and all available East Mediterranean cedar forest chronologies and historical Ottoman chronologies at the dendrochronologically determined date. The crossdating results were then examined to determine if the forest reference chronologies yielding the highest statistical and visual matches with the Jaffa chronologies were concentrated in one geographic area or bioclimatic zone, indicating the most likely geographic origin of the timbers. The dendrochronologically determined provenance and site histories of historical chronologies that had strong visual and statistical correlation with the Jaffa chronologies were also evaluated to determine if these sites were part of the same timber trade network.

As a secondary test, the Jaffa cedar chronologies were crossdated against Kuniholm's (2001) and Touchan et al.'s (2005) *Juniperus excelsa* chronologies from southern Turkey. This was done, because this species of juniper frequently co-occurs with cedars in Turkey, and inter-species correlation between juniper and cedars growing in the same forest is usually significant. However, because the trees differ physiologically and therefore have somewhat different responses to climate and their local environment, inter-species correlation decreases considerably between cedars and junipers growing in increasingly distant forests. Additionally, juniper chronologies have been sampled in Mersin province in southeastern Turkey, where cedar also grows but has not at present been sampled for dendrochronology. Consequently juniper chronologies that have significant correlation with the Jaffa

chronologies give additional strong evidence that the Jaffa timbers were from that sampled forest area.

The geographic locations of the cedar and juniper forest reference chronologies and historical chronologies were plotted, along with their statistical correlation with the Jaffa cedar chronologies. The t_H-value of the match between the Jaffa chronologies and reference chronologies was used to visualize strength in correlation geographically (following Bridge 2012; Daly 2007, 2011; and Haneca et al. 2005). However, it should be emphasized that all available statistical values and the visual fit of between each reference chronology and the Jaffa chronologies were considered when determining the timber provenance of the cedars.

RESULTS

Timber Identification and Dating

***Qishle* Complex**

All 12 of the floorboards from the *Qishle* complex are made from cedar of Lebanon (*Cedrus libani* A. Rich.). Cedar of Lebanon is not native to Israel; its forests grow today in fragmentary stands extending across the Taurus Mountains of southern Turkey down through the coastal mountains of Cilicia, Syria, and Lebanon (Boydak 2003; Hajar et al. 2010; Quézel and Médail 2003). A subspecies, *Cedrus libani* subsp. *brevifolia* (Hook.f.) Meikle, grows in a small area in western Cyprus (Ciesla 2004). Therefore this material was imported to Jaffa from one of these areas.

The timber was heavily shaped and squared during the cutting process. Timbers were generally radially cut: that is, cut approximately along the log's radius and perpendicular to the rings, and several samples (JOK 5, 7, 8, 9, 10) were cut from

slow-growing trees that were likely part of an old growth forest. These cutting and timber selection techniques created high quality, structurally stable boards containing over 100 to 200 rings, which also made them useful for dendrochronological analysis. However, the heavy shaping process removed the outermost rings from all of the samples, since neither the bark nor vascular cambium is present in any of the samples.

Ten of the 12 pieces collected were successfully crossdated to build a 320-year chronology, whose final measured ring dates to 1810 (Figure 5.5, 5.6). Visual and statistical correlation between two of the samples (JOK 11 and JOK 12) is so strong that it is likely that these boards were cut from the same tree; the measurement sequences from these samples were therefore averaged together and treated as one sequence (JOK 11+12) in the site chronology.

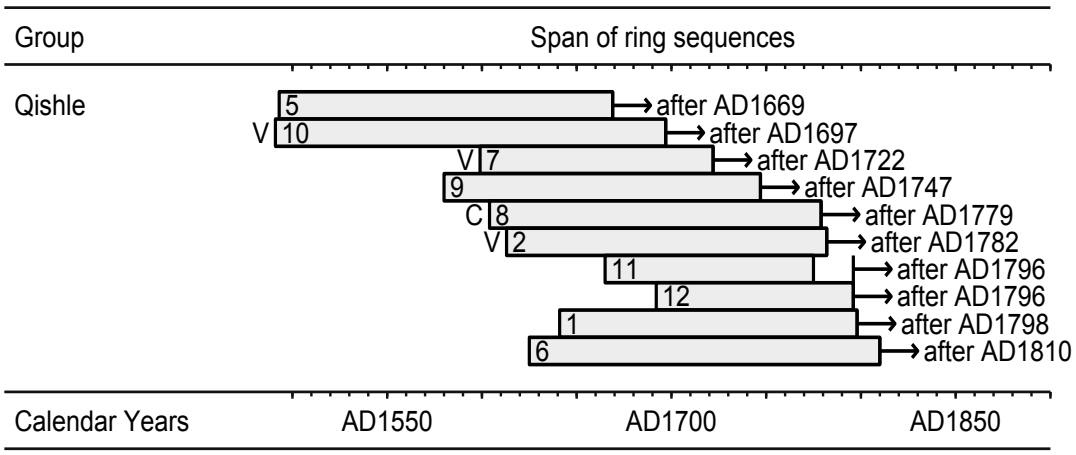

Figure 5.5. Bar graph showing the dendrochronologically dated measurement sequences for each of the samples in the *Qishle* chronology. Measurement sequences with a 'V' at the beginning indicate samples in which the tree's innermost rings but not the pith were present. Measurement sequences with a 'C' indicate samples in which the tree's innermost rings and pith were present.

The individual components of the chronology are divided into four main clusters (samples JOK 1, 2, 11+12; JOK 7, 9; and JOK 5, 8, 10; and JOK 6 as a

distinct individual sequence) with high correlation within each cluster and moderate- to- moderately-poor correlation with the other clusters in the chronology (see: Appendix 5.1 for the internal crossdating statistics of the JOK cedar chronology). Many of the components in the chronology overlap each other by fewer than 100 years, which often lowers correlation dramatically, especially in a typically noisy species like cedar. However, six of the ten individual sample sequences in the chronology, and all of the summed clusters mentioned above, have strong, significant visual and statistical correlation with multiple forest reference chronologies, indicating that their dating placement is correct (see: Appendices 5.2, and 5.3).

The clusters and individual components all correlate best with the same forest reference chronologies, so this suggests that the samples are all likely from the same region, although perhaps not from the same exact stand area. However it should be noted that examination by the author of samples from modern cedar forest stands showed that cedar sample intercorrelation from the same site can sometimes also be low, particularly between trees growing on different slope exposures, trees in different age classes, or at slightly different elevations. In some cases, (like sample JOK-8), local injuries (as evidenced by lines of so-called "traumatic resin ducts" in the wood, which commonly form in cedar after mechanical injury) (Schweingruber 1990) may have slightly altered and caused decreased ring growth, so it is not entirely out of the question that all of the timbers sampled in the *Qishle* chronology were culled from the same forest stand. Thus the site sequences are analyzed as one composite sum.

The last 12 years of the chronology were represented by only one sample, JOK 6, which has a sharp growth decline in 1801–1802 from an indeterminate mechanical

injury to the tree, followed by a sharp growth release from 1803-1810. This growth represents the individual tree's response to a local event and is not indicative of overall growth in the stand. Since this unusual growth response could potentially bias the crossdating results, the ring-width measurements for the last 10 years of the *Qishle* chronology were removed and a truncated chronology was used for crossdating and provenancing.

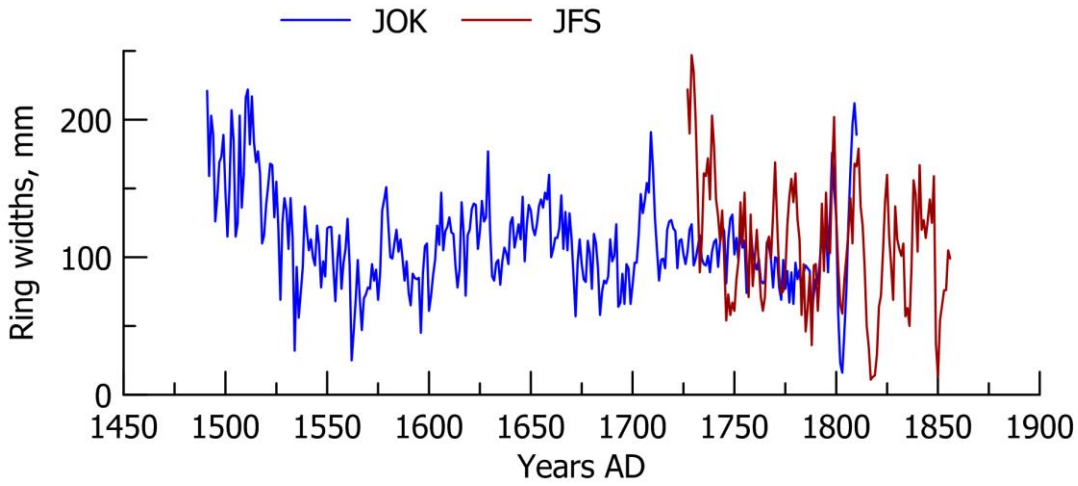

Figure 5.6. Plot showing the crossmatch between the Jaffa *Qishle* (JOK) (*blue*) and Sisters of St. Joseph School (JFS) (*red*) raw cedar chronologies.

Sisters of St. Joseph School

Of the ten samples taken from the Sisters of St. Joseph School, three samples were cedar of Lebanon (*Cedrus libani* A.Rich.), one was cypress (*Cupressus sempervirens* L.), and six were Norway spruce (*Picea abies* (L.) H.Karst.). All of the timbers had been heavily shaped into square and rectangular pieces, so neither the bark nor the vascular cambium is present in any of the samples.

Of the three species found in the building, only cypress is native (although the species has also been planted during the modern era and during antiquity) (Zohary 1962). However, cypress has a broad distribution throughout the Mediterranean; native populations (determined from recent genetic studies and paleobotanical analysis) grow in the eastern Mediterranean from Israel, Lebanon, Syria, Anatolia, the Greek islands, and Italy (Bagnoli et al. 2009), as well as much of the remainder of the Mediterranean basin, where the tree was introduced as a planted species (Meiggs 1982). Furthermore, according to Liphschitz and Biger (1989), cypress trees were rare in Israel during the 19th century and generally grew only in cultivated areas near religious sites, so it is therefore much more likely that the cypress timber analyzed here was also imported to Jaffa.

Dendrochronologically dating cypress timber is not always possible or reliable, since the species is capable of producing multiple rings in one year (Liphschitz et al. 1981) and often produces false rings that are difficult to identify (Schweingruber 1993). The tree's cambium can also remain active during the entire year if sufficient water is available (Stankova et al. 1999), leading to unclear ring boundaries. However Ważny's (2010) recent work with high-elevation cypress trees in Crete has demonstrated that crossdating and building chronologies from historical cypress timbers is possible. The cypress sample from the Sisters of St. Joseph is generally lacking in false rings and density fluctuations, which suggests that the tree grew in a less stressed environment and had a distinct dormant period. The timber yielded a 105-year ring width sequence, but no secure crossdates were found.

The Sisters of St. Joseph cedar timbers, like those found in the *Qishle*, were cut from trees native to the eastern Mediterranean. Two of the three cedar samples (labeled JFS-4 and JFS-7) crossdate to build a 130-year chronology whose final measured ring dates to 1856. The strong visual fit and significant statistical correlation, despite the relatively short overlap between the samples JFS-4 and 7 (t_H= 7.60 and *GL*= 85%, where *n*= 48), suggests that these two samples were cut from slightly different areas on the same tree stem.

Norway spruce is a European species whose wide distribution stretches from the Arctic in Norway across central Europe to the western Alps and east into the Balkans in northern Greece and Bulgaria up to Poland and Russia (Farjon 1990). The spruce timbers in the Sisters of St. Joseph roof were cut from low quality, fast-growing trees with wide, relatively complacent rings, suggesting that they were either from a lower elevation forest or sheltered environment with optimal growth conditions. In general, the timbers were cut from the inner part of the tree stem and included the pith or the area near the tree center.

Four of the six spruce timbers crossdated one another to build a 107-year chronology (Table 5.3). The first 20 years of the chronology were removed for the crossdating exercise, because local environmental conditions caused growth suppression and reaction wood in sample JFS-3 (the only sample in the chronology during this time period), leading to non-representative ring growth (Figure 5.7).

Table 5.3. Internal crossdating statistics for the Sisters of St. Joseph spruce chronology. Dates for each sample sequence are given in relative years, beginning with relative year 1001. Sample sequences that correlate significantly with one another are shaded in gray. t_{BP}= Baillie-Pilcher *t*-value; t_H= Hollstein *t*-value; *GL*= *Gleichläufigkeit* values and their associated *p*-values; *n*= years overlap between the pairs of chronologies. For the *GL* *p*-values, ***= $p<0.001$; **= $p<0.01$; and *= $p<0.05$.

	JFS-1 *1021-1107*	JFS-3 *1001-1100*	JFS-8 *1051-1105*	JFS-10 *1027-1092*
JFS-3	**t_H=6.2** **t_{BP}=5.1** ***GL*=63*** ***n*=80**			
JFS-8	t_H=4.1 t_{BP}=4.1 *GL*=57 *n*=55	**t_H=5.9** **t_{BP}=5.9** ***GL*=56*** ***n*=50**		
JFS-10	**t_H=5.4** **t_{BP}=4.8** ***GL*=65**** ***n*=66**	**t_H=10.7** **t_{BP}=6.2** ***GL*=75****** ***n*=66**	**t_H=4.7** **t_{BP}=2.9** ***GL*=66*** ***n*=42**	

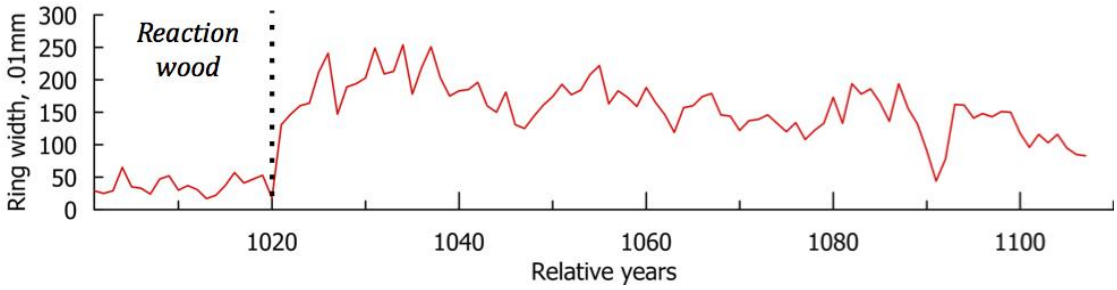

Figure 5.7. Relatively dated spruce chronology from the Sisters of St. Joseph School. There was unusual growth suppression and reaction wood in the rings from the first 20 years of the chronology (*before the dashed line*).

At present, the Sisters of St. Joseph spruce chronology cannot be absolutely dated and is therefore only a relative chronology. The lack of a significant crossdate is likely because the chronology is relatively short (87 years) and complacent. Furthermore, many of the existing European spruce chronologies have been built for the purpose of dendroclimatic reconstruction and are therefore comprised of trees with sensitive ring growth (Wilson et al. 2004). Additionally many European spruce chronologies have been developed for the dating of musical instruments, which require slower-growing, high-quality spruce timber (Bernabei et al. 2010; Burckle and Grissino-Mayer 2003). Previous studies of spruce ring growth along altitudinal transects have demonstrated that spruce tree-ring chronologies built from high elevation forests cannot be used to date spruce timbers from low elevation sites (and vice versa) (Wilson and Hopfmueller 2001). Therefore additional sampling of low elevation spruce forests in Europe will be needed before this material can be dated successfully.

Dendroprovenancing

***Qishle* Complex**

Chronologies built from cedar forests in the western area of the Antalya province in western Turkey–both Kuniholm's chronology (2000b) from Çığlıkara Forest in the Avlan Section and Touchan et al.'s (2005) chronology near Hüseyin Kuyusu and Kocagüney–have by far the highest correlation with the *Qishle* chronology (Table 5.4; Figure 5.8). There is also significant correlation between the *Qishle* chronology and Touchan et al.'s (2005) chronology from the Katrandağı Forest in the Burdur province.

Correlation between the *Qishle* chronology and forest chronologies from further east in Turkey (both at inland and coastal sites), Cyprus, and Lebanon is low. There is moderate correlation between the Jaffa *Qishle* and Touchan et al.'s (2005) chronology from Bcharrê Forest in Lebanon (especially if the t_{BP}-value rather than the t_{H}-value is considered), although this is likely because the two chronologies overlap one another for a long period of time and more of the long-term similarities between the Turkish and Lebanese cedar chronologies are available to compare (which strengthens the statistical correlation). However, the Jaffa *Qishle* chronology's statistical correlation and particularly its visual fit with the Bcharrê chronology is still nowhere near as high as the statistical and visual matches between the *Qishle* and western Antalya forest chronologies in Turkey.

It is also notable that many of the individual sequences of the *Qishle* chronology (which are shorter and preserve the more localized environmental responses of each tree, which generally lowers correlation with composite reference chronologies) have significant fits with the western Antalya forest chronologies (see: Appendix 5.2). This is especially impressive, given how cedar often produces tree-rings with a more localized response and therefore 'noisier' tree-ring sequences than those of other tree species like oak or juniper.

The Jaffa *Qishle* chronology has strong visual and statistical correlation with historical cedar chronologies built from Toplou Monastery in Lassithi, eastern Crete; historical buildings in the Old Town in Rhodes; the Karatay Medrese in Konya, Turkey; and the Sisters of St. Joseph School in Jaffa. The chronology also had significant correlation with, and was instrumental in confirming the

dendrochronological date of, a pair of painted post-Byzantine cedar icons from the Rhodes Museum, which depict the birth of the Virgin Mary (*γενιστα της θεοτοκου*) and her presentation to the Temple (*εισοδια της θεοτοκου*). All of these chronologies contain timbers that were cut while these sites were under Ottoman administration and correlate with cedar forest chronologies from western Turkey and not with those from Lebanon, Cyprus, or eastern Turkey. One of the timbers sampled from the Old Town in Rhodes even had the stamp of a Turkish forester on it, providing further confirmation of cedar importation from Turkey.

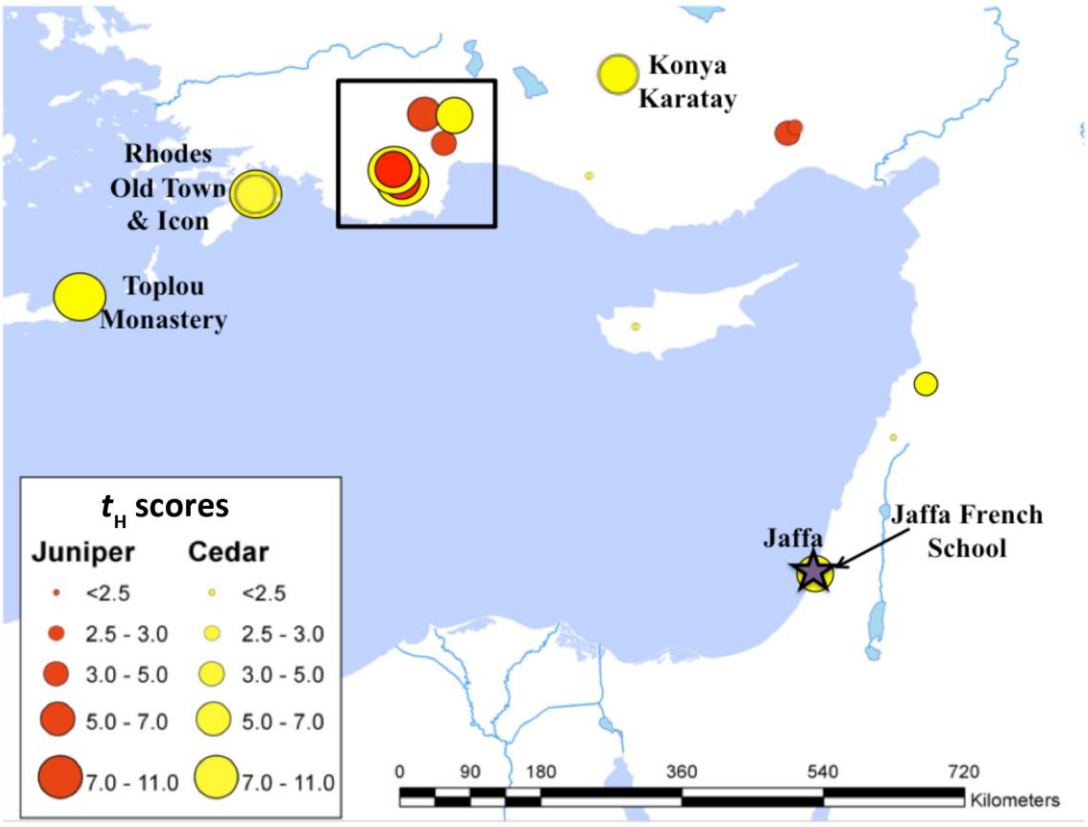

Figure 5.8. **Map showing distribution of t_H-values for cedar (*yellow*) and juniper (*red*) forest and historical chronologies (*labeled*) in the eastern Mediterranean compared with the Jaffa *Qishle* chronology. Increasing circle size corresponds to increasing t_H-value magnitude. The forest sites showing the strongest correlation with the Jaffa *Qishle* timbers are clustered around the western area of Antalya and Burdur provinces in Turkey (*outlined with a rectangle*).**

Table 5.4. Crossdating statistics between the JOK chronology and cedar and juniper reference chronologies. Reference chronologies that are significantly correlated with the JOK chronology are shaded in gray. t_{BP}= Baillie-Pilcher *t*-value; t_H= Hollstein *t*-value; and *GL= Gleichläufigkeit* values and their associated *p*-values. For *GL p*-values, ***= $p<0.001$; **= $p<0.01$; and *= $p<0.05$.

Reference Chronology	Author	Chronology dates (AD)	t_H	t_{BP}	GL (%)	Overlap years
Turkey, Antalya, Elmalı İşletmesi, Çığlıkara Forest	Kuniholm 2000b	1370-2001	9.0	10.0	66***	310
Turkey, Antalya, Elmalı Hüseyin Kuyusu and Kocagüney Forest	Touchan et al. 2005	1449-2000	8.1	10.2	69***	310
Greece, Crete, Toplou Monastery	Ważny, *unpublished*	1596-1856	7.7	8.1	70***	205
Turkey, Antalya, Elmalı juniper	Touchan et al. 2005	1017–2006	6.8	5.6	63***	310
Greece, Rhodes, Old Town	Kuniholm, *unpublished*	1592-1876	6.7	6.9	62***	209
Turkey, Burdur, Katrandağı Forest	Touchan et al. 2005	1693-2000	6.2	5.6	71***	108
Greece, Rhodes, *Ta Hodia tes Theotokou*	Kuniholm, *unpublished*	1614-1780	5.5	6.7	60**	167
Israel, Jaffa, Sisters of St. Joseph School	Lorentzen, *this study*	1727-1856	5.4	3.9	67**	74
Turkey, Konya, Karatay Medrese	Kuniholm 2000b	1551-1831	5.4	5.0	64***	250
Turkey, Burdur, Su Batan juniper	Touchan et al. 2005	1246-2000	5.2	6.3	63***	310
Turkey, Antalya, Elmalı İşletmesi juniper	Kuniholm 2001	1360–1988	5.1	5.8	60***	310
Turkey, Antalya, Göller juniper	Touchan et al. 2005	1152-2000	4.5	6.2	57***	310
Lebanon, Bcharrê Forest	Touchan et al. 2005	1382-2002	4.0	5.4	61***	310
Turkey, Antalya, Akseki, Murtiçi, Salamut Yaylası	Kuniholm and Groneman 2001	1551-1998	3.6	4.0	65***	250
Turkey, Mersin, Neseli juniper	Touchan et al. 2005	1235-2001	3.3	4.5	57**	310
Turkey, Mersin, Silpisli juniper	Touchan et al. 2005	1350-2001	2.7	3.8	60***	310
Turkey, Mersin, Ananardiç juniper	Touchan et al. 2005	1330–2001	2.6	3.3	60***	310
Turkey, Antalya, Yelliç Belli Forest	Touchan et al. 2005	1628-2000	2.5	1.8	59**	173
Cyprus, Tripylos Forest	Touchan et al. 2005	1532-2002	1.6	1.1	56*	269
Lebanon, Maaser Forest	Touchan et al. 2005	1730–2002	0.9	1.3	58	71

Sisters of St. Joseph School

The Sisters of St. Joseph cedar chronology did not yield any statistically significant fits against the available modern forest chronologies. The chronology has moderate correlation with Touchan et al.'s (2005) chronologies from Yelliç Belli in the eastern part of the Antalya province and Katrandağı in Burdur province (Table 5.5), although these results are still not statistically significant.

The chronology does have strong visual and statistical correlation with the historical chronologies from the Old Town in Rhodes and the Jaffa *Qishle*. There is also moderate correlation between the chronology from the Sisters of St. Joseph and the post-Byzantine icon chronology from Rhodes, which although not significant, has a good visual fit and moderate correlation, despite the relatively short overlap (n= 54).

The Sisters of St. Joseph chronology may lack a significant fit against the forest chronologies because of its shorter sequence represented by only one or two individual trees, or possibly because the building's timbers were cut from a forest whose regional chronological signal is not well-represented by the current cedar tree-ring data. However, since the Rhodes and Jaffa *Qishle* chronologies are strongly correlated with that from the Sisters of St. Joseph and provenanced to forests in western Turkey in the area of Antalya and not Syria, Lebanon, or Cyprus, the Sisters of St. Joseph school cedars are most likely also from Turkey.

Table 5.5. Crossdating statistics between the JFS cedar chronology and cedar and juniper reference chronologies. Reference chronologies that are significantly correlated with the JFS chronology are shaded in gray. t_{BP}= Baillie-Pilcher *t*-value; t_H= Hollstein *t*-value; and *GL= Gleichläufigkeit* values and their associated *p*-values. For *GL p*-values, ***= $p<0.001$; **= $p<0.01$; and *= $p<0.05$.

Reference Chronology	Author	Chronology dates (AD)	t_H	t_{BP}	GL (%)	Overlap years
Greece, Rhodes, Old Town	Kuniholm, *unpublished*	1592-1876	6.4	5.0	64***	130
Israel, Jaffa, *Qishle*	Lorentzen, *this study*	1492-1810	5.4	3.9	66**	74
Turkey, Antalya, Yelliç Belli Forest	Touchan et al. 2005	1628-2000	3.8	3.0	60*	130
Turkey, Burdur, Katrandağı Forest	Touchan et al. 2005	1693-2000	3.3	3.0	59*	130
Greece, Rhodes, *Ta Hodia tes Theotokou*	Kuniholm, *unpublished*	1614-1780	3.2	4.0	68**	54
Turkey, Mersin, Neseli juniper	Touchan et al. 2005	1235-2001	3.1	2.3	62*	74
Lebanon, Maaser Forest	Touchan et al. 2005	1730–2002	3.0	2.8	60*	127
Turkey, Antalya, Elmalı İşletmesi, Çığlıkara Forest	Kuniholm 2000b	1370-2001	2.8	2.9	63**	130
Cyprus, Tripylos Forest	Touchan et al. 2005	1532-2002	2.8	2.5	61**	130
Turkey, Antalya, Elmalı Hüseyin Kuyusu and Kocagüney Forest	Touchan et al. 2005	1449-2000	2.7	2.6	62**	130
Turkey, Konya, Karatay Medrese	Kuniholm 2000b	1551-1831	2.6	2.8	60*	105
Lebanon, Arz Jaj Forest	Touchan et al. 2005	1778–2002	2.1	1.7	59	79
Turkey, Antalya, Akseki, Murtiçi, Salamut Yaylası	Kuniholm and Groneman 2001	1551-1998	1.9	1.6	53	130
Turkey, Mersin, Ananardiç juniper	Touchan et al. 2005	1330-2001	1.4	1.6	60	130
Turkey, Antalya, Elmalı İşletmesi juniper	Kuniholm 2001	1360–1988	1.2	0.4	56	130
Turkey, Antalya, Göller juniper	Touchan et al. 2005	1152-2000	1.0	1.1	60*	64
Turkey, Antalya, Elmalı juniper	Touchan et al. 2005	1017–2006	0.9	0.3	62*	74
Greece, Crete, Toplou Monastery	Ważny, *unpublished*	1596-1856	0.6	0.1	57	130
Lebanon, Bcharrê Forest	Touchan et al. 2005	1382-2002	0.5	0.3	55	130

DISCUSSION

Dendrochronological Dates

None of the samples from the *Qishle* complex or the Sisters of St. Joseph School had bark or the vascular cambium present. The dendrochronological dates from both sites accordingly provide a *terminus post quem* for their construction.

The sample (JOK 6) containing the end date of the *Qishle* site chronology has one more partial, unmeasured ring after the last measured ring in 1810. Therefore the Jaffa *Qishle* floorboards provide a *terminus post quem* construction date of 1811 and were likely part of the original building construction. The 1811 date precedes the proposed 1886/7 construction date for the complex by about 75 years, and other timbers (such as samples JOK-5 and 10) precede this date by an even longer period of time. While it is possible that the timbers may have been reused from the earlier buildings near the site, it is far more likely, especially given the heavy modification required to shape the floorboards, that the trees used to make this timber were cut in the late 1880s, but that the outermost rings of the tree were removed when the boards were cut. In four of the samples, the innermost rings of the tree and, in one case, the pith (the cells at the center of the tree stem) are present, so it is clear that these boards were cut from the area near the center of the tree trunk. Many of these boards were also cut from old-growth trees, where the rings are small and densely packed, so it would be very easy to remove decades and even one to two centuries of ring growth during the shaping process.

The sample (JFS-7) containing the end date of the Sisters of St. Joseph school chronology also had one partial, unmeasured ring after the last measured ring of 1856,

so it provides a *terminus post quem* of 1857 for the building's construction and was likely part of the original roof timbers. All of the sampled timbers also had carpenter's assembly marks using the same truss numbering system, suggesting that they were installed at the same time during the original roof's construction. The dendrochronological date precedes the building's documented 1882 construction, but like the *Qishle* complex timbers, the timbers were heavily shaped, and so the tree's outermost rings were also likely removed during the timber cutting process.

Dendroprovenancing

The growing population of European communities and the development of new transportation routes and more efficient transport during Jaffa's Late Ottoman florescence brought increased access to, and usage of, timber from European forests. While long-distance timber trade between Europe and the southern Levant existed prior to the 19th century, the building of the Suez Canal, new railroads, and the creation of faster steamships dramatically increased traffic from European ships and made it easier for traders to bring timbers from more distant locations. The establishment of European consulates in Jaffa and the influx of European religious immigrants to Palestine increased ties between Europe and Palestine. These groups used timber that either they brought with them from Europe, or that were available in Jaffa for their building projects, like the spruce found in the Sisters of St. Joseph School, as well as countless other timbers of European tree species found in Jaffa (Biger and Liphschitz 1991a), Jerusalem (Biger and Liphschitz 1991b), and other communities in Palestine (Biger and Liphschitz 1992).

Despite the growing importation of European timber during the Late Ottoman Period, the data from the *Qishle* and Sisters of St. Joseph School indicates that, contrary to the assertion of Biger and Liphschitz (1991a), Anatolian/Mediterranean timbers were still used in both European and Ottoman building projects after the 1870s. An account by the French geographer Vital Cuinet (1896) of timbers being imported to Jaffa during the year 1895 supports this, since he lists timber coming from both the Danube and *Karamania* (southern Turkey) into Jaffa during this time.

The presence of timbers of native Mediterranean cedar and cypress in addition to European spruce in the Sisters of St. Joseph roof suggests that instead of bringing timbers specifically from France for the building's construction, the school's builders used whatever suitable timbers were available for purchase in Jaffa, which included wood from both East Mediterranean and European trees. Similar results were found in Crete, where late 19th-century buildings like Toplou Monastery contained both cedar timber dendroprovenanced to southwestern Anatolia; silver fir (*Abies alba*) cut during the same time period and dendroprovenanced to central Europe; and (currently undated) Norway spruce, also from Europe (Ważny, *unpublished data*).

The presence of cedar of Lebanon wood in both the *Qishle* and the Sisters of St. Joseph School demonstrates the continued value of this tree's timber for building projects in the southern Levant and confirms the importance of the Anatolian cedar forests as a natural resource for the Ottoman Empire.[3] In antiquity, cedar wood was prized by carpenters, because it is durable, easy to work with, has a straight grain,

[3] For a longer discussion of the role of the Anatolian forests in the Ottoman economy, and timber trade between Anatolia and Egypt especially, see: Mikhail 2011.

takes a good polish, has a pleasant smell, and can produce long, straight timbers for large-scale building projects and shipbuilding (Bikai 1991; Meiggs 1982). Cedar wood was imported, likely from Lebanon, to Egypt as early as the 4th millennium BC (Kuniholm, et al. 2007), and cedar wood has been found in several archaeological sites in Israel beginning in at least the Early Bronze Age (Liphschitz 2007). Biblical authors name Jaffa itself as the port receiving cedar wood from Lebanon for building both the First and Second Temples (2 Chronicles 2:15; Ezra 3:7).

In addition to the timber in the *Qishle* and Sisters of St. Joseph, cedar wood has been found in 19th and early 20th century buildings at over 44 sites in Israel (Liphschitz and Biger 1992). However, by that time, cedar forests, particularly old growth forests like those used to make the *Qishle* floor and the Sisters of St. Joseph posts, grew in Lebanon only in degraded, fragmentary stands after several centuries of overexploitation (Mikesell 1969; Porter 1866; Tristram 1882). In contrast, an extremely active trade in timber, including cedar, is documented between Ottoman Anatolia and Palestine (Cuinet 1896; McNeill 1992; Mikhail 2011). In fact, Cuinet (1896) reports that by at least 1895, cities in Lebanon, including Beirut, were also importing timber from southern Anatolia, the Danube River valley, and Trieste (the main port of the Austro-Hungarian Empire), further indicating that Anatolia, not Lebanon, was the major source of cedar timber in the southern Levant at that time. This documentation and oral accounts from local inhabitants in Israel (Liphschitz and Biger 1991a) indicate that Anatolia was the likely source of these 19th century timbers, not Lebanon.

The dendroprovenancing data from the *Qishle* complex and Sisters of St. Joseph strongly supports this conclusion and more specifically gives scientific evidence that the *Qishle* cedars were cut from forests in the western area of the Antalya province. This information fits well with historical records, which confirm that the Antalya port, along with the ports of Alanya, Finike, and Mersin (Figure 5.9), exported high volumes of timber culled from mountain forests further inland and floated downriver to the ports during the late 19th century (McNeill 1992).

CONCLUSIONS

The high correlation between the southwestern Turkish cedar and *Qishle* chronologies, as well as strong correlation between the *Qishle* and the Sisters of St. Joseph chronologies with those from other historical Ottoman sites, indicates that Jaffa was part of a far-reaching maritime and overland trading network that also supplied inland Anatolia (i.e., Konya Karatay Medrese) and the Aegean islands. The builders of the *Qishle* and Sisters of St. Joseph School were therefore able to take advantage of Jaffa's position in these well-developed Anatolian and European timber trading networks to obtain suitable materials for their construction projects in the expanding Late Ottoman city. Further dendrochronological dating and provenancing of timbers from other historical buildings in Jaffa and other important sites in the Levant and Egypt will provide additional information on exploitation of the Mediterranean and European forests, timber trade, and the environmental history of the region.

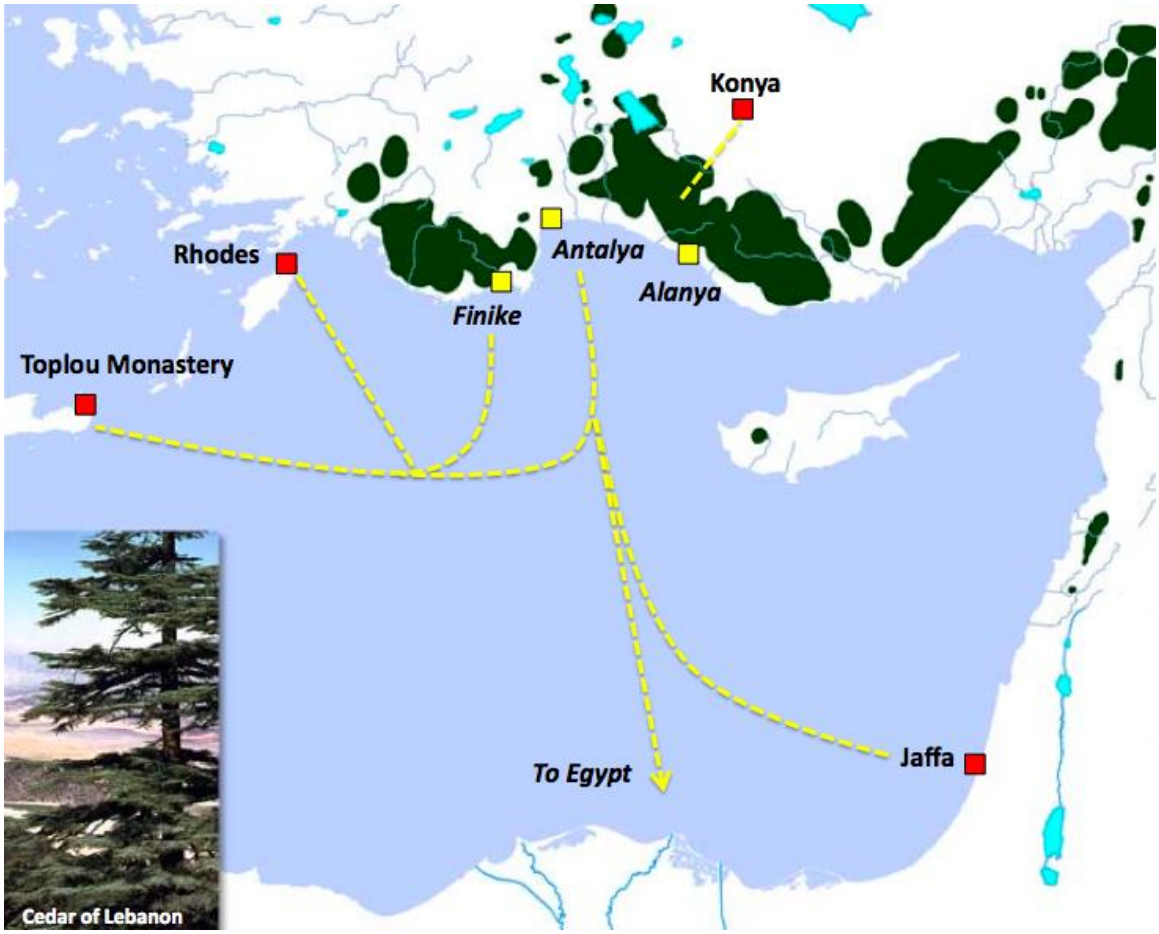

Figure 5.9. Reconstruction of Ottoman cedar trade routes from dendro-provenancing data and historical sources. The modern distribution of cedar of Lebanon (*inset*) is shaded in green. *Photo credit*: *Peter I. Kuniholm*.

APPENDIX 5.1

Internal crossdating statistics for the Jaffa *Qishle* (JOK) cedar chronology. Samples that correlate significantly with one another are shaded in gray. t_{BP}= Baillie-Pilcher *t*-value; t_H= Hollstein *t*-value; *GL= Gleichläufigkeit* values and their associated *p*-values; *n*= years overlap between the pairs of tree-ring sequences. For *GL p*-values, ***= $p<0.001$; **= $p<0.01$; and *= $p<0.05$. The statistical crossmatch between samples JOK-11 and 12 (*in bold*) is so high that the samples are likely cut from the same tree and were summed together as one composite sequence in the JOK cedar chronology.

	1 *1641-1798*								
2	t_H=8.9 t_{BP}=8.6 *GL*=68*** *n*=142	2 *1613-1782*							
5	*n*=29	t_H=2.1 t_{BP}=4.0 *GL*=57 *n*=57	5 *1493-1669*						
6	t_H=3.7 t_{BP}=4.9 *GL*=63*** *n*=158	t_H=5.1 t_{BP}=4.8 *GL*=63*** *n*=158	*n=45*	6 *1625-1800*					
7	t_H=1.2 t_{BP}=2.8 *GL*=58 *n*=82	t_H=3.1 t_{BP}=3.4 *GL*=57 *n*=110	t_H=1.9 t_{BP}=1.8 *GL*=60* *n*=71	t_H=2.8 t_{BP}=2.5 *GL*=67*** *n*=98	7 *1599-1722*				
8	t_H=2.0 t_{BP}=3.0 *GL*=59* *n*=139	t_H=3.4 t_{BP}=3.6 *GL*=61** *n*=167	t_H=1.6 t_{BP}=2.4 *GL*=63* *n*=66	t_H=2.2 t_{BP}=2.7 *GL*=67*** *n*=155	t_H=3.2 t_{BP}=3.3 *GL*=67*** *n*=119	8 *1604-1779*			
9	t_H=1.8 t_{BP}=2.5 *GL*=54 *n*=107	t_H=2.9 t_{BP}=3.8 *GL*=56 *n*=135	t_H=4.7 t_{BP}=4.8 *GL*=57 *n*=90	t_H=3.1 t_{BP}=3.8 *GL*=66*** *n*=123	t_H=5.1 t_{BP}=6.1 *GL*=66*** *n*=124	t_H=1.5 t_{BP}=2.8 *GL*=58* *n*=144	9 *1580-1747*		
10	t_H= 1.6 t_{BP}=2.8 *GL*= 51 *n*=57	t_H=3.5 t_{BP}=3.8 *GL*=64** *n*=85	t_H=6.9 t_{BP}=8.3 *GL*=70*** *n*=177	t_H=1.9 t_{BP}=2.0 *GL*=61* *n*=73	t_H=4.0 t_{BP}=4.1 *GL*=70*** *n*=99	t_H=4.9 t_{BP}=6.0 *GL*=73*** *n*=94	t_H=3.6 t_{BP}=5.2 *GL*=59* *n*=118	10 *1491-1697*	
11	t_H=7.8 t_{BP}=9.0 *GL*=72*** *n*=111	t_H=4.4 t_{BP}=5.4 *GL*=72*** *n*=111	*n=5*	t_H=1.7 t_{BP}=3.2 *GL*=64** *n*=111	t_H=1.3 t_{BP}=2.7 *GL*=69** *n*=58	t_H=4.4 t_{BP}=5.2 *GL*=64** *n*=111	t_H=0.5 t_{BP}=2.3 *GL*=53 *n*=93	*n*=33	11 *1665-1775*
12	t_H=5.5 t_{BP}=6.0 *GL*=66*** *n*=105	t_H=3.4 t_{BP}=3.4 *GL*=66** *n*=91	*n=0*	t_H=2.5 t_{BP}=2.6 *GL*=64** *n*=105	*n*=31	t_H=3.8 t_{BP}=2.5 *GL*=59* *n*=88	t_H=1.3 t_{BP}=1.4 *GL*=53 *n*= 56	*n=6*	**t_H=16.3 t_{BP}=14.5 *GL*=79*** *n*=84**

12
1692-1796

APPENDIX 5.2

Crossdating statistics between individual sample sequences in the JOK chronology (given by sample number) and cedar reference chronologies from forests and historical sites in the East Mediterranean. Sample sequences and reference chronologies that correlate significantly with one another are shaded in gray; crossmatches in which t_{BP} and t_H > 5.0 are in bold. t_{BP}= Baillie-Pilcher *t*-value; t_H= Hollstein *t*-value; *GL= Gleichläufigkeit* values and their associated *p*-values; *n*= years overlap between the pairs of tree-ring sequences. For the *GL p*-values, *= *p*<0.001; **= *p*<0.01; and *= *p*<0.05.**

Reference Chronology

Cyprus, Tripylos Forest	**1**	**2**	**5**	**6**	**7**	**8**	**9**	**10**	**11+12**
t_H	0.9	2.5	1.3	1.9	0.4	0.3	0.9	0.2	1.8
t_{BP}	2.1	4.3	1.7	3.0	0.8	1.3	2.4	0.1	1.5
GL	53	56	57	54	55	51	54	52	55
n	158	170	138	176	124	176	168	166	105
Lebanon, Bcharrê Forest	**1**	**2**	**5**	**6**	**7**	**8**	**9**	**10**	**11+12**
t_H	2.4	1.7	2.2	2.5	0.1	0.2	2.2	2.5	1.3
t_{BP}	2.4	1.9	3.5	2.8	0.3	0.8	2.7	2.8	3.2
GL	61**	55*	59**	60**	49	57*	62***	58*	53
n	158	170	177	176	124	176	168	207	105
Turkey, Antalya, Elmalı İşletmesi, Çığlıkara Forest	**1**	**2**	**5**	**6**	**7**	**8**	**9**	**10**	**11+12**
t_H	4.6	**5.4**	**5.6**	**6.3**	3.7	2.7	**5.8**	4.0	3.2
t_{BP}	4.8	**5.6**	**6.0**	**5.6**	3.8	4.0	**6.5**	6.7	3.3
GL	61**	**61****	**57***	**65*****	72***	58*	**63*****	63***	63**
n	158	**170**	**177**	**176**	124	176	**168**	207	105
Turkey, Antalya, Elmalı Hüseyin Kuyusu and Kocagüney Forest	**1**	**2**	**5**	**6**	**7**	**8**	**9**	**10**	**11+12**
t_H	3.4	3.9	**5.9**	**8.9**	3.5	0.8	**6.5**	**5.2**	2.7
t_{BP}	3.8	5.1	**6.8**	**9.0**	3.9	2.4	**7.9**	**8.0**	2.9
GL	60**	63***	**63*****	**72*****	62**	57*	**69*****	**61*****	61*
n	158	170	**177**	**176**	124	176	**168**	**207**	105
Turkey, Antalya, Akseki, Murtiçi, Salamut Yaylası	**1**	**2**	**5**	**6**	**7**	**8**	**9**	**10**	**11+12**
t_H	3.2	3.2	0.6	1.8	3.7	0.5	4.8	3.0	1.9
t_{BP}	3.8	4.2	0.3	2.6	5.0	1.4	3.1	2.7	3.3
GL	60**	58*	58*	58*	64***	58*	61**	60**	65**
n	158	170	119	176	124	176	168	147	105
Turkey, Antalya, Yelliç Belli Forest	**1**	**2**	**5**	**6**	**7**	**8**	**9**	**10**	**11+12**
t_H	1.2	1.3	0.9	1.7	0.8	0.2	0.6	0.5	1.8
t_{BP}	1.2	1.0	0.5	0.9	0.3	0.0	0.8	0.2	1.9
GL	56	51	64*	61**	62*	52	58*	56	63**
n	168	155	42	173	95	152	120	70	105
Turkey, Burdur, Katrandağı Forest	**1**	**2**	**5**	**6**	**7**	**8**	**9**	**10**	**11+12**
t_H	4.4	4.8		3.3	0.9	0.7	0.5		2.9
t_{BP}	4.1	4.5		3.0	2.7	1.2	1.9		3.5
GL	60*	69***		59*	48	45	53		62**
n	106	90	*0*	108	30	86	55	*5*	104

APPENDIX 5.2 (*continued*)

Reference Chronology

Greece, Crete, Toplou Monastery	**1**	**2**	**5**	**6**	**7**	**8**	**9**	**10**	**11+12**
t_H	4.4	4.3	3.8	**6.2**	3.3	2.1	3.9	3.2	3.3
t_{BP}	4.3	4.4	4.8	**6.8**	4.5	3.8	6.4	5.4	3.4
GL	63***	60**	69***	**65*** **	69***	58*	61**	62*	64**
n	158	170	74	**176**	124	176	152	102	105
Greece, Rhodes, Old Town	**1**	**2**	**5**	**6**	**7**	**8**	**9**	**10**	**11+12**
t_H	**5.1**	3.6	4.0	3.5	3.1	1.2	3.5	3.1	2.8
t_{BP}	**5.5**	3.8	4.3	3.3	3.7	3.0	4.8	4.7	3.2
GL	**62****	58*	60*	65***	67***	58*	57*	61*	60*
n	**158**	170	78	176	124	176	156	106	105
Greece, Rhodes, *Ta Hodia tes Theotokou*	**1**	**2**	**5**	**6**	**7**	**8**	**9**	**10**	**11+12**
t_H	3.9	4.2	1.7	2.4	2.4	0.9	3.1	2.8	1.8
t_{BP}	4.6	4.6	2.5	3.5	2.5	1.5	4.6	2.4	3.2
GL	58*	57*	61*	57*	62**	51	63**	64**	65**
n	140	167	56	156	109	166	134	84	89
Israel, Jaffa, Sisters of St. Joseph School	**1**	**2**	**5**	**6**	**7**	**8**	**9**	**10**	**11+12**
t_H	4.4	1.9		4.9		0.4			3.7
t_{BP}	4.0	2.2		3.4		0.5			3.9
GL	65**	63*		70***		61			62*
n	72	56	*0*	74	*0*	53	*21*	*0*	70
Turkey, Konya, Karatay Medrese	**1**	**2**	**5**	**6**	**7**	**8**	**9**	**10**	**11+12**
t_H	**5.1**	4.9	1.2	**6.3**	1.5	1.7	2.8	2.1	2.4
t_{BP}	**5.0**	5.6	1.4	**5.5**	1.1	2.4	3.2	2.1	3.6
GL	**63*****	66***	56	**63*****	58*	59**	57*	51	64**
n	**158**	170	119	**176**	124	176	168	147	105

APPENDIX 5.3

Crossdating statistics between groups of samples within the JOK chronology that have high correlation with one another (sample numbers comprising each group given) and cedar reference chronologies from forests and historical sites in the East Mediterranean. Sample groups and reference chronologies that correlate significantly with one another are shaded in gray; crossmatches in which t_{BP} and t_H > 5.0 are in bold. t_{BP}= Baillie-Pilcher *t*-value; t_H= Hollstein *t*-value; *GL*= *Gleichläufigkeit* values and their associated *p*-values; *n*= years overlap between the pairs of tree-ring sequences. For the *GL* *p*-values, ***= $p<0.001$; **= $p<0.01$; and *= $p<0.05$.

Reference Chronology	JOK-1, 2, 11, 12	JOK- 5, 8, 10	JOK-7,9
Cyprus, Tripylos Forest	t_H= 2.2 t_{BP}= 3.3 *GL*= 55 *n*= 186	t_H= 1.5 t_{BP}= 1.9 *GL*= 51 *n*= 248	t_H= 0.7 t_{BP}= 1.7 *GL*= 54 *n*= 168
Lebanon, Bcharrê Forest	t_H= 2.3 t_{BP}= 2.7 *GL*= 57* *n*= 186	t_H= 2.6 t_{BP}= 3.5 *GL*= 58** *n*= 289	t_H= 0.9 t_{BP}= 1.4 *GL*= 56 *n*= 168
Turkey, Antalya, Elmalı İşletmesi, Çığlıkara Forest	**t_H= 5.5** **t_{BP}= 6.0** ***GL*= 66***** ***n*= 186**	**t_H= 5.6** **t_{BP}= 7.1** ***GL*= 60***** ***n*= 289**	**t_H= 5.7** **t_{BP}= 6.0** ***GL*= 68***** ***n*= 168**
Turkey, Antalya, Elmalı Hüseyin Kuyusu and Kocagüney Forest	t_H= 4.2 t_{BP}= 5.1 *GL*= 64*** *n*= 186	t_H= 3.3 t_{BP}= 5.3 *GL*= 61*** *n*= 289	**t_H= 5.2** **t_{BP}= 6.3** ***GL*= 67***** ***n*= 168**
Turkey, Antalya, Akseki, Murtiçi, Salamut Yaylası	t_H= 3.8 t_{BP}= 5.2 *GL*= 63*** *n*= 186	t_H= 1.5 t_{BP}= 1.6 *GL*= 54 *n*= 229	t_H= 3.2 t_{BP}= 5.0 *GL*= 66*** *n*= 168
Turkey, Antalya, Yelliç Belli Forest	t_H= 2.0 t_{BP}= 1.9 *GL*= 58* *n*= 171	t_H= 0.4 t_{BP}= 0.4 *GL*= 51 *n*= 152	t_H= 0.5 t_{BP}= 0.1 *GL*= 57 *n*= 120
Turkey, Burdur, Katrandağı Forest	**t_H= 5.3** **t_{BP}= 5.2** ***GL*= 74***** ***n*= 106**	t_H= 0.4 t_{BP}= 0.7 *GL*= 55 *n*= 87	t_H= 0.6 t_{BP}= 1.8 *GL*= 57 *n*= 55

APPENDIX 5.3 (*continued*)

Reference Chronology	JOK-1,2,11, 12	JOK-5,8,10	JOK-7,9
Greece, Crete, Toplou Monastery	t_H= 4.4 t_{BP}= 4.8 *GL*= 65*** *n*= 186	t_H= 3.9 t_{BP}= 5.4 *GL*= 62*** *n*= 184	t_H= 4.4 t_{BP}= 6.8 *GL*= 66*** *n*= 152
Greece, Rhodes, Old Town	t_H= 4.7 t_{BP}= 5.0 *GL*= 59** *n*= 186	t_H= 3.2 t_{BP}= 4.8 *GL*= 59** *n*= 188	t_H= 3.5 t_{BP}= 4.6 *GL*= 64*** *n*= 156
Greece, Rhodes, *Ta Hodia tes Theotokou*	t_H= 3.9 t_{BP}= 4.9 *GL*= 62** *n*= 167	t_H= 1.4 t_{BP}= 2.2 *GL*= 54 *n*= 166	t_H= 3.3 t_{BP}= 4.2 *GL*= 66*** *n*= 134
Israel, Jaffa, Sisters of St. Joseph School	t_H= 4.7 t_{BP}= 4.5 *GL*= 66** *n*= 72	t_H= 0.4 t_{BP}= 0.5 *GL*= 61 *n*= 53	*n=21*
Turkey, Konya, Karatay Medrese	t_H= 4.5 t_{BP}= 5.0 *GL*= 67*** *n*= 186	t_H= 3.2 t_{BP}= 3.4 *GL*= 59 *n*= 229	t_H= 2.0 t_{BP}= 2.3 *GL*= 56 *n*= 168

REFERENCES

Akkemik, Ü., 2003. Tree rings of *Cedrus libani* at the northern boundary of its natural distribution. *IAWA Journal* 24 (1): 63–73.

Akkemik, Ü., Caner, H., Conyers, G.A., Dillon, M.J., Karlıoğlu, N., Rauh, N.K., Theller, L.O., 2012. The archaeology of deforestation in south coastal Turkey. *International Journal of Sustainable Development and World Ecology* 19 (5): 395–405.

Arbel, Y., 2009. Yafo, the *Qishle*. Hadashot Arkhaeologiyot–Excavations and Surveys in Israel 121. Electronic document, http://www.hadashot-esi.org.il/report_detail_eng.asp?id=1051&mag_id=115. Accessed 1 October, 2012. (Hebrew with English abstract)

Avitzur, S., 1972. *Jaffa Port: Rise and Fall, 1865-1965*. Milo Press, Tel Aviv. (Hebrew)

Bagnoli, F., Vendramin, G.G., Buonamici, A., Doulis, G., Gonzalez-Martinez, S.C., La Porta, N., Magri, D., Raddi, P., Sebastiani, F., Fineschi, S., 2009. Is *Cupressus sempervirens* native in Italy? An answer from genetic and paleobotanical data. *Molecular Ecology* 18: 2276–2286.

Baillie, M. G.L., Pilcher, J.R., 1973. A simple crossdating program for tree-ring research. *Tree-Ring Bulletin* 33: 7–14.

Bernabei, M., Bontadi, J., Rossi Rognoni, G., 2010. A dendrochronological investigation of stringed instruments from the collection of the Cherubini Conservatory in Florence, Italy. *Journal of Archaeological Science* 37: 192–200.

Biger, G., Liphschitz, N., 1993. Tree ring research of the 19th century American Constructions in Israel. *Dendrochronologia* 11: 139–150.

Biger, G., Liphschitz, N., 1992. Timber usage in the first immigrant colonies. *Horizons in Geography* 33–34: 43–57. (Hebrew)

Biger, G., Liphschitz, N., 1991a. Regional dendrohistory and timber analysis: The use of wood in the buildings of nineteenth-century Jaffa. *Mediterranean Historical Review* 6 (1): 86–104.

Biger, G., Liphschitz, N., 1991b. Historical geography and botany: Timber in the nineteenth century Old City of Jerusalem. *Palestine Exploration Quarterly* 123: 4–18.

Bikai, P., 1991. *The Cedar of Lebanon: Archaeological and Dendrochronological Perspectives*. Unpublished Ph.D. dissertation, University of California, Berkeley.

Bonine, M.E., 1998. The introduction of railroads in the eastern Mediterranean: Economic and social impacts. In: Philipp, T., Schäbler, B. (Eds.), *The Syrian Land: Processes of Integration and Fragmentation, Bilad al-Sham from the 18th to the 20th Century*. Franz Steiner Verlag, Stuttgart, 54–78.

Boydak, M., 2003. Regeneration of Lebanon cedar (*Cedrus libani* A. Rich.) on karstic lands in Turkey. *Forest Ecology and Management* 178: 231–243.

Boydak, M., 1990. Monumental forests and trees of *Cedrus libani* in Turkey. In: *Proceedings of the International Cedar Symposium, October 22-27, 1990, Antalya*. Ormancılık Araş. Ens. Dergisi (Ankara) 36 (1) 71, 7-21.

Brewer, P.W., Sturgeon, K., Madar, L., Manning, S.W., 2010. A new approach to dendrochronological data management. *Dendrochronologia* 28: 131–134.

Bridge, M., 2012. Locating the origins of wood resources: a review of dendroprovenancing. *Journal of Archaeological Science* 39: 2828–2834.

Burckle, L., Grissino-Mayer, H.D., 2003. Stradivari, violins, tree rings, and the maunder minimum: a hypothesis. *Dendrochronologia* 21: 41–45.

Burke, A.A., 2011. Early Jaffa: From the Bronze Age to the Persian Period. In: Peilstöcker, M.P., Burke, A.A. (Eds.), *The History and Archaeology of Jaffa 1*. Monumenta Archaeologica 26. Cotsen Institute of Archaeology Press, University of California, Los Angeles, pp. 63–78.

Ciesla, W.M., 2004. Forests and forest protection in Cyprus. *The Forestry Chronicle* 80 (1): 107–113.

Cook, E.R., Kairiukstis, L.A. (Eds.), 1990. *Methods of Dendrochronology*. Kluwer Academic Publishers, Dordrecht.

Cuinet, V., 1896. *Syrie, Liban et Palestine: Géographie Administrative, Statistique, Descriptive et Raisonnée*. E. Leroux, Paris.

Cuinet, V., 1894. *La Turqie d'Asie: Géographie Administrative, Statistique, Descriptive et Raisonnée de Chaque Province de l'Asie Mineure*. E. Leroux, Paris.

Daly, A., 2011. Dendro-geography. Mapping the Northern European historic timber trade. In: Fraiture, P. (Ed.), *Tree Rings, Art, and Archaeology*. Proceedings of the Conference, Royal Institute for Cultural Heritage, Brussels, 10–12th February 2010. Scientia artis collection, Brussels, pp. 107–123.

Daly, A., 2007. *Timber, Trade, and Tree-Rings*. Unpublished Ph.D. dissertation, University of Southern Denmark, Odense.

Eckstein, D., Bauch, J., 1969. Ein Beitrag zur Rationalisierung eines dendrochronologischen Verfahrens und zur Analyse seiner Aussagesicherheit. *Forstwissenschaftliches Centralblatt* 88: 230–250.

Fahn, A., Werker, E., Baas, P., 1986. *Wood Anatomy and Identification of Trees and Shrubs from Israel and Adjacent Regions*. Israel Academy of Sciences and Humanities, Jerusalem.

Farjon, A., 1990. Pinaceae. *Drawings and Descriptions of the Genera*. Koeltz Scientific Books, Königstein.

Hajar, L., François, L., Khater, C., Jomaa, I., Déqué, M., Cheddadi, R., 2010. *Cedrus libani* (A. Rich) distribution in Lebanon: Past, present and future. *C.R. Biologies* 333: 622–630.

Haneca, K., Ważny, T., Van Acker, J, Beeckman, H., 2005. Provenancing Baltic timber from art historical objects: Success and limitations. *Journal of Archaeological Science* 32: 261–271.

Hoffsummer, P., 2009. From wood to roof carpentry. In: Hoffsummer, P. (Ed.), *Roof Frames from the 11th to the 19th Century: Typology and Development in Northern France and in Belgium, Analysis of CRMH Documentation*. Architectura Mediiaevi 3. Brepols, Turnhout, pp. 53–72.

Hollstein, E., 1980. *Mitteleuropäische Eichenchronologie: Trierer dendrochronologische Forschungen zur Archäologie und Kunstgeschichte*. Trierer Grabungen und Forschungen 11. P. von Zabern, Mainz am Rhein.

InsideWood, 2004–onwards. InsideWood. Online database, http://insidewood.lib.ncsu.edu/search. Accessed 12 August, 2011.

Jansma, E., Brewer, P.W., Zandhuis, I., 2010. TRiDaS 1.1: The tree-ring data standard. *Dendrochronologia* 28: 99–130.

Kark, R., 2011. Ottoman Jaffa: From ruin to central city in Palestine. In: Peilstöcker, M., Burke, A.A. (Eds.), *The History and Archaeology of Jaffa 1*. Monumenta Archaeologica 26. Cotsen Institute of Archaeology Press, University of California, Los Angeles, pp. 129–136.

Kark, R., 1984. *Jaffa: A City in Evolution, 1799-1917*. Yad Izhak Ben-Zvi Press, Jerusalem.

Kuniholm, P.I., 2001. International Tree-Ring Databank. IGBP PAGES/World Data Center for Paleoclimatology Data Contribution Series #noaa-tree-3798. NOAA/NCDC Paleoclimatology Program, Boulder, Colorado, USA.

Kuniholm, P.I., 2000a. Dendrochronologically dated Ottoman monuments. In: Baram, U., Carroll, L. (Eds.), *A Historical Archaeology of the Ottoman Empire: Breaking New Ground*. Plenum Press, New York, pp. 93–136.

Kuniholm, P.I., 2000b. International Tree-Ring Databank. IGBP PAGES/World Data Center for Paleoclimatology Data Contribution Series #noaa-tree-3797. NOAA/NCDC Paleoclimatology Program, Boulder, Colorado, USA.

Kuniholm, P.I., Griggs, C.B., Newton, M.W. 2007. Evidence for early timber trade in the Mediterranean. In: Belke, K., Kisslinger, E.A.K., Stassinopoulou, M.A. (Eds.), *Byzantina Mediterranea: Festschrift für Johannes Koder zum 65. Geburtstag*. Böhlau Verlag, Vienna, pp. 365–385.

Kuniholm, P.I., Groneman, C., 2001. International Tree-Ring Databank. IGBP PAGES/World Data Center for Paleoclimatology Data Contribution Series #noaa-tree-3811. NOAA/NCDC Paleoclimatology Program, Boulder, Colorado, USA.

Kuniholm, P.I., Striker, C.L., 1987. Dendrochronological investigations in the Aegean and neighboring regions, 1983–1986. *Journal of Field Archaeology* 14: 385–398.

Lev-Yadun, S., 2000. Wood structure and the ecology of annual growth ring formation in *Pinus halepensis* and *P. brutia*. In: Ne'eman, G., Trabaud, L. (Eds.), *Ecology and Biodiversity and Management of* Pinus halepensis *and* P. brutia *Forest Ecosystems in the Mediterranean Basin*. Backhuys, Leiden, pp. 67–78.

Liphschitz, N., 2007. *Timber in Ancient Israel: Dendroarchaeology and Dendrochronology*. Monograph Series of the Institute of Archaeology of Tel Aviv University, 26. Emery and Claire Yass Publications in Archaeology, Tel Aviv.

Liphschitz, N., Biger, G., 1992. Israel: Historical timber trade in the Levant: The use of imported *Cedrus libani* in construction of buildings in Israel from ancient times to the early twentieth century. *LUNDQUA Report* 34: 202–206.

Liphschitz, N., Biger, G., 1991. Cedar of Lebanon (*Cedrus libani*) in Israel during antiquity. *Israel Exploration Journal* 41: 167–175.

Liphschitz, N., Biger, G., 1989. *Cupressus sempervirens* in Israel during antiquity. *Israel Journal of Botany* 38: 35–45.

Liphschitz, N., Biger, G., 1988. Identification of timber and dating of historical buildings in Eretz Israel (Palestine), by dendrochronological methods. *Dendrochronologia* 6: 99–110.

Liphschitz, N., Lev-Yadun, S., Rosen, E., Waisel, Y., 1981. The annual rhythm of activity of the lateral meristems (cambium and phellogen) in *Cupressus sempervirens* L. *Annals of Botany* 47: 485–496.

McNeill, J.R., 1992. *The Mountains of the Mediterranean World*. Cambridge University Press, Cambridge.

Meiggs, R., 1982. *Trees and Timber in the Ancient Mediterranean World*. Clarendon Press, Oxford.

Mikesell, M.W., 1969. The deforestation of Mount Lebanon. *The Geographical Review* 59: 1–28.

Mikhail, A., 2011. *Nature and Empire in Ottoman Egypt: An Environmental History*. Cambridge University Press, Cambridge.

Or, E., Feder, S., Shaham, T., Jacobson, J.C., 1988. *Jaffa Guide: A Visitor's Guide to Old Jaffa*. Antiquities Museum of Tel Aviv-Jaffa, Tel Aviv.

Peilstöcker, M., 2011. The history of archaeological research in Jaffa, 1948–2009. In: Peilstöcker, M., Burke, A.A. (Eds.), *The History and Archaeology of Jaffa 1*. Monumenta Archaeologica 26. Cotsen Institute of Archaeology Press, University of California, Los Angeles, pp. 17–32.

Peilstöcker, M., Burke, A.A. (Eds.), 2011. *The History and Archaeology of Jaffa 1*. Monumenta Archaeologica 26. Cotsen Institute of Archaeology Press, University of California, Los Angeles.

Porter, J.L., 1871. *The Giant Cities of Bashan and Syria's Holy Places*. Thomas Nelson and Sons, New York.

Quézel, P., Médail, F., 2003. *Écologie et Biogéographie des Forêts du Bassin Méditerranéen*. Elsevier, Paris.

Sander, C., Levanič, T., 1996. Comparison of *t*-values calculated in different dendrochronological programmes. *Dendrochronologia* 14: 269–272.

Schweingruber, F.H., 1993. *Trees and Wood in Dendrochronology: Morphological, Anatomical, and Tree-Ring Analytical Characteristics of Trees Frequently Used in Dendrochronology*. Springer-Verlag, Berlin.

Schweingruber, 1990. *Anatomy of European Woods*. Verlag Paul Haupt, Bern.

Shaham, Zvi. *forthcoming*. The northeastern bastion of Jaffa's fortifications. In: Arbel, Y. (Ed.), *Excavations at the Qishle Site, Yafo*. The Jaffa Cultural Heritage Project. Cotsen Institute of Archaeology, Los Angeles.

Stankova, T., Stankov, H., Panetsos, K., 1999. Seasonality in the primary growth of *Cupressus sempervirens* L. from western Crete. *Silvae Genetica* 48 (2): 53–61.

Tolkowsky, S., 1924. *The Gateway of Palestine: A History of Jaffa*. George Routledge and Sons, London.

Touchan, R., Xoplaki, E., Funkhouser, G., Luterbacher, J., Hughes, M.K., Erkan, N., Akkemik, Ü., Stephan, J., 2005. Reconstructions of Spring/Summer Precipitation for the Eastern Mediterranean from Tree-Ring Widths and Its Connection to Large-Scale Atmospheric Circulation. *Climate Dynamics* 25: 75–98.

Tristram, H.B., 2012. *The Land of Israel: A Journal of Travels in Palestine*. 2nd ed. Cambridge University Press, Cambridge, UK.

Ważny, T., Rackham, O., Moody, J., 2010. *The Cretan Tree-Ring Project: Investigating the Dendrochronological and Dendroclimatological Potential of the Mediterranean Cypress (*Cupressus sempervirens *L.)*. Unpublished report to the Institute for Aegean Prehistory Study Center for East Crete.

Wigley, T.M.L., Jones, P.D., Briffa, K.R., 1987. Cross-dating methods in dendrochronology. *Journal of Archaeological Science* 14: 51–64.

Wilson, R.J.S., Hopfmueller, M., 2001. Dendrochronological investigations of Norway spruce along an elevational transect in the Bavarian Forest, Germany. *Dendrochronologia* 19 (1): 67–79.

Zohary, M., 1962. *Plant Life of Palestine: Israel and Jordan*. Ronald Press, New York.